

Storey-Based Stability Analysis for Multi-Storey Unbraced Frames Subjected to Variable Loading

by

Xiaohong Wang

A thesis
presented to the University of Waterloo
in fulfillment of the
thesis requirement for the degree of
Doctor of Philosophy
in
Civil Engineering

Waterloo, Ontario, Canada, 2008

©Xiaohong Wang 2008

I hereby declare that I am the sole author of this thesis. This is a true copy of the thesis, including any required final revisions, as accepted by my examiners.

I understand that my thesis may be made electronically available to the public.

Abstract

For decades, structural engineers have been using various conventional design approaches for assessing the strength and stability of framed structures for various loads. Today, engineers are still designing without some critical information to insure that their stability assessment yields a safe design for the life of the structure with consideration for extreme loads. Presented in this thesis is new critical information provided from the study of stability analysis and design of steel framed structures accounting for extreme loads associated to load patterns that may be experienced during their lifetime. It is conducted in five main parts. A literature survey is first carried out reviewing the previous research of analyzing frame stability including the consideration of initial geometric imperfections, and also evaluating research of the analysis and design of the increased usage of cold-formed steel (CFS) storage racks. Secondly, the elastic buckling loads for single-storey unbraced steel frames subjected to variable loading is extended to multi-storey unbraced steel frames. The formulations and procedures are developed for the multi-storey unbraced steel frames subjected to variable loading using the storey-based buckling method. Numerical examples are presented as comparisons to the conventional proportional loading approach and to demonstrate the effect of connection rigidity on the maximum and minimum frame-buckling loads. Thirdly, the lateral stiffness of axially loaded columns in unbraced frames accounting for initial geometric imperfections is derived based on the storey-based buckling. A practical method of evaluating column effective length factor with explicit accounting for the initial geometric imperfections is developed and examined using numerical examples. The fourth part is an investigation of the stability for multi-storey unbraced steel frames under variable loading with accounting for initial geometric imperfections. Finally, the stability of CFS storage racks is studied. The effective length factor of CFS storage racks with accounting for the semi-rigid nature of the beam-to-column connections of such structures are evaluated based on experimental data. A parametric study on maximum and minimum frame-buckling loads with or without accounting for initial geometric imperfections is conducted.

The proposed stability analysis of multi-storey unbraced frames subjected to variable loading takes into consideration the volatility of live loads during the life span of structures and frame buckling characteristics of the frames under any possible load pattern. From the proposed method, the maximum and minimum frame-buckling loads together with their associated load patterns provides critical information to clearly define the stability capacities of frames under extreme loads. This

critical information in concern for the stability of structures is generally not available through a conventional proportional loading analysis. This study of work ends with an appropriate set of conclusions.

Acknowledgements

I would like to express my most sincere appreciation to my supervisor, Prof. L. Xu for his support, valuable guidance to complete this research. Without his insightful discussions, comments and suggestions, this thesis would have been impossible to complete.

I greatly appreciate all the members of the examining committee Prof. Sanjeev Bedi, especially to Prof. Donald E. Grierson who taught me about optimization theory and application and Prof. Reinhold M. Schuster who taught me the theory and applications of cold formed steel and also provided experimental data that was of enormous value to my research. Special thanks to Professor K.S. Sivakumaran, McMaster University, Canada for serving as the external examiner and for improving the quality of my thesis. Thanks are due to my colleague, Dr. Yuxin Liu for his valuable discussions and help.

Thanks are due to the research scholarship award provided by the Natural Sciences and Engineering Research Council of Canada; the University of Waterloo Faculty of Engineering Graduate Scholarships; the University of Waterloo President's Graduate Scholarship for 2006-2008; Provost Doctoral Entrance Award for Women - Engineering and the Teaching Assistantships granted by the Department of Civil and Environmental Engineering.

Finally, I dedicate this thesis to my husband Gary Lindahl. I am forever indebted to his help with revising the drafts of this thesis, his computer application skills, his love, understanding, endless patience, encouragements, support, and sacrifice when it was most required. I am also very grateful to my parents Mingzhang Wang and Zhenzhen Yang, my parents-in-law Tom Lindahl and Lee Ann Lindahl, and my Canadian parents Rober Korfman and Merilyn Korfman for their love, support and encouragements as well as my brothers, sisters and friends.

To Gary, my husband and my family

Table of Contents

List of Figures	x
List of Tables.....	xii
Symbols	xvi
Chapter I Introduction	1
1.1 Background	1
1.2 Objectives of this Research	4
1.3 Outline of Research	5
Chapter II Literature Survey.....	7
2.1 Introduction	7
2.2 Stability of Steel Frames	7
2.2.1 Effective Length Factor Method.....	8
2.2.2 Initial Geometric Imperfections.....	10
2.2.3 Notional Load Approach	11
2.3 CFS Structure Applications	12
2.3.1 Analysis and Design of CFS Structures	12
2.3.2 Design of CFS Storage Racks	15
Chapter III Storey Stability of Multi-Storey Unbraced Frames Subjected to Variable Loading	18
3.1 Introduction	18
3.2 Lateral Stiffness of an Axially Loaded Semi-Rigid Column	19
3.3 Storey-Based Stability Equation.....	22
3.4 Decomposition of Multi-Storey Frames	25
3.5 Stability Analysis for Multi-Storey Unbraced Frames Subjected to Variable Loading	26
3.6 Numerical Example	28
3.7 Conclusions	43
Chapter IV Storey-Based Stability Analysis for Unbraced Frame with Initial Geometric Imperfections	45
4.1 Introduction	45
4.2 Lateral Stiffness of an Axially Loaded Column with Initial Geometric Imperfections	46
4.3 Evaluation of Column Effective Length Factor Accounting for Initial Geometric Imperfections	51
4.4 Numerical Examples	55

4.5 Conclusions.....	76
Chapter V Multi-Storey Unbraced Frames with Initial Geometric Imperfections Subjected to Variable Loading	78
5.1 Introduction.....	78
5.2 Numerical Examples.....	79
5.2.1 Single-Storey Unbraced Frame Example.....	79
5.2.2 Multi-Storey Unbraced Frame Example	86
5.2.3 Effects of Semi-Rigid Connections.....	96
5.3 Conclusions.....	104
Chapter VI Application of Storey-Based Stability Analysis to CFS Storage Racks	105
6.1 Introduction.....	105
6.2 Members Design	106
6.2.1 Introduction.....	106
6.2.2 Elastic Buckling Strength of Perforated Members.....	107
6.2.3 Effective Design of Cross-Sectional Area	112
6.3 Beam to Column Connections	115
6.3.1 Introduction.....	115
6.3.2 Beam to Column Connection Tests.....	117
6.3.3 Test Specimens and Set-up	118
6.3.4 Evaluation of Test Results	119
6.4 Elastic Buckling Strength of Storage Racks	120
6.4.1 Introduction.....	120
6.4.2 Column Effective Length Factor for Geometrically Perfect Storage Racks.....	121
6.4.3 Effective Length Factor for Initial Geometric Imperfect Storage Racks	124
6.5 Stability Analysis of Storage Racks Subjected to Variable Loading.....	128
6.5.1 Introduction.....	128
6.5.2 Numerical Studies	128
6.6 Conclusions.....	150
Chapter VII Conclusions and Future Research.....	151
7.1 Conclusions.....	151
7.1.1 Storey Stability of Multi-Storey Unbraced Frames Subjected to Variable Loading.....	151

7.1.2 Storey-Based Stability Analysis for Unbraced Frame with Initial Geometrical Imperfections.....	153
7.1.3 Multi-storey Unbraced Frames with Initial Geometric Imperfections Subjected to Variable Loading.....	154
7.1.4 Application of Storey-based Stability Analysis to CFS Storage Racks	155
7.2 Future Research.....	156
Appendix A	158
Appendix B.....	164
Appendix C.....	167
Appendix D	169
Appendix E.....	181
Bibliography	182

List of Figures

Figure 2-1: Typical cross-section types of CFS members	12
Figure 2-2: Cold-formed steel framing—Example 1	13
Figure 2-3: Cold-formed steel framing—Example 2	13
Figure 2-4: Cold-formed steel members used in storage rack systems - Example 1	15
Figure 2-5: Cold-formed steel members used in storage rack systems - Example 2	15
Figure 3-1: Axially loaded column of an unbraced frame with deformations and forces.....	19
Figure 3-2: Relationship between the end-fixity factor and connection stiffness.....	20
Figure 3-3: (m-1)-bay by n-storey unbraced frame.....	23
Figure 3-4: Decomposed single storey model.....	25
Figure 3-5: 2-bay by 2-storey steel frame – Case 1	29
Figure 3-6: 2-bay by 2-storey steel frame – Case 2	30
Figure 3-7: 2-bay by 2-storey steel frame – Cases 3 and 5	30
Figure 3-8: 2-bay by 2-storey steel frame – Case 4	31
Figure 3-9: Load patterns associated with max. and min. frame-buckling loads – Case 1	34
Figure 3-10: Load patterns associated with max. and min. frame-buckling loads – Case 2.....	35
Figure 3-11: Load patterns associated with max. and min. frame-buckling loads – Case 3.....	36
Figure 3-12: Load patterns associated with max. and min. frame-buckling loads – Case 4.....	37
Figure 3-13: Load patterns associated with max. and min. frame-buckling loads – Case 5.....	38
Figure 4-1: Influence of imperfection on column behavior (Trahair and Bradford,1991).....	46
Figure 4-2: The deformed shapes of an axially loaded column with initial geometric imperfections.	47
Figure 4-3: 2-bay by 1-storey frame of Example 1 (Schimdt, 1999).....	56
Figure 4-4: Example 1 - comparison results of K factors vs end-fixity factor r	59
Figure 4-5: Example 1 - K factors vs out-of-straightness (δ_0)	60
Figure 4-6: Example 1 - K factors vs out-of-plumbness (Δ_0).....	61
Figure 4-7: Example 1 - lateral stiffness coefficients $\beta_{0,ij}$ vs. out-of-straightness (δ_0).....	64
Figure 4-8: Example1 - lateral stiffness coefficients $\beta_{1,ij}$ vs. out-of-straightness (δ_0).....	65
Figure 4-9: Example1 - lateral stiffness coefficients $\beta_{2,ij}$ vs. out-of-straightness (δ_0).....	65
Figure 4-10: Example 1 - lateral stiffness coefficients of $\beta_{0,ij}$ vs. out-of-plumbness (Δ_0).....	66
Figure 4-11: Example1 - lateral stiffness coefficients of $\beta_{1,ij}$ vs. out-of-plumbness(Δ_0).....	66
Figure 4-12: Example1 - lateral stiffness coefficients of $\beta_{2,ij}$ vs. out-of-plumbness (Δ_0).....	67
Figure 4-13: Example 1 - column buckling load vs out-of-straightness (δ_0)	67

Figure 4-14: Example 1 - column buckling load vs out-of-plumbness (Δ_0)	68
Figure 4-15: 1-bay by 3-storey frame of Example 2 (Shanmugan et al., 1995)	69
Figure 4-16: Example 2 - column K factors of stories 1 to 3 vs out-of-straightness δ_0	72
Figure 4-17: Example 2 - column K factors of stories 1 to 3 vs out-of-plumbness (Δ_0).....	72
Figure 4-18: Example 2 - factored axial strength vs out-of-straightness (δ_0).....	75
Figure 4-19: Example 2 - the effect of factored axial strength vs out-of-plumbness (Δ_0).....	75
Figure 5-1: 2-bay by 1-storey frame of Example 1 (Xu, 2002).....	79
Figure 5-2: 15 frames with different beam-to-column connections used in study	80
Figure 5-3: Relative differences of the critical buckling loads($(P_{max}-P_{min})/P_{min}$) of three schemes	85
Figure 5-4: Relative differences of the critical buckling loads($(P_{max}-P_{min})/P_{min}$) of three schemes	85
Figure 5-5: Load patterns associated with max. and min. frame-buckling loads – Case 1	97
Figure 5-6: Load patterns associated with max. and min. frame-buckling loads – Case 2	98
Figure 5-7: Load patterns associated with max. and min. frame-buckling loads – Case 3	99
Figure 5-8: Load patterns associated with max. and min. frame-buckling loads – Case 4	100
Figure 5-9: Load patterns associated with max. and min. frame-buckling loads – Case 5	101
Figure 6-1: Typical storage rack configuration and components (CSA, 2005).....	106
Figure 6-2: Elastic buckling axial load for C_1	111
Figure 6-3: Elastic buckling axial load for C_2	111
Figure 6-4: Elastic buckling axial load for C_3	112
Figure 6-5: Typical rack moment connection (NEHRP, 2003).....	115
Figure 6-6: Typical rack bracing members and connection (NEHRP, 2003).....	116
Figure 6-7: Typical column base plate connection (NEHRP, 2003)	116
Figure 6-8: Cantilever test – beam to column connection test (RMI, 2000)	117
Figure 6-9: Portal test – beam to column connection test (RMI, 2000)	117
Figure 6-10: Typical box and ledge beam sections in tests (Schuster, 2004).....	118
Figure 6-11: Cantilever rack beam/column test (Schuster, 2004)	119
Figure 6-12: 2-bay by 2-storey storage rack example	122
Figure 6-13: 2-bay by 3-storey storage rack example	124
Figure 6-14: 3-bay by 3-storey storage rack example	129

List of Tables

Table 3-1: 2-bay by 2-storey steel frames with different connections.....	32
Table 3-2: Results of the unbraced steel frames shown in Figure 3-5 – Case 1	34
Table 3-3: Results of the unbraced steel frames shown in Figure 3-6 – Case 2	35
Table 3-4: Results of the unbraced steel frames shown in Figure 3-7 – Case 3	36
Table 3-5: Results of the unbraced steel frames shown in Figure 3-8 – Case 4	37
Table 3-6: Results of the unbraced steel frames shown in Figure 3-7 – Case 5	38
Table 3-7: Results verification of the unbraced steel frames shown in Figure 3-5 – Case 1	39
Table 3-8: Results verification of the unbraced steel frames shown in Figure 3-8 – Case 4.....	42
Table 4-1: Example 1 - Comparison of K factors of 2-bay by 1-storey.....	57
Table 4-2: Example 1 – comparison study of three approaches	58
Table 4-3: Example 1 - effects of out-of-straightness on K factors	62
Table 4-4: Example 1- effects of out-of-plumbness on K factors	62
Table 4-5: Example 1 - effects of out-of-straightness and out-of-plumbness on K factors	63
Table 4-7: Example 2 - comparison study of three approaches	70
Table 4-8: Example 2 - effects of out-of-straightness on K factors	73
Table 4-9: Example 2 - effects of out-of-plumbness on K factors	74
Table 4-10: Example 2 - effects of out-of-straightness and out-of-plumbness on K factors	74
Table 5-1: Comparison of the max. and min. buckling loads together with their relative difference with three different schemes (1).....	82
Table 5-2: Comparison of the max. and min. buckling loads together with their relative difference with three different schemes (2).....	83
Table 5-3: Comparison of the max. and min. buckling loads together with their relative difference with three different schemes (3).....	84
Table 5-4: The effect of out-of-straightness (δ_0) to frame buckling loadings (1)	88
Table 5-5: The effects of out-of-straightness (δ_0) to frame buckling loadings (2).....	89
Table 5-6: The effects of out-of-straightness (δ_0) to frame buckling loadings (3).....	90
Table 5-7: The effects of out-of-plumbness (Δ_0) to frame buckling loadings (4).....	91
Table 5-8: The effects of out-of-plumbness (Δ_0) to frame buckling loadings (5).....	92
Table 5-9: The effects of combined out-of-straightness (δ_0) and out-of-plumbness (Δ_0) to frame buckling loadings (6)	93

Table 5-10: The effects of combined out-of-straightness (δ_0) and out-of-plumbness (Δ_0) to frame buckling loadings (7).....	94
Table 5-11: Results of the unbraced steel frames shown in Figure 3-5 – Case 1 ($\delta_0=L/1000$ and $\Delta_0=L/500$)	97
Table 5-12: Results of the unbraced steel frames shown in Figure 3-6 – Case 2 ($\delta_0=L/1000$ and $\Delta_0=L/500$)	98
Table 5-13: Results of the unbraced steel frames shown in Figure 3-7 – Case 3 ($\delta_0=L/1000$ and $\Delta_0=L/500$)	99
Table 5-14: Results of the unbraced steel frames shown in Figure 3-8 – Case 4 ($\delta_0=L/1000$ and $\Delta_0=L/500$)	100
Table 5-15: Results of the unbraced steel frames shown in Figure 3-7 – Case 5 ($\delta_0=L/1000$ and $\Delta_0=L/500$)	101
Table 6-1: Section C ₁ dimensions and properties (Sarawit and Peköz, 2003)	108
Table 6-2: Section C ₂ dimensions and properties (Sarawit and Peköz, 2003)	109
Table 6-3: Section C ₃ dimensions and properties (Sarawit and Peköz, 2003)	110
Table 6-4: Properties of column and beam (Schuster, 2004)	122
Table 6-5: <i>K</i> factors for three types of column and beam in study.....	123
Table 6-6: Comparison of <i>K</i> factors of two-bay by three-storey frame – Rack Type I.....	125
Table 6-7: <i>K</i> factors of two-bay by three-storey frame – Rack Type I.....	126
Table 6-8: Effects of out-of-straightness - 2-bay by 3-storey.....	126
Table 6-9: Effects of out-of-plumbness - 2-bay by 3-storey	127
Table 6-10: Effects of out-of-straightness and out-of-plumbness - 2-bay by 3-storey.....	127
Table 6-11: There different end connections in study	129
Table 6-12: Results of the storage rack for Connection 1 ($r = 0.029$) –Figure 6-14.....	131
Table 6-13: Results of the storage rack for Connection 2 ($r = 0.228$) – Figure 6-14	132
Table 6-14: Results of the storage rack for Connection 3 ($r = 0.596$) – Figure 6-14.....	133
Table 6-15: Results verification of rack shown in Figure 6-14 – Connection 1.....	134
Table 6-16: Effects of out-of-straightness (δ_0) to Maximum frame-buckling loads	136
Table 6-17: Effects of out-of-straightness (δ_0) to minimum loading with lateral instability - storey 1: $S_1 = 0, S_2 > 0, S_3 > 0$	137
Table 6-18: Effects of out-of-straightness (δ_0) to minimum loading with lateral instability - storey 2: $S_2 = 0, S_1 > 0, S_3 > 0$	138

Table 6-19: Difference between the maximum and minimum frame-buckling loads - out-of-straightness (δ_0).....	139
Table 6-20: Effects of out-of-plumbness (Δ_0) to maximum frame-buckling loads.....	141
Table 6-21: Effects of out-of-plumbness (Δ_0) to minimum loading with lateral instability - storey 1: $S_1 = 0, S_2 > 0, S_3 > 0$	142
Table 6-22: Effects of out-of-plumbness (Δ_0) to minimum loading with lateral instability - storey 2: $S_2 = 0, S_1 > 0, S_3 > 0$	143
Table 6-23: Difference between the maximum and minimum frame-buckling loads - out-of-plumbness (Δ_0).....	144
Table 6-24: Effects of both out-of-straightness (δ_0) and out-of-plumbness (Δ_0) to maximum frame-buckling loading.....	146
Table 6-25: Effects of both out-of-straightness (δ_0) and out-of-plumbness (Δ_0) to minimum loading with lateral instability - storey 1: $S_1 = 0, S_2 > 0, S_3 > 0$	147
Table 6-26: Effects of both out-of-straightness (δ_0) and out-of-plumbness (Δ_0) to minimum loading with lateral instability - storey 2: $S_2 = 0, S_1 > 0, S_3 > 0$	148
Table 6-27: Difference between the maximum and minimum frame-buckling loads – out-of-straightness (δ_0) and out-of-plumbness (Δ_0).....	149
Table D-1: $\beta_0 (\times 10^{-1})$ values corresponding to the column end-fixity factors ($\delta_0=L/1000$ and $\Delta_0=L/500$).....	169
Table D-2: $\beta_0 (\times 10^{-1})$ values corresponding to the column end-fixity factors ($\delta_0=L/800$ and $\Delta_0=L/400$).....	170
Table D-3: $\beta_0 (\times 10^{-1})$ values corresponding to the column end-fixity factors ($\delta_0=L/600$ and $\Delta_0=L/300$).....	171
Table D-4: $\beta_0 (\times 10^{-1})$ values corresponding to the column end-fixity factors ($\delta_0=L/400$ and $\Delta_0=L/200$).....	172
Table D-5: $\beta_1 (\times 10^{-2})$ values corresponding to the column end-fixity factors ($\delta_0=L/1000$ and $\Delta_0=L/500$).....	173
Table D-6: $\beta_1 (\times 10^{-2})$ values corresponding to the column end-fixity factors ($\delta_0=L/800$ and $\Delta_0=L/400$).....	174
Table D-7: $\beta_1 (\times 10^{-2})$ values corresponding to the column end-fixity factors ($\delta_0=L/600$ and $\Delta_0=L/300$).....	175

Table D-8: $\beta_1 (\times 10^{-2})$ values corresponding to the column end-fixity factors ($\delta_0=L/400$ and $\Delta_0=L/200$)	176
Table D-9: $\beta_2 (\times 10^{-4})$ values corresponding to the column end-fixity factors ($\delta_0=L/1000$ and $\Delta_0=L/500$)	177
Table D-10: $\beta_2 (\times 10^{-4})$ values corresponding to the column end-fixity factors ($\delta_0=L/800$ and $\Delta_0=L/400$)	178
Table D-11: $\beta_2 (\times 10^{-4})$ values corresponding to the column end-fixity factors ($\delta_0=L/600$ and $\Delta_0=L/300$)	179
Table D-12: $\beta_2 (\times 10^{-4})$ values corresponding to the column end-fixity factors ($\delta_0=L/400$ and $\Delta_0=L/200$)	180

Symbols

A	Area of cross section
A_e	Effective area at stress F_n
$A_{net\ min}$	Net minimum cross-sectional area obtained by passing a plane through the section normal to axis of the column
A_{nm}	Net minimum cross-sectional area obtained by passing a plane through the section normal to axis of the column
b	Flange width
C_w	Torsional warping constant of cross-section
d	Depth of section
E	Young's modulus of steel
$EI_{c,ij}/L_{c,ij}$	Flexural stiffness of the column
F	Constant connection stiffness
F_c	Critical buckling stress based on σ_{ex} , σ_{ey} and σ_{et}
F_n	Nominal buckling stress and determined in Section C4 of CSA/S136S1-04.
F_y	Yield point used for design
F'_y	Actual yield stress of the column material if no cold work of forming affects considered
F_u	Ultimate (tensile) strength of steel
G	Shear modulus of steel
H	Length of the storey
i	Index of storey
$I_{c,ij}$	Moment of inertia of column
$I_{c,y-net}$	Net moment of inertia of column section about y-axis
I_x	Moment of inertia of beam section about x-axis
I_{xb}	Moment of inertia of beam section about x-axis
I_{xy}	Product of inertia of full unreduced section about major and minor centroidal axes
I_y	Moment of inertia of beam section about y-axis
j	Index of column
J	St. Venant torsion constant of cross section

$K_{\text{braced},ij}$	Effective length factor of the column associated with non-sway-buckling
K_{ij}	Effective length factor for unbraced frame
l	Index of storey
L	Member length
$L_{c,ij}$	Length of column
L_b	Beam length
L_c	Column length
$L_{c,ij}$	The length axial load of column j in the i th storey
m	Number of columns in one storey
M	Moment in the column
M_e	Elastic flexural buckling moment
M_r	Factored moment resistance
M_l	End moment at the lower end
M_u	End moment at the upper end
M_y	Moment causing initial yield at the extreme compression fiber of the full unreduced gross section
n	Number of the storey of the frame
P	Axial loading
$P_{a,ij}$	Applied axial load for the column
$P_{e,ij}$	Euler buckling load for the column
P_{cr}	Elastic buckling strength of the end-restrained column
P_l	First yield takes place at a load
P_r	Factored compressive resistance
$P_{u,ij}$	Ultimate load for the column
P_{ij}	Column axial load
$P_{0.85}$	0.85 times ultimate test load
P_{ult}	Ultimate compressive strength of stub column by tests
P_{max}	Summation of the maximum loads
P_{min}	Summation of the minimum loads
P_y	Axial load causing the yield of the full unreduced gross section
$P-\delta$	Member stability

$P-\Delta$	Frame stability
Q	Perforation factor
$r_{l,ij}$	End-fixity factors for the lower end of the column
$r_{u,ij}$	End-fixity factors for the upper end of the column
$R_{l,ij}$	Rotational restraining stiffness of connected beams at lower joints
$R_{u,ij}$	Rotational restraining stiffness of connected beams at upper joints
$R.F.$	Reduction factor to provide safety considering scatter of test data and recommend being 1 in this study
S_1	Lateral stiffness of the columns in storey 1
S_2	Lateral stiffness of the columns in storey 2
S_c	Elastic section modulus of effective section calculated relative to extreme compression or tension fibre at F_c
S_e	Elastic section modulus of the effective section calculated with extreme compression or tension fiber at F_y
S_f	Elastic section modulus of full unreduced section relative to extreme compression fiber
S_k	Lateral stiffness of the columns in the k th storey
S_l	Lateral stiffness of the columns in the l th storey
S_{ij}	Lateral stiffness of an axially loaded column in an unbraced frame
t	Thickness of cross section
y_1	Member imperfection function
y_2	Frame imperfection function
Y_i	Design gravity load applied at level i ,
Z	Summation of extreme loadings
Z_l	Summation of extreme loadings
β_{ij}	Modification factor of the lateral stiffness
$\beta_{0,ij}$	Modification factor of the lateral stiffness
$\beta_{1,ij}$	Modification factor of the lateral stiffness
$\beta_{2,ij}$	Modification factor of the lateral stiffness
ν	Poisson's ratio
δ_0	Out-of- straightness of the columns

$\delta_{0.85}$	Displacement of free end of cantilever beam at load $P_{0.85}$
Δ_0	Out-of-plumbness of the frames
Δ_l	Deflection of the joints of the member
θ	Angle between the column and the connecting beam
θ_l	End rotation of the column at the lower end
θ_u	End rotation of the column at the upper end
θ_{l0}	End rotation of the column at the lower end
θ_{u0}	End rotation of the column at the upper end
λ_{icr}	Critical load multiplier associated with the i th storey
λ_{cr}	Most critical load multiplier associated with the multi-storey frame
$\lambda_{icr-1st-order}$	Critical load multiplier of the i th storey associated with 1 st -order approximation
$\lambda_{icr-2nd-order}$	Critical load multiplier of the i th storey associated with 2 nd -order approximation
σ_{ex}	Lateral-torsional buckling about x-axis defined as $\sigma_{ex} = \frac{\pi^2 E}{(K_x L_x / r_x)^2}$
σ_{ey}	Lateral-torsional buckling about y-axis defined as $\sigma_{ey} = \frac{\pi^2 E}{(K_y L_y / r_y)^2}$
σ_{et}	Torsional buckling defined as $\sigma_{et} = \frac{1}{A r_0^2} [GJ + \frac{\pi^2 E C_w}{(K_t L_t)^2}]$
ϕ_b	Resistance factor for bending strength
ϕ_c	Resistance factor for concentrically loaded compression member
ϕ_{ij}	Applied load ratio, defined as $\phi_{ij} = \sqrt{\frac{P L_{ij}^2}{E I_{c,ij}}} = \pi \sqrt{P_{ij} / P_{e,ij}}$

Chapter I

Introduction

1.1 Background

Stability is the fundamental safety criterion for steel structures during their construction period and lifetime of operation. Although the research on the stability of structures can be traced back to 264 years ago when Euler published his famous Euler equation on the elastic stability of steel bars in 1744, adequate solutions are still not available for many types of structures. The stability of structures has been exercising the minds of many eminent engineers and applied mathematicians for several decades. Even today in 2008, structural engineers are still facing the challenges of determining the stability of a structure under different types of loads. One of these more difficult challenges is in determining the critical load under which a structure collapses due to the loss of stability in the structural design because of the complexity of this phenomenon and because of the many material property influences due to imperfections and inelasticity. In addition to the complex challenges, the improvement of the industrial processes in both hot-rolled and cold formed steel (CFS) members and the use of high strength steel provides a competitive design solution to structural weight reduction, resulting from the increase of member slenderness, structural flexibility and therefore being more vulnerable to instability.

The approaches for considering column stability in the design of steel frames vary between different design standards and specifications throughout the world. Within the context of using elastic analysis, in general, there are three types of methods available for stability analysis of framed structures subjected to proportional loading, i.e. 1) theoretical method which is so-called the system buckling method, 2) the effective-length based method and 3) storey-based buckling method (Galambos, 1988; Julian and Lawrence, 1959; Majid, 1972; Chen and Lui, 1987). Among these methods, the system buckling method is considered to be impractical as it involves solving for the minimum positive eigenvalue from either a highly nonlinear or a transcendental equation (Galambos, 1988). With the effective-length based method, the alignment chart method (Julian and Lawrence,

1959) is the most widely used method in practice for designing a frame, while this method uses certain simplifications which may result in the inaccuracy of the estimated column strengths in certain cases. The storey-based buckling method, which is an alternative to the effective length method that does not use the simplifications corresponding to the alignment chart method is considered to be practical and provides accurate results (Yura, 1971; LeMessurier, 1977; Xu and Liu, 2002; Liu and Xu, 2005; Xu and Wang, 2007, 2008). This method is based on the idea that lateral sway instability of an unbraced frame is a storey phenomenon involving the interaction of lateral sway resistance of each column in the same storey and the total gravity load in the columns of that storey. A storey-based buckling method developed by Xu and Liu (2002) will be adopted and extended in this research to facilitate the stability analysis of multi-storey steel frames subjected to variable loading.

Considering current design practice and research activities involving the stability analysis and design of framed structures are almost exclusively based on the assumption of proportional loading, where the obtained stability capacity of the structure corresponds to a specified load pattern that may not apply to any other load pattern. Therefore, structural engineers have to anticipate the possible load patterns caused by various types of loads that may be encountered during the life span of the building, and this is usually accomplished by specifying different load combinations in accordance with existing design standards, if available. However, the worst case load patterns are not always guaranteed in the load combinations specified in the standards or by the engineers due to the unpredictable nature to varying types of loads. The variability of loads in both magnitudes and locations need to be accounted for in assessing the stability of structures, otherwise, public safety may be jeopardized.

The study of stability of multi-storey unbraced steel frames subjected to variable loading will be considered in this research because this is of primary importance as variable loading accounts for the variability of applied loads, which will represent realistic conditions during the life span of the structures. This research includes obtaining the maximum and minimum frame-buckling loads and the associated load patterns from a frame stability analysis under any possible load combinations. The associated load patterns clearly define the stability capacities of frames under extreme load cases. Since this research proposes an innovative variable loading approach, it enables the prediction of the characteristics of stability of unbraced multi-storey frames under variable loadings. The variable loading approach captures the load patterns that cause instability failure of frames at the maximum

load levels (the most favorable load pattern) and minimum (the worst load pattern). The approach clearly identifies the stability capacities of frames under the extreme load cases; such critical information is generally not available through the current proportional loading stability analysis.

All structural frames in reality are geometrically imperfect, hence, deflection commences as soon as the loads are applied. In the practical stability design and analysis of framed structures, geometric imperfections to be accounted for are out-of-straightness, which is a lateral deflection of the column relative to a straight line between its end points, and frame out-of-plumbness, which is lateral displacement of one end of the column relative to the other. In the absence of more accurate information, evaluation of imperfection effects should be based on the permissible fabrication and erection tolerances specified in the appropriate building code. As an example, in the U.S.A, the initial geometric imperfections are assumed to be equal to the maximum fabrication and erection tolerances permitted by the AISC *Code of Standard Practice for Steel Building and Bridge* (AISC, 1992) and AISC (2005). For columns and frames, this implies a member out-of-straightness equal to $L/1000$, where L is the member length brace or framing points, and a frame out-of-plumbness equal to $H/500$, where H is the storey height, and these two initial geometric imperfections values will be adopted in this current research.

In this research, an analytical investigation on the effective length based procedure such that the effects of the out-of-straightness of column and out-of-plumbness of frame on column strength can be evaluated explicitly and independently. Within the concept of the storey-based buckling method introduced by Yura (1971), a practical method to evaluate the effective length factor for columns in an unbraced frame with initial geometric imperfections is developed in this study.

The method investigated to evaluate the stability capacities for a multi-storey unbraced frame under extreme load cases is an innovative approach, which is currently not available through the current proportional loading stability analysis. For an extreme loading case accounting for the initial geometric imperfections, this innovative variable loading approach will help improve upon existing methods used in applications for the engineering practice from this research.

The structural application of CFS has increased rapidly in recent times due to significant improvements of manufacturing technologies producing thin, high-strength steels and research

achievements on the design and construction of CFS framing. Cold formed steel members have a unique structural stability issues primarily due to the large width-to-thickness comparison element ratios, which is not commonly the use with in sections of hot-rolled steel. One of the largest applications of CFS structures is found in the storage rack industry, ranging from relatively small shelving systems to extremely large and sophisticated pallet storage rack systems. In current design practice, the nature of randomly applied loads, both in applied locations and magnitudes, are often found as one of the primary contributing factors causing structural failures. This not considered in the design of the storage racks and as a result the appropriate analysis method is not available at the present time. Considering that CFS storage racks are extensively used in large and crowded warehouse type shopping facilities in Canada and the U.S.A, public safety may be a concern due to the factors involved with structural stability. For the purposes of safety and performance, research on assessing the integrity of the CFS storage racks subjected to variable loading is imperative and considered far overdue. It is an essential part of this research to apply for the proposed method in the application of CFS storage racks to help improve upon existing methods.

1.2 Objectives of this Research

The overall objective of this research involves the stability issues that the design professional is facing in the structural design of both conventional steel structures and CFS storage racks to ensure the stability of structural frame and its individual members while considering the uncertainty and variability of the applied loads. The specific objectives of this thesis are:

- Develop an analytical approach for the stability analysis of multi-storey unbraced frames subjected to variable loading with regard to frame stability.
- Develop a practical approach of calculating storey-based column effective length factors with explicitly accounting for initial geometric imperfections and the effects of initial geometric imperfections on the column strength.
- Investigate the effect of initial geometric imperfections on the stability of multi-storey unbraced frames subjected to variable loading.
- Apply the proposed method for evaluating the effective length factor method of CFS storage rack frame structures with consideration for semi-rigid connections.

- Conduct an analytical investigation on the stability of CFS storage rack frame structures subjected to variable loading with or without accounting for initial geometric imperfections.

1.3 Outline of Research

This thesis is organized in the following manner:

In Chapter 2, a literature survey is presented which includes the reviews of selected previous works on frame stability analysis including the consideration of the stability analysis of frames, the effects of initial geometric imperfections in the design of frame structures, research work about CFS including the application of CFS used for storage rack frame structures.

Presented in Chapter 3 is the study to extend the method for elastic stability of multi-storey unbraced frames subjected to variable loading from the method developed by Xu (2002) for single-storey frames. This study will establish the problem of determining the maximum and minimum frame-buckling loads of multi-storey unbraced semi-rigid frames under variable loading based on the concept of storey-based buckling. The established problem is formulated as a pair of maximization and minimization problems with stability constraints that can be solved by a linear programming method. A 2-bay by 2-storey semi-rigid unbraced frame subjected to variable loading is presented to demonstrate the proposed approach. This proposed approach clearly identifies the stability capacities of frames under extreme load cases. The maximum and minimum frame-buckling loads together with their associated load patterns obtained from this proposed approach, are generally not available through a conventional proportional loading stability analysis.

Given in Chapter 4 is the study of the storey-based stability analysis for multi-storey unbraced frames accounting for initial geometric imperfections. By following the derivation of the lateral stiffness of an axially loaded column in an unbraced frame and accounting for the initial geometric imperfections, the formulation and the procedure of evaluating the column effective length factor with explicitly accounting for the initial geometric imperfections are developed. The comparison among the results of the 1st-order, 2nd-order Taylor series approximations and the storey-based method is examined by using numerical examples. Parametric studies are presented to illustrate the effects of the initial geometric imperfections on the column effective length factor and column strengths. In this

chapter a method is developed to enable practitioners to better evaluate column strengths by explicitly using any given value of initial geometric imperfections, which is not available in the current design practice.

Based on the studies presented in Chapters 3 and 4, the study presented in Chapter 5 is focused on the effects of the initial geometric imperfections for maximum and minimum frame-buckling loads of the multi-storey unbraced semi-rigid frames under variable loading. The maximization and minimization problems presented in Chapter 3 are reformulated by replacing the column lateral stiffness, which accounts for the initial geometric imperfections. The numerical example in Chapter 3 is examined with consideration for the imperfections. A parametric study is also carried out to investigate the influences of the imperfections on the maximum and minimum frame-buckling loads.

Presented in Chapter 6 is the application of CFS storage racks using the methods developed in the previous Chapters 3 to 5. The effects of the perforations to the member design code for CFS storage racks are also examined and the semi-rigid connection is evaluated with the experimental data for such structures in this chapter. The numerical examples of CFS storage racks with different beam-to-column connections are given to predict the column effective length factor accounting for the initial geometric imperfections. Also the parametric study to provide the results for unbraced CFS storage racks subjected to variable loading is presented in this chapter.

Conclusions of the current research and recommendations on the future research are presented in Chapter 7.

Chapter II

Literature Survey

2.1 Introduction

The structural use of steel in the construction industry is continually growing rapidly across the world. New challenges in the structural use of steel are arising all the time, and research has been called upon to provide appropriate solutions. The use of steel as a construction material has, of course, its advantages, such as strength, lightness, ductility, etc., but it also possesses, as is well-known, considerable challenges with regard to slenderness, stability, fire resistance, geometric imperfections and other structural requirements. Thus, with the understanding accruing from the numerous studies of the mechanics of steel structures at both member and system levels, it becomes necessary to develop appropriate analysis procedures to quantify the relevant effects in the structures, and to develop appropriate design procedures for the actual construction of these structures.

2.2 Stability of Steel Frames

Since the mid-18th century, the phenomenon of elastic stability, or buckling, has given rise to extensive theoretical and experimental investigations. The first study about the stability analysis for rigidly jointed plane frameworks can be found in Zimmermann (1909), Müller-Breslau (1908) and Bleich (1919). Later, Pager (1936) developed a method using the stability condition of a column with elastic end restraints. Chwalla (1938) presented a study on lateral stability of a rigidly jointed one-storey symmetric portal frame subjected to symmetrical concentrated transverse loads. In his study, the elastic buckling strength of a frame was defined as being equivalent to the elastic critical load of the frame and the strengths of the frame and columns were interrelated and the relationship between the two was identified to be complicated. Since the 18th century, there have been tremendous research efforts made in frame stability with goals to provide more accurate and practical solutions for the engineering practice and since then there are three types of methods available for stability

analysis of framed structures, i.e. theoretical method, the effective-length based method and storey-based buckling method.

The theoretical method of stability analysis of frames, which is also called the system buckling method, often involves solving the critical loads from either a highly nonlinear equation or a transcendental equation (Majid, 1972; Livesley, 1975; Bhatt, 1981), which accounts for the stiffness interactions of all members in the frame. Although the system buckling method provides accurate results, this method is generally considered impractical because of the cumbersomeness and difficulty in solving for the critical load multiplier of the structural system as the least non-negative eigenvalue from either a highly nonlinear or a transcendental equation (Galambos, 1988). In design practice, the effective length based methods still are the general methods of evaluating the column compressive strength and have been recommended in almost all of the current design specifications (AISC, 2005).

2.2.1 Effective Length Factor Method

In current design practice, the effective-length based method has become the most common method to evaluate the column compressive strength. Based on the effective length concept, the compressive strength of a member with length L in a frame is equated to the length of an equivalent pin-ended member with length KL , in which K is called the effective length factor, or K factor. This concept is considered an essential part of many analysis procedures and has been recommended by almost all current design specifications (AISC, 1989, 1994, 2001, 2005) and Canadian Standard CAN/CSA S16.1-2000 (CSA, 2000). There are several methods to calculate the K factors within the concept of effective length. Among these methods, the alignment chart method that was investigated by Julian and Lawrence (1959) is the most widely used method for frame design. This method assumes that all individual columns in a storey buckle simultaneously under their individual proportionate share of the total gravity load (Duan and Chen, 1989) and it also takes into account the rotational restraints provided by upper and lower beam column assemblages to provide a direct means to evaluate the K factors. However, since this method relies on several assumptions, the evaluated K factors may be inaccurate when the assumptions are violated. Bridge and Fraster (1977) presented a modified G -factor method to improve the effectiveness of the alignment chart method. Duan and Chen (1988, 1989) proposed a procedure to evaluate the K factors of compressive members in both braced and

unbraced frames, in which the far ends of the columns above and below are not necessarily continuous but can either be hinged or fixed.

The alignment chart method takes into account the rotational restraints by upper and lower assemblages but it neglects the interaction of lateral stiffness among the columns in the same storey resisting lateral sway buckling of unbraced frames. In contrast to the alignment chart method, the concept of storey-based buckling introduced by Yura (1971) acknowledged that sidesway buckling of unbraced frames is a total storey phenomenon, and a single individual column cannot fail by sidesway without all the columns in the same storey also buckling in the same sway mode. LeMessurier (1977) presented a method of evaluating the K factor based on the concept of the storey-based buckling, which accounts for the lateral restraining effect among columns in the same storey, i.e., the stronger columns brace the weaker columns until sidesway buckling of the storey occurs. LeMessurier's method requires using the alignment charts and involves an iterative procedure. Compared with the alignment charts method, LeMessurier's method provided a more accurate estimation of effective length factor. Lui (1992) proposed a simplified method that accounts for both the member stability ($P-\delta$) and the frame stability ($P-\Delta$) in the calculation of the effective length factor. The method involves a first-order frame analysis without the need for special charts or iterative procedures required. The concept of storey-based buckling was adopted by the LRFD specification (AISC, 2005) because the destabilizing effects of lean-on column in a frame were not considered in the alignment charts method.

In the determination of the effective length factor for columns in semi-rigid frames, Chen and Lui (1991) modified the values of the moment of inertia of the restraining beams while using the alignment chart method in order to incorporate connection flexibility. The modification factors were derived for both the braced and unbraced frames based on the assumption that the beam-to-column connection stiffness at both ends are identical. These modification factors were developed to consider the different values of connection stiffness at the ends of the beam (Bjorhovde, 1984; Chen et al., 1996; Christopher and Bjorhoved, 1999). However, the modification factors were based on the rotational conditions at the ends of the beam. Based on the adoption of the concept end-fixity factor, Xu (1994) derived a comprehensive expression for the modification factors regardless of the rotational conditions at each end of a beam for braced and unbraced frames. Kishi et al., (1997) presented a study of evaluating the effective length factor for columns in semi-rigid unbraced frames

using a sub assemblage model with two columns and then comparing the results with those of the alignment chart method. Also investigated in this study was the nonlinear behaviour of the semi-rigid connection on the effective length factor. Shanmugan and Chen (1995) presented an assessment of K factors of columns within frames of different geometry based on four methods, including the alignment charts, LeMessurier's formula, Lui's formula and the system buckling method. The study concluded that Lui's method is the most appropriate for general use in design practice.

Roddis et al. (1998) presented a parametric study based on variations of bay-width, moment of inertia of columns, loading, and column height for a 2-bay by 3-storey frame. This study demonstrated that the approach of evaluating effective length factors based on the concept of storey-based buckling yielded more accurate results and, therefore, is recommended for general use. The foregoing storey-based buckling method often requires using either a first order elastic analysis or the alignment chart while evaluating the storey-based effective length factor; as a result, an efficient storey-based buckling method was proposed by Xu (2001) and Xu and Liu (2002). This improved method was based on the single-storey frame mode that required neither a conducting frame analysis nor using the alignment chart.

2.2.2 Initial Geometric Imperfections

In stability design and analysis of framed structures, one must allow for a frame's initial imperfections and it is imperative to account for the effects of out-of-plumbness of framing and out-of-straightness of columns. In steel structure analysis and design, member out-of-straightness has been closely examined and its effects included in column strength curves. The inclusion of geometric imperfections in the design procedure for frames is much more complex. Eurocode 3 (1996) recommends that frame imperfections be included in the elastic global analysis of the frame. Although the influence of the number of columns in a plane and the number of stories is considered, only limited guidance is given with respect to the shape and distribution of imperfections.

AS4100-1900 (SA, 1990) and the CAN/CSA-S16.1-2000 (CSA, 2000) include the effect of frame imperfections through the use of an equivalent notional lateral load, a procedure also allowed in Eurocode 3 (CEN, 1992). In the study of Clarke et al. (1992), an advanced analysis based on the finite element method accounted for the effects of geometrical imperfection and this study found that for

the simple sway portal frame, the out-of-plumbness imperfections reduced frame strength to a greater extent than the member out-of-straightness imperfections. A comprehensive review of geometric imperfections included in design specifications around the world can be found in the SSRC World View document (SSRC, 1996). In this book, the geometric imperfections are defined as the combination of member out-of-straightness and frame out-of-plumbness. These initial geometric imperfections are the basic limits specified by AISC as member out-of-straightness equal to $L/1000$, where L is the member length brace or framing points, and a frame out-of-plumbness equal to $H/500$, where H is the storey height (AISC, 2005). It is indicated from this book, with the absence of a reliable database of measured frame imperfections, the maximum erection tolerances be used as the basis of frame stability checks in design, while the individual storey instabilities should be checked using the maximum out-of-plumbness tolerance.

2.2.3 Notional Load Approach

For decades, structural engineers have been exploring various approaches for assessing column and frame stability in the design of steel building structures for decades. The approaches for considering column stability in the design of steel frames vary widely between different codes and specifications throughout the world. Current AISI (2004), AISC (2005) and RMI (2000) Specifications use the effective length approach for assessing frame stability. An alternative approach, which is called the notional load approach is to use the actual column length (i.e., $K=1$) in conjunction with “notional” lateral loads acting at each storey level and a second-order elastic analysis is then conducted on the geometrically perfect structures. The notional load approach, also termed the equivalent imperfection approach takes into account the storey out-of-plumbness imperfection under gravity loads and it is widely used in the British Standard BS5950: Part 1 (BSI, 1990), the Australian Standard AS4100-1990 (SA, 1990), the Canadian Standard CAN/CSA-S.16.1-2000 (CSA, 2000) and the Eurocode 3 (CEN, 1992).

A comprehensive discussion of the notional load approach and design procedure can be found in the 1995 Research Report from the University of Sydney (Clarke and Bridge, 1995). In this report, a detailed study of the calibration and verification of the notional load approach for the assessment of frame stability is presented. Compared to the traditional effective length approach, the notional load

approach is an engineering procedure intended to be applied in conjunction with second-order elastic analysis of the geometrically perfect structure.

It is noted that the Direct Analysis Method accounting for geometric imperfections and residual stresses is presented in Appendix 7 of the AISC (2005), in which the specified 0.002 notional load coefficient to account for geometric imperfections is based on an assumed initial storey out-of-plumbness ratio of 1/500. A different notional load can be used if the known or anticipated out-of-plumbness is different, and the imperfections can be modeled explicitly instead of applying notional loads. Therefore, it will be desirable to develop an applicable method of accounting for the effects of the out-of-straightness of column and out-of-plumbness of frame explicitly and independently in the stability analysis for steel buildings and it is one of the objectives of this current research.

2.3 CFS Structure Applications

2.3.1 Analysis and Design of CFS Structures

CFS structures are structural products that are made by forming flat sheets of steel at an ambient temperature into various shapes that can be used to satisfy both structural and functional requirements. The most common structural shapes are cross-section types of CFS members (U, C, Z, L and Hat) shown in Figure 2-1.

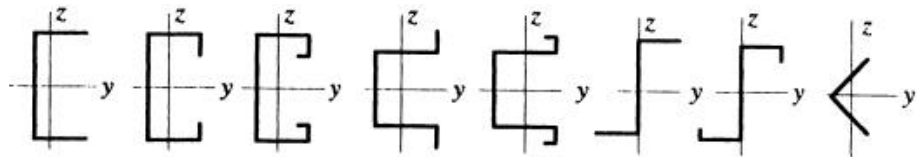


Figure 2-1: Typical cross-section types of CFS members

CFS members used in structural applications for lightweight constructions have many advantages due to its high strength-to-self weight ratio, where they can carry tension, compression, bending forces, and other structural performance benefits. Since 1990, there has been a growing trend to use

CFS sections as the primary structural members in building construction, such as low-to-mid rise residential buildings shown in Figures 2-2 and 2-3.



Figure 2-2: Cold-formed steel framing—Example 1



Figure 2-3: Cold-formed steel framing—Example 2

Consequently, much research has been done to understand the structural behaviour and to develop design procedure. Hancock and his co-workers (Hancock et al., 1985, 2003) conducted extensive research work on the analysis and design of CFS structures (Lau and Hancock, 1987, 1990; Kwon and Hancock, 1992). In his very comprehensive review article of CFS structures, Hancock et al. (2003) reviewed and summarized the significant developments that continue to take place in the design of CFS structural members and connections. He indicated this is to be expected since the growth in the use of CFS has significantly outstripped that for hot-rolled steel structural members, particularly with the increased use in residential construction throughout the world.

Other researchers, like Sivakumaran (1998) proposed a study of a finite element analysis model for the behavior of CFS members subjected to axial compression and concluded the finite element analysis gives accurate and consistent results compared with the test results. The study by Davies (2000) includes developments in CFS section technology, developments in applications, developments in design procedures for cold-formed sections, the application of generalized beam theory (GBT) to buckling problems, current design models and their deficiencies, and design using whole section models.

To assist practicing engineers in CFS design, there are a number of codes of practice (AISI, 1996, 2004; AS/NZ 4600, 1996; CEN, 1996; BS5950, 1998) available in published literature together with complementary design guides and working examples (Rhodes, 1991; Hancock, 1998; Yu, 2000; Schuster, 1975, 2004). Current design standards for CFS members in North America use the *North American Specification for the Design of Cold-Formed Steel Structural Members* published by the American Iron and Steel Institute (AISI, 2004) and the Canadian Standards Association, CAN/CSA-S136S1-04, (CSA, 2004). One distinguished monograph on CFS design is that of the *Direct Strength Method* (DSM) written by Schafer (2006). The DSM is an entirely new design method adopted in 2004 as shown in Appendix 1 of the *North American Specification for the Design of Cold-Formed Steel Structural Members*; this guide provides practical and detailed advice on the use of these new and powerful design methods.

2.3.2 Design of CFS Storage Racks

CFS has many structural applications, and one of them is used for storage systems, such as drive-in and drive-through rack systems, usually called racks, which are widely used throughout the world for storing materials in many distribution facilities. Figures 2-4 and 2-5 are two examples of CFS storage rack systems.



Figure 2-4: Cold-formed steel members used in storage rack systems - Example 1



Figure 2-5: Cold-formed steel members used in storage rack systems - Example 2

CFS rack systems provide high density storage, allowing for the storage for a large amount of products in a small area. In addition, such systems also allow greater accessibility to the stored products and materials. CFS storage racks are composed of CFS structural members that are used as columns, beams and braces. The CFS racks present some peculiar features in their structural analysis and design because of the presence of manufactured perforations into the columns to facilitate assemblage of the rack system, and semi-rigid beam-to-column connections. Much research has been aimed to develop more accurate and efficient analysis and design for CFS storage racks. The research of Peköz and Winter (1973) provided background information on the development of the storage rack design standards proposed by the manufacturers associations, the *Rack Manufacturers Institute* (RMI). The design standards used in the United States is carried out according to the 1997 edition of the Specification published by RMI.

Lewis (1991) studied the stability of storage racks including the effects of the semi-rigid nature of beam-to-column connections and initial imperfections. His study showed how the maximum load of pallet rack system frameworks can be affected by the beam end connector characteristics, and the initial imperfection of the structure. In a study by Olsson et al. (1999), the influence on the load carrying capacity of storage rack columns was investigated. This study showed that even very minor defects in the thin-walled columns could significantly reduce the axial load-carrying capacity and the results showed a correlation with actual damages found in industrial racks and shelving systems. Freitas et al. (2005) presented a study about analysis of steel storage rack columns using commercial finite element software, ANSYS and their study showed that the comparison between code prescriptions (RMI) and finite element results indicated conservative values. Peköz and Rao (2001) summarized a study of design of industrial storage racks that carried out a critical review of the current RMI Specification in his study and the RMI Specification was found to be conservative with regard to strength estimates. Sarawit and Peköz (2006) presented the study of effective length approach and notional load approach for CFS storage racks design. This study recommended that the notional load approach be considered as an alternative means for industrial steel storage racks design.

In the design of CFS storage racks, the specification (RMI, 2000) of the RMI was applied in both the USA and Canada along with the AISI Specification (AISI, 2004). In 2005, the Canadian Standards Association published the first edition of CSA/A344.1-05/A344.2-05, *User guide for steel storage racks/Standard for the design and construction of steel storage racks* (CSA, 2005). The

Federation Europeene De La Manutention (FEM) is the European manufactures association of material handling, lifting and storage equipment. The FEM and the European Federation of Maintenance, in cooperation with RMI, has conducted research standards and development activities for the European Union (EU). FEM published their design code specifications for storage racks with working examples (FEM 10.2.02, 2001), code specification (FEM 10.2.03, 2003) and user code specification (FEM 10.2.04, 2001). These specifications represent the interests of manufacturers of racking, shelving and other storage products through the FEM National Committees of Germany, France, Italy, Great Britain, Sweden, Belgium, Spain and Holland.

In the present, the design of industrial steel storage racks in the United States is based on the effective length method according to the RMI Specification (RMI, 2000). Notional loads are introduced to account for the effect of out-of-plumbness on the stability of a framed structure and the out-of-plumbness effects are assumed to be those that result from an erection tolerance of 0.5 in 10 ft (1:240) stated in Clause 6.2.2 of CSA A344.1 for industrial steel storage racks (CSA, 2005). This corresponds to the maximum fabrication and erection tolerance permitted by the RMI Specification and is roughly twice the value of 1/500 recommended by the AISC Specification used for structural steel buildings (RMI, 2000; AISC, 2005).

Chapter III

Storey Stability of Multi-Storey Unbraced Frames Subjected to Variable Loading

3.1 Introduction

Current design practice concerning stability analysis and design of framed structures is almost exclusively based on the assumption of proportional loading, where the obtained stability capacity of the structure corresponds to a specified load pattern that may not apply to any other load pattern. Therefore, structural engineers have to anticipate the possible load patterns caused by various types of loads that may be encountered during the life span of the building, and this is usually accomplished by investigating different load combinations in accordance with existing design standards, if available. However, the worst load patterns are not always guaranteed by the load combinations specified in the standards or by the engineers due to the unpredictable nature of varying types of loads. The variability of loads in both magnitudes and locations need to be accounted for when assessing the stability of structures; otherwise, structural damage and public safety may be jeopardized.

In the case of variable loading, the conventional assumption of proportional loading is abandoned where different load patterns may cause the frame to buckle at different levels of critical loads. In contrast to current frame stability analysis involving only proportional loads, the proposed approach in this study permits individual applied loads on the frame to vary independently and it captures the load patterns that cause instability failure of frames at the maximum load levels (the most favorable load pattern) and minimum (the worst load pattern). The proposed approach clearly identifies the stability capacities of frames under the extreme load cases; such critical information is generally not available through current proportional loading stability analysis.

In light of the use of the storey-based buckling concept to characterize the lateral sway buckling of unbraced framed structures, presented in this chapter is an extension of the previous study by Xu

(2002) on the stability of single-storey unbraced frames subjected to variable loading to the multi-storey unbraced frames.

3.2 Lateral Stiffness of an Axially Loaded Semi-Rigid Column

The lateral stiffness of an axially loaded semi-rigid column is schematically illustrated in Figure 3-1. Let $EI_{c,ij}/L_{c,ij}$ be the flexural stiffness of the column axial load, and $R_{l,ij}$ and $R_{u,ij}$ be the rotational restraining stiffness provided by the connected beams at the lower and upper joints, respectively.

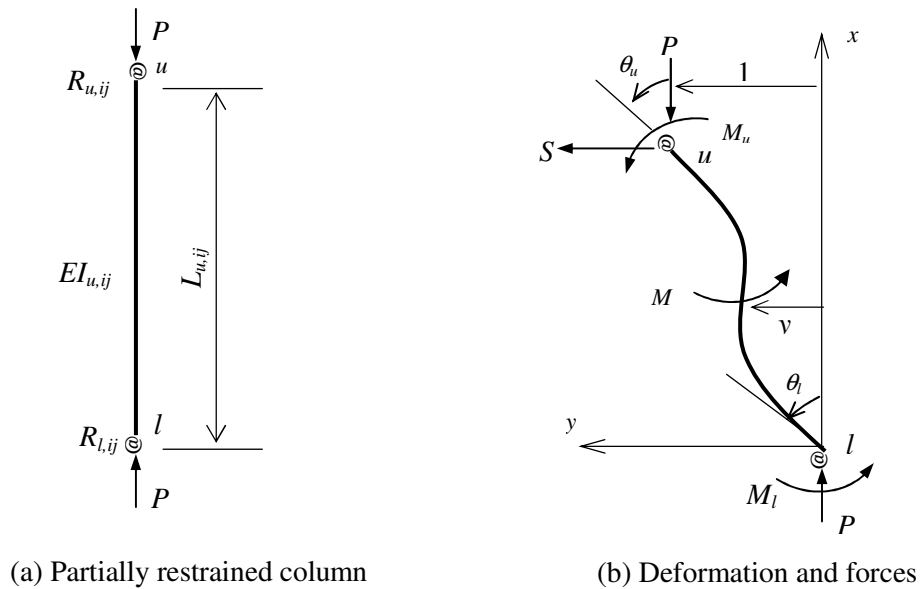


Figure 3-1: Axially loaded column of an unbraced frame with deformations and forces (Xu and Liu, 2002)

The effect of beam-to-column end rotational restraints can be characterized by the end-fixity factors as follows (Monforton and Wu, 1963):

$$r_{l,ij} = \frac{1}{1 + 3EI_{c,ij} / R_{l,ij} L_{c,ij}} ; \quad r_{u,ij} = \frac{1}{1 + 3EI_{c,ij} / R_{u,ij} L_{c,ij}} \quad (3.1a;b)$$

where $r_{l,ij}$ and $r_{u,ij}$ are the end-fixity factors for the upper and lower end of the column, respectively.

The end-fixity factors in Eq. (3.1) define the stiffness of each end connection relative to the attachment member. For flexible, i.e., pinned connections, the rotational stiffness of the connection is idealized as zero; thus, the value of the corresponding end-fixity factor is zero. For fully restrained or so-called rigid connections, the end-fixity factor is unity, because the connection rotational stiffness is taken to be infinite. A semi-rigid connection has an end-fixity factor between zero and unity.

Based on Eq. (3.1), the relationship between the end-fixity factor and the connection stiffness is nonlinear, as shown in Figure 3-2.

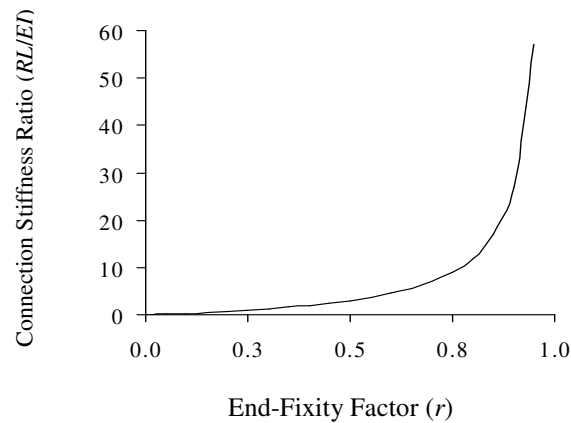


Figure 3-2: Relationship between the end-fixity factor and connection stiffness
(Xu and Liu, 2002)

It can be observed from Figure 3-2 that the relationship between the connection stiffness and the end-fixity factor is almost linear when the connection is relatively flexible with a value of the end-fixity factor between 0.0 and 0.5; then it becomes nonlinear with an end-fixity factor between 0.5 and 1.0. Upon the introduction of the end-fixity factor, different member-end restraint conditions can be readily modeled, such as rigid-pinned, rigid to semi-rigid and pinned to semi-rigid, simply by evaluating the end-fixity factors at the two ends of the member according to Eq. (3.1) with appropriate values of rotational stiffness of end connections.

After the introduction of the end-fixity factors, the lateral stiffness of an axially loaded column of an unbraced frame can be expressed as (Xu and Liu, 2002)

$$S_{ij} = \beta_{ij}(\phi_{ij}, r_{l,ij}, r_{u,ij}) \frac{12EI_{c,ij}}{L_{c,ij}^3} \quad (3.2)$$

where subscripts i and j are the indices of storey and column, respectively; E is Young's modulus and $I_{c,ij}$ and $L_{c,ij}$ are the moment of inertia and the length of column, respectively. ϕ_{ij} is the applied load ratio and defined as

$$\phi_{ij} = \sqrt{\frac{PL_{ij}^2}{EI_{c,ij}}} = \pi \sqrt{P_{ij} / P_{e,ij}} \quad (3.3)$$

in which P_{ij} is the column axial load and $P_{e,ij}$ is the Euler buckling load for the column with pinned connections.

$\beta_{ij}(\phi_{ij}, r_{l,ij}, r_{u,ij})$ in Eq. (3.2) is the modification factor of the lateral stiffness that takes into account the effects of both axial force and column end rotational restraints. A zero value of $\beta_{ij}(\phi_{ij}, r_{l,ij}, r_{u,ij})$ indicates the column has completely lost its lateral stiffness and lateral buckling of the column is about to occur. A column with a negative value of $\beta_{ij}(\phi_{ij}, r_{l,ij}, r_{u,ij})$ signifies that the column relies upon the lateral restraint provided by other columns in the same storey in order to maintain the axial load. A column with a positive value of $\beta_{ij}(\phi_{ij}, r_{l,ij}, r_{u,ij})$ indicates that the column can provide lateral support to other columns to sustain the stability of the storey.

The modification factor $\beta_{ij}(\phi_{ij}, r_{l,ij}, r_{u,ij})$ in terms of the end-fixity factors can be expressed as (Xu, 2003)

$$\beta_{ij}(\phi_{ij}, r_{l,ij}, r_{u,ij}) = \frac{\phi_{ij}^3}{12} \left[\frac{a_1 \phi_{ij} \cos \phi_{ij} + a_2 \sin \phi_{ij}}{18r_{l,ij}r_{u,ij} - a_3 \cos \phi_{ij} + a_4 \phi_{ij} \sin \phi_{ij}} \right] \quad (3.4)$$

where

$$a_1 = 3[r_{l,ij}(1 - r_{u,ij}) + r_{u,ij}(1 - r_{l,ij})] \quad (3.5a)$$

$$a_2 = 9r_{l,ij}r_{u,ij} - (1 - r_{l,ij})(1 - r_{u,ij})\phi_{ij}^2 \quad (3.5b)$$

$$a_3 = 18r_{l,ij}r_{u,ij} + [3r_{l,ij}(1 - r_{u,ij}) + 3r_{u,ij}(1 - r_{l,ij})]\phi_{ij}^2 \quad (3.5c)$$

$$a_4 = -9r_{l,ij}r_{u,ij} + 3r_{l,ij}(1 - r_{u,ij}) + 3r_{u,ij}(1 - r_{l,ij}) + (1 - r_{u,ij})(1 - r_{l,ij})\phi_{ij}^2 \quad (3.5d)$$

In the case that the axial force $P_{ij} \rightarrow 0$, which leads to $\phi_{ij} \rightarrow 0$, the modification factor of the lateral stiffness is reduced to the result of the first-order analysis in which only the end rotational effect has been taken into account as

$$\beta_{0,ij}(r_{l,ij}, r_{u,ij}) = \lim_{\phi_{ij} \rightarrow 0} \beta_{ij}(\phi_{ij}, r_{l,ij}, r_{u,ij}) = \frac{(r_{l,ij} + r_{u,ij} + r_{l,ij}r_{u,ij})}{4 - r_{l,ij}r_{u,ij}} \quad (3.6)$$

3.3 Storey-Based Stability Equation

The lateral stability of single-storey unbraced frames subjected to variable loading was first investigated by (Xu et al., 2001; Xu, 2002). Based on the concept of storey-based buckling, the problem of determining the elastic buckling loads of the frames under non-proportional loading is expressed as a pair of maximization and minimization problems with stability constraints. The study revealed that in the case of variable loading, the difference between the maximum and minimum elastic buckling loads associated lateral instability of the single-storey unbraced frames can be as high as 20% in some cases. When the beam-to-column connections are considered either as purely pinned or fully rigid in the study, further investigation was carried out on the single-storey unbraced semi-rigid frames (Xu, 2002). It was discovered that the difference between the maximum and minimum buckling loads is insignificant for frames whose connection rigidities are approximately the same and evenly distributed among the columns and beams. However, the difference can still be substantial in some cases with lean-on columns, but it is not as significant as in the case where connections are simplified as ideally pinned or fully rigid.

Considering elastic buckling of multi-storey unbraced frames, the concept of storey-based buckling indicates that lateral sway instability of an unbraced frame is a storey phenomenon involving the interaction of lateral stiffness among columns in the same storey. This means that the columns with a larger stiffness are able to provide lateral support for the weaker columns in the same storey to resist the lateral sway instability while the columns with a smaller stiffness depend on such lateral support to maintain the lateral stability. Therefore, the condition for multi-column storey-based buckling in a lateral sway mode is the sum of the lateral stiffness of the storey reduced to zero.

Based on Eq. (3.2), the stability equation of a single-storey semi-rigid frame buckling in a lateral sway mode is given by (Xu and Liu, 2002; Liu and Xu, 2005)

$$S_i = \sum_{j=1}^m S_{ij} = \sum_{j=1}^m \beta_{ij}(\phi_{ij}, r_{l,ij}, r_{u,ij}) \frac{12EI_{c,ij}}{L_{c,ij}^3} = 0 \quad (3.7)$$

where i is the i th storey and m is the number of the columns in i th storey.

For the multi-storey frame shown in Figure 3-3, once the lateral stiffness of any one storey vanishes, the frame becomes laterally unstable.

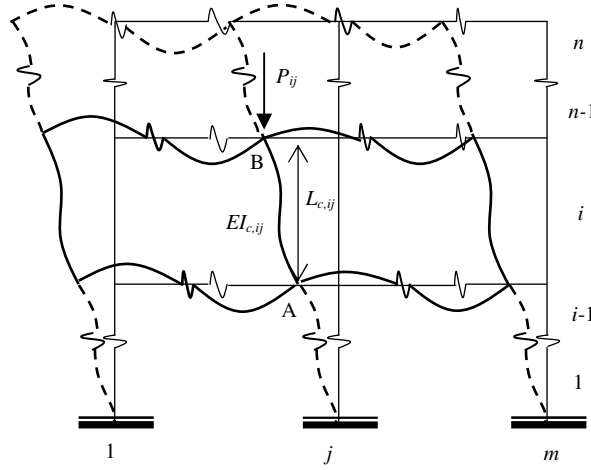


Figure 3-3: (m-1)-bay by n-storey unbraced frame

Therefore, the lateral instability of a multi-storey frame can be defined as a case with at least one storey of the frame, say storey k having its lateral stiffness vanished, that is S_k becomes zero. Based on Eq. (3.7), the lateral stability equation for unbraced multi-storey frames is given by

$$\prod_{i=1}^n S_i = \prod_{i=1}^n \left(\sum_{j=1}^m \beta_{ij}(\phi_{ij}, r_{l,ij}, r_{u,ij}) \frac{12EI_{c,ij}}{L_{c,ij}^3} \right) = 0 \quad (3.8)$$

This equation implies that if any one of the stories fails to maintain its lateral stability, storey-based buckling of an unbraced multi-storey frame will occur. It is impractical to evaluate a column buckling load in multi-column frames directly from Eq. (3.4) due to the transcendental relationship of $\beta_{ij}(\phi_{ij}, r_{l,ij}, r_{u,ij})$ and ϕ_{ij} . Applying the 2nd-order Taylor series expansion, Eq. (3.4) for a column j in the i th floor of a multi-storey frame is simplified as follows (Xu and Liu, 2002)

$$\beta_{ij}(\phi_{ij}, r_{l,ij}, r_{u,ij}) = \beta_{0,ij}(r_{l,ij}, r_{u,ij}) - \beta_{1,ij}(r_{l,ij}, r_{u,ij})\phi_{ij}^2 - \beta_{2,ij}(r_{l,ij}, r_{u,ij})\phi_{ij}^4 \quad (3.9)$$

where $\beta_{0,ij}$, $\beta_{1,ij}$ and $\beta_{2,ij}$ are given by

$$\beta_{0,ij}(r_{l,ij}, r_{u,ij}) = \frac{r_{l,ij} + r_{u,ij} + r_{l,ij}r_{u,ij}}{4 - r_{l,ij}r_{u,ij}} \quad (3.10a)$$

$$\beta_{1,ij}(r_{l,ij}, r_{u,ij}) = \frac{8(5 + r_{u,ij}^2) - (34 - r_{u,ij})r_{u,ij}r_{l,ij} + (8 + r_{u,ij} + 3r_{u,ij}^2)r_{l,ij}^2}{30(4 - r_{l,ij}r_{u,ij})^2} \quad (3.10b)$$

$$\beta_{2,ij}(r_{l,ij}, r_{u,ij}) = \frac{g_0 + g_1r_{l,ij} + g_2r_{l,ij}^2 + g_3r_{l,ij}^3}{25200(4 - r_{l,ij}r_{u,ij})^2} \quad (3.10c)$$

where

$$g_{0,ij} = 2560r_{u,ij}^2 - 1792r_{u,ij}^3 \quad (3.11a)$$

$$g_{1,ij} = -4960r_{u,ij} + 1844r_{u,ij}^2 - 1792r_{u,ij}^3 \quad (3.11b)$$

$$g_{2,ij} = 2560 + 1844r_{u,ij} - 1492r_{u,ij}^2 - 41r_{u,ij}^3 \quad (3.11c)$$

$$g_{3,ij} = -1792 + 704r_{u,ij} - 41r_{u,ij}^2 - 17r_{u,ij}^3 \quad (3.11d)$$

From previous research investigated by Xu and Liu (2002), the 1st-order Taylor approximation yields satisfactory results and it is recommended for use in practice due to the simplicity of the method. Therefore, substituting Eqs. (3.10a) and (3.10b) into Eq. (3.7), the lateral stiffness of column ij becomes

$$S_{ij} = 12 \left(\frac{EI_{c,ij}}{L_{c,ij}^3} \beta_{0,ij}(r_{l,ij}, r_{u,ij}) - \frac{P_{ij}}{L_{c,ij}} \beta_{1,ij}(r_{l,ij}, r_{u,ij}) \right) \quad (3.12)$$

where $L_{c,ij}$ and P_{ij} are the length and applied axial load of column j in the i th storey, respectively.

3.4 Decomposition of Multi-Storey Frames

Equation (3.8) defines the stability condition for multi-storey unbraced frames based on the concept of storey-based buckling. However, even with the simplification of column lateral stiffness as shown in Eq. (3.12), it is difficult for practitioners to facilitate a stability analysis using Eq. (3.8) due to the high-order of nonlinearity. To overcome this difficulty, Liu and Xu (2005) proposed a strategy of decomposing a multi-storey frame into a series of single storey frames.

In the case of a single storey frame, the beam-to-column rotational restraints are directly applied to the upper ends of the connected columns. For a multi-storey frame, floor beams provide rotational restraints for both the lower and upper columns at a joint. Therefore, the appropriate distribution of the beam-to-column rotational-restraining stiffness between the lower and upper columns with consideration of the effects of axial load on column end rotational stiffness is the key issue to be resolved in the decomposition process.

Figure 3-4 illustrates a deformed profile of the single storey model decomposed from a typical storey of the multi-storey frame shown in Figure 3-3.

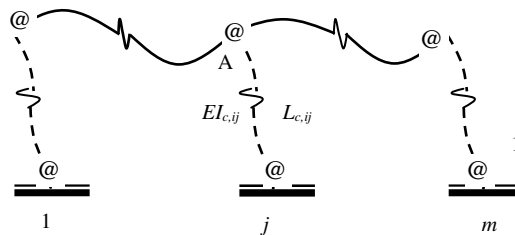


Figure 3-4: Decomposed single storey model

In determining the distribution factor of the beam-to-column rotational-restraint stiffness, three approaches are proposed by Liu and Xu (2005). The first approach referred to as the geometrical stiffness distribution (GSD) is a method of accounting for the effect of the column axial force on column end rotational stiffness. The second approach, named frame-based stiffness distribution (FSD), is basically the same as the GSD except the effects of axial loads are neglected. The third approach is defined as column-based stiffness distribution (CSD), which is similar to that of the FSD approach except that the rotational stiffnesses of the beams at the far end of the column in adjacent stories is taken as infinite.

It is noted that in these three approaches, the GSD or FSD approach requires the end-fixity factor at the far end of the column $r_{l,ij}$ to be known, in which the decomposition process can be conveniently evaluated from the first storey since the end-fixity factors associated with the column bases are known and continued toward to the upper stories. In the case of using the CSD approach, the decomposition process can be initiated from any storey. Between the approaches of GSD and FSD to account for the effects of axial force or not, it is found that in a frame buckling analysis, the critical axial force of each column at the buckling state is unknown in advance, and as the axial force and column end rotational stiffness are interrelated, the numerical iterations are required to obtain the results. As we already know, the iterative process can be quite cumbersome for the engineering practice. From the study of Liu and Xu (2005), it is recommended to initiate the process of evaluating the stiffness distribution factors with either the FSD or CSD approach. In this current study, the column base is known; therefore, the FSD approach is chosen to carry out the following studies. The detailed procedure of applying the FSD approach is presented in Appendix A.

3.5 Stability Analysis for Multi-Storey Unbraced Frames Subjected to Variable Loading

To investigate the stability of unbraced frames under variable loading can be formulated as two problems of seeking the maximum and minimum bounds of buckling loads of the frames. The simplified form of Eqs. (3.4) and (3.9) are adopted for the column stiffness modification factor and consequently, the problem of seeking the maximum frame-buckling loads can be stated as follows:

$$\text{Maximize: } Z = \sum_{i=1}^n \sum_{j=1}^m P_{ij} \quad (3.13a)$$

$$\text{Subject to: } S_k = 12 \sum_{j=1}^m \left(\frac{EI_{kj}}{L_{kj}^3} \beta_{0,ij}(r_{l,ij}, r_{u,ij}) - \frac{\beta_{1,kj}(r_{l,ij}, r_{u,ij})}{L_{kj}} \sum_{i=k}^n P_{ij} \right) \geq 0 \quad (3.13b)$$

$$0 \leq \sum_{i=i}^n P_{ij} \leq P_{u,ij} = \frac{\pi^2 EI_{ij}}{K_{braced,ij}^2 L_{ij}^2} \quad (3.13c)$$

$$(k=1,2\dots n; i=1,2\dots n; j=1,2\dots m)$$

where n is the number of the stories in the frame and m is the number of columns in one storey. P_{ij} is the applied load associated with column ij and is the variable of the maximum problem. Z is the objective function corresponding with either the maximum or the minimum elastic buckling loads of the frame and it is the sum of variable loading P_{ij} .

Equation (3.13b) represents the storey-based stability condition for the k th storey of the frame, in which the column stiffness modification factor $\beta_{0,ij}(r_{l,ij}, r_{u,ij})$ and $\beta_{1,ij}(r_{l,ij}, r_{u,ij})$ are defined in Eq. (3.9). In the case that the lateral stiffness of storey, S_k is greater than zero, the storey is laterally stable; otherwise, the storey becomes laterally unstable if $S_k=0$. Equation (3.13c) is a side constraint for each applied column load, which is to be less than an associated upper bound load. The upper bound, $\pi^2 EI_{c,ij} / K_{braced,ij}^2 L_{c,ij}^2$, is imposed to ensure that the magnitude of the applied load will not exceed the buckling load associated with non-sway buckling of the individual column. The factor $K_{braced,ij}$ is the effective length factor of the column associated with non-sway-buckling that is related to the rotational restraints of the column ends. In this study, $K_{braced,ij}$ is evaluated as the following (Newmark, 1949),

$$K_{braced,ij}^2 = \frac{(2 + \pi^2 R_{u,ij} L_{ij} / EI_{ij}) \times (2 + \pi^2 R_{l,ij} L_{ij} / EI_i)}{(4 + \pi^2 R_{u,ij} L_{ij} / EI_{ij}) \times (4 + \pi^2 R_{l,ij} L_{ij} / EI_{ij})} \quad (3.14)$$

where $R_{l,ij}$ and $R_{u,ij}$ are the rotational restraining stiffnesses provided by the beams connected at the lower and upper ends of the column, respectively, and $EI_{c,ij}/L_{c,ij}$ is the flexural stiffness of the column. Expressed in terms of the end-fixity factors defined in Eq. (3.1), Eq. (3.14) becomes

$$K_{braced,ij}^2 = \frac{[(\pi^2 + (6 - \pi^2)r_{u,ij}) \times (\pi^2 + (6 - \pi^2)r_{l,ij})]}{[\pi^2 + (12 - \pi^2)r_{u,ij}] \times [\pi^2 + (12 - \pi^2)r_{l,ij}]} \quad (3.15)$$

The problem of seeking the minimum frame-buckling loads of a multi-storey unbraced frame subjected to variable loading can be stated as: (Xu and Wang, 2007)

$$\text{Minimum } Z = \min \left\{ Z_l = \sum_{i=1}^n \sum_{j=1}^m P_{ij} \mid l = 1, 2, 3 \dots n \right\} \quad (3.16)$$

where n is the number of stories in the frame and m is the number of columns in one storey. Z_l ($l = 1, 2, 3 \dots n$) is obtained from the minimization problem as follows,

$$\text{Minimize: } Z_l = \sum_{i=1}^n \sum_{j=1}^m P_{ij} \quad (3.17a)$$

$$\text{Subject to: } S_l = 12 \sum_{j=1}^m \left(\frac{EI_{lj}}{L_{lj}^3} \beta_{0,ij}(r_{l,ij}, r_{u,ij}) - \frac{\beta_{1,lj}(r_{l,ij}, r_{u,ij})}{L_{lj}} \sum_{i=l}^n P_{ij} \right) = 0 \quad (3.17b)$$

$$S_k = 12 \sum_{j=1}^m \left(\frac{EI_{kj}}{L_{kj}^3} \beta_{0,ij}(r_{l,ij}, r_{u,ij}) - \frac{\beta_{1,kj}(r_{l,ij}, r_{u,ij})}{L_{kj}} \sum_{i=k}^n P_{ij} \right) > 0 \quad (3.17c)$$

$$0 \leq \sum_{i=i}^n P_{ij} \leq P_{u,ij} = \frac{\pi^2 EI_{ij}}{K_{braced,ij}^2 L_{ij}^2} \quad (3.17d)$$

$$(k = 1, 2, \dots, n; k \neq l; i = 1, 2, \dots, n; j = 1, 2, \dots, m)$$

It is noticed that both the formulation and procedure of seeking the minimum frame-buckling load are different from those of the maximum frame-buckling loads. First, an equality constraint, Eq. (3.17b), is imposed in the minimization problem to ensure that the minimum value of the loads obtained from Eq.(3.17b) will result in lateral instability at least in one storey, say storey l in this case. Second, the minimization problem shown in Eq.(3.17a) needs to be solved by n times with $l = 1, 2, 3, \dots, n$, and the minimum frame-buckling load obtained from Eq.(3.16) is the minimum of the minimum frame-buckling loads associated with the instability of each storey (Xu and Wang, 2007).

It should be noticed that Eqs. (3.13) and (3.17) are linear programming problems. Thus, the maximum or minimum frame-buckling loads under variable loading can be solved with the use of a linear programming algorithm such as the simplex method, which will be demonstrated in the next section with an numerical example.

3.6 Numerical Example

A numerical example is presented in this section to demonstrate the validity and efficiency of the foregoing proposed method for stability analysis of multi-storey unbraced steel frames subjected to variable loading. This example is a 2-bay by 2-storey steel frame which is a bench mark case for stability analysis and has been investigated by different researchers to validate different analytical methods (Lui, 1992; Liu and Xu, 2005). To investigate the effects of a semi-rigid connection behaviour on the frame stability, especially on the maximum or minimum frame-buckling loads under

variable loading, cases with different values of end-fixity factor for beam-to-column and column base connections in this example is being studied in this research.

The 2-bay by 2-storey frames with five different beam-to-column and column base connections as shown in Figures 3-5 to 3-8 are investigated to illustrate the influence of the different connections on the maximum and minimum buckling loads of frames and associated variable load patterns.

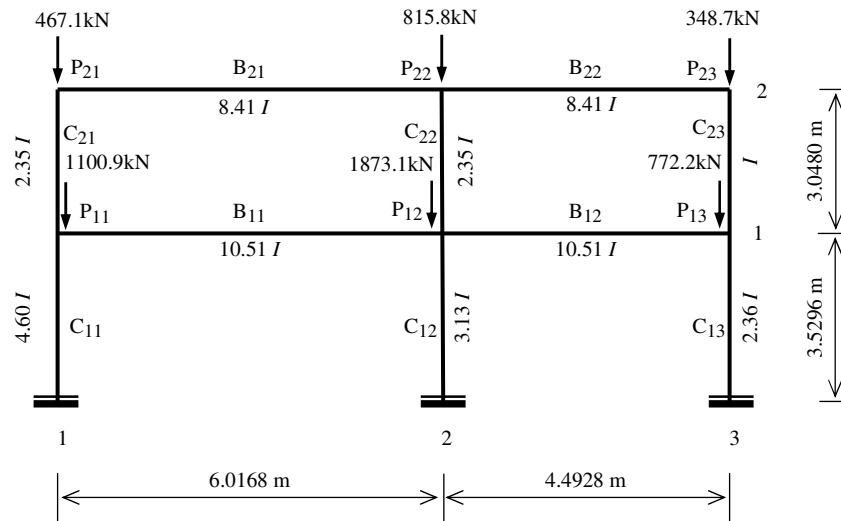


Figure 3-5: 2-bay by 2-storey steel frame – Case 1

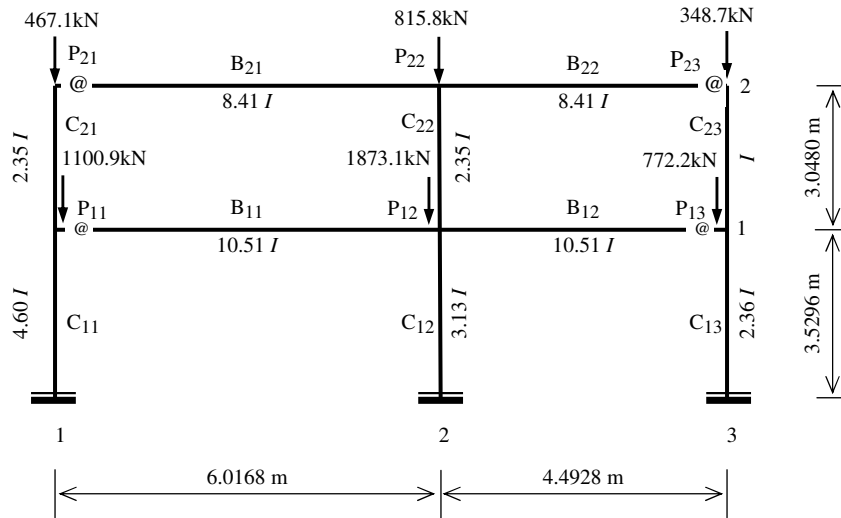


Figure 3-6: 2-bay by 2-storey steel frame – Case 2

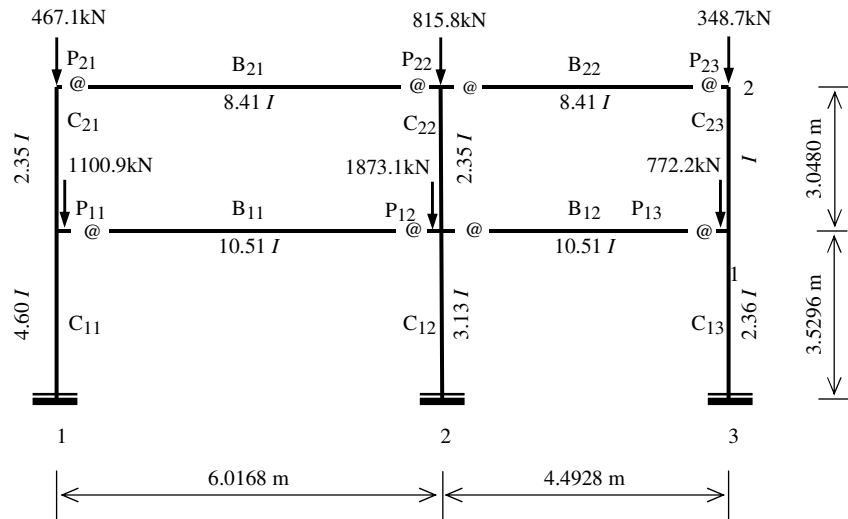


Figure 3-7: 2-bay by 2-storey steel frame – Cases 3 and 5

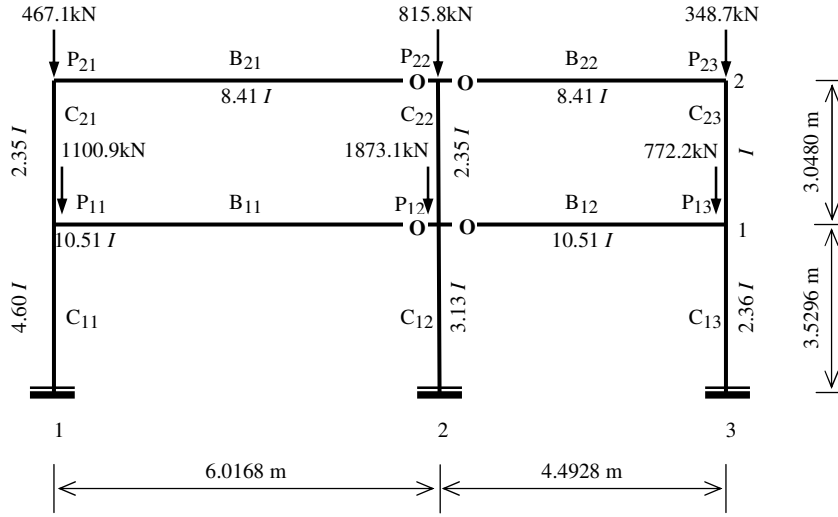


Figure 3-8: 2-bay by 2-storey steel frame – Case 4

Based on Eq.(3.13b), the maximum buckling loads for the 2-bay by 2-storey steel frame shown in Figures 3-5 to 3-9 can be expressed in the following forms: (Xu and Wang, 2007)

$$\text{Maximize: } Z = P_{11} + P_{12} + P_{13} + P_{21} + P_{22} + P_{23} \quad (3.18)$$

Subject to:

$$S_1 = \frac{12EI_{11}}{L_{11}^3} \beta_{0,11} - \frac{12}{L_{11}} \beta_{1,11} (P_{11} + P_{21}) + \frac{12EI_{12}}{L_{12}^3} \beta_{0,12} - \frac{12}{L_{12}} \beta_{1,12} (P_{12} + P_{22}) + \frac{12EI_{13}}{L_{13}^3} \beta_{0,13} - \frac{12}{L_{13}} \beta_{1,13} (P_{13} + P_{23}) > 0 \quad (3.19a)$$

$$S_2 = \frac{12EI_{21}}{L_{21}^3} \beta_{0,21} - \frac{12}{L_{21}} \beta_{1,21} P_{21} + \frac{12EI_{22}}{L_{22}^3} \beta_{0,22} - \frac{12}{L_{22}} \beta_{1,22} P_{22} + \frac{12EI_{23}}{L_{23}^3} \beta_{0,23} - \frac{12}{L_{23}} \beta_{1,23} P_{23} > 0 \quad (3.19b)$$

$$0 \leq P_{11} + P_{21} \leq P_{u,11}; 0 \leq P_{12} + P_{22} \leq P_{u,12}; 0 \leq P_{13} + P_{23} \leq P_{u,13}$$

$$0 \leq P_{21} \leq P_{u,21}; 0 \leq P_{22} \leq P_{u,22}; 0 \leq P_{23} \leq P_{u,23} \quad (3.19c)$$

Similarly, based on Eqs. (3.16) and (3.17), the minimum buckling loads for the 2-bay by 2-storey steel frame ($n=2, m=3$) can be obtained from following forms:

$$\text{Minimum } Z = \min \left\{ Z_l = \sum_{i=1}^2 \sum_{j=1}^3 P_{ij} \mid l = 1, 2, 3 \right\} \quad (3.20)$$

$$\text{Minimize: } Z = P_{11} + P_{12} + P_{13} + P_{21} + P_{22} + P_{23} \quad (3.21)$$

Subject to:

$$S_1 = \frac{12EI_{11}}{L_{11}^3} \beta_{0,11} - \frac{12}{L_{11}} \beta_{1,11} (P_{11} + P_{21}) + \frac{12EI_{12}}{L_{12}^3} \beta_{0,12} - \frac{12}{L_{12}} \beta_{1,12} (P_{12} + P_{22}) \\ + \frac{12EI_{13}}{L_{13}^3} \beta_{0,13} - \frac{12}{L_{13}} \beta_{1,13} (P_{13} + P_{23}) = 0 \quad (3.22a)$$

$$S_2 = \frac{12EI_{21}}{L_{21}^3} \beta_{0,21} - \frac{12}{L_{21}} \beta_{1,21} P_{21} + \frac{12EI_{22}}{L_{22}^3} \beta_{0,22} - \frac{12}{L_{22}} \beta_{1,22} P_{22} \\ + \frac{12EI_{23}}{L_{23}^3} \beta_{0,23} - \frac{12}{L_{23}} \beta_{1,23} P_{23} > 0 \quad (3.22b)$$

$$0 \leq P_{11} + P_{21} \leq P_{u,11}; \quad 0 \leq P_{12} + P_{22} \leq P_{u,12}; \quad 0 \leq P_{13} + P_{23} \leq P_{u,13}$$

$$0 \leq P_{21} \leq P_{u,21}; \quad 0 \leq P_{22} \leq P_{u,22}; \quad 0 \leq P_{23} \leq P_{u,23} \quad (3.22c)$$

For the 2-bay by 2-storey steel frames shown in Figures 3-5 to 3-8, the end fixity factors associated with column bases and beam-to-column connections are summarized in Table 3-1.

Table 3-1: 2-bay by 2-storey steel frames with different connections

Case	Column base	Beam-to-column connections	
	Co nnections	Interior column	Exterior column
1	rigid: $r = 1$	rigid: $r = 1$	rigid: $r = 1$
2	rigid: $r = 1$	rigid: $r = 1$	semi-rigid: $r = 0.8$
3	rigid: $r = 1$	semi-rigid: $r = 0.8$	semi-rigid: $r = 0.8$
4	rigid: $r = 1$	pinned: $r = 0$	rigid: $r = 1$
5	rigid: $r = 1$	semi-rigid: $r = 0.2$	semi-rigid: $r = 0.2$

The Young's modulus of steel is $E = 2 \times 10^5$ MPa where the reference moment of inertia for beams and columns is $I = 8.3246 \times 10^7 \text{ mm}^4$. The dimensions of frames and the moment of inertia of each member are shown in Figures 3-5 to 3-8. The detailed process of evaluating stiffness distribution

factors, beam-to-column rotational-stiffness, end-fixity factors and column stiffness modification factors for unbraced multi-storey frames are presented in Appendix A.

Following the procedures described in the previous section, the maximum and minimum frame-buckling loads associated with the two-storey and two-bay unbraced steel frames subjected to variable loading can be obtained from solving the maximization and minimization problems stated in Eqs. (3.18) to (3.20). For the foregoing five cases in Table 3-1, the values of the coefficients including the end-fixity factors, the effective length factor and the buckling loads associated with non-sway buckling corresponding with the maximum and minimum frame-buckling loads, together with their relative differences, are presented in Tables 3-2 to 3-6. Also presented in the Tables are the column elastic flexural stiffness $12EI_{ij}\beta_{0,ij}/L_{ij}^3$ and the coefficients associated with column lateral stiffness modification factors $\beta_{1,ij}(r_{l,ij}, r_{u,ij})$. New results for a frame subjected to proportional loading are also obtained in this study and the results are presented in Tables 3-2 to 3-6. The load patterns associated with the maximum and minimum frame-buckling loads are illustrated in Figures 3-9 to 3-13.

In case of proportional loading, the pattern of applied loads on the frame is given and the loads can be evaluated using the following equation

$$P = \sum_{i=1}^n \sum_{j=1}^m P_{ij} \quad (3.23)$$

in which,

$$P_{ij} = \lambda_{cr} P_{a,ij} \quad (3.24)$$

where $P_{a,ij}$ is the applied load of an individual column which is shown in the Figures 3-4 to 3-8 and λ_{cr} is the critical load multiplier associated with the multi-storey frame and is defined in the following equation (Liu and Xu, 2005)

$$\lambda_{cr} = \min\{\lambda_{1cr}, \lambda_{2cr}, \lambda_{3cr} \dots \lambda_{ncr}\} \quad (i=1,2,3 \dots n) \quad (3.25)$$

where

$$\lambda_{icr} = \sum_{j=1}^m \frac{EI_{c,ij} \beta_{0,ij}}{L_{c,ij}^3} / \sum_{j=1}^m \frac{P_{a,ij} \beta_{1,ij}}{L_{c,ij}} \quad (3.26)$$

The detailed studies for obtaining the critical load multiplier λ_{cr} can be referred in Chapter 4.

Table 3-2: Results of the unbraced steel frames shown in Figure 3-5 – Case 1

Col. <i>ij</i>	$r_{l,ij}$	$r_{u,ij}$	$\frac{12EI_{ij}}{L_{ij}^3} \beta_{0,ij}$ (kN/m)	$\beta_{1,ij}$	K_{braced}	$P_{u,ij}$ (kN)	Max. (kN)	Min. (kN)	
								$S_1 = 0$ $S_2 > 0$	$S_2 = 0$ $S_1 > 0$
11	1.000	0.635	14100.000	0.094	0.575	183700.000	32995.120	0.000	0.000
12	1.000	0.834	11980.000	0.096	0.534	144700.000	0.000	34205.970	0.000
13	1.000	0.826	8956.000	0.096	0.536	108500.000	0.000	0.000	0.000
21	0.614	0.784	8854.000	0.089	0.630	106200.000	76848.140	0.000	0.000
22	0.828	0.895	12530.000	0.093	0.558	133900.000	0.000	73278.69	15394.100
23	0.822	0.919	5431.000	0.093	0.554	57570.000	0.000	0.000	57570.000
Critical frame buckling loads $\sum P_{ij} =$							109843.260	107484.660 ($S_2=0.000$)	72964.100 ($S_1=11311.300$)
Difference of max. & min. frame-buckling loads (%)							$\frac{\max - \min}{\min} \%$	2.2%	50.5%
Proportional loading: $P_p = \lambda_{cr} \sum P_{a,ij}$ (kN)							P_p	108200.000	
Difference of proportional loading & max. frame-buckling loads (%)							$\frac{\max - P_p}{\min} \%$	0.7%	
Difference of proportional loading & min. frame-buckling loads (%)							$\frac{P_p - \min}{\min} \%$	48.3%	

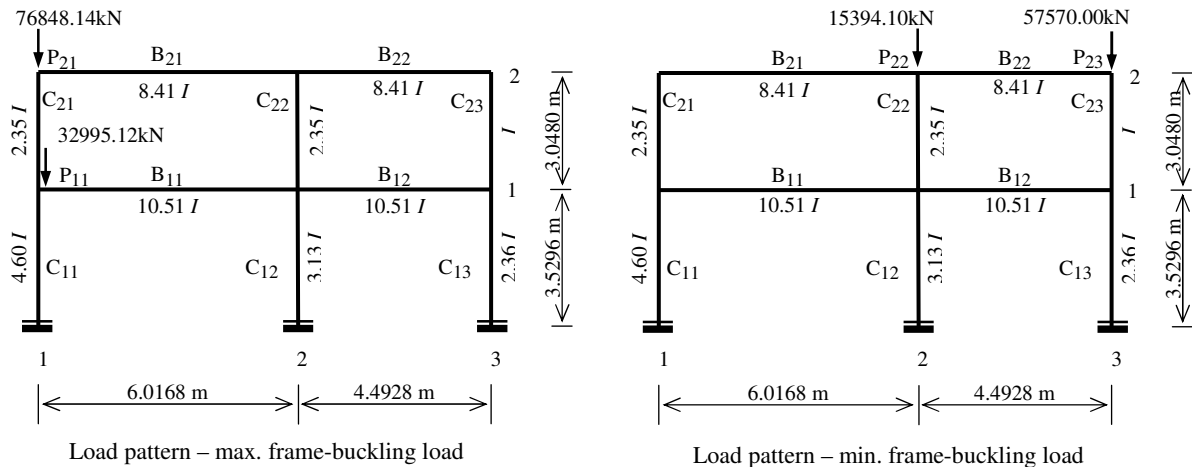


Figure 3-9: Load patterns associated with max. and min. frame-buckling loads – Case 1

Table 3-3: Results of the unbraced steel frames shown in Figure 3-6 – Case 2

Col. <i>ij</i>	$r_{l,ij}$	$r_{u,ij}$	$\frac{12EI_{ij}}{L_{ij}^3} \beta_{0,ij}$ (kN/m)	$\beta_{1,ij}$	K_{braced}	$P_{u,ij}$ (kN)	Max. (kN)	Min. (kN)	
								$S_1 = 0$ $S_2 > 0$	$S_2 = 0$ $S_1 > 0$
11	1.000	0.568	13010.00	0.094	0.588	175300.000	35951.570	0.000	0.000
12	1.000	0.815	11740.000	0.096	0.538	142700.000	0.000	37237.400	0.000
13	1.000	0.781	8534.000	0.095	0.545	104900.000	0.000	0.000	0.000
21	0.484	0.731	7136.000	0.088	0.672	91970.000	68405.800	0.000	0.000
22	0.771	0.881	11650.000	0.092	0.573	126400.000	0.000	65193.370	65193.370
23	0.733	0.895	4821.000	0.092	0.578	52860.000	0.000	0.000	0.000
Critical frame buckling loads $\sum P_{ij} =$							104357.370	102430.770 ($S_2=0.000$)	65193.370 ($S_1=12102.200$)
Difference of max. & min. frame-buckling loads (%)							$\frac{\max - \min}{\min} \%$	1.9%	60.1%
Proportional loading: $P_p = \lambda_{cr} \sum P_{a,ij}$ (kN)							P_p	103200.000	
Difference of proportional loading & max. frame-buckling loads (%)							$\frac{\max - P_p}{\min} \%$	1.1%	
Difference of proportional loading & min. frame-buckling loads (%)							$\frac{P_p - \min}{\min} \%$	58.3%	

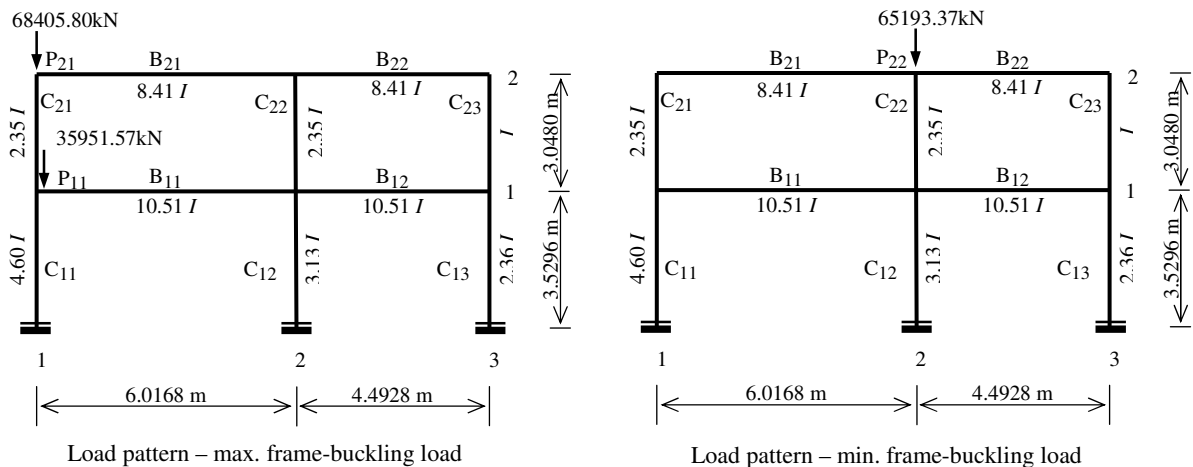


Figure 3-10: Load patterns associated with max. and min. frame-buckling loads – Case 2

Table 3-4: Results of the unbraced steel frames shown in Figure 3-7 – Case 3

Col. <i>ij</i>	$r_{l,ij}$	$r_{u,ij}$	$\frac{12EI_{ij}}{L_{ij}^3} \beta_{0,ij}$ (kN/m)	$\beta_{1,ij}$	K_{braced}	$P_{u,ij}$ (kN)	Max. (kN)	Min. (kN)	
								$S_1 = 0$ $S_2 > 0$	$S_2 = 0$ $S_1 > 0$
11	1.000	0.540	12570.000	0.094	0.594	171900.000	36634.980	0.000	0.000
12	1.000	0.771	11200.000	0.095	0.547	138100.000	0.000	37899.160	0.000
13	1.000	0.760	8343.000	0.095	0.549	103300.000	0.000	0.000	0.000
21	0.453	0.707	6669.000	0.087	0.685	93930.000	64023.320	0.000	0.000
22	0.718	0.850	10660.000	0.091	0.592	123300.000	0.000	61512.610	9764.310
23	0.709	0.884	4640.000	0.091	0.586	53460.000	0.000	0.000	51460.000
Critical frame buckling loads $\sum P_{ij} =$							100658.310	99411.760 ($S_2=0.000$)	61224.310 ($S_1=12386.010$)
Difference of max. & min. frame-buckling loads (%)							$\frac{\max - \min}{\min} \%$	1.3%	64.4%
Proportional loading: $P_p = \lambda_{cr} \sum P_{a,ij}$ (kN)							P_p	99890.000	
Difference of proportional loading & max. frame-buckling loads (%)							$\frac{\max - P_p}{\min} \%$	0.8%	
Difference of proportional loading & min. frame-buckling loads (%)							$\frac{P_p - \min}{\min} \%$	63.2%	

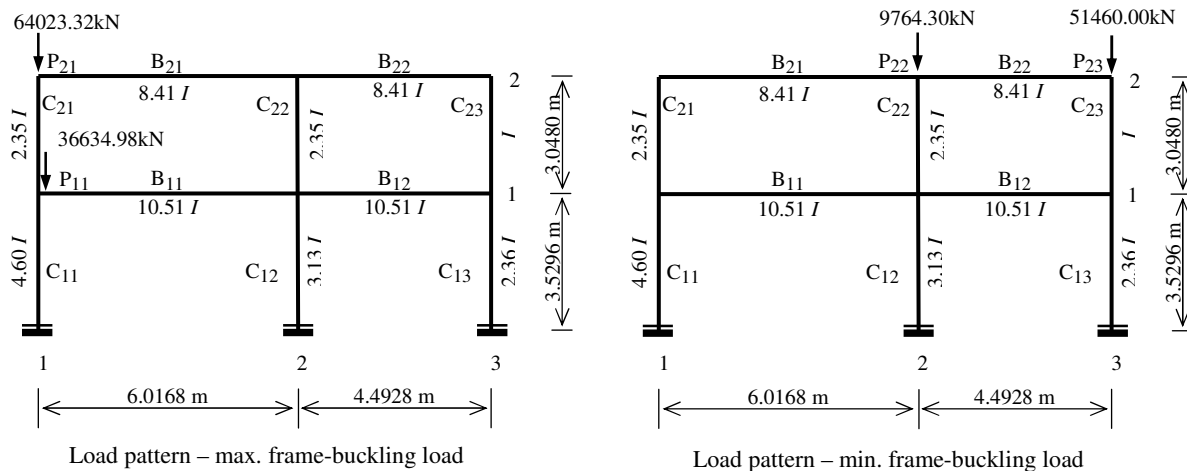


Figure 3-11: Load patterns associated with max. and min. frame-buckling loads – Case 3

Table 3-5: Results of the unbraced steel frames shown in Figure 3-8 – Case 4

Col. <i>ij</i>	$r_{l,ij}$	$r_{u,ij}$	$\frac{12EI_{ij}}{L_{ij}^3} \beta_{0,ij}$ (kN/m)	$\beta_{1,ij}$	K_{braced}	$P_{u,ij}$ (kN)	Max. (kN)	Min. (kN)	
								$S_1 = 0$ $S_2 > 0$	$S_2 = 0$ $S_1 > 0$
11	1.000	0.420	10740.000	0.094	0.573	158400.000	51596.840	0.000	0.000
12	1.000	0.000	3555.000	0.100	0.707	82570.000	0.000	45588.770	0.000
13	1.000	0.705	7843.000	0.095	0.560	97700.000	0.000	0.000	0.000
21	0.377	0.644	5577.000	0.086	0.719	80370.000	28685.290	0.000	0.000
22	0.00	0.000	0.000	0.083	1.000	41570.000	0.000	29734.760	0.000
23	0.644	0.851	4176.000	0.090	0.608	47880.000	0.000	0.000	27473.240
Critical frame buckling loads $\sum P_{ij} =$							80282.130	75323.530 ($S_2=0.000$)	27473.240 ($S_1=16818.560$)
Difference of max. & min. frame-buckling loads (%)							$\frac{\max - \min}{\min} \%$	6.5%	192.2%
Proportional loading: $P_p = \lambda_{cr} \sum P_{a,ij}$ (kN)							P_p	77650.000	
Difference of proportional loading & max. frame-buckling loads (%)							$\frac{\max - P_p}{\min} \%$	3.1%	
Difference of proportional loading & min. frame-buckling loads (%)							$\frac{P_p - \min}{\min} \%$	182.6%	

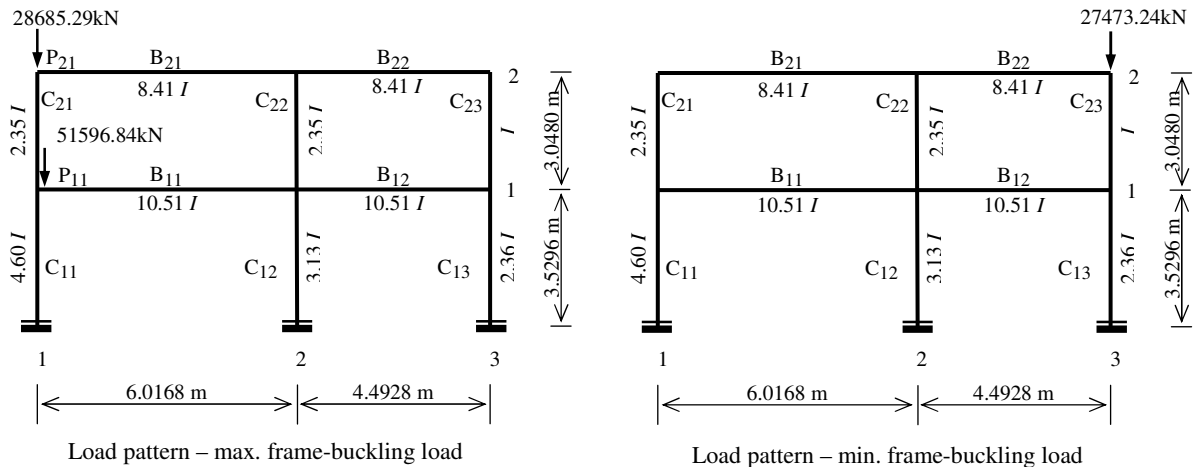


Figure 3-12: Load patterns associated with max. and min. frame-buckling loads – Case 4

Table 3-6: Results of the unbraced steel frames shown in Figure 3-7 – Case 5

Col. ij	$r_{l,ij}$	$r_{u,ij}$	$\frac{12EI_{ij}}{L_{ij}^3} \beta_{0,ij}$ (kN/m)	$\beta_{1,ij}$	K_{braced}	$P_{u,ij}$ (kN)	Max. (kN)	Min. (kN)	
								$S_1 = 0$ $S_2 > 0$	$S_2 = 0$ $S_1 > 0$
11	1.000	0.184	7489.000	0.097	0.668	136000.000	0.000	37376.260	0.000
12	1.000	0.384	6955.000	0.095	0.626	105300.000	39118.180	0.000	0.000
13	1.000	0.359	5060.000	0.095	0.631	78070.000	0.000	0.000	0.000
21	0.090	0.287	1681.000	0.084	0.889	52560.000	0.000	21894.260	0.000
22	0.269	0.485	3794.000	0.085	0.787	67090.000	0.075	0.000	0.000
23	0.262	0.559	1772.000	0.086	0.769	29890.000	21440.250	0.000	21440.830
Critical frame buckling loads $\sum P_{ij} =$							60559.010	59270.520 ($S_2=0.000$)	21440.830 ($S_1=12596.100$)
Difference of max. & min. frame-buckling loads (%)							$\frac{\text{max} - \text{min}}{\text{min}} \%$	2.2%	182.4%
Proportional loading: $P_p = \lambda_{cr} \sum P_{a,ij}$ (kN)							P_p	60200.000	
Difference of proportional loading & max. frame-buckling loads (%)							$\frac{\text{max} - P_p}{\text{min}} \%$	0.6%	
Difference of proportional loading & min. frame-buckling loads (%)							$\frac{P_p - \text{min}}{\text{min}} \%$	180.8%	

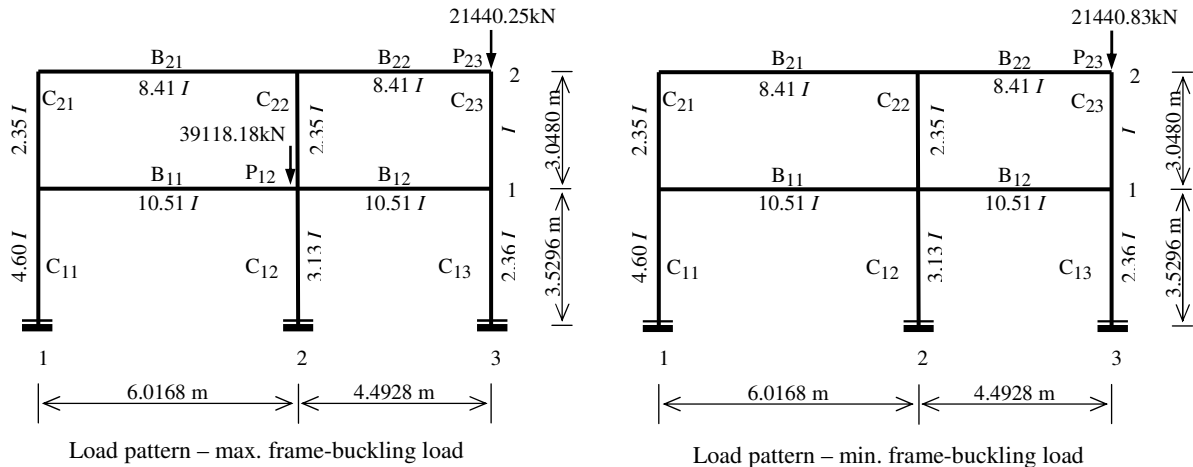


Figure 3-13: Load patterns associated with max. and min. frame-buckling loads – Case 5

For Case 1, in which both the column base and beam-to-column connections are rigidly connected, it is observed from Table 3-2 that the maximum frame-buckling load, 109843.3 kN is achieved when lateral instability takes place in both the first and the second stories of the frame. The minimum storey-buckling loads associated with lateral instability of the first and second stories are 107484.66 kN and 72964.1 kN, respectively. Therefore, the relative difference between the maximum and minimum frame-buckling loads is 50.5%, which is significant. It is also observed from Table 3-2 that the load patterns associated with the minimum frame-buckling loads are different. The load pattern corresponding to the maximum frame-buckling loads tends to place the loads only on exterior columns 11 and 21. In contrast to that, the load pattern associated with the minimum frame-buckling load applies the loading both on the exterior and interior columns.

The load patterns corresponding to the maximum and minimum frame-buckling loads of Case 1 are verified using structural analysis software MASTAN2 (McGuire et al., 2000) and the results are presented in Table 3-7. From Table 3-7, it is found that when the load patterns associated with the maximum and minimum frame-buckling load is applied on the frame, the applied load ratio with respect to the elastic critical load is equal to one which verifies the current study results are correct.

Table 3-7: Results verification of the unbraced steel frames shown in Figure 3-5 – Case 1

Storey	Columns	Current study		
		Max. (kN)	Min. (kN)	
			$S_1 = 0, S_2 > 0$	$S_2 = 0, S_1 > 0$
1	11	32995.120	0.000	0.000
	12	0.000	34205.970	0.000
	13	0.000	0.000	0.000
2	21	76848.140	0.000	0.000
	22	0.000	73278.690	15394.100
	23	0.000	0.000	57570.000
MASTAN2 – Elastic critical load: applied load ratio		1.000	1.000	1.040

In Case 2, the column base and the interior beam-to-column connections are rigid. The exterior column is semi-rigidly connected with the corresponding end-fixity factor being 0.8. The presence of semi-rigid connections yields a flexible frame, which is evidenced by decreasing the magnitudes of the elastic flexural stiffness compared to that of Case 1. Consequently, the maximum frame-buckling load of Case 2 reduces to 104357.4 kN, and the corresponding minimum frame-buckling load decreases to 65193.4 kN, which yields the relative difference between the maximum and minimum frame-buckling loads to be 60.1%, which is significant too. It is also observed that the first and second stories are unstable simultaneously when they are subjected to a maximum frame-buckling load.

For Case 3, the beam-to-column connections for both the interior and exterior columns are semi-rigidly connected with the corresponding end-fixity factor being 0.8. Compared to Cases 1 and 2, the frame of Case 3 is more flexible; thus, the magnitudes of the maximum and minimum frame-buckling loads are reduced to 100658.3 kN and 61224.3 kN, respectively, which leads to a difference of 64.4% between the extreme buckling loads. Like Cases 1 and 2, it is found that lateral instability occurs simultaneously for both first and second stories and the load patterns are identical when they are subjected to the maximum frame-buckling load.

Table 3-5 presents the results of Case 4 and the detailed hand calculation of illustrating the process of evaluating the end-fixity factors and the lateral stiffness modification factors of Case 4 is also presented as an example in Appendix A. In Case 4, the column base uses rigid connections having $r_{l,11} = r_{l,12} = r_{l,13} = 1$. The beam-to-column connections of the exterior columns are rigid and the interior columns are pinned, in which we can get other end-fixity factors associated with the upper and lower ends of the columns (see details in Appendix A) with the values of $r_{u,11} = 0.42$, $r_{u,12} = 0.0$, $r_{u,13} = 0.705$, $r_{l,21} = 0.377$, $r_{l,22} = 0.0$, $r_{l,23} = 0.644$, $r_{u,21} = 0.644$, $r_{u,22} = 0.0$, $r_{u,23} = 0.851$. Once we obtain the values of end-fixity factors for the columns, we can calculate the lateral stiffness modification factors of $\beta_{0,ij}(r_{l,ij}, r_{u,ij})$ and $\beta_{1,ij}(r_{l,ij}, r_{u,ij})$ with the value $\beta_{0,11} = 0.68$, $\beta_{0,12} = 0.25$, $\beta_{0,13} = 0.731$, $\beta_{0,21} = 0.336$, $\beta_{0,22} = 0.0$, $\beta_{0,23} = 0.592$, $\beta_{1,11} = 0.094$, $\beta_{1,12} = 0.1$, $\beta_{1,13} = 0.094$, $\beta_{1,21} = 0.086$, $\beta_{1,22} = 0.083$, $\beta_{1,23} = 0.09$. Therefore, the

maximization and minimization problems stated in Eqs. (3.18) to (3.22) can be evaluated and the details are presented in Appendix B.

The results demonstrate that the maximum and minimum frame-buckling loads are 80282.1 kN and 27473.3 kN, respectively. The load patterns corresponding to the maximum frame-buckling loads applied to the exterior columns, which are characterized by the rigid beam-to-column connections. The difference between the maximum and minimum frame-buckling loads is 192.2%, which is considerably significant. It is observed that the load patterns associated with the maximum frame-buckling load are applied only on exterior columns, which are the same with cases 1, 2 and 3. It is also found that load patterns associated with the minimum frame-buckling load are applied on interior or exterior columns. To verify the constraint conditions shown in Eq. (B.5) in Appendix B, the loading of column C_{23} , $P_{23}=27473.24$ kN is substituted into the Eq. (B.5a), $S_1 = 25610 - 0.319(P_{11} + P_{21}) - 0.34(P_{12} + P_{22}) - 0.32(P_{13} + P_{23})$, it yields $S_1=16818.56>0$. If substituting $P_{23}=27473.24$ kN into the Eq. (B.5b), $S_2 = 9753 - 0.34P_{21} - 0.328P_{22} - 0.355P_{23}$, it produces $S_2=0$, which verifies the results presented in Table 3-5.

The verification results obtained from computer program MASTAN2 (McGuire et al., 2000) are given in Table 3-8 with respect to the maximum and minimum frame-buckling loads. It is noted that once the load patterns corresponding to the maximum and minimum frame-buckling loads are applied on the frame, the frame is just within its critical load condition which can be verified to be equal to one for the applied load ratio with respect to the elastic critical load.

Table 3-8: Results verification of the unbraced steel frames shown in Figure 3-8 – Case 4

Storey	Columns	Current study		
		Max. (kN)	Min. (kN)	
			$S_1 = 0, S_2 > 0$	$S_2 = 0, S_1 > 0$
1	11	51596.840	0.000	0.000
	12	0.000	45588.770	0.000
	13	0.000	0.000	0.000
2	21	28685.290	0.000	0.000
	22	0.000	29734.760	0.000
	23	0.000	0.000	27473.240
MASTAN2 – Elastic critical load: applied load ratio		1.000	1.030	0.980

In Case 5, the column base connection is rigid, while the beam-to-column connections for both the interior and exterior columns are quite flexible with the corresponding end-fixity factor being 0.2. Consequently, the elastic flexural stiffness decrease largely compared to the other cases. The maximum and minimum frame-buckling loads are 60559.0 kN and 21440.8 kN as shown in Table 3-6, which yields a considerable difference of 182.4%. The load patterns corresponding to the maximum frame-buckling loads tend to apply the loads both on the interior and exterior columns and the load patterns corresponding to the minimum frame-buckling loads tend to apply only on exterior.

The frame-buckling strengths associated with storey-based buckling subjected to proportional loading for the frames in the foregoing cases are also presented in Tables 3-2 to 3-6. It is found that the differences between the maximum and proportional loadings are 0.7%, 1.1%, 0.8%, 3.1% and 0.6% for Cases 1 to 5, respectively. For these five cases, the differences between the proportional and the minimum loadings are found to be 48.3%, 58.3%, 63.2%, 182.6% and 180.8%, respectively. A concern may be raised from such significant differences in this particular example and other studies (Xu et al., 2001; Xu, 2002; Deierlein, 1992) as to the appropriateness of using the conventional proportional loading approach to evaluate frame-buckling strength for unbraced steel frames such as the ones investigated in this example.

3.7 Conclusions

The stability of single-storey unbraced frames subjected to variable loading proposed by Xu (2002) has been extended to the multi-storey unbraced frames in this study. The difference of solving an extreme loading problem between single-storey and multi-storey frames using the case of a multi-storey frame, to obtain the minimum frame-buckling load, the minimization problem needs to be solved for each storey while the maximum frame-buckling load can be acquired by solving the maximization problem only once.

The maximum and minimum frame-buckling loads and their associated load patterns can be obtained by solving the maximization and minimization problems, respectively, with a linear programming method. These problems represent the maximum and minimum bounds of the frame buckling loads of the structures, which characterize the stability capacity of the frame under extreme loading conditions. It can also be observed from the presented 2-bay by 2-storey frame example that the corresponding maximum frame-buckling load is always associated with the lateral instability of both the first and second storey simultaneously, which indicated a further increase in any one of the applied loads is impossible as each storey has already reached the limit state of lateral instability. This study reveals that the differences between the maximum and minimum frame-buckling loads could be substantial for multi-storey unbraced steel frames. This study also found the maximum and minimum frame-buckling loads are influenced by the beam-to-column connection. For instance, when the end-fixity factor of beam-to-column connection reduces from 1, 0.8 and 0.2 for Cases 1, 3 and 5, respectively, the frame becomes more flexible which can be evidenced by decreasing the maximum and minimum frame-buckling loads and their relative differences increase from 50.5%, 64.4% and 182.4% for Cases 1, 3 and 5, respectively. Comparing the results obtained from the proportional and variable loading cases, one can conclude that the frame-buckling loads associated with proportional loading are always between the maximum and minimum loads subjected to variable loading. The comparison results also indicate that the proportional load was very close to the maximum frame-buckling load. However, to ensure that the minimum frame-buckling strength of the frame is being accounted for in the design, the stability analysis of the frames subjected to variable loading proposed herein is recommended for the frames in either of the following cases:

1. There is a considerable variation in lateral stiffness among columns in the same storey of any storey of the frame;

2. There is a considerable variation in connection stiffness among beam-to-column connections in the same storey of any storey of the frame or column base connection; and
3. There is an expected substantial volatility in applied loads.

Chapter IV

Storey-Based Stability Analysis for Unbraced Frame with Initial Geometric Imperfections

4.1 Introduction

The steel framework is one of the most commonly used structural systems in modern construction and is often designed using planar unbraced moment frames for the lateral-load resisting systems along with a significant number of gravity columns throughout the structure. In the foregoing proposed research, the idealizations are made by assuming that the joints of the multi-storey frame are precisely aligned while the column is perfectly straight. It should also be understood that such idealizations are not practically achievable.

In the current design practice, the effect for the out-of-straightness of columns is taken into account inexplicitly in the development of the column strength curve by calibrating column strength to that associated with a specific value of out-of-straightness. Out-of-straightness is often to be the maximum allowable value of out-of-straightness specified in applicable design standards. The effect of out-of-plumbness of the frame, on the other hand, can be accounted for by conducting a second-order analysis and applying so called notional loads of $0.002Y_i$ at each storey level, where Y_i is the design gravity load applied at level i , and $0.002Y_i$ represents an initial out-of-plumbness in each storey of the structure of $1/500$ times the storey height (AISC, 2005).

In this chapter, the stability of columns in multi-storey unbraced frames with the initial geometric imperfections has been investigated. The lateral stiffness of the axially loaded column in unbraced frame is derived with the incorporation of effects of the initial geometric imperfections. Based on the concept of storey-based buckling, a practical method of determining the effective length factor for columns in unbraced frames with explicit accounting for the out-of-straightness of member and the out-of-plumbness of frame has been developed and the numerical examples have been examined.

4.2 Lateral Stiffness of an Axially Loaded Column with Initial Geometric Imperfections

For a perfect slender column under an axial load only, elastic buckling occurs suddenly when the critical load is attained. The column does not deflect laterally prior to the failure. In practice, columns are actually imperfect, subject to both material imperfections and geometrical imperfections. The influence of out-of-straightness of column is presented in Figure 4-1 from Trahair and Bradford (1991). For a straight member with initial out-of-straightness, the lateral deformations (curve A) occur immediately upon loading and then follow the elastic second-order bending curve until the first yield takes place at a load P_l .

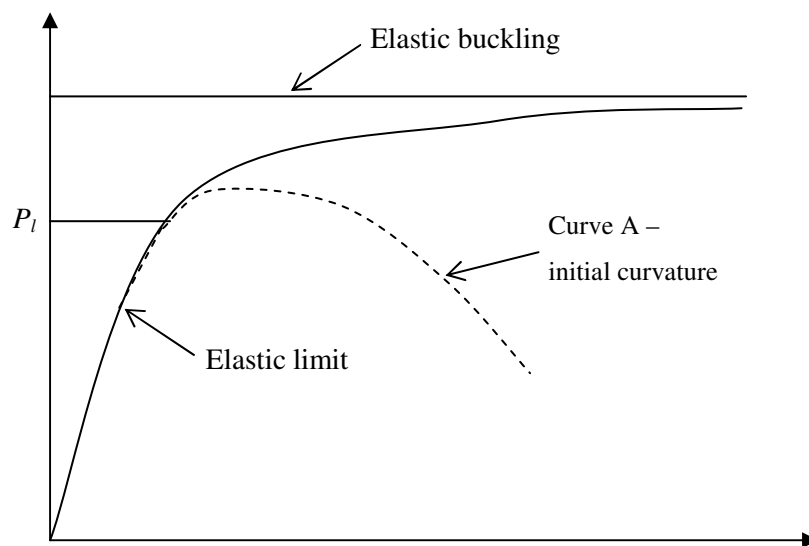


Figure 4-1: Influence of imperfection on column behavior (Trahair and Bradford,1991)

The deformed shapes of an axially loaded column with initial imperfections associated with out-of-plumbness of framing and out-of-straightness of column are shown in Figure 4-2.

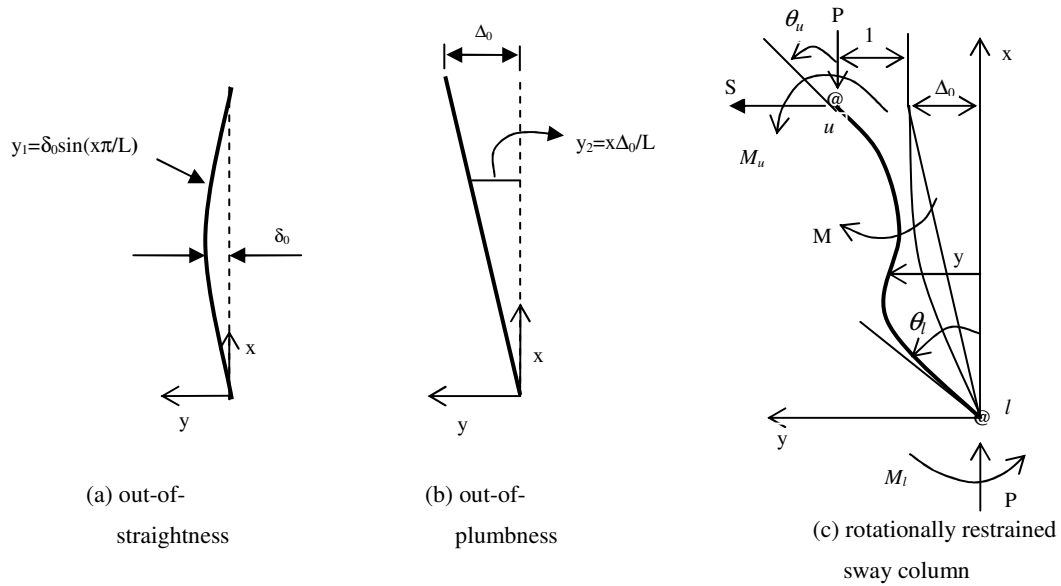


Figure 4-2: The deformed shapes of an axially loaded column with initial geometric imperfections

In engineering practice, these initial geometric imperfections shall not exceed the fabrication (out-of-straightness) and erection (out-of-plumbness) tolerances stipulated in the applicable engineering standards. For instance, the AISC (2005) specifies a fabrication tolerance (out-of-straightness) for compression members of $L/1000$ between lateral supports, and an erection tolerance (out-of-plumbness) of $L/500$ for individual columns. To account for out-of-straightness of column, a half-sine curve is typically adopted to simulate the member imperfection as shown in Figure 3a. Thus, the imperfection function associated with out-of-straightness of column is,

$$y_1 = \delta_0 \sin \frac{\pi x}{L} \quad (4.1)$$

where δ_0 is the initial out-of-straightness at the middle of the column.

Let Δ_0 be the initial out-of-plumbness at the upper joint of the column as shown in Figure 3b, and then the corresponding imperfection function of frame is,

$$y_2 = \frac{x \Delta_0}{L} \quad (4.2)$$

With a unit lateral deflection at the upper end as shown in Figure 3c, the internal moment of the column with both column out-of-straightness and frame out-of-plumbness can be expressed as

$$M = -M_u - P(1 + \Delta_0 - y) - S(L - x) \quad (4.3)$$

where M is the internal moment of the column; M_u is the end moment at the column upper end; P is the applied axial load; L is the column length; S , the lateral force associated with the unit lateral deflection at column upper end, is defined as the lateral stiffness of the column; and y is the lateral deflection of the column including the member imperfection function y_1 and frame imperfection function y_2 . Therefore, the equilibrium condition of the column subjected to the axial load and end moment can be expressed as

$$EI \frac{d^2 y}{dx^2} = M_u + S(L - x) + P(1 + \Delta_0 - y) \quad (4.4)$$

Similarly, the end moment at the lower end can be obtained from Eq. (4.3)

$$M_l = -M_u - SL - P(1 + \Delta_0) \quad (4.5)$$

Let $\theta_{l,ij}$ and $\theta_{u,ij}$ be the end rotations of the column related to the lower and upper ends, respectively, the boundary conditions of the column are described in the following:

$$M_u = R_{u,ij} \theta_{u0}; \quad M_l = -R_{l,ij} \theta_{l0} \quad (4.6a, b)$$

$$y|_{x=0} = 0; \quad y|_{x=L} = \Delta_0 + 1 \quad (4.7a, b)$$

$$\left. \frac{dy}{dx} \right|_{x=0} = \theta_l; \quad \left. \frac{dy}{dx} \right|_{x=L} = -\theta_u \quad (4.8a, b)$$

in which

$$\theta_{l0} = \theta_l - \Delta_0 / L - \delta_0 \pi / L \quad (4.9a)$$

$$\theta_{u0} = \theta_u - \Delta_0 / L + \delta_0 \pi / L \quad (4.9b)$$

where the column rotational-restraining stiffness $R_{u,ij}$ and $R_{l,ij}$ are contributed by beams connected to the upper and lower ends of the column, respectively.

The detailed process to derive the lateral stiffness of an axially loaded column with accounting for the initial geometric imperfections is discussed in Appendix C. Based on Eq. (C5) in Appendix C, the lateral stiffness of the column is given as

$$S = \frac{\phi^2 CEI}{L^3} = \beta \frac{12EI}{L^3} \quad (4.10)$$

in which $\beta = \frac{C\phi^2}{12}$ is the lateral stiffness modification factor that takes the effects of axial force and column end rotational restraints into account, and is given as follows.

$$\beta = \frac{\phi^3}{12} \left[\frac{f_1 + (-f_1 + f_2\phi^2)\cos\phi - (f_3\phi^2 + f_4 + f_5 + f_6)\phi\sin\phi}{f_7 - (f_7 + f_8\phi^2)\cos\phi + (f_9\phi^2 + f_{10})\phi\sin\phi} \right] \quad (4.11)$$

where

$$f_1 = -\frac{9}{50}\delta_0\pi r_l r_u \quad (4.11a)$$

$$f_2 = 3\left(1 + \frac{\Delta_0}{100}\right)(r_l + r_u - 2r_l r_u) \quad (4.11b)$$

$$f_3 = \left(1 + \frac{\Delta_0}{100}\right)(1 - r_l - r_u + r_l r_u) \quad (4.11c)$$

$$f_4 = \frac{3}{100}\Delta_0(r_l - r_u - 3r_l r_u) \quad (4.11d)$$

$$f_5 = \frac{3\Delta_0}{100}(r_l + r_u - 2r_l r_u) \quad (4.11e)$$

$$f_6 = -9r_l r_u \quad (4.11f)$$

$$f_7 = 18r_l r_u \quad (4.11g)$$

$$f_8 = 3(r_l + r_u - 2r_l r_u) \quad (4.11h)$$

$$f_9 = 1 - r_l - r_u + r_l r_u \quad (4.11i)$$

$$f_{10} = 3(r_l + r_u - 5r_l r_u) \quad (4.11j)$$

As stated previously in Chapter 3, the transcendental relationship between β and ϕ in Eqs. (4.11) based on Eq. (C9) of Appendix C are too complicated for solving the critical buckling load of the column. By applying 1st-order or 2nd-order Taylor series approximations, the lateral stiffness modification factor β with initial geometrical imperfections presented in Eq. (4.11) can be expressed as

$$\beta_{ij}(r_{l,ij}, r_{u,ij}, \delta_0, \Delta_0, \phi_{ij}) = \beta_{0,ij}(r_{l,ij}, r_{u,ij}, \delta_0, \Delta_0) - \beta_{1,ij}(r_{l,ij}, r_{u,ij}, \delta_0, \Delta_0)\phi_{ij}^2 \quad (4.12a)$$

$$\beta_{ij}(r_{l,ij}, r_{u,ij}, \delta_0, \Delta_0, \phi_{ij}) = \beta_{0,ij}(r_{l,ij}, r_{u,ij}, \delta_0, \Delta_0) - \beta_{1,ij}(r_{l,ij}, r_{u,ij}, \delta_0, \Delta_0)\phi_{ij}^2 - \beta_{2,ij}(r_{l,ij}, r_{u,ij}, \delta_0, \Delta_0)\phi_{ij}^4 \quad (4.12b)$$

in which

$$\beta_{0,ij}(r_{l,ij}, r_{u,ij}) = \frac{(1 - \pi\delta_0/100)(r_{l,ij} + r_{u,ij} + r_{l,ij}r_{u,ij}) - \frac{\Delta_0}{100}r_{u,ij}(2 + r_{l,ij})}{4 - r_{l,ij}r_{u,ij}} \quad (4.13a)$$

$$\beta_{1,ij} = \frac{\alpha_{0,ij} + \pi\delta_0\alpha_{1,ij} + \Delta_0\alpha_{2,ij}}{60(4 - r_{l,ij}r_{u,ij})^2} \quad (4.13b)$$

where

$$\alpha_{0,ij} = 2(40 + 8r_{l,ij}^2 - 34r_{l,ij}r_{u,ij} + r_{l,ij}^2r_{u,ij} + 8r_{u,ij}^2 + r_{l,ij}r_{u,ij}^2 + 3r_{l,ij}^2r_{u,ij}^2) \quad (4.14a)$$

$$\alpha_{1,ij} = \frac{1}{100}(16r_{l,ij}^2 - 28r_{l,ij}r_{u,ij} + 2r_{l,ij}^2r_{u,ij} + 16r_{u,ij}^2 + 2r_{l,ij}r_{u,ij}^2 + r_{l,ij}^2r_{u,ij}^2) \quad (4.14b)$$

$$\alpha_{2,ij} = \frac{1}{50}[40 + 16r_{u,ij}^2 + r_{l,ij}^2r_{u,ij}(8 + 3r_{u,ij}) - 2r_{l,ij}r_{u,ij}(17 + 3r_{u,ij})] \quad (4.14c)$$

$$\beta_{2,ij} = \frac{(1 + \frac{1}{100}\pi\delta_0)(\zeta_0 + \zeta_1r_{l,ij} + \zeta_2r_{l,ij}^2 + \zeta_3r_{l,ij}^3) + \frac{1}{100}\Delta_0(\zeta_4 + \zeta_5r_{l,ij} + \zeta_6r_{l,ij}^2 + \zeta_7r_{l,ij}^3)}{25200(4 - r_{l,ij}r_{u,ij})^4} \quad (4.15)$$

where

$$\zeta_0 = 2560r_{u,ij}^2 - 1792r_{u,ij}^3 \quad (4.16a)$$

$$\zeta_1 = -4960r_{u,ij} + 1844r_{u,ij}^2 + 704r_{u,ij}^3 \quad (4.16b)$$

$$\zeta_2 = 2560 + 1844r_{u,ij} - 1492r_{u,ij}^2 - 41r_{u,ij}^3 \quad (4.16c)$$

$$\zeta_3 = -1792 + 704r_{u,ij} - 41r_{u,ij}^2 - 17r_{u,ij}^3 \quad (4.16d)$$

$$\zeta_4 = -5120r_{u,ij}^2 + 3584r_{u,ij}^3 \quad (4.16e)$$

$$\zeta_5 = +4960r_{u,ij} + 2008r_{u,ij}^2 - 3200r_{u,ij}^3 \quad (4.16f)$$

$$\zeta_6 = -5696r_{u,ij} + 1492r_{u,ij}^2 + 898r_{u,ij}^3 \quad (4.16g)$$

$$\zeta_7 = 1792r_{u,ij} - 816r_{u,ij}^2 + 17r_{u,ij}^3 \quad (4.16h)$$

It is noted that in the consideration of initial geometric imperfections, $\beta_{0,ij}(r_{l,ij}, r_{u,ij}, \delta_0, \Delta_0)$, $\beta_{1,ij}(r_{l,ij}, r_{u,ij}, \delta_0, \Delta_0)$ and $\beta_{2,ij}(r_{l,ij}, r_{u,ij}, \delta_0, \Delta_0)$ are functions of the column end-fixity factors ($r_{l,ij}$, $r_{u,ij}$) and the initial geometric imperfections of out-of-straightness (δ_0) and out-of-plumbness (Δ_0).

4.3 Evaluation of Column Effective Length Factor Accounting for Initial Geometric Imperfections

Maintaining the adequacy of column strength and frame stability is of primary importance to the structural design of such a structural system. For nearly 40 years, stability design of columns under the American Institute of Steel Construction Specification for Structural Steel Building (AISC, 2005) has been traditionally based upon the concept of effective length. According to this concept, the elastic buckling strength of a column of length L is equated to an equivalent pin-ended member of length KL , subject to axial load only, by means of K factor $K = \sqrt{P_e / P_{cr}}$, where P_{cr} is the elastic buckling strength of the end-restrained column, and P_e is the Euler buckling strength of a pin-end column given by $P_e = \pi^2 EI / L^2$ in which E is the Young's modulus and I is the moment of inertia of the column section about the axis of buckling.

There are different methods of calculating the K factors within the concept of effective length and along with adopted idealizations of the structure. Among them, the most widely adopted procedure

for the frame design is the alignment chart method that was originally proposed by Julian and Lawrence (1959) based on the assumption that all individual columns in a storey buckle simultaneously under their individual proportionate share of the total gravity load. This method corresponds to the side-sway-inhibited and side-sway-permitted cases. The procedure takes into account the rotational restraints provided by upper and lower beam-column assemblage and provides a direct means to obtain K factors. One significant drawback of the alignment chart method is that it does not account for the fact that a stronger column can provide effective bracing to a weaker column in resisting the lateral instability of a storey assemblage.

A more accurate approach to determine K is given by LeMessurier (1977). In this approach, the following assumptions have to be satisfied to evaluate the K factors: (1) the sum of the gravity load that causes lateral instability of a storey is equal to the sum of the individual buckling loads of columns that provide storey side-sway resistance; (2) the individual column buckling loads are determined based on the K factors obtained from the alignment chart. Later, a practical approach to determine the effective length factor for unbraced frames was proposed by Lui (1992), which involved the first-order frame analysis but without any special charts or iterative procedures required.

In the study of the storey-based buckling analysis discussed in Chapter 3, a practical method to evaluate the effective length factor for unbraced frame with initial imperfections is investigated in this chapter. By substituting Eq. (4.12b) into Eq. (3.2), the lateral stiffness of column ij associated with 2nd–order Taylor series approximation can be written as

$$S_{ij} = 12 \left(\frac{EI_{c,ij}}{L_{c,ij}^3} \beta_{0,ij} - \frac{P_{a,ij}}{L_{c,ij}} \beta_{1,ij} \lambda_i - \frac{P_{a,ij}^2 L_{ij}}{EI_{ij}} \beta_{2,ij} \lambda_i^2 \right) \quad (4.17)$$

in which $L_{c,ij}$ and $P_{a,ij}$ are the length and applied axial load of column j in the i th storey, respectively. λ_i is the proportional load multiplier associated with the i th storey of the frame. Substituting Eq. (4.17) into Eq. (3.7), the stability equation for storey i , buckling in a lateral sway mode can be expressed as

$$S_i = \sum_{j=1}^m 12 \left(\frac{EI_{c,ij}}{L_{c,ij}^3} \beta_{0,ij} - \frac{P_{a,ij}}{L_{c,ij}} \beta_{1,ij} \lambda_i - \frac{P_{a,ij}^2 L_{ij}}{EI_{ij}} \beta_{2,ij} \lambda_i^2 \right) = 0 \quad (4.18)$$

Let

$$a_i = \sum_{j=1}^m \frac{P_{a,ij}^2 L_{ij}}{EI_{ij}} \beta_{2,ij} \quad (4.19a)$$

$$b_i = \sum_{j=1}^m \frac{P_{a,ij}}{L_{ij}} \beta_{1,ij} \quad (4.19b)$$

$$c_i = \sum_{j=1}^m \frac{EI_{ij}}{L_{ij}^3} \beta_{0,ij} \quad (4.19c)$$

by substituting Eqs. (4.19) into Eq. (4.18), one can obtain the following equation

$$a_i \lambda_i^2 + b_i \lambda_i - c_i = 0 \quad (4.20)$$

Thus, the critical load multiplier associated with the lateral instability of i -th storey can be solved from the smaller positive root of Eq. (4.20) as follows

$$\lambda_{icr-2nd-order} = \frac{\sqrt{1 + 4(a_i / b_i)(c_i / b_i)} - 1}{2(a_i / b_i)} \quad (4.21)$$

Noted that if only 1st-order Taylor series approximation in Eq. (4.12a) adopted, in which only the first two terms of this equation is used, then the corresponding stability Eq. (4.20) is reduced to

$$b_i \lambda_i - c_i = 0 \quad (4.22)$$

from which the critical load multiplier associated with lateral instability of i -th storey can be obtained from Eq. (4.22) as

$$\lambda_{icr-1st-order} = \frac{c_i}{b_i} \quad (4.23)$$

It is noted that since the applied axial compressive load $P_{a,ij}$ on the columns are defined as positive values in this study, then the values of a_i and b_i expressed in Eqs. (4.19a) and (4.19b) will be dependent on the lateral stiffness modification factors of $\beta_{2,ij}(r_{l,ij}, r_{u,ij}, \delta_0, \Delta_0)$ and $\beta_{1,ij}(r_{l,ij}, r_{u,ij}, \delta_0, \Delta_0)$. The coefficient c_i in Eq. (4.19c) is the function of the lateral stiffness modification factors $\beta_{0,ij}(r_{l,ij}, r_{u,ij}, \delta_0, \Delta_0)$. The lateral stiffness modification factors of $\beta_{0,ij}(r_{l,ij}, r_{u,ij}, \delta_0, \Delta_0)$, $\beta_{1,ij}(r_{l,ij}, r_{u,ij}, \delta_0, \Delta_0)$ and

$\beta_{2,ij}(r_{l,ij}, r_{u,ij}, \delta_0, \Delta_0)$ can be evaluated from Eqs. (4.13) and the values are given in Tables D-1 to D-12 in Appendix D with respect to combined effects of the out-of-straightness (δ_0) and out-of-plumbness (Δ_0). The end-fixity factors $r_{l,ij}$ and $r_{u,ij}$ vary between 0 and 1. From Tables D-1 to D-12 in Appendix D, it is noted that the values of $\beta_{0,ij}(r_{l,ij}, r_{u,ij}, \delta_0, \Delta_0)$, $\beta_{1,ij}(r_{l,ij}, r_{u,ij}, \delta_0, \Delta_0)$ and $\beta_{2,ij}(r_{l,ij}, r_{u,ij}, \delta_0, \Delta_0)$ are positive as well as the values of coefficients a_i , b_i and c_i expressed in Eqs. (4.19). Based on the above statements, an inequality expression can be obtained with respect to Eqs. (4.21) and (4.23), which is given as:

$$\lambda_{icr-2nd-order} < \lambda_{icr-1st-order} \quad (4.24a)$$

substituting Eqs. (4.21) and (4.23) into this condition, which will yield the following expression:

$$\frac{\sqrt{1 + 4(a_i / b_i)(c_i / b_i)} - 1}{2(a_i / b_i)} < \frac{b_i}{c_i} \quad (4.24b)$$

reordering the left side of expression of (4.24a), we will have the following expression:

$$\frac{\sqrt{b_i^2 + 4a_i c_i} - b_i}{2a_i} < \frac{c_i}{b_i} \quad (4.24c)$$

As the coefficients of a_i and b_i are the positive values in current study, then both sides of expression (4.24c) multiply a positive coefficient of $2a_i b_i$, we can obtain the following expression:

$$a_i^2 c_i^2 > 0 \quad (4.24d)$$

which is always true and the expression of (4.24a) can be proved as true with a_i and b_i having the positive values together.

The expression of (4.24a) is indicated the critical load multiplier associated with 1st-order Tayler series approximation is less conservative than the critical load multiplier associated with 2nd-order Tayler series approximation. In the following numerical examples, we will compare the results based on 1st-order and 2nd-order Tayler series approximations as well as the results directly from the Eq. (4.11).

Once we obtained the critical load multiplier associated with lateral instability of i -th storey from Eq. (4.21) or (4.23), and the corresponding elastic buckling load of the column is

$$P_{ij} = \lambda_{icr} P_{a,ij} \quad (j = 1, 2, 3 \dots m) \quad (4.25)$$

Finally, the storey-based effective length factor of the column can be evaluated as (Lui, 1992; Xu and Liu, 2005; Xu and Wang, 2008)

$$k_{ij} = \frac{\pi}{L_{c,ij}} \sqrt{\frac{EI_{c,ij}}{\lambda_{icr} P_{a,ij}}} \quad (j = 1, 2, 3 \dots m) \quad (4.26)$$

Upon the previous study discussed in Chapter 3, the end-rotational stiffness of each beam and beam-to-column restraining stiffness of each joint can be evaluated using the decomposition process FSD approach given in Appendix A (Liu and Xu, 2005). Therefore, the distribution of the beam-to-column rotational-restraining stiffness to the upper and lower columns can be calculated by the column end-rotational stiffness, as demonstrated in Appendix A. The summary of storey-based effective length factor for columns in a multi-storey unbraced frame with initial geometrical imperfections is carried out as follows:

- (1) Calculate the end-fixity factors $r_{l,ij}$ and $r_{u,ij}$ from Eq.(3.1) for all the columns.
- (2) Compute the lateral stiffness modification coefficients $\beta_{0,ij}(r_{l,ij}, r_{u,ij}, \delta_0, \Delta_0)$, $\beta_{1,ij}(r_{l,ij}, r_{u,ij}, \delta_0, \Delta_0)$ and $\beta_{2,ij}(r_{l,ij}, r_{u,ij}, \delta_0, \Delta_0)$ in accordance with Eqs. (4.13a,b) and (4.15) based on the specified values of initial geometric imperfections, δ_0 or Δ_0 .
- (3) Evaluate the critical load multiplier based on Eq.(4.21) or (4.23) for each storey and obtain the corresponding storey-based effective length factor K_{ij} from Eq.(4.26) for all the columns of the storey.

4.4 Numerical Examples

The objectives of the numerical examples are to investigate the effects of the initial geometric imperfections δ_0 and Δ_0 on the column elastic buckling strength. Also the results of the critical buckling multiplier λ and the effective length factor K among the approaches of 1st-order and 2nd-

order approximations, and the storey-based buckling analysis are evaluated and one method is recommended for the engineering practice. The maximum tolerance of out-of-straightness ($\delta_0=L/1000$) for columns is used to simulate the member imperfection. The initial misalignment ($\Delta_0=L/500$) at the upper joint of the column is used to demonstrate the frame instability.

Example 1

The stability of a 2-bay by 1-storey unbraced steel frame shown in Figure 4-3 was investigated by LeMessurier (1977) and several other researchers (Lui, 1992; Shanmugam and Chen, 1995; Schmidt, 1999). The frame dimensions, member sizes and the applied loads are also shown in this figure.

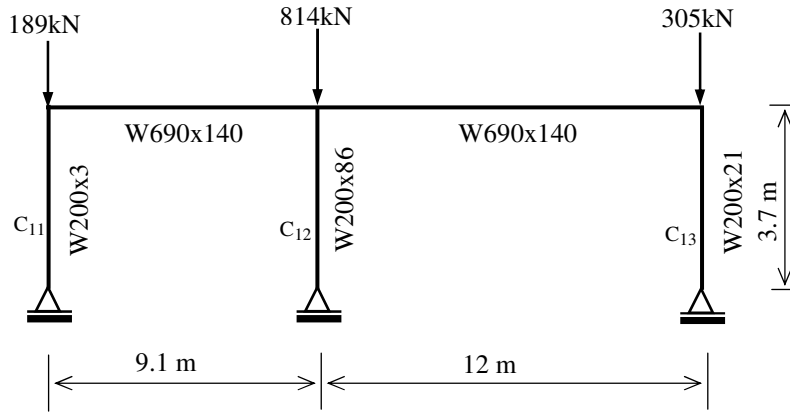


Figure 4-3: 2-bay by 1-storey frame of Example 1 (Schmidt, 1999)

The study to evaluate the column effective length factor among the approaches of the 1st-order and 2nd-order approximations, and the storey-based buckling method without the consideration of the initial geometric imperfections is investigated first and the results are given in Table 4-1. The results associated with the 1st-order and 2nd-order approximations are obtained from Eqs. (4.23) and (4.21) with $\delta_0=0$ and $\Delta_0=0$. The storey-based buckling results are computed using Eq. (4.11) based on the condition of the summation of the columns lateral stiffness of each storey becomes zero. Also presented in this table are the column effective length factor based on the alignment chart method and LeMessurier's method.

Table 4-1: Example 1 - Comparison of K factors of 2-bay by 1-storey

Col.	K factors				
	Alignment chart	LeMessurier's method	Current study ($\Delta_0=0, \delta_0=0$)		
			1 st -order approximation	2 nd -order approximation	Storey-based buckling method
C ₁₁	2.020	2.110	2.100	2.115	2.128
C ₁₂	2.030	1.770	1.750	1.770	1.781
C ₁₃	2.070	2.600	2.580	2.600	2.616

There is generally good agreement among the results of LeMessurier's method and the current study corresponding to the three approaches, except for those obtained with the alignment chart method. Based on the LeMessurier's method and storey-based buckling method, the K factors are mostly within 0.6% for columns C₁₂ and C₁₃, but a maximum difference of 0.84% is noted for column C₁₁.

In Table 4-1, it is found the maximum difference of the effective length factor K between 1st-order and 2nd-order approximations are only 0.66%, 0.68% and 0.65% for columns C₁₁, C₁₂ and C₁₃, respectively. For column C₁₁, the maximum differences of K factors between the storey-based buckling method and the two approximations are 1.26% and 0.61%, respectively. 1.3% and 0.62% are found for the maximum differences of K factors between the storey-based buckling method and the two approximations for column C₁₂. And the maximum differences of K factors between the storey-based buckling method and the two approximations are 1.26% and 0.61% for column C₁₃.

The maximum difference of up to 1.3% is noted for K factors between the storey-based buckling method and the 1st-order approximation. This 1st-order approximation results are acceptable and can be recommended for use in the practice due to its simplified equations.

In the case of considering the initial geometric imperfections to evaluate the effective length factor K , the maximum of out-of-straightness ($\delta_0=L/1000$) for columns is used to simulate the member imperfection. The initial misalignment $\Delta_0=L/500$ at the upper joint of the column is used to demonstrate the frame instability. The critical loading multipliers together with their effective length

factors are obtained from Eqs. (4.23) and (4.21), which are corresponding to the 1st-order and 2nd-order approximations of λ in the Taylor series approximation of Eq. (4.11) and the results are presented in Table 4-2. For comparison, the results based on the current study without the consideration of initial geometric imperfections are also given in Table 4-2.

Table 4-2: Example 1 – comparison study of three approaches

Col	Effective length factors (K) ($\delta_0=0, \Delta_0=0$)			Critical loading multiplier (λ_{cr}) ($\delta_0=L/1000, \Delta_0=L/500$)			Effective length factors (K) ($\delta_0=L/1000, \Delta_0=L/500$)		
	1 st – order approx.	2 nd – order approx.	Storey- based buckling	1 st – order Eq. (4.23)	2 nd – order Eq. (4.21)	Storey- based buckling	1 st – order approx.	2 nd – order approx.	Storey- based buckling
C ₁₁	2.100	2.115	2.128	3.619	3.584	3.540	2.573	2.582	2.601
C ₁₂	1.750	1.770	1.781	3.619	3.584	3.540	2.153	2.161	2.177
C ₁₃	2.580	2.600	2.616	3.619	3.584	3.540	3.163	3.175	3.198

In Table 4-2, upon the storey-based buckling results, it is noticed that there is a considerable difference between the results of with and without considering the imperfections. For column C₁₁, K value increases from 2.128 (no initial imperfections) to 2.601 (out-of-straightness: $\delta_0 = L/1000$ and out-of-plumbness: $\Delta_0 = L/500$), which would result in 18% reduction of the axial strength of the column (AISC, 2005). For column C₁₂, K value increases from 1.781 to 2.177 and the corresponding reduction on the factored axial strength is about 15%. K value increases from 2.616 to 3.198 for column C₁₃, which results in a decrease of the factored axial strength by about 29%. It should be pointed out that as the reductions of the factored axial strengths are based on the column factored axial strength evaluated in accordance with the specification of AISC (2005) in which the effects of the initial geometrical imperfections have been accounted for in the formulation of evaluating column axial strength in some degree. Therefore, the effects of the initial geometrical imperfections maybe somewhat doubly accounted for herein. However, the purpose of the foregoing discussion is to demonstrate the influence of the initial geometrical imperfections on the column strength, therefore

only the relevant percentages of the strength reductions and not the actual magnitudes of the strength are given for the reason of comparison.

From Table 4-2, it is found that the critical loading multiplier λ_{cr} obtained from Eqs. (4.21) and (4.23) are 3.584, and 3.619, respectively which also satisfies the inequality expression (4.24a) and the difference of the λ_{cr} is 0.96%. Consequently, for column C_{11} , the maximum difference of the corresponding K factor between 1st-order and 2nd-order approximations is only 0.46%, which is insignificant. The differences of the corresponding K factors are found to be 0.46% and 0.50% for columns C_{12} and C_{13} , respectively. The maximum differences of K factors between the storey-based buckling results and the 1st-order approximation are 1.08%, 1.1% and 1.09% for columns C_{11} , C_{12} and C_{13} , respectively. Compared to the 2nd-order approximation for columns C_{11} , C_{12} and C_{13} , the maximum differences are found to be 0.62%, 0.64% and 0.59%, respectively. In Table 4-1, the K factors based on Eq. (4.23) (2nd-order approximation) are less than the results obtained from Eq. (4.21) (1st-order approximation), which proved the results based on 2nd-order approximation are more conservative than the results from 1st-order approximation. Figure 4-4 illustrates the K factors with the 1st-order and 2nd-order approximations, and the storey buckling method, corresponding to the end-fixity factors of the columns base.

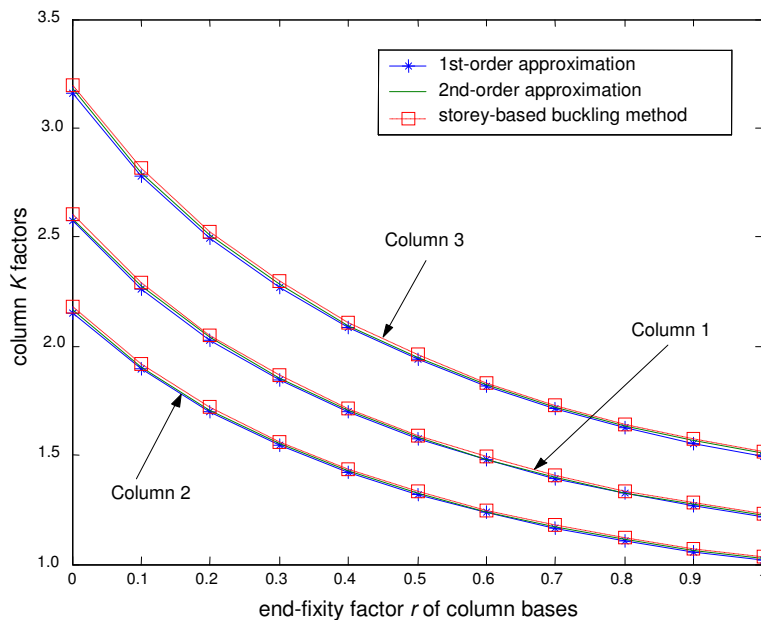


Figure 4-4: Example 1 - comparison results of K factors vs end-fixity factor r

Figure 4-4 demonstrates good accordance for columns K factors within the 1st-order and 2nd-order approximations and the storey-based buckling results for all the columns in the frame. It is also noted the K factors decrease while the end-fixity factors of the column bases increase.

Illustrated in Figures 4-5 and 4-6 are the effects of initial geometric imperfections on the columns K factors obtained from 1st-order and 2nd-order approximations, and the storey-based buckling analysis. Similarly to Figure 4-4, the three methods present almost matching results for the K factors with respect to the initial geometric imperfections of out-of-straightness (δ_0) or out-of-plumbness (Δ_0). These two figures also show the K factors increase when the imperfection coefficients of δ_0 or Δ_0 increases.

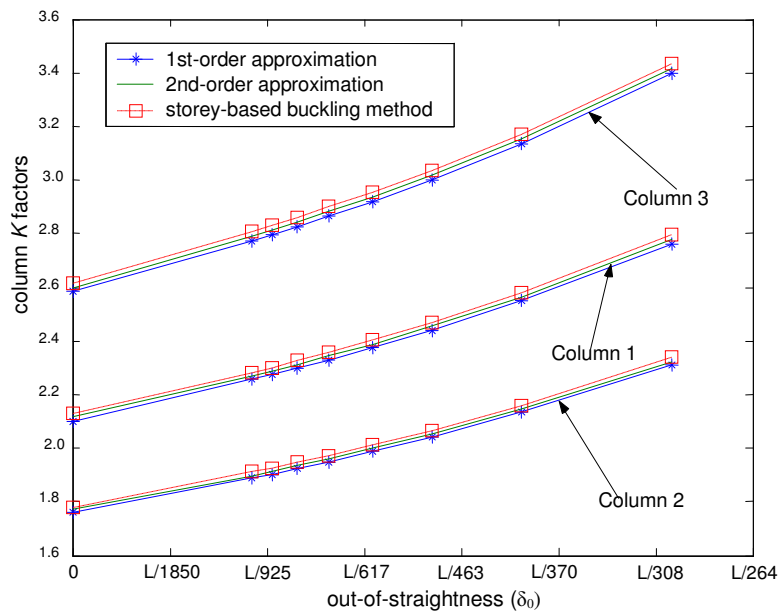


Figure 4-5: Example 1 - K factors vs out-of-straightness (δ_0)

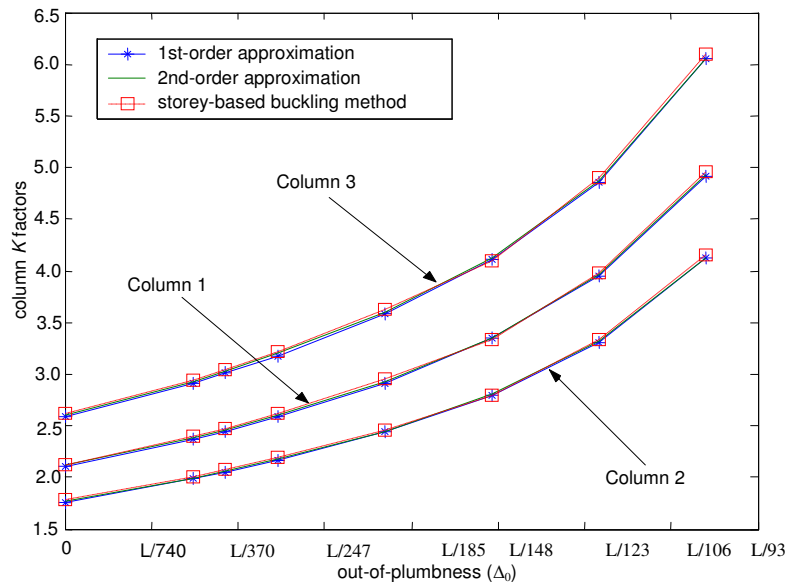


Figure 4-6: Example 1 - K factors vs out-of-plumbness (Δ_0)

From the comparison study, it is found the difference between 1st-order approximation and the storey-based buckling method is less than 1.2%, which is acceptable in the engineering practice. Therefore, it is recommended that the simplified Eq. (4.23) can be used to calculate the critical loading multiplier λ_{cr} together with the K factors in Eq.(4.26) in practice due to the simplicity of this method.

In the following parametric studies, the effects of only considering the out-of-straightness on K factors are demonstrated in Table 4-3 while the effects with consideration of the out-of-plumbness alone on K factors is presented in Table 4-4. Compared to the effects of out-of-straightness and out-of-plumbness on the K factors, it is found that the out-of-straightness has greater influence than that of the out-of-plumbness, which is observed by comparing the K factors associated with values of the imperfections to be $L/500$, $L/400$, $L/300$ in Tables 4-3 and 4-4. The combined effects of the out-of-straightness and out-of-plumbness on column K factors are illustrated in Table 4-5. Also presented in Tables 4-3 to 4-5 are the compared results between the 1st-order and 2nd-order approximations.

Table 4-3: Example 1 - effects of out-of-straightness on K factors

Column		K factors ($\Delta_0=0$)						
		$\delta_0=$ 0	$\delta_0=$ $L/1000$	$\delta_0=$ $L/800$	$\delta_0=$ $L/600$	$\delta_0=$ $L/500$	$\delta_0=$ $L/400$	$\delta_0=$ $L/300$
1 st -order Approximation	C ₁₁	2.101	2.255	2.298	2.374	2.440	2.549	2.763
	C ₁₂	1.758	1.887	1.923	1.987	2.042	2.133	2.312
	C ₁₃	2.583	2.772	2.825	2.919	3.001	3.134	3.397
2 nd -order Approximation	C ₁₁	2.115	2.268	2.312	2.388	2.454	2.563	2.776
	C ₁₂	1.770	1.898	1.934	1.998	2.054	2.145	2.323
	C ₁₃	2.600	2.789	2.842	2.936	3.017	3.151	3.413

Table 4-4: Example 1- effects of out-of-plumbness on K factors

Column		K factors ($\delta_0=0$)				
		$\Delta_0=0$	$\Delta_0=L/500$	$\Delta_0=L/400$	$\Delta_0=L/300$	$\Delta_0=L/200$
1 st -order Approximation	C ₁₁	2.101	2.371	2.448	2.587	2.916
	C ₁₂	1.758	1.984	2.049	2.165	2.440
	C ₁₃	2.583	2.916	3.010	3.181	3.585
2 nd -order Approximation	C ₁₁	2.115	2.384	2.461	2.599	2.927
	C ₁₂	1.770	1.995	2.059	1.175	2.449
	C ₁₃	2.600	2.931	3.025	3.196	3.598

Table 4-5: Example 1 - effects of out-of-straightness and out-of-plumbness on K factors

Column		K factors				
		$\delta_0=0$ $\Delta_0=0$	$\delta_0=L/1000$ $\Delta_0=L/500$	$\delta_0=L/800$ $\Delta_0=L/400$	$\delta_0=L/600$ $\Delta_0=L/300$	$\delta_0=L/400$ $\Delta_0=L/200$
1 st -order Approximation	C ₁₁	2.101	2.573	2.728	3.04	4.044
	C ₁₂	1.758	2.153	2.283	2.54	3.384
	C ₁₃	2.583	3.163	3.354	3.74	4.973
2 nd -order Approximation	C ₁₁	2.115	2.585	2.740	3.040	4.054
	C ₁₂	1.770	2.163	2.293	2.544	3.392
	C ₁₃	2.600	3.179	3.369	3.738	4.984

From Tables 4-3 to 4-5, it is noticed that the K factors increase when the value of either one of the initial imperfections increases. The combined effects of the initial geometric imperfections would have the most severe impact on the column K factors. For instance, the value of K factor for column C₁₁ increases from 2.10 (without accounting for the initial geometric imperfections) to 2.26 (out-of-straightness: $\delta_0 = L/1000$ alone) and 2.37 (out-of-plumbness: $\Delta_0 = L/500$ alone). However, for combined effects (out-of-straightness: $\delta_0 = L/1000$ and out-of-plumbness: $\Delta_0 = L/500$), the resulted K factor is 2.57. Consequently, the factored axial strength reductions for column C₁₁ are 6%, 10% and 18%, respectively. In Tables 4-3 to 4-5, the comparison results provide less than 0.6 percent between 1st-order and 2nd-order approximations, which further indicated the 1st-order approximation can yield satisfied results in practice.

Illustrated in Figures 4-7 to 4-14 are the effects of the initial geometric imperfections on the lateral stiffness modification factors of column $\beta_{0,ij}$, $\beta_{1,ij}$ and $\beta_{2,ij}$. As shown in Eq. (4.18), it is noted that $\beta_{0,ij}$ is associated with the elastic lateral stiffness of the column while $\beta_{1,ij}$ and $\beta_{2,ij}$ correspond to the effect of the applied axial load (second-order effect) on the column stiffness. It can be seen from the figures, as any of the initial geometric imperfections, δ_0 or Δ_0 increases, the value of $\beta_{0,ij}$ will decrease and the value of $\beta_{1,ij}$ and $\beta_{2,ij}$ will increase, which indicates that the initial geometric imperfections will reduce the column stiffness and amplify the second-order effect. Consequently, the frame is more laterally

flexible when the combined effects of δ_0 or Δ_0 are taken into consideration. Demonstrated in Figures 4-13 and 4-14 are the influences of the out-of-straightness (δ_0) and out-of-plumbness (Δ_0) on the column buckling loads using 1st-order approximation.

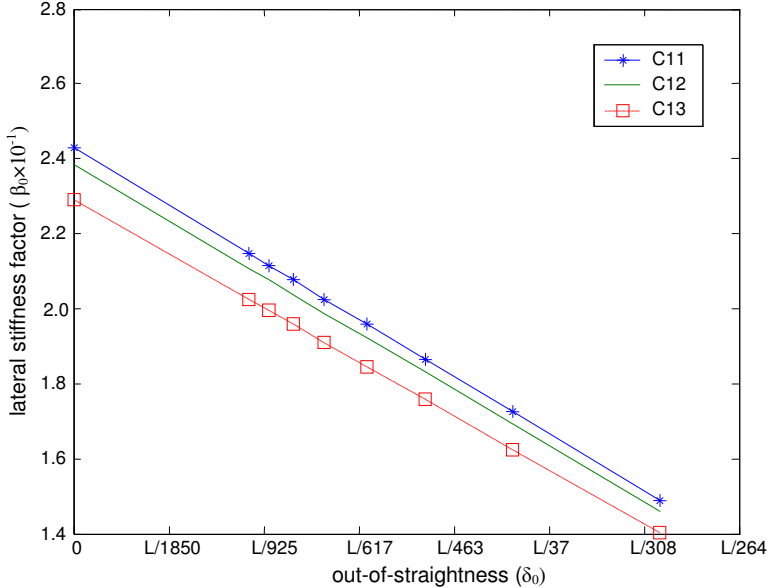


Figure 4-7: Example 1 - lateral stiffness coefficients $\beta_{0,ij}$ vs. out-of-straightness (δ_0)

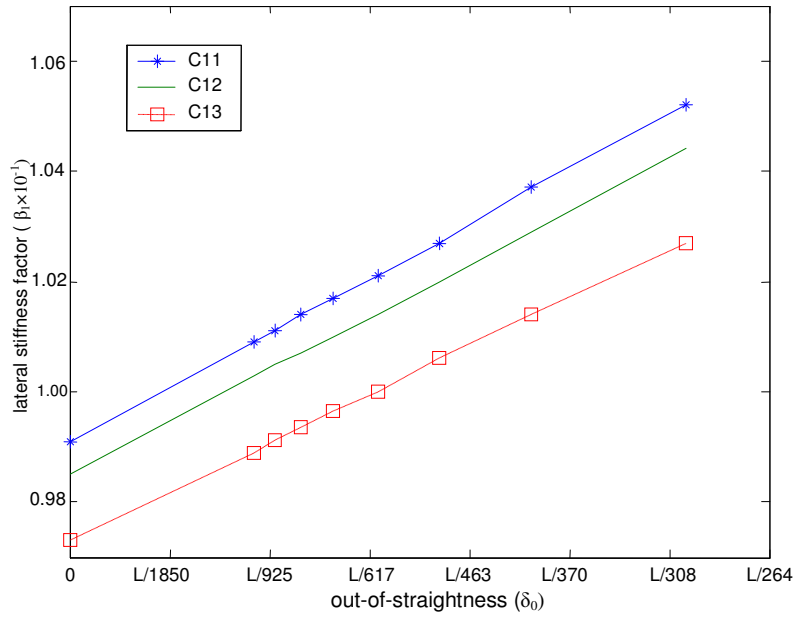


Figure 4-8: Example1 - lateral stiffness coefficients $\beta_{1,ij}$ vs. out-of-straightness (δ_0)

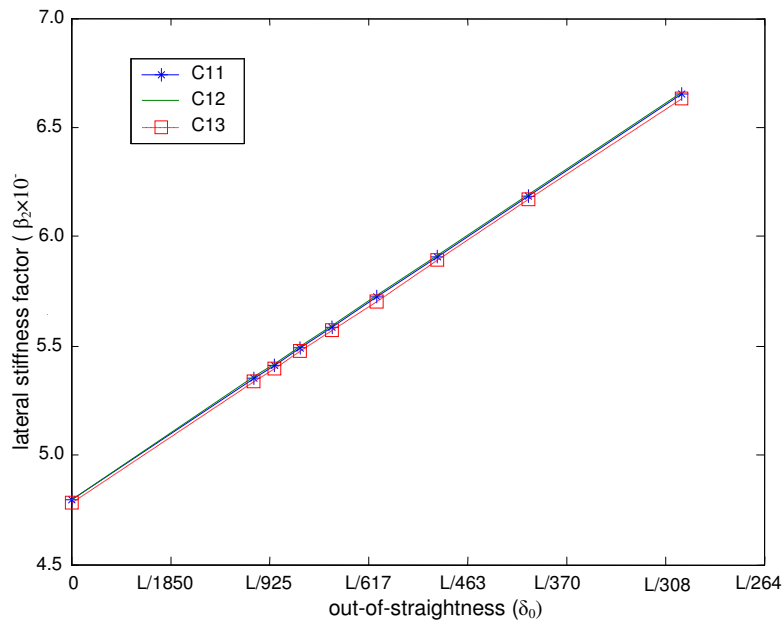


Figure 4-9: Example1 - lateral stiffness coefficients $\beta_{2,ij}$ vs. out-of-straightness (δ_0)

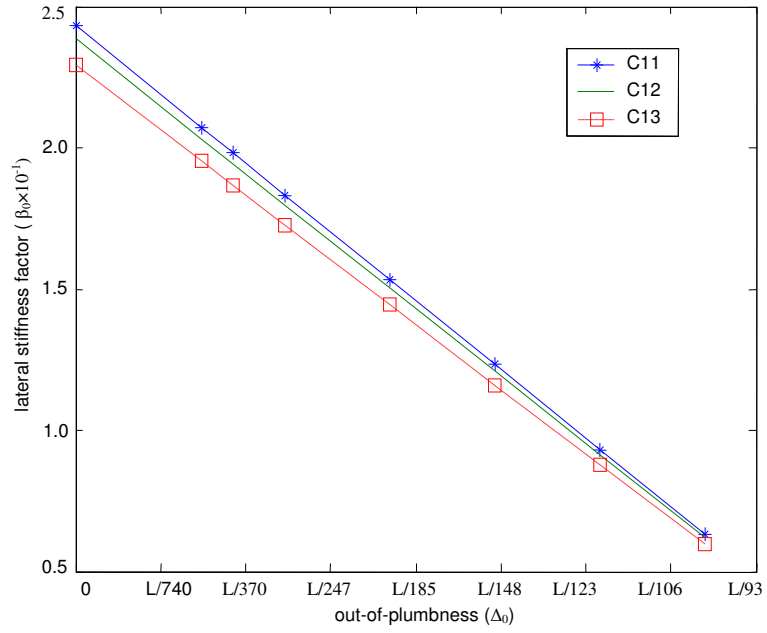


Figure 4-10: Example 1 - lateral stiffness coefficients of $\beta_{0,ij}$ vs. out-of-plumbness (Δ_0)

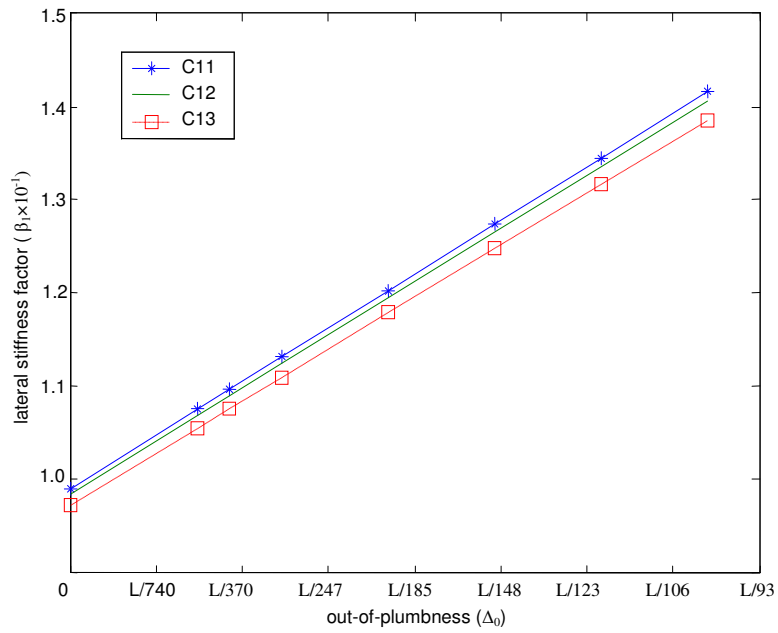


Figure 4-11: Example1 - lateral stiffness coefficients of $\beta_{1,ij}$ vs. out-of-plumbness(Δ_0)

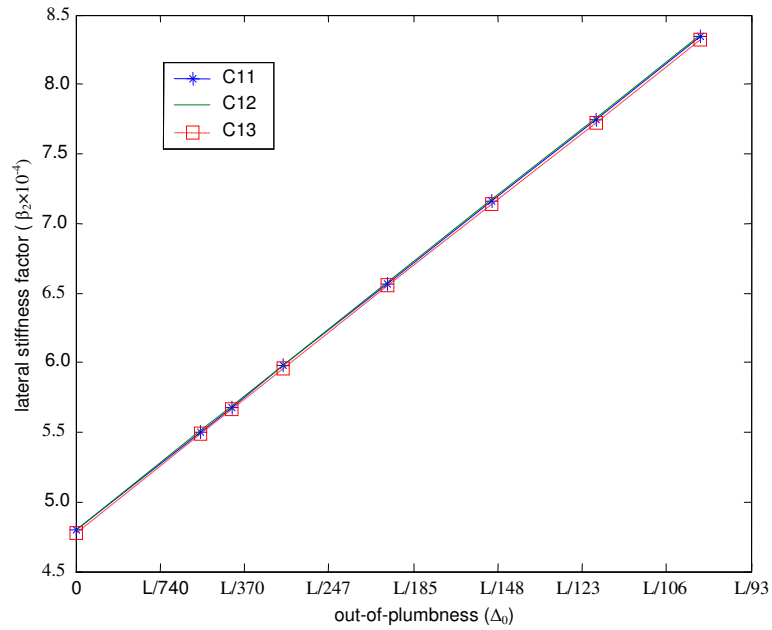


Figure 4-12: Example1 - lateral stiffness coefficients of $\beta_{2,ij}$ vs. out-of-plumbness (Δ_0)

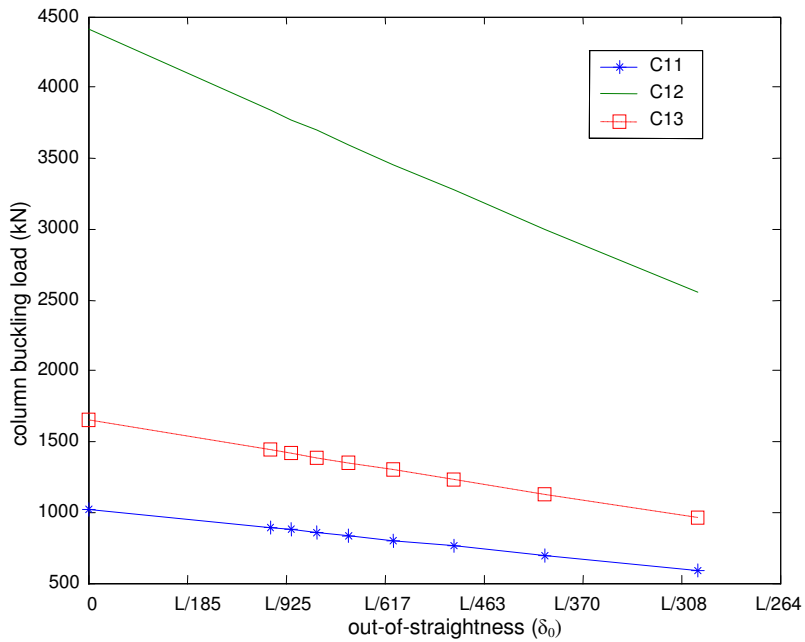


Figure 4-13: Example 1 - column buckling load vs out-of-straightness (δ_0)

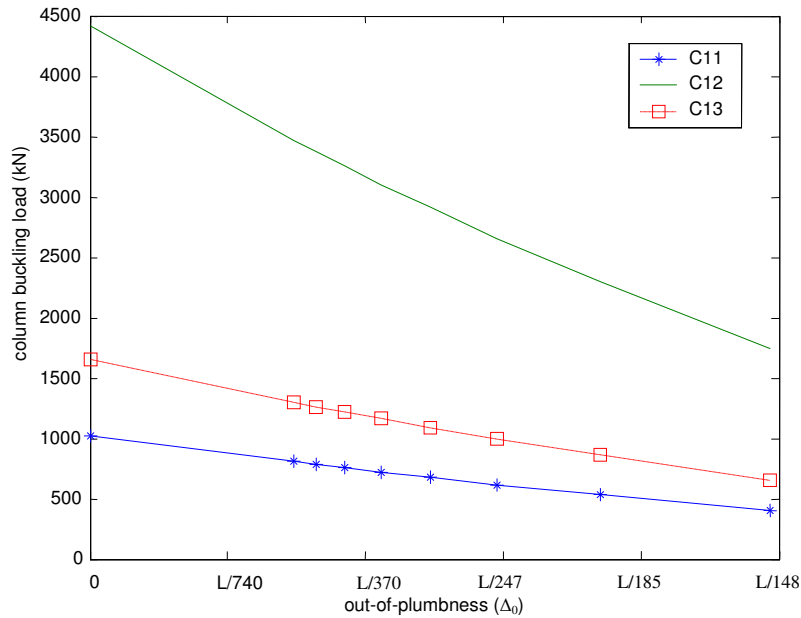


Figure 4-14: Example 1 - column buckling load vs out-of-plumbness (Δ_0)

Example 2

The second example shown in Figure 4-15 is a 1-bay by 3-storey frame that was investigated by Shanmugan et al. (1995), and Liu and Xu (2005). The frame dimension and the material properties are given in Figure 4-15. The applied axial loads are also presented in this figure. Table 4-6 presents the comparison results of the K factors with respect to the 1st-order and 2nd-order approximations of the Taylor series approximation, and the storey-based buckling analysis without accounting for the initial geometric imperfections. Also presented in Table 4-6 are the K factors obtained from the alignment chart method, LeMessurier's method and Lui's method.

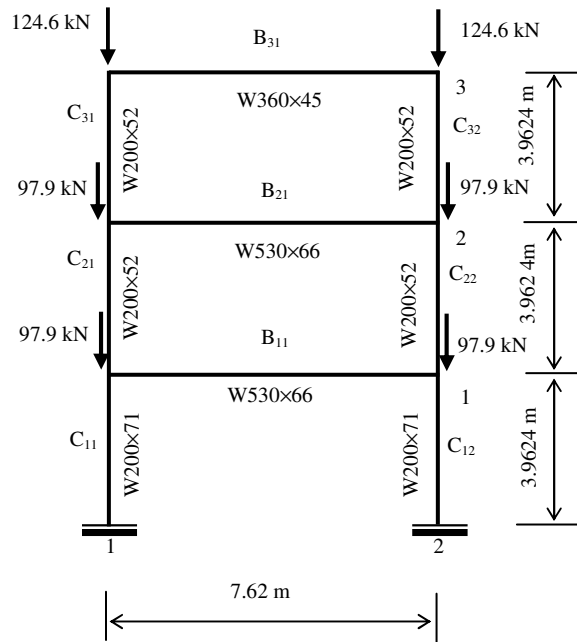


Figure 4-15: 1-bay by 3-storey frame of Example 2 (Shanmugan et al., 1995)

Table 4-6: Example 2 - comparison of K factors

Column	K factors					
	Alignment chart	LeMessurier	Lui	Current study ($\Delta_0=0, \delta_0=0$)		
				1 st -order approxi.	2 nd -order approxi.	Storey-based buckling
$C_{11} = C_{12}$	1.110	1.120	1.140	1.107	1.112	1.112
$C_{21} = C_{22}$	1.210	1.210	1.210	1.207	1.211	1.212
$C_{31} = C_{32}$	1.230	1.230	1.230	1.226	1.229	1.229

In Table 4-6, the column K factors agree very well when comparing three stories among the storey-based buckling method and Alignment charts of LeMessurier and Lui methods, except for the maximum difference noted of 2.5% in storey 1 between the storey-based buckling method and Lui' method. For the comparison K factors within the current study, it is found the maximum difference of

the effective length factor K between 1st-order and 2nd-order approximations are only 0.45%, 0.33% and 0.24% for the columns in stories 1 to 3, respectively. It is noted that the columns K factors of stories 1 and 3 are the same between the 2nd-order approximation and storey-based method, and only a difference of 0.08% is found for storey 2. Comparing the columns K factors between the 1st-order approximation and storey-based method, 0.45%, 0.41 and 0.24% are noted for stories 1, 2 and 3, respectively. Based on the good accordance among the comparisons in this example, it is concluded that the 1st-order approximation can be used to obtain the satisfied K factors in practice.

Similar to Example 1, considering the initial geometric imperfections to evaluate the effective length factor K for Example 2, the maximum allowable out-of-straightness $\delta_0 = L/1000$ and out-of-plumbness $\Delta_0 = L/500$ (AISC, 2005) represent the initial geometric imperfections in this study. The critical loading multipliers together with their effective length factors are obtained from Eqs. (4.23) and (4.21), which correspond to the 1st-order and 2nd-order approximations of λ in the Taylor series approximation of Eq. (4.11) and the results are presented in Table 4-2. The results based on the current study without the consideration of initial geometric imperfections are also given in Table 4-2 for comparison.

Table 4-7: Example 2 - comparison study of three approaches

Col.	Effective length factors (K) ($\delta_0=0, \Delta_0=0$)			Critical loading multiplier (λ_{cr}) ($\delta_0=L/1000, \Delta_0=L/500$)			Effective length factors (K) ($\delta_0=L/1000, \Delta_0=L/500$)		
	1 st - order appro.	2 nd - order appro.	Storey- based buckling	1 st - order Eq. (4.23)	2 nd - order Eq. (4.21)	Storey- based buckling	1 st - order appro.	2 nd - order appro.	Storey- based buckling
$C_{11}=C_{12}$	1.107	1.112	1.112	18.145	18.022	18.006	1.287	1.291	1.292
$C_{21}=C_{22}$	1.207	1.211	1.212	14.952	14.887	14.854	1.413	1.416	1.418
$C_{31}=C_{32}$	1.226	1.229	1.229	26.121	25.998	25.973	1.429	1.432	1.432

It is obvious the initial geometric imperfections would result in a decrease of the lateral stiffness of columns, which consequently increases the values of column K factors and reduces column strengths. For the three column sizes shown in Figure 4-15, based on the storey-based buckling method, the resulting factored axial strength reductions of the columns in the first, second and top stories associated with initial imperfections ($\delta_0=L/1000$ and $\Delta_0=L/500$) are 5%, 6% and 10%, respectively. By examining the columns sizes, it appears to be that the initial geometric imperfections would have a greater impact on columns that are laterally more flexible.

It is observed in Table 4-7, the critical loading multiplier λ_{cr} obtained for the 1st-order and 2nd-order approximations for storey 1 are 18.145 and 18.022, which also verifies the inequality expression (4.24a) and the difference of the λ_{cr} is 0.68%. Therefore, for the columns in storey 1, the differences of the corresponding K factors are only 0.31%. The differences of the corresponding K factors are found only to be 0.21% and 0.21% for the columns in stories 2 and 3, respectively. It is noted that the columns K factors are the same for stories 1 and 3, and a difference of 0.14% is found for storey 2 with respect to the 2nd-order approximation and storey-based buckling methods. Compared to the 1st-order approximation and storey-based buckling methods, the K factors differences are found to be 0.39%, 0.35% and 0.21% with respect to stories 1 to 3, respectively. The good agreement between the 1st-order approximation and storey-based buckling methods indicates the 1st-order approximation can provide satisfactory results and can be recommended for the engineering practice. Also, Figures 4-16 and 4-17 illustrate the K factors from the 1st-order and 2nd-order approximations, and the storey-based buckling results associated with out-of-straightness δ_0 and out-of-plumbness Δ_0 for the columns in stories 1 to 3.

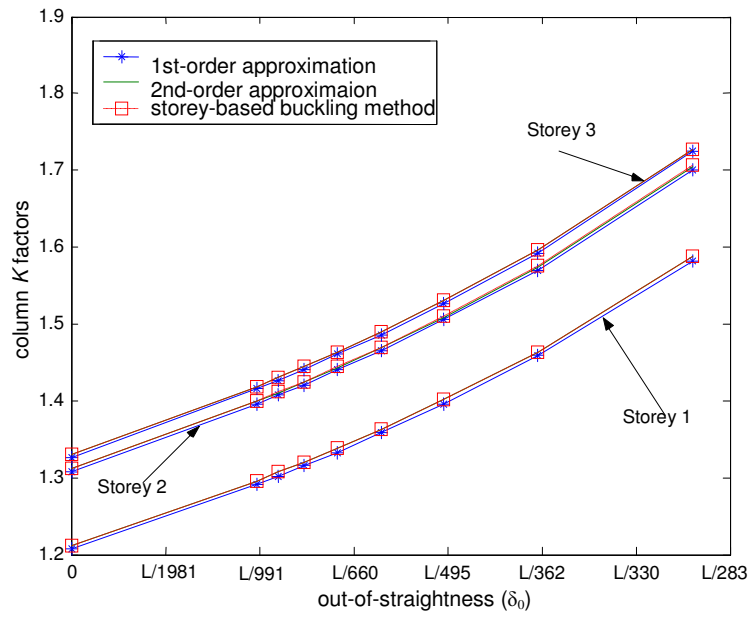


Figure 4-16: Example 2 - column K factors of stories 1 to 3 vs out-of-straightness δ_0

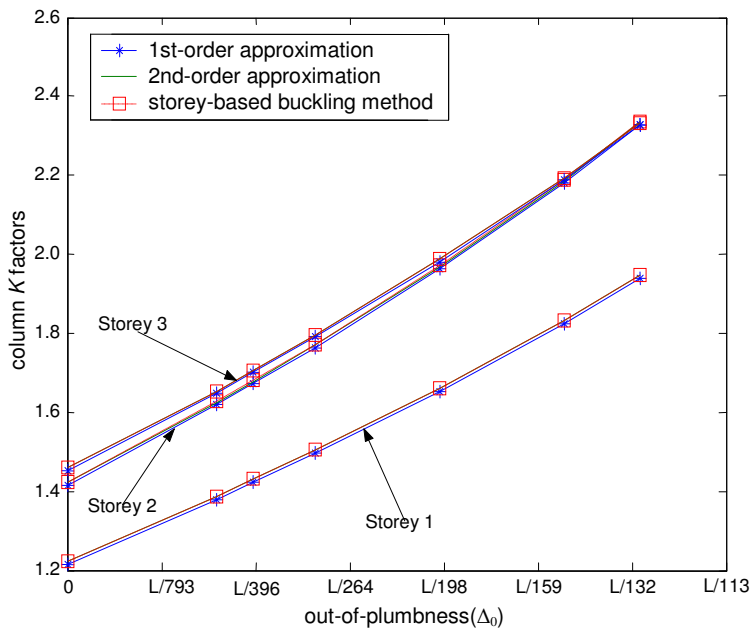


Figure 4-17: Example 2 - column K factors of stories 1 to 3 vs out-of-plumbness (Δ_0)

In Figures 4-16 and 4-17 present the effects of initial geometric imperfections to the columns K factors obtained from 1st-order and 2nd-order approximations, and the storey-based buckling analysis for columns in stories 1 to 3. These two figures demonstrate the K factors increase when increasing the imperfection coefficients of δ_0 or Δ_0 . Comparing the results in Figures 4-16 and 4-17, the matching results among these three approaches demonstrate the 1st-order approximation can be recommended for use in practice.

Presented in Tables 4-8 to 4-10 are parametric studies of the individual and combined effects of the initial imperfections on columns effective length factor including 1st-order and 2nd-order approximation results. Similar to the results obtained from the parametric studies of Example 1, it is noticed that the out-of-straightness (δ_0) has greater influence on the column K factors than that of the out-of-plumbness (Δ_0), which is observed by comparing the K factors associated with the imperfections to be $L/500$, $L/400$, $L/300$ in Tables 4-8 and 4-9. The effects of out-of-straightness (δ_0) and out-of-plumbness (Δ_0) on the factored axial strength of the columns using 1st-order approach are illustrated in Figures 4-18 and 4-19, respectively.

Table 4-8: Example 2 - effects of out-of-straightness on K factors

Column		K factors ($\Delta_0=0$)						
		$\delta_0=$ 0	$\delta_0=$ $L/1000$	$\delta_0=$ $L/800$	$\delta_0=$ $L/600$	$\delta_0=$ $L/500$	$\delta_0=$ $L/400$	$\delta_0=$ $L/300$
1 st -order Approxima tion	$C_{11}= C_{12}$	1.107	1.191	1.215	1.258	1.296	1.358	1.482
	$C_{21}= C_{22}$	1.207	1.296	1.321	1.366	1.405	1.470	1.601
	$C_{31}= C_{32}$	1.226	1.315	1.341	1.386	1.426	1.492	1.624
2 nd -order Approxima tion	$C_{11}= C_{12}$	1.112	1.196	1.220	1.263	1.301	1.363	1.487
	$C_{21}= C_{22}$	1.211	1.299	1.324	1.369	1.409	1.474	1.604
	$C_{31}= C_{32}$	1.229	1.319	1.344	1.390	1.430	1.496	1.628

Table 4-9: Example 2 - effects of out-of-plumbness on K factors

Column		K factors ($\delta_0=0$)				
		$\Delta_0=0$	$\Delta_0=L/500$	$\Delta_0=L/400$	$\Delta_0=L/300$	$\Delta_0=L/200$
1 st -order Approximation	$C_{11}=C_{12}$	1.107	1.190	1.211	1.249	1.327
	$C_{21}=C_{22}$	1.207	1.309	1.336	1.382	1.481
	$C_{31}=C_{32}$	1.226	1.324	1.350	1.395	1.490
2 nd -order Approximation	$C_{11}=C_{12}$	1.112	1.194	1.215	1.253	1.331
	$C_{21}=C_{22}$	1.211	1.312	1.339	1.385	1.484
	$C_{31}=C_{32}$	1.229	1.327	1.353	1.398	1.493

Table 4-10: Example 2 - effects of out-of-straightness and out-of-plumbness on K factors

Column		K factors				
		$\delta_0=0$	$\delta_0=L/1000$	$\delta_0=L/800$	$\delta_0=L/600$	$\delta_0=L/400$
		$\Delta_0=0$	$\Delta_0=L/500$	$\Delta_0=L/400$	$\Delta_0=L/300$	$\Delta_0=L/200$
1 st -order Approximation	$C_{11}=C_{12}$	1.107	1.287	1.341	1.443	1.710
	$C_{21}=C_{22}$	1.207	1.413	1.476	1.595	1.914
	$C_{31}=C_{32}$	1.226	1.429	1.491	1.607	1.915
2 nd -order Approximation	$C_{11}=C_{12}$	1.112	1.291	1.346	1.447	1.713
	$C_{21}=C_{22}$	1.211	1.416	1.479	1.598	1.916
	$C_{31}=C_{32}$	1.229	1.432	1.494	1.610	1.918

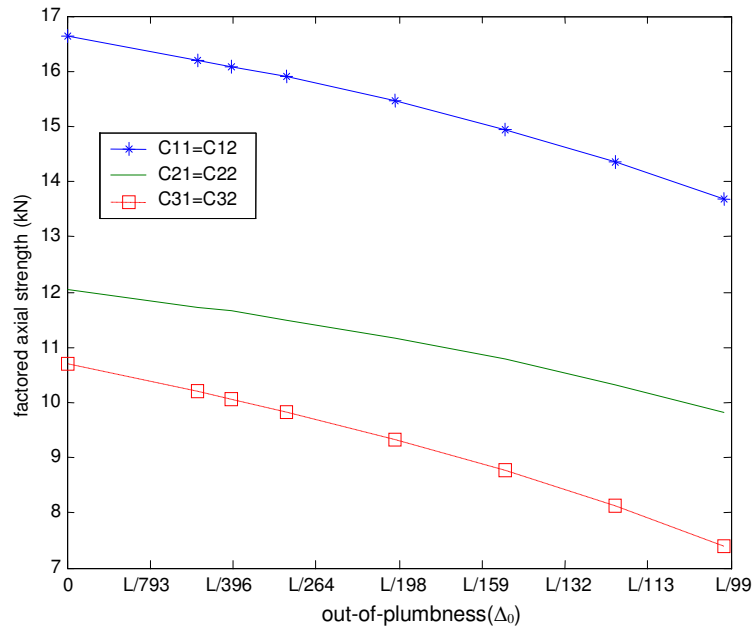


Figure 4-18: Example 2 - factored axial strength vs out-of-straightness (δ_0)

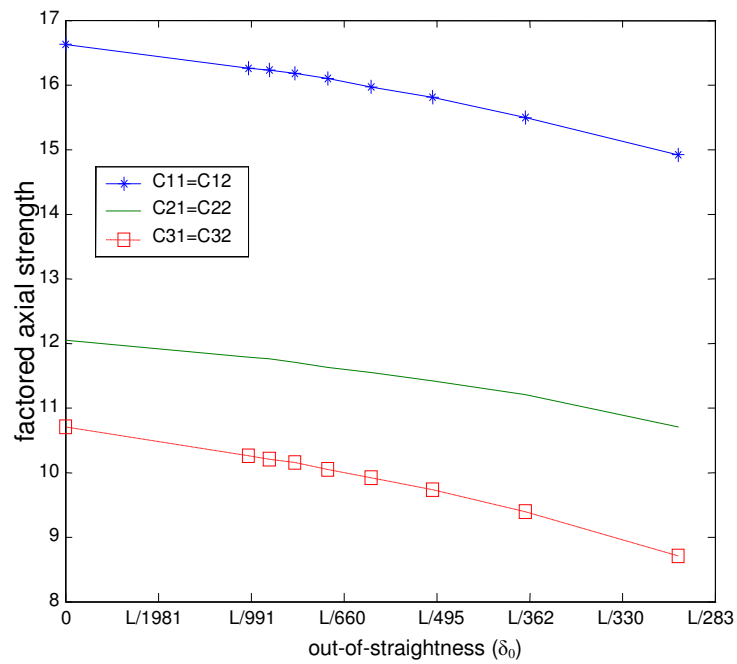


Figure 4-19: Example 2 - the effect of factored axial strength vs out-of-plumbness (Δ_0)

4.5 Conclusions

The stability of columns in multi-storey unbraced frames with initial geometric imperfections has been investigated in this study. The lateral stiffness of the axially loaded column in unbraced frames was derived by incorporating the effects of initial geometric imperfections. The Taylor series expansions including 1st-order and 2nd-order approximations were employed to simplify the stability equation used in the engineering practice. The comparison among the methods of 1st-order and 2nd-order approximations and the storey-based buckling analysis was studied using three numerical examples. The numerical examples demonstrate that the 1st-order approximation can provide sufficient results, thus it should be recommended for use in the design practice.

The results based on the proposed method for the unbraced frames without considering the geometrical imperfection show good agreements with results provided in the literature. In comparing the results with and without geometrical imperfection, it is clear that the K factors increase when considering the geometrical imperfection, and the K factors continue to increase when increasing the initial values of the geometrical imperfections. The results presented for unbraced frames with the initial geometrical imperfections indicate that the geometric imperfections play a key role in the structural analysis and they have to be considered in the design for stability of frames. The parametric studies associated with the effective length factor together with the effects of initial geometric imperfections demonstrated that both the initial geometric imperfections of out-of-straightness and out-of-plumbness influence the K factors. The results presented further indicate that the initial geometric imperfection of out-of-plumbness has a stronger influence for the frame stability than the initial geometric imperfections of out-of-straightness. The K factors have higher values when considering the effects of both out-of-straightness and out-of-plumbness together. In the parametric studies corresponding to the effects between geometric imperfections and lateral stiffness modification factors, the results demonstrated increasing values of geometric imperfections and decreasing values of lateral stiffness modification factors. These effects are major concerns in the practice of structural engineering since these results indicate that the geometric imperfections influence the structural behavior and result in the reductions in stiffness, which will affect the distribution of internal forces in the structural system.

With the literature on the stability design of unbraced frames, much has been studied about the stability analysis on the structures performance assuming perfectly straight and perfectly plumb

members. While the current work is important, typically much less attention has been devoted to explicitly account for the geometric imperfections including out-of-straightness and out-of-plumbness. Furthermore, established design procedures for checking the effective length factor based on storey-based stability analysis in this study is very practical and can be of interest to researchers and design engineers.

Chapter V

Multi-Storey Unbraced Frames with Initial Geometric Imperfections Subjected to Variable Loading

5.1 Introduction

In Chapter 3, the stability of multi-storey unbraced frames subjected to variable loading has been investigated without accounting for initial geometric imperfections. For the single-storey unbraced perfect frames subjected to variable loading, previous research (Xu, 2002) found that the difference between the maximum and minimum elastic buckling loads can be as high as 20% in some cases. In this chapter, the investigation will be focused on the maximum and minimum frame-buckling loadings with initial geometric imperfections including single-storey and multi-storey unbraced frames. As discussed in Chapter 3, the maximization and minimization problems based on 1st-order approximation of the lateral stiffness of an axially loaded column can be solved by a linear programming method to obtain the maximum and minimum bounds of the frame buckling loads subjected to variable loading. In the case of considering the initial geometric imperfections, the study from Chapter 4 indicated that the 1st-order approximation of the column lateral stiffness can provide satisfactory results accounting for the initial geometric imperfections. Therefore, the 1st-order approximation of column lateral stiffness accounting for the initial geometric imperfections will be used to carry out the maximization and minimization problems in this chapter. Following the maximization and minimization problems described in Chapter 3 and stated on Eqs.(3.13),(3.16) and (3.17), the lateral stiffness modification factors of $\beta_{0,ij}(r_{l,ij}, r_{u,ij})$ and $\beta_{1,ij}(r_{l,ij}, r_{u,ij})$ with respect to these equations will be replaced by $\beta_{0,ij}(r_{l,ij}, r_{u,ij}, \delta_0, \Delta_0)$ and $\beta_{1,ij}(r_{l,ij}, r_{u,ij}, \delta_0, \Delta_0)$ given in Eqs. (4.13) accounting for the initial geometric imperfections. Then the linear programming method can be adopted again to obtain the maximum and minimum bounds of the multi-storey unbraced frame buckling loads subjected to variable loading while accounting for the initial geometric imperfections.

5.2 Numerical Examples

5.2.1 Single-Storey Unbraced Frame Example

A 2-bay by 1-storey unbraced steel frame shown in Figure 5-1 is used in Example 1 (Xu, 2002). It is a similar example studied in Example 1 in Chapter 4.

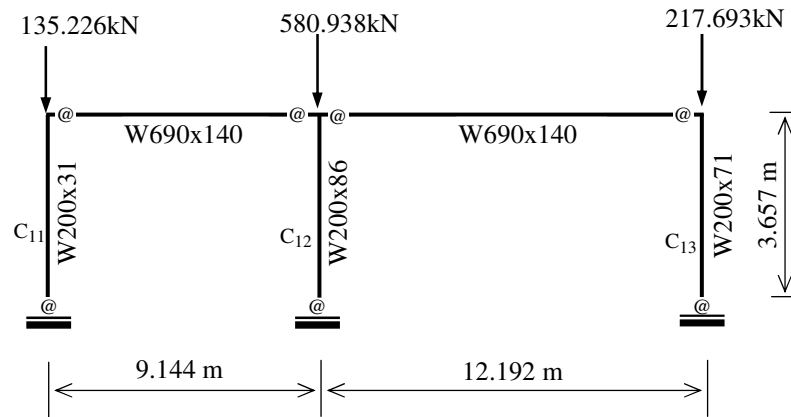


Figure 5-1: 2-bay by 1-storey frame of Example 1 (Xu, 2002)

Evaluated in this section will be what the imperfection effects have on the extreme loadings with different beam-to-column connections for single-storey frame and will be compared with the results without accounting for the initial geometric imperfections previously studied by Xu (2002). In engineering practice a connection can neither be ideally rigid with a member end-fixity factor $r = 1$ nor purely pinned with $r = 0$. From previous research in connections of building design, Gerstle (1988), Craig (2000) and Xu (2002) recommended that three different values of $r = 1.0, 0.9,$ and 0.8 can be used for rigid connection and $r = 0.0, 0.1,$ and 0.2 can be used for pinned connection.

The 15 different combinations of beam-to-column connection frames are illustrated in Figure 5-2. Three schemes of rigid and pinned connections, in which scheme 1 ($r = 1, r = 0$), scheme 2 ($r = 0.9, r = 0.1$) and scheme 3 ($r = 0.8, r = 0.2$) are used for the comparison of the relative difference of the maximum and minimum buckling loads. In the case of not accounting for the initial geometric imperfections, the previous research (Xu, 2002) found that the difference between the maximum and minimum elastic buckling loads can be as high as 20% illustrated in Figure 5-3 for the 15 different combinations of beam-to-column connections frames shown Figure 5-2.

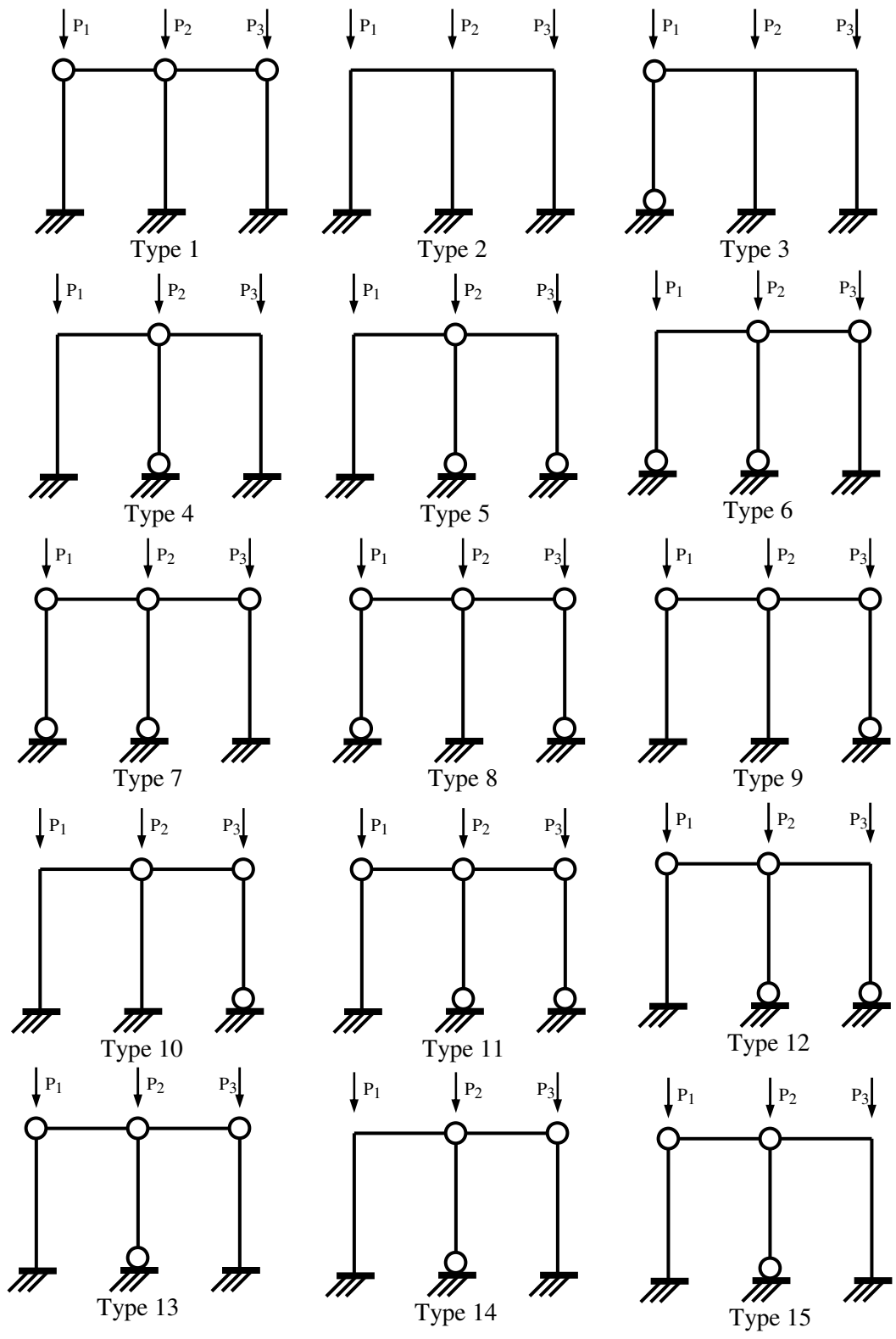


Figure 5-2: 15 frames with different beam-to-column connections used in study

Knowing the initial geometric imperfections of out-of-straightness ($\delta_0=L/1000$) and out-of-plumbness ($\Delta_0=L/500$) (AISC, 2005), the results of the relative difference of the maximum and minimum frame-buckling loads for the 15 frame types (shown in Figure 5-2) together with the three schemes of rigid and pinned connections are presented in Tables 5-1 to 5-3 and Figure 5-3. The results without accounting for the out-of-straightness and out-of-plumbness are also presented in Tables 5-1 to 5-3.

Table 5-1: Comparison of the max. and min. buckling loads together with their relative difference with three different schemes (1)

Frame Type	Scheme	out-of-straightness: $\delta_0=0$ out-of-plumbness: $\Delta_0=0$			out-of-straightness: $\delta_0=L/1000$ out-of-plumbness: $\Delta_0=L/500$		
		Max. frame buckling load (kN)	Min. frame buckling load (kN)	$\frac{Max. - Min.}{Min.}$	Max. frame buckling load (kN)	Min. frame buckling load (kN)	$\frac{Max. - Min.}{Min.}$
1	Scheme 1 ($r=1, r=0$)	7475.800	7475.800	0%	6126.200	6126.200	0%
	Scheme 2 ($r=0.9, r=0.1$)	16685.000	16534.000	0.91%	12852.000	12744.000	0.85%
	Scheme 3 ($r=0.8, r=0.2$)	19136.000	18795.000	1.81%	14538.000	14146.000	2.78%
2	Scheme 1 ($r=1, r=0$)	28894.000	28490.000	1.42%	21606.000	21222.000	1.81%
	Scheme 2 ($r=0.9, r=0.1$)	26683.000	26259.000	1.61%	19920.200	19516.000	2.07%
	Scheme 3 ($r=0.8, r=0.2$)	24298.000	23851.000	1.87%	18095.000	17667.000	2.42%
3	Scheme 1 ($r=1, r=0$)	24952.000	24200.000	3.11%	18873.000	18088.000	4.34%
	Scheme 2 ($r=0.9, r=0.1$)	23816.000	23360.000	1.95%	17792.000	17376.000	2.39%
	Scheme 3 ($r=0.8, r=0.2$)	21956.000	21742.000	0.99%	16310.000	16124.000	1.16%
4	Scheme 1 ($r=1, r=0$)	16257.000	14057.000	15.65%	12619.000	10520.000	19.96%
	Scheme 2 ($r=0.9, r=0.1$)	17302.000	15930.000	8.62%	12837.000	11747.000	9.28%
	Scheme 3 ($r=0.8, r=0.2$)	16974.000	16307.000	4.09%	12497.000	11947.000	4.61%
5	Scheme 1 ($r=1, r=0$)	7820.200	6618.900	18.15%	5725.700	4773.000	19.96%
	Scheme 2 ($r=0.9, r=0.1$)	10706.000	9843.600	8.76%	7712.700	7057.500	9.28%
	Scheme 3 ($r=0.8, r=0.2$)	12177.000	11653.000	4.50%	8783.300	8396.300	4.61%

Table 5-2: Comparison of the max. and min. buckling loads together with their relative difference with three different schemes (2)

Frame Type	Scheme	out-of-straightness: $\delta_0=0$ out-of-plumbness: $\Delta_0=0$			out-of-straightness: $\delta_0=L/1000$ out-of-plumbness: $\Delta_0=L/500$		
		Max. frame buckling load (kN)	Min. frame buckling load (kN)	$\frac{Max. - Min.}{Min.}$	Max. frame buckling load (kN)	Min. frame buckling load (kN)	$\frac{Max. - Min.}{Min.}$
6	Scheme 1 ($r=1, r=0$)	4666.600	38889.000	20.00%	3681.200	3037.400	21.20%
	Scheme 2 ($r=0.9, r=0.1$)	10056.000	9124.200	10.21%	7470.100	6657.000	12.21%
	Scheme 3 ($r=0.8, r=0.2$)	14947.000	14323.000	4.36%	10935.000	10297.000	6.20%
7	Scheme 1 ($r=1, r=0$)	3436.000	2863.300	20.00%	2834.000	2346.400	20.78%
	Scheme 2 ($r=0.9, r=0.1$)	9505.800	8961.400	6.08%	7108.200	6734.600	5.55%
	Scheme 3 ($r=0.8, r=0.2$)	12180.000	11931.000	2.09%	9043.900	8704.100	3.90%
8	Scheme 1 ($r=1, r=0$)	4329.000	3532.500	20.00%	3496.300	2894.800	20.78%
	Scheme 2 ($r=0.9, r=0.1$)	11633.000	10823.000	7.48%	8787.100	8178.600	7.44%
	Scheme 3 ($r=0.8, r=0.2$)	14176.000	13483.000	5.14%	10559.000	9922.600	6.41%
9	Scheme 1 ($r=1, r=0$)	5535.000	4612.500	20.00%	4565.200	3779.800	20.78%
	Scheme 2 ($r=0.9, r=0.1$)	13799.000	12803.000	7.78%	10495.000	9717.000	8.00%
	Scheme 3 ($r=0.8, r=0.2$)	16019.000	15217.000	5.28%	11998.000	11337.000	5.83%
10	Scheme 1 ($r=1, r=0$)	9165.900	7638.300	20.00%	7230.000	5986.200	20.78%
	Scheme 2 ($r=0.9, r=0.1$)	15496.000	13740.000	12.77%	11753.000	10282.500	14.31%
	Scheme 3 ($r=0.8, r=0.2$)	16889.000	15574.000	8.44%	12626.000	11497.000	9.83%

Table 5-3: Comparison of the max. and min. buckling loads together with their relative difference with three different schemes (3)

Frame Type	Scheme	out-of-straightness: $\delta_0=0$ out-of-plumbness: $\Delta_0=0$			out-of-straightness: $\delta_0=L/1000$ out-of-plumbness: $\Delta_0=L/500$		
		Max. frame buckling load (kN)	Min. frame buckling load (kN)	$\frac{Max. - Min.}{Min.}$	Max. frame buckling load (kN)	Min. frame buckling load (kN)	$\frac{Max. - Min.}{Min.}$
11	Scheme 1 ($r=1, r=0$)	1296.000	1080.000	20.00%	1068.900	885.000	20.78%
	Scheme 2 ($r=0.9, r=0.1$)	8071.300	7270.500	11.01%	5943.100	5339.400	11.31%
	Scheme 3 ($r=0.8, r=0.2$)	10659.000	10097.000	5.57%	7791.200	7362.000	5.83%
12	Scheme 1 ($r=1, r=0$)	4189.200	3491.000	20.00%	3060.800	2534.300	20.78%
	Scheme 2 ($r=0.9, r=0.1$)	9494.400	8870.700	7.03%	6853.200	6333.200	8.21%
	Scheme 3 ($r=0.8, r=0.2$)	11631.000	11300.000	2.93%	8404.900	8127.600	3.41%
13	Scheme 1 ($r=1, r=0$)	4731.900	3943.300	20.00%	3902.800	3231.400	20.78%
	Scheme 2 ($r=0.9, r=0.1$)	11625.000	10959.000	6.08%	8871.700	8310.700	5.55%
	Scheme 3 ($r=0.8, r=0.2$)	13971.000	13645.000	2.39%	10444.000	10140.000	3.00%
14	Scheme 1 ($r=1, r=0$)	8362.900	6969.100	20.00%	6567.700	5437.800	20.78%
	Scheme 2 ($r=0.9, r=0.1$)	12852.000	11741.000	9.46%	9634.700	8749.900	10.11%
	Scheme 3 ($r=0.8, r=0.2$)	14598.000	13823.000	5.60%	10918.000	10214.000	6.89%
15	Scheme 1 ($r=1, r=0$)	11682.000	10140.000	15.20%	8885.600	7630.800	16.44%
	Scheme 2 ($r=0.9, r=0.1$)	14046.000	13136.000	6.93%	10381.000	9692.300	7.11%
	Scheme 3 ($r=0.8, r=0.2$)	14680.000	14336.000	2.40%	10767.000	10499.000	2.55%

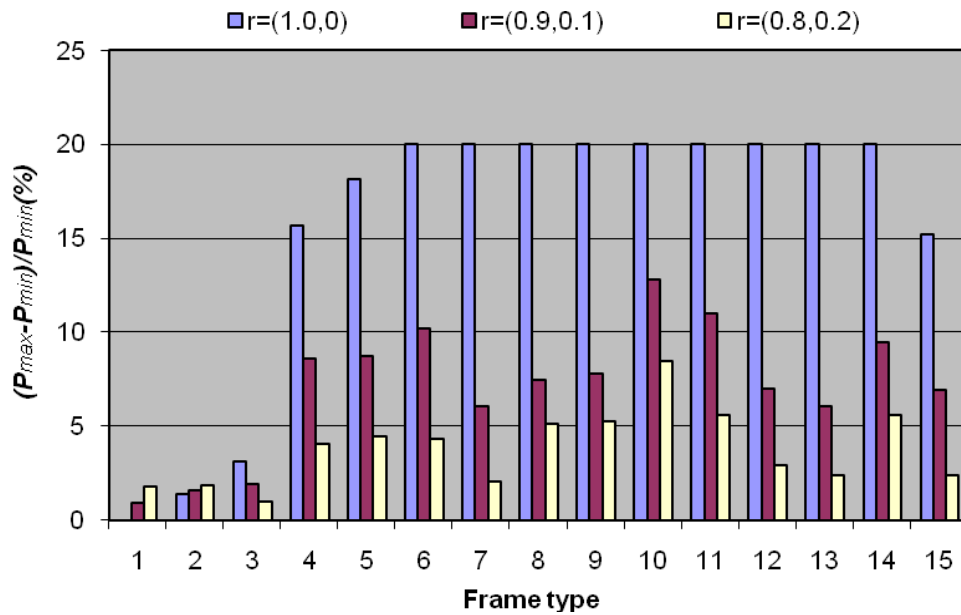


Figure 5-3: Relative differences of the critical buckling loads($(P_{max}-P_{min})/P_{min}$) of three schemes without initial geometric imperfections

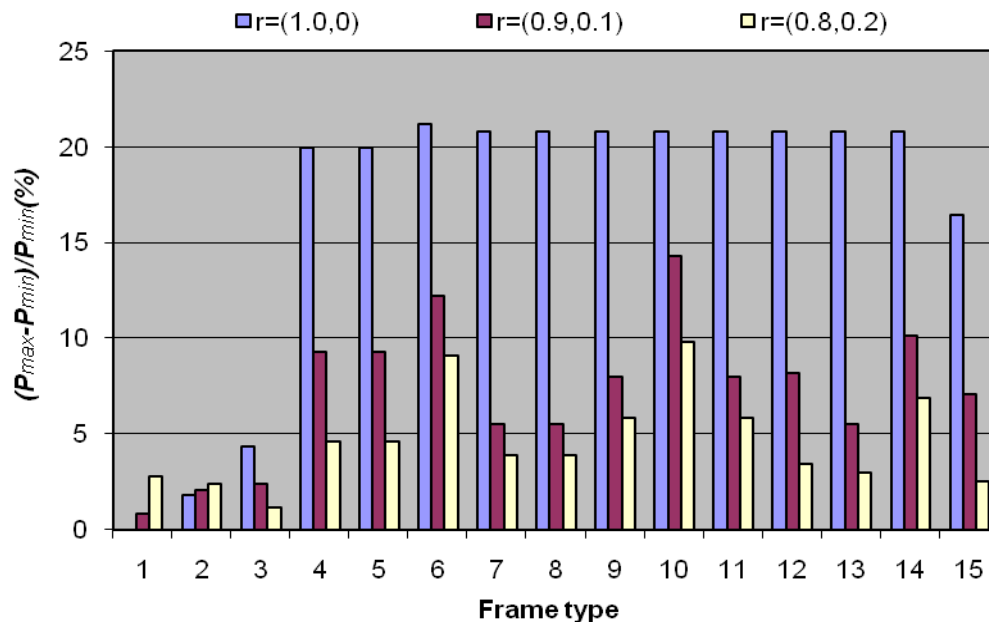


Figure 5-4: Relative differences of the critical buckling loads($(P_{max}-P_{min})/P_{min}$) of three schemes with initial geometric imperfections

It is noted in Figure 5-2 and Tables 5-1 to 5-3, that for each frame with three schemes, the presence of the initial geometric imperfections reduce the maximum and minimum frame-buckling loads and increase the relative difference between these two extreme frame-buckling loads. From Tables 5-1 to 5-3, it is also found for these 15 frames with or without initial geometric imperfections, the magnitudes of the maximum and minimum frame-buckling loads increase when the beam-to-column connection rigidity reduce from Schemes 1 to 3, except types 2, 3 and 4 frames. In Tables 5-1 to 5-3, it is noted that the relative difference between the extreme frame-buckling loads of the same frame type with respect to initial geometric imperfections higher than those without accounting for initial geometric imperfection except for frame types 1, 7, 8 and 13.

When accounting for the initial geometric imperfections, for frame type 1, in which all the column base connections are fully rigid and the beam-to-column connections are pinned, there is no difference between the maximum and minimum buckling loads of scheme 1. It is also observed that relative differences between the extreme buckling loads among the three schemes are negligible for frame types 1 and 2 since the relative differences are less than 3%. For frame type 3, the relative differences for schemes 1 and 2 can be also negligible. Table 4-16 and Figure 4-20 presented that in scheme 1 with ($r = 1, r = 0$), the relative difference for frame types 4 and 5 obtain their maximum of 20%, frame 6 obtains the largest maximum of 21.2% and the other frames 7 to 14 reach their maximum of 20.78%. For frame 15, its relative difference is 16.44% for scheme 1. It is also seen that there is at least one lean-on column in frames 4 to 15. However in schemes 2 ($r = 0.9, r = 0.1$) and 3 ($r = 0.8, r = 0.2$), the maximum relative differences between the buckling loads are much lower than that of scheme 1 for frames 4 to 15. This study also finds that in the case of initial geometric imperfection, the increase of the critical buckling loads is primarily due to the increase of the end-fixity factor for pinned connections from $r = 0$, to $r = 0.1$ and $r = 0.2$.

5.2.2 Multi-Storey Unbraced Frame Example

In this study, the multi-storey unbraced frame example used in Chapter 3 will be investigated again to evaluate the influences of the initial geometric imperfections to the multi-storey unbraced frames subjected to the variable loadings. The effects of semi-rigid connections are also considered in this study. For the 2-bay by 2-storey steel frames shown in Figures 3-5 to 3-8, the same procedures described in Chapter 3 with respect to the effects of initial geometric imperfections to the lateral

stiffness of column investigated in Chapter 4 will be adopted in this study. Then the critical buckling loads of the 2-bay by 2-storey unbraced steel frames associated with the effects of initial geometric imperfections subjected to variable loading can be obtained from Eqs. (3.1) to (3.5). The objectives of this example are to demonstrate the proposed method for evaluating the extreme loadings in a frame with accounting for initial geometric imperfections of out-of-straightness and out-of-plumbness and the different beam-to-column connections with these geometrically imperfect considerations.

In the foregoing studies described in Table 3-1 of Chapter 3, the first case of the rigid frame (Figure 3-5) was considered in the parametric studies to demonstrate the influences of the geometric imperfections to frame buckling loadings. The values of the geometric imperfections including the out-of-straightness (δ_0) effect, out-of-plumbness (Δ_0) effect and combined effects of out-of-straightness (δ_0) and out-of-plumbness (Δ_0) are given in Tables 5-4 to 5-10. Also presented in these tables are the values of the buckling loads corresponding to the maximum and minimum frame-buckling loads, together with their relative differences.

Table 5-4: The effect of out-of-straightness (δ_0) to frame buckling loadings (1)

Col.	$\delta_0=L/1000, \Delta_0=0$			$\delta_0=L/800, \Delta_0=0$		
	Max. (kN)	Min. (kN)		Max. (kN)	Min. (kN)	
		$S_1 = 0, S_2 > 0$	$S_1 > 0, S_2 = 0$		$S_2 = 0$	$S_1 = 0, S_2 > 0$
11	27341.140	0.000	0.000	25997.680	0.000	0.000
12	0.000	28611.160	0.000	0.000	27260.700	0.000
13	0.000	0.000	0.000	0.000	0.000	0.000
21	69068.640	0.000	57551.410	67121.730	0.000	0.000
22	0.000	65611.470	0.000	0.000	63697.710	5801.400
23	0.000	0.000	0.000	0.000	0.000	57570.000
$\sum P_{ij}$	96409.780	94222.630	65299.950	93119.410	90958.410	63371.400
$\frac{\text{max.} - \text{min.}}{\text{min.}} \%$	$S_2=0.000$	$S_1=9590.620$	$\frac{\text{max.} - \text{min.}}{\text{min.}} \%$	$S_2=0.000$	$S_1=91867.910$	
	2.3% (storey-buckling)	47.6% (storey-buckling)		2.4% (storey-buckling)	46.9% (storey-buckling)	
$\frac{\text{max.} - \text{min.}}{\text{min.}} \%$	47.6% (frame-buckling)			$\frac{\text{max.} - \text{min.}}{\text{min.}} \%$	46.9% (frame-buckling)	

Table 5-5: The effects of out-of-straightness (δ_0) to frame buckling loadings (2)

Col.	$\delta_0=L/600, \Delta_0=0$			$\delta_0=L/500, \Delta_0=0$		
	Max. (kN)	Min. (kN)		Max. (kN)	Min. (kN)	
		$S_1 = 0, S_2 > 0$	$S_1 > 0, S_2 = 0$		$S_1 = 0, S_2 > 0$	$S_1 > 0, S_2 = 0$
11	23755.030	0.000	0.000	21995.460	0.000	0.000
12	0.000	25021.340	0.000	0.000	23237.980	0.000
13	0.000	0.000	0.000	0.000	0.000	0.000
21	63933.030	0.000	0.000	61399.040	0.000	51218.600
22	0.000	60564.520	2669.520	0.000	58092.180	182.800
23	0.000	0.000	57570.000	0.000	0.000	57570.000
ΣP_{ij}	87688.060	85585.860	60239.520	83394.500	81330.150	57752.800
$\frac{\text{max.} - \text{min.}}{\text{min.}} \%$	$S_2=0.000$	$S_1=8486.860$	45.6% (storey-buckling)	$S_2=0.000$	$S_1=7940.030$	44.4% (storey-buckling)
	2.5% (storey-buckling)			2.5% (storey-buckling)		
$\frac{\text{max.} - \text{min.}}{\text{min.}} \%$	45.6% (frame-buckling)			$\frac{\text{max.} - \text{min.}}{\text{min.}} \%$	44.4% (frame-buckling)	

Table 5-6: The effects of out-of-straightness (δ_0) to frame buckling loadings (3)

Col.	$\delta_0=L/400, \Delta_0=0$			$\delta_0=L/300, \Delta_0=0$		
	Max. (kN)	Min. (kN)		Max. (kN)	Min. (kN)	
		$S_1 = 0, S_2 > 0$	$S_1 > 0, S_2 = 0$		$S_1 = 0, S_2 > 0$	$S_1 > 0, S_2 = 0$
11	19377.880	0.000	0.000	15183.210	0.000	0.000
12	0.000	20604.460	0.000	0.000	16398.280	0.000
13	0.000	0.000	0.000	0.000	0.000	0.000
21	57582.600	0.000	0.000	51292.860	0.000	0.000
22	0.000	54373.330	0.000	0.000	48267.650	0.000
23	0.000	0.000	54041.880	0.000	0.000	47963.210
$\sum P_{ij}$	76960.490	74977.790	54041.880	66476.080	64666.280	47963.210
$\frac{\max - \min}{\min} \%$		$S_2=0.000$	$S_1=7102.480$	$\frac{\max - \min}{\min} \%$	$S_2=0.000$	$S_1=5734.550$
		2.6% (storey-buckling)	42.4% (storey-buckling)		2.8% (storey-buckling)	38.6% (storey-buckling)
$\frac{\max - \min}{\min} \%$		42.4% (frame-buckling)		$\frac{\max - \min}{\min} \%$	38.5% (frame-buckling)	

Table 5-7: The effects of out-of-plumbness (Δ_0) to frame buckling loadings (4)

Col.	$\delta_0=0, \Delta_0=L/500$			$\delta_0=0, \Delta_0=L/400$		
	Max. (kN)	Min. (kN)		Max. (kN)	Min. (kN)	
		$S_1 = 0, S_2 > 0$	$S_1 > 0, S_2 = 0$		$S_1 = 0, S_2 > 0$	$S_1 > 0, S_2 = 0$
11	29081.520	0.000	0.000	28170.560	0.000	0.000
12	0.000	29817.500	0.000	0.000	28785.640	0.000
13	0.000	0.000	0.000	0.000	0.000	0.000
21	67618.530	0.000	0.000	65472.400	0.000	0.000
22	0.000	64574.220	6678.380	0.000	62550.710	4659.580
23	0.000	0.000	57570.000	0.000	0.000	57570.000
$\sum P_{ij}$	96700.060	94391.720	64248.380	93642.96 0	91336.350	62229.580
$\frac{\max - \min}{\min} \%$		$S_2=0.000$	$S_1=10509.620$		$S_2=0.000$	$S_1=10315.050$
		2.5% (storey-buckling)	50.5% (storey-buckling)		2.5% (storey-buckling)	50.5% (storey-buckling)
$\frac{\max - \min}{\min} \%$		50.5% (frame-buckling)		$\frac{\max - \min}{\min} \%$	50.5% (frame-buckling)	

Table 5-8: The effects of out-of-plumbness (Δ_0) to frame buckling loadings (5)

Col.	$\delta_0=0, \Delta_0=L/300$			$\delta_0=0, \Delta_0=L/200$		
	Max. (kN)	Min. (kN)		Max. (kN)	Min. (kN)	
		$S_1 = 0, S_2 > 0$	$S_1 > 0, S_2 = 0$		$S_1 = 0, S_2 > 0$	$S_1 > 0, S_2 = 0$
11	26760.400	0.000	0.000	24036.810	0.000	0.000
12	0.000	27206.040	0.000	0.000	24239.330	0.000
13	0.000	0.000	0.000	0.000	0.000	0.000
21	62046.630	0.000	0.000	55687.440	0.000	0.000
22	0.000	59296.860	1399.020	0.000	53263.950	0.000
23	0.000	0.000	57570.000	0.000	0.000	53263.950
ΣP_{ij}	88807.030	86502.900	58969.020	79724.250	77503.290	53263.950
$\frac{\max - \min}{\min} \%$	$S_2=0.000$	$S_1=10010.060$	$\frac{\max - \min}{\min} \%$	$S_2=0.000$	$S_1=9223.070$	
	2.7% (storey-buckling)	50.6% (storey-buckling)		2.9% (storey-buckling)	49.7% (storey-buckling)	
$\frac{\max - \min}{\min} \%$	50.6% (frame-buckling)		$\frac{\max - \min}{\min} \%$	49.7% (frame-buckling)		

Table 5-9: The effects of combined out-of-straightness (δ_0) and out-of-plumbness (Δ_0) to frame buckling loadings (6)

Col.	$\delta_0=L/1000$ and $\Delta_0=L/500$			$\delta_0=L/800$ and $\Delta_0=L/400$		
	Max. (kN)	Min. (kN)		Max. (kN)	Min. (kN)	
		$S_1 = 0, S_2 > 0$	$S_1 > 0, S_2 = 0$		$S_1 = 0, S_2 > 0$	$S_1 > 0, S_2 = 0$
11	23876.000	0.000	0.000	21870.860	0.000	0.000
12	0.000	24663.670	0.000	0.000	22531.770	0.000
13	0.000	0.000	0.000	0.000	0.000	0.000
21	60369.780	0.000	0.000	56577.910	0.000	0.000
22	0.000	57430.540	0.000	0.000	53797.940	0.000
23	0.000	0.000	57081.330	0.000	0.000	53462.880
ΣP_{ij}	84245.780	82094.210	57081.330	78448.770	76329.710	53462.880
		$S_2=0.000$	$S_1=8848.790$		$S_2=0.000$	$S_1=8248.900$
	$\frac{\text{max}-\text{min}}{\text{min}}\%$	2.6% (storey-buckling)	47.6% (storey-buckling)	$\frac{\text{max}-\text{min}}{\text{min}}\%$	2.8% (storey-buckling)	46.7% (storey-buckling)
	$\frac{\text{max}-\text{min}}{\text{min}}\%$	47.6% (frame-buckling)		$\frac{\text{max}-\text{min}}{\text{min}}\%$	46.7% (frame-buckling)	

Table 5-10: The effects of combined out-of-straightness (δ_0) and out-of-plumbness (Δ_0) to frame buckling loadings (7)

Col.	$\delta_0=L/600$ and $\Delta_0=L/300$			$\delta_0=L/400$ and $\Delta_0=L/200$		
	Max. (kN)	Min. (kN)		Max. (kN)	Min. (kN)	
		$S_1 = 0, S_2 > 0$	$S_1 > 0, S_2 = 0$		$S_1 = 0, S_2 > 0$	$S_1 > 0, S_2 = 0$
11	18605.780	0.000	47681.300	12763.800	0.000	0.000
12	0.000	19183.720	0.000	0.000	13143.450	0.000
13	0.000	0.000	0.000	0.000	0.000	0.000
21	50526.590	0.000	0.000	39316.240	0.000	0.000
22	0.000	47987.310	0.000	0.000	37277.150	0.000
23	0.000	0.000	47673.290	0.000	0.000	37011.490
ΣP_{ij}	69132.370	67121.030	47673.290	52080.040	50420.600	37011.490
$\frac{\text{max}-\text{min}}{\text{min}}\%$	$S_2=0.000$	$S_1=7249.490$	$\frac{\text{max}-\text{min}}{\text{min}}\%$	$S_2=0.000$	$S_1=5290.000$	
	3.0% (storey-buckling)	45% (storey-buckling)		3.3% (storey-buckling)	40.7% (storey-buckling)	
$\frac{\text{max}-\text{min}}{\text{min}}\%$	45% (frame-buckling)			$\frac{\text{max}-\text{min}}{\text{min}}\%$	40.7% (frame-buckling)	

Presented in tables 5-4 to 5-6 are the results of the frame-buckling loads associated with the initial geometric imperfection of out-of-straightness δ_0 (only). The first stability constraint described as $S_1 = 0, S_2 > 0$ represents the case of laterally unstable for first storey found in Tables 5-4 to 5-6. The minimum storey-buckling load is only applied onto the interior columns 12 and 22 and the second storey becomes lateral unstable simultaneously. The second stability constraint defined as $S_1 > 0, S_2 = 0$, shows the frames with respect to the case of laterally unstable for second storey and the load pattern corresponding to the minimum storey-buckling loads is applied onto both the interior and exterior columns 22 and 23 and the first storey is lateral stable. Another observation can be seen that the load magnitudes and patterns are identical when the frames are subjected to maximum frame-buckling loads and the load patterns applied on the exterior columns 11 and 21. Also it is noted the first second stories become lateral unstable simultaneously when the frame archived to its maximum

frame-buckling loads. And It is seen that the extreme frame-buckling loads together with the load patterns decrease when the initial geometric imperfection of out-of-straightness (δ_0). Also from Tables 5-4 to 5-6, the relative difference between the maximum and minimum frame-buckling loads are found to be 47.6%, 46.9%, 45.6%, 44.4%, 42.4% and 38.6% with respect to the δ_0 values of $L/1000$, $L/800$, $L/600$, $L/500$, $L/400$ and $L/300$, respectively, which are significant.

In Tables 5-7 and 5-8, the results show that the maximum frame-buckling loads are decreased when increasing the values of the member out-of-plumbness Δ_0 (only). It can also be ascertained that the maximized frame-buckling loads occur when the first and second stories become laterally unstable simultaneously. From Tables 5-7 and 5-8 we can see that the minimum frame-buckling loads with respect to lateral instability of the first and second stories decrease when increasing the initial geometric imperfection out-of-plumbness (Δ_0). Also in Tables 5-7 and 5-8 we can see the relative difference between the maximum and minimum frame-buckling loads are all very close to 50.5% with respect to the Δ_0 values of $L/500$, $L/400$, $L/300$ and $L/200$ respectively, which may suggest that the values of Δ_0 appear to be not have much influence on the difference between the maximum and minimum frame-buckling loads.

Once the frames are subjected to combined initial geometric imperfections of an out-of-straightness member and an out-of-plumbness frame, the frames become more flexible and the magnitudes of the maximum and minimum frame-buckling loads decrease as shown in Tables 5-9 and 5-10.

In Tables 5-9 and 5-10, the values exhibit similar trends is the result of Tables 5-4 to 5-8. It is seen that the extreme buckling loads decrease when increasing the values of member out-of-straightness (δ_0) and frame out-of-plumbness (Δ_0). It is also seen that the maximum frame-buckling loads are achieved when the lateral instability occurs in first and second stories simultaneously. Also from Tables 5-9 and 5-10, it is seen that the relative difference between the maximum and minimum frame-buckling loads are 47.5%, 46.8%, 45% and 40.7% associated with the values of δ_0 and Δ_0 of $L/1000$, $L/500$; $L/800$, $L/400$; $L/600$, $L/300$; and $L/400$, $L/200$ respectively.

5.2.3 Effects of Semi-Rigid Connections

The behaviour of the beam-to-column semi-rigid connections is another primary contributing factor to structural stability, hence, the connection rigidity will be considered in this section. The five cases with different beam-to-column and column base connection rigidities shown in Table 3-1 will be investigated with geometric imperfections of member out-of-straightness ($\delta_0 = L/1000$) and frame out-of-plumbness ($\Delta_0 = L/500$). The values of the coefficients including the end-fixity factors, the effective length factor and the buckling loads associated with non-sway buckling corresponding to the maximum and minimum frame-buckling loads, together with their relative differences, are presented in Tables 5-11 to 5-15. The column elastic flexural stiffness $12EI_{ij}\beta_{0,ij}/L_{ij}^3$ and the coefficients associated with column lateral stiffness modification factors $\beta_{1,ij}(r_{l,ij}, r_{u,ij})$ are also provided in these tables. Also presented in Tables 5-11 to 5-15 are the results for a frame subjected to proportional loading obtained in this study. The load patterns associated the maximum and minimum frame-buckling loads are illustrated in Figures 5-5 to 5-9.

**Table 5-11: Results of the unbraced steel frames shown in Figure 3-5 –
Case 1 ($\delta_0=L/1000$ and $\Delta_0=L/500$)**

Col. <i>ij</i>	$r_{l,ij}$	$r_{u,ij}$	$\frac{12EI_{ij}}{L_{ij}^3} \beta_{0,ij}$ (kN/m)	$\beta_{1,ij}$	K_{braced}	$P_{u,ij}$ (kN)	Max. (kN)	Min. (kN)	
								$S_1 = 0$ $S_2 > 0$	$S_2 = 0$ $S_1 > 0$
11	1.000	0.635	11700.000	0.101	0.575	183700.000	23876.000	0.000	0.000
12	1.000	0.834	9860.000	0.104	0.534	144800.000	0.000	24663.670	0.000
13	1.000	0.826	7373.000	0.104	0.536	108500.000	0.000	0.000	0.000
21	0.635	0.784	7418.000	0.095	0.630	106200.000	60369.780	0.000	0.0000
22	0.834	0.895	10500.000	0.100	0.558	133900.000	0.000	57430.540	0.000
23	0.826	0.919	4565.000	0.100	0.554	57570.000	0.000	0.000	57081.330
Critical frame buckling loads $\sum P_{ij} =$							84245.780	82094.210 ($S_2=0.000$)	57081.330 ($S_1=8848.790$)
Difference of max. & min. frame-buckling loads (%)							$\frac{\max - \min}{\min} \%$	2.6%	47.6%
Proportional loading: $P_p = \lambda_{cr} \sum P_{a,ij}$ (kN)							P_p	82750.000	
Difference of proportional loading & max. frame-buckling loads (%)							$\frac{\max - P_p}{\min} \%$	0.8%	
Difference of proportional loading & min. frame-buckling loads (%)							$\frac{P_p - \min}{\min} \%$	44.9%	

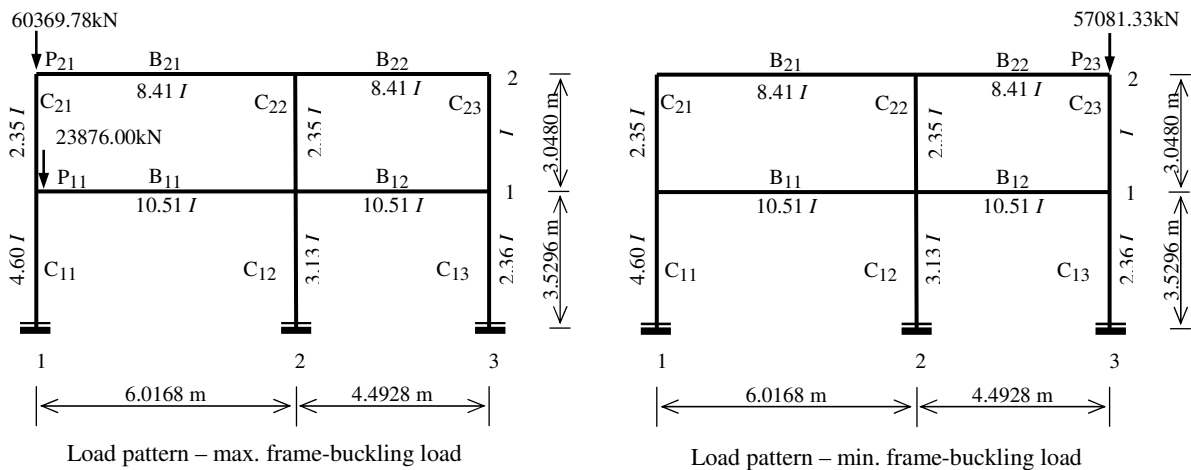


Figure 5-5: Load patterns associated with max. and min. frame-buckling loads – Case 1

**Table 5-12: Results of the unbraced steel frames shown in Figure 3-6 –
Case 2 ($\delta_0=L/1000$ and $\Delta_0=L/500$)**

Col. <i>ij</i>	$r_{l,ij}$	$r_{u,ij}$	$\frac{12EI_{ij}}{L_{ij}^3} \beta_{0,ij}$ (kN/m)	$\beta_{1,ij}$	K_{braced}	$P_{u,ij}$ (kN)	Max. (kN)	Min. (kN)	
								$S_1 = 0$ $S_2 > 0$	$S_2 = 0$ $S_1 > 0$
11	1.000	0.568	10830.000	0.101	0.588	175300.000	26191.210	0.000	0.000
12	1.000	0.815	9697.000	0.100	0.538	142700.000	0.000	27406.670	0.000
13	1.000	0.781	7037.000	0.103	0.545	104900.000	0.000	0.000	0.000
21	0.568	0.731	5947.000	0.094	0.672	97460.000	54194.080	0.000	0.000
22	0.815	0.881	9782.000	0.098	0.573	130600.000	0.000	51032.520	0.000
23	0.781	0.895	4043.000	0.098	0.578	54780.000	0.000	0.000	51032.520
Critical frame buckling loads $\sum P_{ij} =$							80385.290	78439.190 ($S_2=0.000$)	51032.520 ($S_1=9622.480$)
Difference of max. & min. frame-buckling loads (%)							$\frac{\max - \min}{\min} \%$	2.5%	57.5%
Proportional loading: $P_p = \lambda_{cr} \sum P_{a,ij}$ (kN)							P_p	79100.000	
Difference of proportional loading & max. frame-buckling loads (%)							$\frac{\max - P_p}{\min} \%$	0.8%	
Difference of proportional loading & min. frame-buckling loads (%)							$\frac{P_p - \min}{\min} \%$	55%	

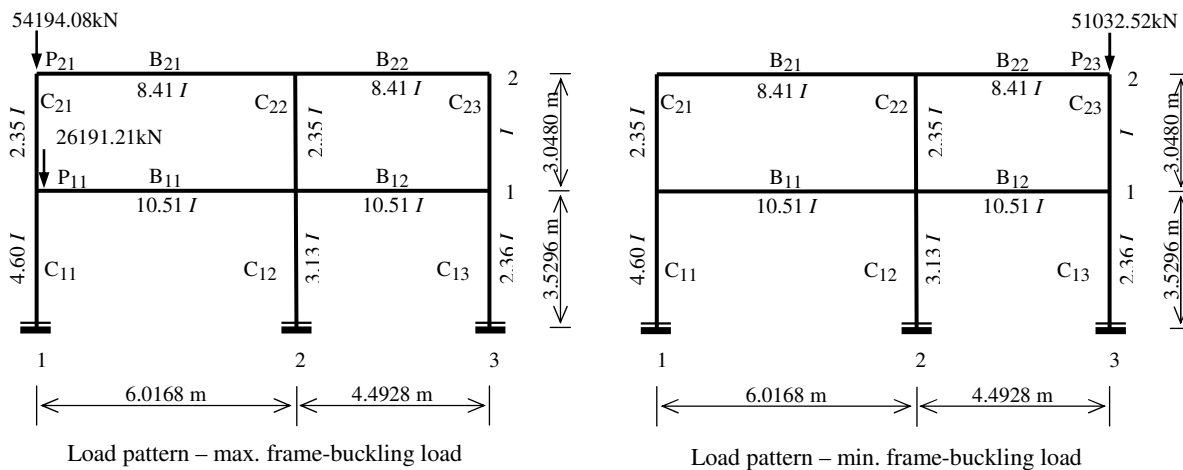


Figure 5-6: Load patterns associated with max. and min. frame-buckling loads – Case 2

**Table 5-13: Results of the unbraced steel frames shown in Figure 3-7 –
Case 3 ($\delta_0=L/1000$ and $\Delta_0=L/500$)**

Col. <i>ij</i>	$r_{l,ij}$	$r_{u,ij}$	$\frac{12EI_{ij}}{L_{ij}^3} \beta_{0,ij}$ (kN/m)	$\beta_{1,ij}$	K_{braced}	$P_{u,ij}$ (kN)	Max. (kN)	Min. (kN)	
								$S_1 = 0$ $S_2 > 0$	$S_2 = 0$ $S_1 > 0$
11	1.000	0.540	10480.000	0.101	0.594	171900.000	27505.250	0.000	0.000
12	1.000	0.771	9235.000	0.103	0.547	138100.000	0.000	28216.980	0.000
13	1.000	0.760	6883.000	0.102	0.549	103300.000	0.000	0.000	0.000
21	0.540	0.707	5555.000	0.093	0.685	93930.000	50136.310	0.000	0.000
22	0.771	0.850	8946.000	0.097	0.592	123300.000	0.000	48153.970	0.000
23	0.760	0.884	4189.000	0.098	0.586	53460.000	0.000	0.000	47766.230
Critical frame buckling loads $\sum P_{ij} =$							77641.560	76370.950 ($S_2=0.000$)	47766.230 ($S_1=10201.850$)
Difference of max. & min. frame-buckling loads (%)							$\frac{\max - \min}{\min} \%$	1.7%	62.5%
Proportional loading: $P_p = \lambda_{cr} \sum P_{a,ij}$ (kN)							P_p	76750.000	
Difference of proportional loading & max. frame-buckling loads (%)							$\frac{\max - P_p}{\min} \%$	0.5%	
Difference of proportional loading & min. frame-buckling loads (%)							$\frac{P_p - \min}{\min} \%$	60.7%	

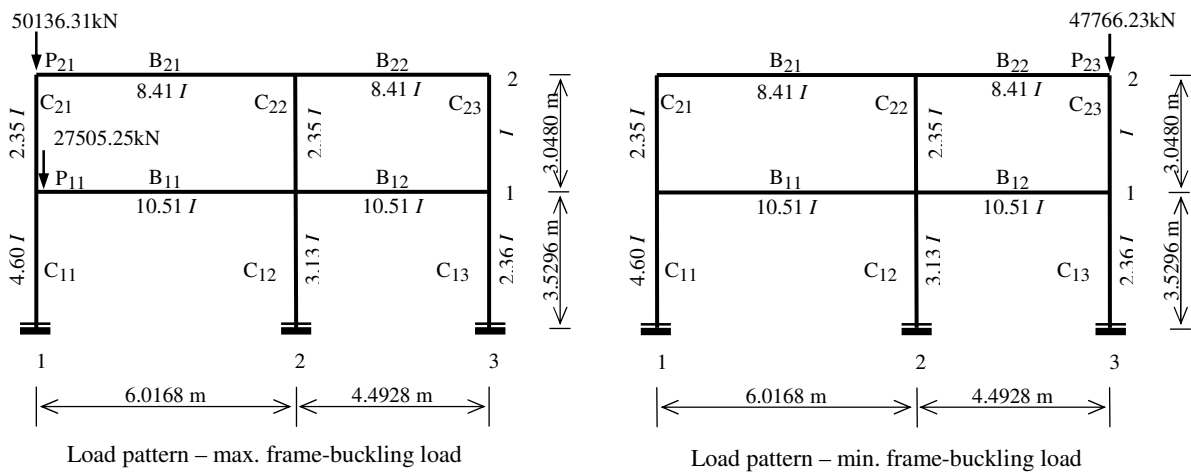


Figure 5-7: Load patterns associated with max. and min. frame-buckling loads – Case 3

**Table 5-14: Results of the unbraced steel frames shown in Figure 3-8 –
Case 4 ($\delta_0=L/1000$ and $\Delta_0=L/500$)**

Col. <i>ij</i>	$r_{l,ij}$	$r_{u,ij}$	$\frac{12EI_{ij}}{L_{ij}^3} \beta_{0,ij}$ (kN/m)	$\beta_{l,ij}$	K_{braced}	$P_{u,ij}$ (kN)	Max. (kN)	Min. (kN)	
								$S_1 = 0$ $S_2 > 0$	$S_2 = 0$ $S_1 > 0$
11	1.000	0.420	9032.000	0.101	0.619	158400.000	31891.220	0.000	0.000
12	1.000	0.00	3161.000	0.108	0.707	82570.000	0.000	27649.710	0.000
13	1.000	0.705	6347.000	0.102	0.560	99130.000	0.000	0.000	0.000
21	0.377	0.644	3696.000	0.092	0.719	80370.000	22363.790	0.000	0.000
22	0.00	0.00	0.0000	0.088	1.00	41570.000	0.000	23346.740	0.000
23	0.644	0.851	1132.000	0.097	0.608	47880.000	0.000	0.000	21392.470
Critical frame buckling loads $\sum P_{ij} =$							54255.010	50996.450 ($S_2=0.000$)	21392.470 ($S_1=11293.180$)
Difference of max. & min. frame-buckling loads (%)							$\frac{\max - \min}{\min} \%$	6.4%	153.6%
Proportional loading: $P_p = \lambda_{cr} \sum P_{a,ij}$ (kN)							P_p	52550.000	
Difference of proportional loading & max. frame-buckling loads (%)							$\frac{\max - P_p}{\min} \%$	3%	
Difference of proportional loading & min. frame-buckling loads (%)							$\frac{P_p - \min}{\min} \%$	145.4%	

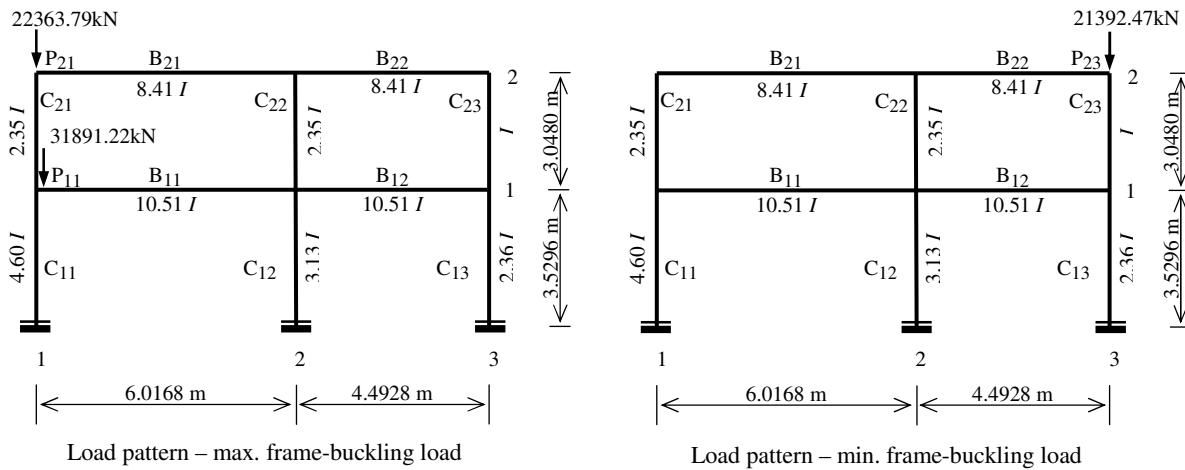


Figure 5-8: Load patterns associated with max. and min. frame-buckling loads – Case 4

**Table 5-15: Results of the unbraced steel frames shown in Figure 3-7 –
Case 5 ($\delta_0=L/1000$ and $\Delta_0=L/500$)**

Col. <i>ij</i>	$r_{l,ij}$	$r_{u,ij}$	$\frac{12EI_{ij}}{L_{ij}^3} \beta_{0,ij}$ (kN/m)	$\beta_{l,ij}$	K_{braced}	$P_{u,ij}$ (kN)	Max. (kN)	Min. (kN)	
								$S_1 = 0$ $S_2 > 0$	$S_2 = 0$ $S_1 > 0$
11	1.000	0.184	6448.000	0.104	0.668	136000.000	0.000	29881.420	0.000
12	1.000	0.384	5863.000	0.102	0.626	105300.000	31293.350	0.000	0.000
13	1.000	0.359	4275.000	0.102	0.631	78070.000	0.000	0.000	0.000
21	0.184	0.287	1367.000	0.089	0.889	55730.000	0.000	16956.520	0.000
22	0.384	0.485	3139.000	0.091	0.787	72300.000	16751.820	0.000	0.000
23	0.359	0.559	1654.000	0.092	0.769	31840.000	0.000	0.000	16552.010
Critical frame buckling loads $\sum P_{ij} =$							48045.180	46837.940 ($S_2=0.000$)	16552.010 ($S_1=10861.350$)
Difference of max. & min. frame-buckling loads (%)							$\frac{\text{max} - \text{min}}{\text{min}} \%$	2.6%	190.3%
Proportional loading: $P_p = \lambda_{cr} \sum P_{a,ij}$ (kN)							P_p	47650	
Difference of proportional loading & max. frame-buckling loads (%)							$\frac{\text{max} - P_p}{\text{min}} \%$	1.7%	
Difference of proportional loading & min. frame-buckling loads (%)							$\frac{P_p - \text{min}}{\text{min}} \%$	183.0%	

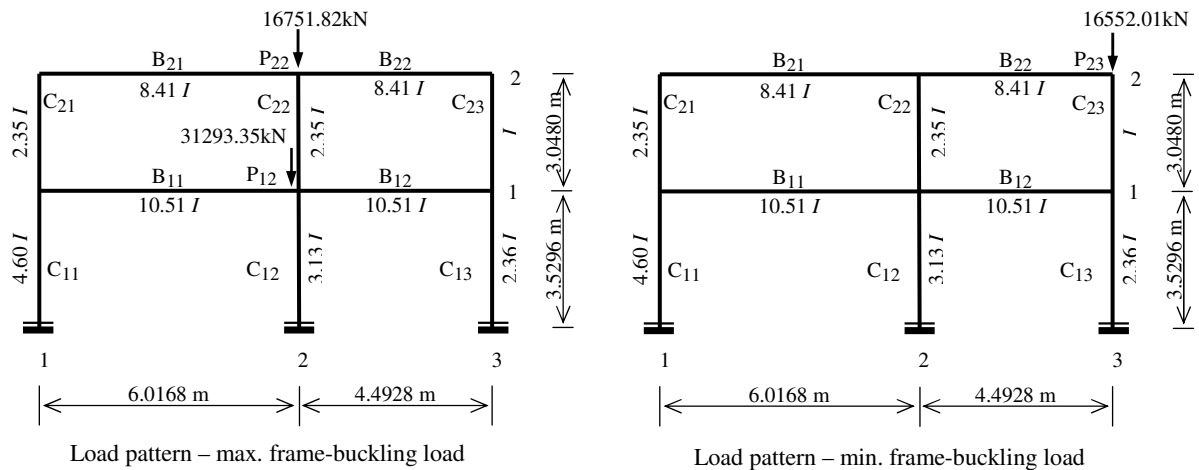


Figure 5-9: Load patterns associated with max. and min. frame-buckling loads – Case 5

Tables 5-11 to 5-15 show the results of the extreme frame-buckling loads accounting for the initial geometric imperfections with different values of the beam-to-column semi-rigid connections. Compared to the results without accounting for the initial geometric imperfections given in Tables 3-2 to 3-6, the presence of the out-of-straightness ($\delta_0 = L/1000$) and out-of-plumbness ($\Delta_0 = L/500$) reduce the lateral stiffness strength for the same case shown in Tables 5-11 to 5-15. Consequently, for the same case, the extreme frame-buckling loads together with their relative difference all reduce.

Summarized in Table 5-11, are the results of Case 1, in which both the column base and beam-to-column connections are rigidly connected. It can be seen from Table 5-11 that the maximum frame-buckling load of 84245.78 kN, is achieved when first and second stories are simultaneously laterally unstable. The minimum storey-buckling loads associated with lateral instability of the first and second stories are 820694.215 kN and 57081.33 kN, respectively. The relative difference between the maximum and minimum frame-buckling loads is 47.6%, which is significant. It can also be seen from Table 5-11 that the load patterns associated with the maximum and minimum frame-buckling loads are different. The load pattern corresponding to the maximum frame-buckling loads are applied only on the exterior columns 11 and 21 for both first and second stories. In contrast, the associated with the minimum frame-buckling load applies the loads both on the exterior and interior columns. Also found in Case 1 are two different loading patterns associated with the minimum frame-buckling loads.

For Case 2, presented in Table 5-12, the exterior column is semi-rigidly connected with the corresponding end-fixity factor being 0.8 whereas the column base and the interior beam-to-column connections are rigid. The presence of semi-rigid connections used with a frame will become flexible and the magnitudes of lateral stiffness decrease compared to that of Case 1. As a result of the frame flexibility, the maximum frame-buckling load of Case 2 reduces to 80385.29 kN, and the corresponding minimum frame-buckling load decreases to 51032.52 kN, which yields the relative difference between the maximum and minimum frame-buckling loads to be 57.5%. The load patterns associated with the maximum frame-buckling load including load locations and magnitudes are identical for the first and second stories. There are two different load patterns associated with minimum frame-buckling load. It is also observed that the first and second storey become unstable simultaneously when they are subjected to maximum frame-buckling load.

For Case 3 given in Table 5-13, the beam-to-column connections for both the interior and exterior columns are semi-rigidly connected with the corresponding end-fixity factor being 0.8. Compared with Cases 1 and 2, the Case 3 frame is more flexible, which can be evidenced by the further decreased value of lateral stiffness; thus, the magnitudes of the maximum and minimum frame-buckling loads are reduced to 77641.56 kN and 47766.23 kN, respectively, which leads to a difference of 62.5% between the buckling loads. Like Case 2, it is found that lateral instability occurs simultaneously for both first and second stories when they are subjected to the maximum frame-buckling load. It is also noticed that the load patterns are identical for both first and second stories when the frames are subjected to a maximum frame-buckling load.

Presented in Table 5-14 are the results of Case 4, in which the column base uses rigid connections. The beam-to-column connections for the exterior columns are rigid, and for the interior columns are pin connections. The maximum and minimum frame-buckling loads are 54255.01 kN and 21392.47 kN, respectively. The load patterns corresponding to the maximum frame-buckling loads applied to the exterior columns, and the load patterns associated with the minimum frame-buckling loads applied to both the exterior columns and interior column. The difference between the maximum and minimum frame-buckling loads is 153.6%, which is very significant compared to cases 1 to 3. It is also found that lateral instability occurs simultaneously for both first and second stories when they are subjected to the maximum frame-buckling load.

In Table 5-15, for Case 5, the column base connection is rigid, while the beam-to-column connections for both the interior and exterior columns are quite flexible with the corresponding end-fixity factor being 0.2. The maximum and minimum frame-buckling loads are 48045.18 kN and 16552.01 kN, which yields a considerable difference of 190.3%. The load patterns associated with the maximum frame-buckling loads is applied on the interior columns C_{12} and C_{22} while the load patterns with respect to the minimum frame-buckling loads trend to apply on the exterior columns, which are the different than Cases 1 to 4. Also similar to Cases 1 to 4, the lateral instability occurs simultaneously for both first and second stories when they are subjected to the maximum frame-buckling load.

The frame-buckling strengths associated with storey-based buckling subjected to proportional loading for the frames are also presented in Tables 4-24 to 4-28. It is observed that the differences

between the proportional and the minimum loading are 51.1%, 55%, 60.7%, 174.8% and 187.8%, respectively.

5.3 Conclusions

The problem of extreme frame-buckling loads and their associated load patterns for unbraced multi-storey frame structures accounting for initial geometric imperfections has been solved using the linear programming method. Comparing the results discussed in Chapter 3, the geometric imperfection results obtained in this chapter show similar trends for the extreme frame-buckling loads and their associated load patterns. Found in this study is that the presence of the initial geometric imperfections reduces the column lateral stiffness and consequently the maximum and minimum frame-buckling loads were all reduced. The results of the parametric studies indicate that both the geometric imperfections of member out-of-straightnesses and frame out-of-plumbnesses affect the extreme frame-buckling loads and their associated load patterns. As well, the numerical examples indicate that the extreme frame-buckling loads and their associated load patterns decreased when increasing the values of member out-of-straightnesses and frame out-of-plumbnesses. The results also demonstrate that the frame out-of-plumbness shows a stronger influence for the frame stability than the member out-of-straightness. Compared to the frame that includes only the out-of-straightness or out-of-plumbness, the relative difference noted between the extreme frame-buckling loads was higher in the case of the frame that includes only the out-of-plumbness. The extreme frame-buckling loads and their associated load patterns showed lower values when considering the effects of combined member out-of-straightness and frame out-of-plumbness together. Comparing the relative differences between the extreme frame-buckling loads with respect to the out-of-straightness or out-of-plumbness, the relative differences between the extreme frame-buckling loads are not affected by combining the initial geometric imperfections of out-of-straightness and out-of-plumbness. In the considerations of comparing the different beam-to-column and column base connections, the results based on geometric imperfections clearly indicate that the geometric imperfections play an important role in the stability analysis. There is also a considerable variation in connection stiffness among beam-to-column connections in the same storey of any frame or column base connection.

Chapter VI

Application of Storey-Based Stability Analysis to CFS Storage Racks

6.1 Introduction

Storage rack manufacturers for warehousing or distribution center applications using CFS members for optimal structural design presents several stability challenges for structural designers. Factors to be considered in the stability design for storage racks include semi-rigid behavior of beam-to-column and column base connections, perforated columns, local buckling and torsional-flexural buckling. In addition, the nature of randomly applied loads both in magnitude and location are often one of the primary factors contributing to structural failures. So far, there have not been any design guidelines and tools available to assess the structural integrity of the variable loading for CFS structures.

In practice, as there was no Canadian standard available prior to 2005, steel racks were designed in accordance with the *Allowable Strength Design* standard developed by RMI in the U.S. Although the first Canadian standard for design and construction of steel storage racks with *Limit State Design* was developed in 2005 (CSA, 2005), the standard is in the infancy stage where many complex issues, as listed in the foregoing, are either overly simplified or not addressed due to the lack of the research in this area.

As the use of storage racks increases around the world, they will be subjected to a more diverse use of loading conditions and as a result the engineering and building code communities are scrutinizing these structures in their stability. Therefore, the variable loading condition discussed in Chapters 3 and 5 is also a key factor in the stability design of a CFS storage rack and it will be addressed in this chapter. Another key factor in causing such structures to have instability issues is through the influence of initial geometric imperfections studied in Chapter 4 and this influence will also be evaluated within this chapter. Also the studies of perforated columns and the behavior of the beam-to-column connection on the CFS storage rack stability are demonstrated in this chapter. Figure 6-1 shows the typical rack structure components. In general for the purposes of describing direction, the

rack industry refers to the longitudinal direction as the down-aisle direction and the transverse direction, as the cross-aisle direction. It can be seen that the lateral load resisting systems of storage racks in down-aisle and cross-aisle directions are unbraced frames and bracing frames, respectively.

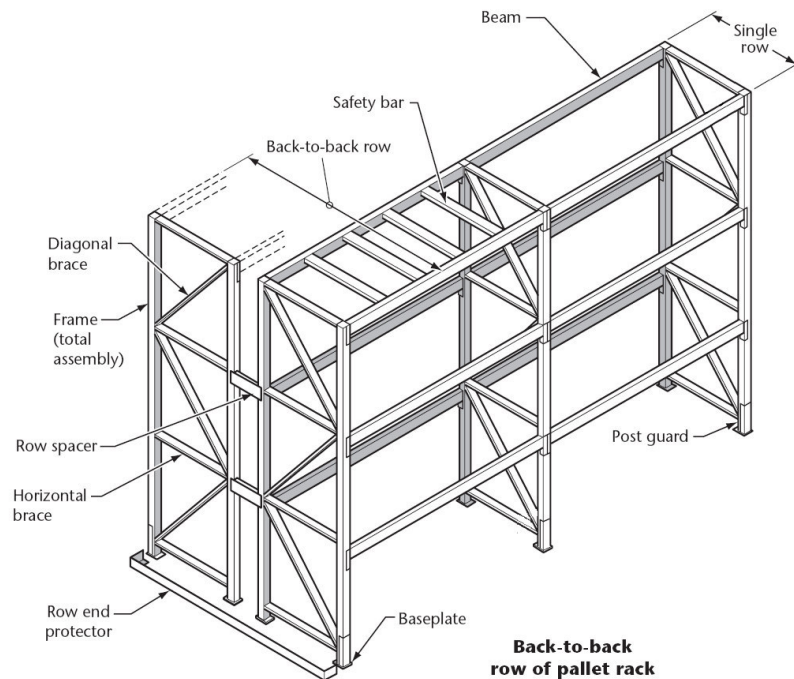


Figure 6-1: Typical storage rack configuration and components (CSA, 2005)

6.2 Members Design

6.2.1 Introduction

The current RMI design provision for CFS members is similar to the AISI specification, which can be described as follows: (RMI, 2000; AISI, 2004)

- (1) the overall stability of the member must be considered, which includes the elastic column buckling stress (flexural, torsional, or torsional-flexural) for the full unreduced section.
- (2) then the design equations are used to determine the nominal failure stress, whether the member will fail from elastic buckling, inelastic buckling, or yielding.
- (3) once the nominal failure stress is known, the corresponding effective section properties can then be computed and will be used to account for the local buckling of thin-walled sections.

- (4) the nominal member strength is determined based on the governing nominal failure stress and the effective section properties.
- (5) the nominal member strength is multiplied by a resistance factor in the case of LRFD and LSD or dividing it by a safety factor in the case of ASD obtaining the design member strength.

Based on the general design steps listed above, studies are carried out in this section to check the current design provisions for member design.

6.2.2 Elastic Buckling Strength of Perforated Members

The column sections in storage racks are perforated for the purpose of easy assembly of the beam end connection elements. It is well known that the presence of such perforation reduces the local buckling strength of the individual component element and the overall buckling strength of the section. The RMI Specification currently allows the use of unperforated section properties to predict the overall elastic buckling strength of perforated members, thus assuming the presence of such perforation does not have a significant influence on the reduction of the overall elastic buckling strength (RMI, 2000). The objective of this study is to check this assumption. The overall buckling equations as given in the CAN/CSA-S136S1-04(CSA, 2004) were used to carry out the perforation affect for the overall buckling strength.

The computer program CU-TWP developed at Cornell University (Sarawit and Peköz, 2003) was designed to compute the perforated column cross section properties and will be used in this study to obtain the perforated column cross section properties. Three C-sections of C_1 , C_2 and C_3 properties are calculated using CU-TWP and their section properties are given in Tables 6-1 to 6-3. In Table 6-1 is the section C_1 property for the full unreduced gross section and perforated web or flanges. Table 6-2 gives the section properties of C_2 with and without section perforation. The cross section properties of C_3 considering without perforation and with perforation are presented in Table 6-3. The cross section should be noted that the geometry of C_1 and C_2 are similar but their section thicknesses are different. In this study, the weighted section shown in Tables 6-1 to 6-3 presents the cross area that uses an average thickness in the perforated segment of the section to account for the absence of the material from the holes along the length of the section.

Table 6-1: Section C₁ dimensions and properties (Sarawit and Peköz, 2003)

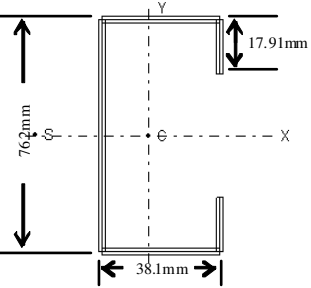
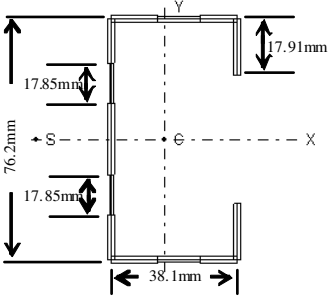
Full unperforated section dimensions	Section Properties
	<p> $A=442.670\text{mm}^2$ $t=2.311\text{mm}$ $I_x=4.250 \times 10^5\text{mm}^4$ $I_{xy}=0.000\text{mm}^4$ $I_y=1.190 \times 10^5\text{mm}^4$ $J=788.330\text{mm}^4$ $C.G.=(15.680\text{mm}, 0)$ $S.C.=(-22.910\text{mm}, 0)$ $C_w=2.110 \times 10^8\text{mm}^8$ </p>
Net section dimensions	Section Properties
	<p> $A=400.280\text{mm}^2$ $t=2.311\text{mm}$ $I_x=3.970 \times 10^5\text{mm}^4$ $I_{xy}=0.000\text{mm}^4$ $I_y=1.100 \times 10^5\text{mm}^4$ $J=640.940\text{mm}^4$ $C.G.=(16.700\text{mm}, 0)$ $S.C.=(-23.560\text{mm}, 0)$ $C_w=2.050 \times 10^8\text{mm}^8$ </p>

Table 6-2: Section C₂ dimensions and properties (Sarawit and Peköz, 2003)

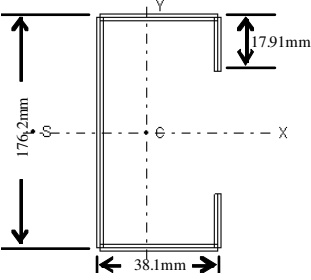
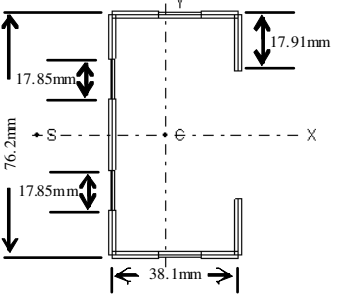
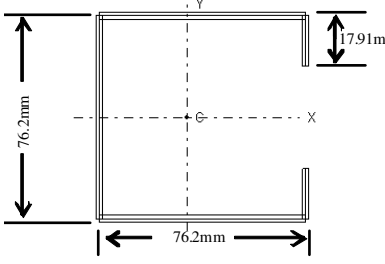
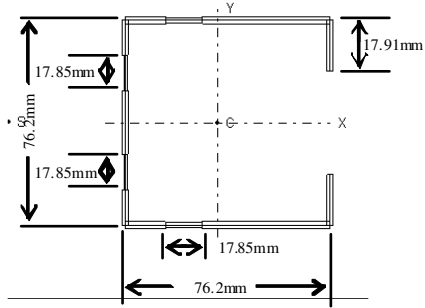
Full unperforated section dimensions	Section Properties
	<p> $A=218.900\text{mm}^2$ $t=1.143\text{mm}$ $I_x=2.100 \times 10^5 \text{mm}^4$ $I_{xy}=0.00 \text{mm}^4$ $I_y=0.587 \times 10^5 \text{mm}^4$ $J=95.330\text{mm}^4$ $C.G.=(15.680\text{mm}, 0)$ $S.C.=(-22.910\text{mm}, 0)$ $C_w=1.040 \times 10^8 \text{mm}^8$ </p>
Net section dimensions	Section Properties
	<p> $A=197.940\text{mm}^2$ $t=1.143\text{mm}$ $I_x=1.960 \times 10^5 \text{mm}^4$ $I_{xy}=0.00 \text{mm}^4$ $I_y=0.546 \times 10^5 \text{mm}^4$ $J=77.510\text{mm}^4$ $C.G.=(16.700\text{mm}, 0)$ $S.C.=(-23.560\text{mm}, 0)$ $C_w=1.010 \times 10^8 \text{mm}^8$ </p>

Table 6-3: Section C₃ dimensions and properties (Sarawit and Peköz, 2003)

Full unperforated section dimensions	Section Properties
	$A=593.260\text{mm}^2$ $t=2.311\text{mm}$ $I_x=5.960 \times 10^5 \text{mm}^4$ $I_{xy}=0.000 \text{mm}^4$ $I_y=4.820 \times 10^5 \text{mm}^4$ $J=1056.510\text{mm}^4$ $C.G.=(31.600\text{mm}, 0)$ $S.C.=(-40.860\text{mm}, 0)$ $C_w=7.820 \times 10^8 \text{mm}^8$
Net section dimensions	Section Properties
	$A=550.870\text{mm}^2$ $t=2.311\text{mm}$ $I_x=5.690 \times 10^5 \text{mm}^4$ $I_{xy}=0.000 \text{mm}^4$ $I_y=4.480 \times 10^5 \text{mm}^4$ $J=909.120\text{mm}^4$ $C.G.=(33.560\text{mm}, 0)$ $S.C.=(-42.140\text{mm}, 0)$ $C_w=7.580 \times 10^8 \text{mm}^8$

The flexural buckling strength of the members will be calculated using a net section to represent the perforated section in this current study. All three sections are studied as both a concentrically loaded compression member and a flexural member subject to bending about the strong axis, which represents the x-axis. Boundary conditions at the ends of the member are pinned connections such that the effective length for flexural buckling of both the strong and weak axis as well as the torsion is equal to the length of the member.

The results of sections C₁, C₂ and C₃ are illustrated in Figures 6-2 to 6-4. The vertical axis in Figures 6-2 to 6-4 are the elastic axial buckling load P_e divided by the axial load causing yielding of the full unreduced gross section $P_y = AF_y$.

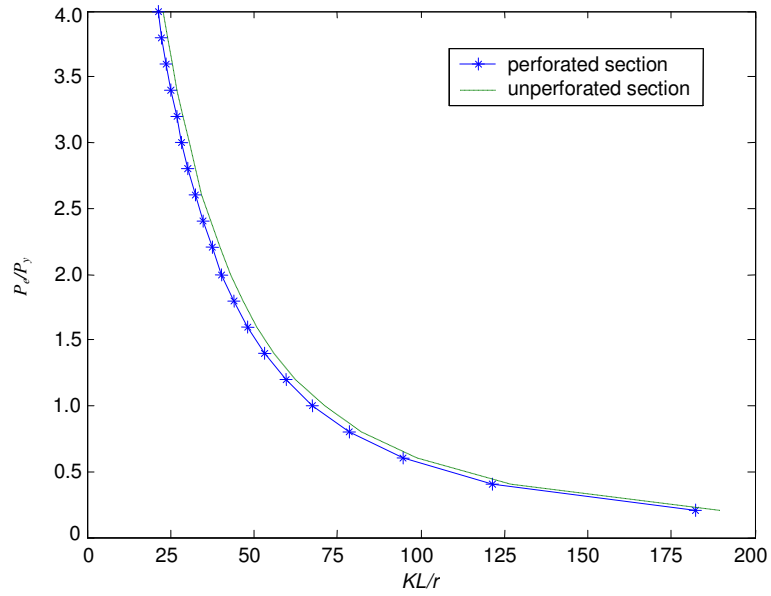


Figure 6-2: Elastic buckling axial load for C₁

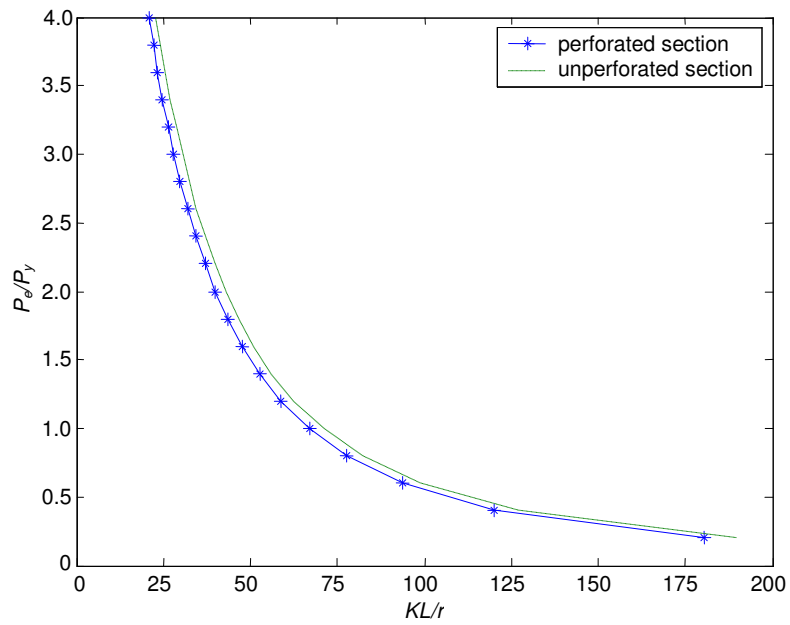


Figure 6-3: Elastic buckling axial load for C₂

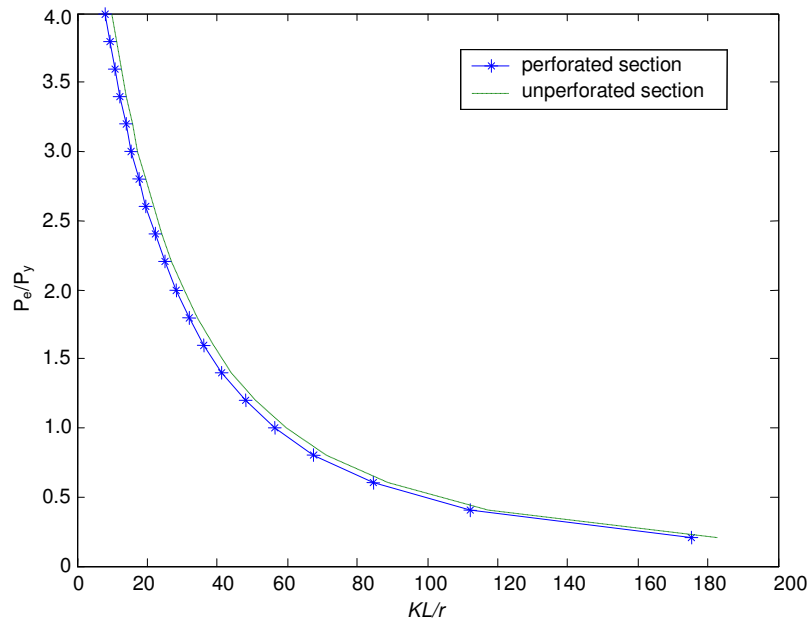


Figure 6-4: Elastic buckling axial load for C₃

Comparison results between the unperforated and perforated members for the axial load of these three sections are demonstrated in Figures 6-2 to 6-4, respectively. From these figures, it can be observed that the buckling strength will reduce with the presence of perforations in the section. In Figures 6-2 to 6-4, it is noted that the maximum difference of the elastic buckling strength between the gross and reduced section is less than 3.3%, which indicates that such perforation does not have significant influence on the reduction of the overall elastic buckling strength. Therefore, the unperforated section to predict the buckling strength of perforated sections assumed in the current RMI Specification will be used in the following studies of this chapter.

6.2.3 Effective Design of Cross-Sectional Area

With the presence of perforations in rack columns, the effective design width equations of the AISI Specification (2004) is not applicable in the design of CFS storage racks (RMI, 2000). Stub-column tests are required in the RMI specifications and to account for the member local behavior (AISI, 2004; CSA, 2004).

By measuring the axial load and the corresponding axial shortening in the stub-column test, the relationship between the stress on the effective section F_n and the effective area A_e can be obtained. However, for tests where only the ultimate strength of the stub-column is measured, the effective design area equation is given as follows: (RMI, 2000; CSA, 2004)

$$\frac{A_e}{A_{net\ min}} = 1 - (1 - Q) \left(\frac{F_n}{F_y} \right)^Q \quad (6.1)$$

in which Q is the perforation factor and can be determined as

$$Q = \frac{P_{ult}}{F'_y A_{nm}} \quad (6.2)$$

Where

A_e : effective area at stress F_n

F_n : nominal buckling stress

A_{nm} : net minimum cross-sectional area obtained by passing a plane through the section normal to axis of the column.

P_{ult} : ultimate compressive strength of stub column by tests.

F'_y : actual yield stress of the column material if no cold work of forming affects are to be considered.

F_y : yield point used for design

6.2.3.1 Concentrically Loaded Compression Members

In accordance with Section C4 of CAN/CSA-S136S1-04 (CSA, 2004), the factored compressive resistance (P_r) can be calculated by the following equation:

$$P_r = \phi_c A_e F_n \quad (6.3)$$

where

ϕ_c : resistance factor for concentrically loaded compression member

A_e : effective area at stress F_n and determined in Eq. (6.1)

F_n : nominal buckling stress and determined in Section C4 of CAN/CSA-S136S1-04.

6.2.3.2 Laterally Supported Members in Bending

According to procedure I in Section C3.1 of CAN/CSA-S136S1-04 (CSA, 2004), the factored moment resistance (M_r) can be obtained as follows:

$$M_r = \phi_b S_e F_y [(Q + 1) / 2] \quad (6.4)$$

where

ϕ_b : resistance factor for bending strength

S_e : elastic section modulus of effective section calculated relative to extreme compression or tension fibre at F_y

Q : perforation factor determined in Eq. (6.2)

The calculations in procedure II of Section 3.1.1 of CAN/CSA-S136S1-04 that utilize inelastic reserve capacity are not used in rack design (CSA, 2004).

6.2.3.3 Laterally Unsupported Members in Bending

In accordance with Section C3.1.2.1 (lateral-torsional buckling resistance of open cross section members) of CAN/CSA-S136S1-04 (CSA, 2004), the factored moment resistance (M_r) can be calculated using the following equation:

$$M_r = \phi_b S_c F_c [(Q + 1) / 2] \quad (6.5)$$

where

ϕ_b : resistance factor for bending strength

S_c : elastic section modulus of effective section calculated relative to extreme compression or tension fibre at F_c

F_c : critical buckling stress based on σ_{ex} , σ_{ey} and σ_{et} , in accordance with Section C3.1.2.1 of CAN/CSA-S136S1-04 (CSA, 2004).

So far, there are no available results from the stub-column test to compute the perforation factor Q at the University of Waterloo and such test will need to be carried out in future research.

6.3 Beam to Column Connections

6.3.1 Introduction

In the storage rack industry, beam end connectors are used to make beam to column connections. The semi-rigid nature of this connection is primarily due to the distortion of the column walls, tearing of the column perforation, and distortion of the beam end connector. Photographs of typical down-aisle moment frame connections, cross-aisle braced frame connections, and column base plate connections are presented in Figures 6-5 to 6-7.



Figure 6-5: Typical rack moment connection (NEHRP, 2003)



Figure 6-6: Typical rack bracing members and connection (NEHRP, 2003)



Figure 6-7: Typical column base plate connection (NEHRP, 2003)

The storage rack stability depends significantly on the behavior of all these connections. The detailed connections vary widely, thus it is impossible to establish general procedures for computing joint stiffness and strength. Therefore, it is necessary to determine these characteristics by tests. These beam to column connection tests are usually carried out to determine the relationship of the moment M at the joint and the change in angle θ between the column and the connecting beam (RMI, 2000).

6.3.2 Beam to Column Connection Tests

The RMI Specification recommends the use of a cantilever test or a portal test. Figures 6-8 and 6-9 show the schematics of these test set-ups (RMI, 2000). The cantilever test provides a simple means of determining the connection moment capacity and rigidity. In this current study, the sections of column and beam and their connection stiffnesses for some numerical examples are obtained from the cantilever beam tests carried out in accordance with the RMI Specification and Commentary (RMI, 2000) at the University of Waterloo (Schuster, 2004).

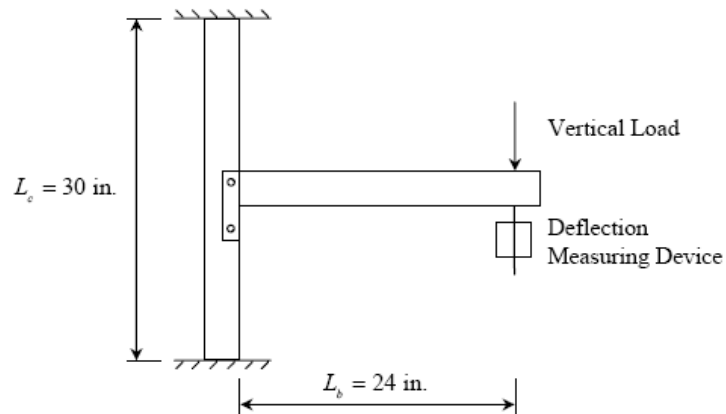


Figure 6-8: Cantilever test – beam to column connection test (RMI, 2000)

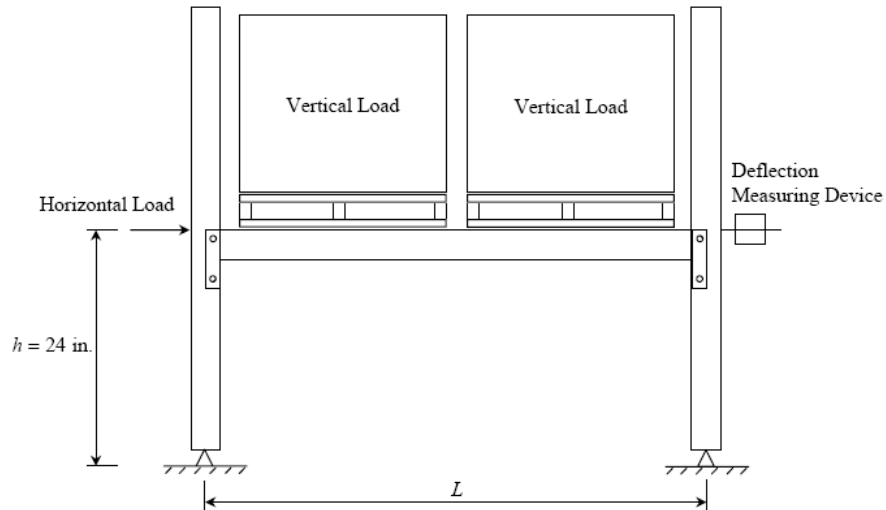


Figure 6-9: Portal test – beam to column connection test (RMI, 2000)

6.3.3 Test Specimens and Set-up

All the specimens were fabricated by the Econo-Rack Group Enrack manufacturing facility in Brantford, Ontario and were delivered to the structures Laboratory of the Department of Civil Engineering at the University of Waterloo prior to actual testing (Schuster, 2004). The rack column section 4" w × 3" d × 13Ga and 3-1/4" w × 2" d × 13Ga was used with both the 'Redirack' style box beam and ledge beams shown in Figure 6-10 in this test.



Figure 6-10: Typical box and ledge beam sections in tests (Schuster, 2004)

The schematic layout of a cantilever test set-up shown in Figure 6-8 was created in accordance with RMI Commentary, Section 9.4.1(RMI, 2000) and the actual test set-up at the University of Waterloo is shown in Figure 6-11(Schuster, 2004).

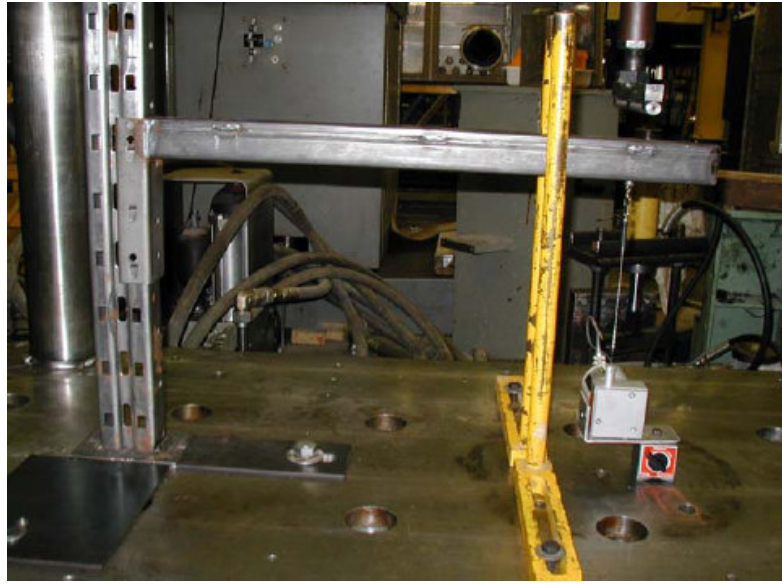


Figure 6-11: Cantilever rack beam/column test (Schuster, 2004)

6.3.4 Evaluation of Test Results

In the cantilever test, the constant connection stiffness, R , relative to the moment and the rotation is expressed as follows:

$$R = \frac{M}{\theta} \quad (6.6)$$

The relationship between the moment and the angular change at a joint is generally nonlinear. The following equation taken from RMI Commentary (RMI, 2000), can be determined a constant value of R which can be used in structural analysis.

$$R = \frac{R.F.}{\frac{\delta_{0.85}}{P_{0.85} L_b^2} - \frac{L_c}{16EI_{c,y-net}} - \frac{L_b}{3EI_{xb}}} \quad (6.7)$$

where

$R.F.$: reduction factor to provide safety considering scatter of test data and recommend being 1 in this study

$I_{c,y-net}$: net moment of inertia of column section about y-axis

I_{xb} : moment of inertia of beam section about x-axis

$P_{0.85}$: 0.85 times ultimate test load

$\delta_{0.85}$: displacement of free end of cantilever beam at load $P_{0.85}$

Therefore, the R obtained from Eq. (6.7) with P equal to 0.85 times the ultimate load and δ equal to the deflection at that load.

All data used to calculate beam-to-column connection stiffness R provided from the test is given in Appendix E (Schuster, 2004). The designation of the beam section is also given in this table. With $M = PL_b$ and R known, θ can be determined from Eq. (6.6) for each load step. Once the beam-to-column connection stiffness R is obtained, the end-fixity factor, discussed in Chapter 3, can be obtained from Eqs. (3.1). In this study, the column base connections are assumed to be a rigid connection, in which the corresponding end-fixity factor will be taken a unity.

6.4 Elastic Buckling Strength of Storage Racks

6.4.1 Introduction

Up to now, the effective length factor, K , method is still the most commonly used method for assessing frame stability in the engineering practice and by the storage rack industry. The design of industrial steel storage racks in the United States is based on the effective length method according to the RMI Specification (RMI, 2000). It should be noted that the cantilever test discussed in the previous section is used to design beams and connections. The beam-to-column connection stiffness, R , obtained from the tests is to account for the semi-rigid behavior of the connection in design with a beam. However, there is an inconsistency in the current practice because the semi-rigid behavior was not accounted for in the evaluation of K factors. In practice, K is simply assumed to be 1.7 as suggested by the RMI Specification and it is not based on the alignment chart or stability analysis. Therefore, it is important to investigate K factors with accounting for R based on the test results.

As discussed in Chapter 2, the Notional loads are introduced to account for the effect of out-of-plumbness on the stability of a framed structure and the out-of-plumbness effect is assumed to be this that results from an erection tolerance of 5mm over 120mm (1:240) stated in Clause 6.2.2 of CSA/A344.1-05/A344.2-05 (CSA, 2005) for industrial steel storage racks. This corresponds to the maximum fabrication and erection tolerance permitted by the RMI specification and is roughly twice the value of 1/500 recommended by the AISC specification used for structural steel buildings (RMI, 2000; AISC, 2005).

The effective length factor based on the storey-based buckling method using the 2nd-order approximation presented in Chapter 4 will be used in this study to carry out the stability analysis for CFS storage rack's compressive members with and without accounting for initial geometric imperfections. Also, the unperforated sections will be considered in the following studies.

6.4.2 Column Effective Length Factor for Geometrically Perfect Storage Racks

The objective of this study is to evaluate the effective length factor K for CFS storage racks from the method previously mentioned from the last section and compare the results with the Alignment chart method. Parameters that influence the value of K for column flexural buckling including the section properties and beam-to-column connections are also examined in this study. The box sections used as columns and beams together with their section designations, section properties and the beam-to-column connection stiffness (R) can be obtained from Appendix E (Schuster, 2004).

2-Bay by 2-Storey Storage Rack Example

A 2-bay by 2-storey storage rack shown in Figure 6-12 is used to carry out this study. The dimension of this storage rack is also given in this figure. Some of the experimental data used in this study from Appendix E is summarized in Table 6-4. The results of effective length factor K , based on different rack types are presented in Table 6-5.

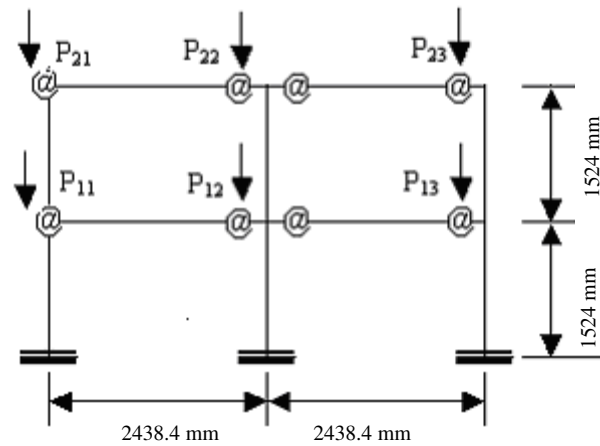


Figure 6-12: 2-bay by 2-storey storage rack example

Table 6-4: Properties of column and beam (Schuster, 2004)

Rack Type	Designation		Section properties	Beam-to-column Connection
	Width (mm)	Depth (mm)	$I_{c, y-net}$ (column) I_{xb} (beam) (mm^4)	R (N-mm/rad)
I Column Beam	82 50.800	2438.4 mm 800 177.800	2438.4 mm^5 4.87×10^6	3.537×10^7
II Column Beam	101.600 50.800	76.200 177.800	1.074×10^6 4.87×10^6	3.537×10^7
III Column Beam	82.550 50.800	50.800 101.600	4.7×10^5 1.22×10^6	2.09×10^7

Table 6-5: *K* factors for three types of column and beam in study

Storey	Column	<i>K</i> factors					
		Rack Type I		Rack Type II		Rack Type III	
		Alignment chart	Current study ($\delta_0=0, \Delta_0=0$)	Alignment chart	Current study ($\delta_0=0, \Delta_0=0$)	Alignment chart	Current study ($\delta_0=0, \Delta_0=0$)
1	C ₁₁	2.080	1.692	2.206	1.814	2.172	1.777
	C ₁₂	1.920	1.692	2.107	1.814	2.051	1.777
	C ₁₃	2.080	1.692	2.206	1.814	2.171	1.777
2	C ₂₁	3.570	3.410	5.262	5.182	4.602	4.484
	C ₂₂	2.620	3.410	3.792	5.182	3.335	4.484
	C ₂₃	3.570	3.410	5.262	5.182	4.602	4.484

In Table 6-4, Rack Types I and II have the same value of beam-to-column connection stiffness (*R*) and the same size beam section using a box section of 50.8mm×177.8mm (2”×7”). The box sections of 82.55mm×50.8mm (3-1/4”×3”) and 101.6mm×76.2mm(4”×3”) are used as column sections in Rack Types I and II, respectively. For Types I and III, only the column size is the same. Compared to Rack Types I and II, it is found that when the column size increases, the *K* factors will increase. It is also observed from Rack Types I and III when the beam size and the connection stiffness is increased, the value of *K* factors will decrease because of the additional restraint from the beam and connection stiffness will prevent the frame from sidesway buckling.

It is noted that the *K* factors values are close to 1.7 for the first storey and are greater than 2 for the second storey. In the RMI Specification, the *K* factor’s default value is equal to 1.7 to provide a reasonable amount of protection against sidesway buckling for most storage racks. However, the results from this study found the actual value of *K* factors for storey 2 is much higher than 1.7. In the RMI Specification, it is also stated that the *K* factor values other than 1.7 may be used if they can be justified on the basis of using a rational analysis. Such rational analysis must properly consider the following: column stiffness, beam stiffness, semi-rigid connection behavior and base fixity properties.

6.4.3 Effective Length Factor for Initial Geometric Imperfect Storage Racks

Considering the initial geometric imperfections to evaluate the effective length factor K , the standard practice of the AISC (2005) specifies a fabrication tolerance for compression members of $L/1000$ between lateral supports will be used as the initial out-of-straightness in storage racks (Sarawit and Peköz, 2006). The maximum erection tolerance of $L/240$ allowed by RMI (2000) and CSA/A344.1-05/A344.2-05 (CSA, 2005) will be used as the out-of-plumbness value for individual columns in storages racks. The critical loading multipliers together with their effective length factor based on each storey are obtained from Eqs. (4.23) corresponding to the 2nd-order approximations of λ in the Taylor series approximation of Eq. (4.11).

2-Bay by 3-Storey Storage Rack Example

A 2-bay by 3-storey storage rack shown in Figure 6-13 is investigated in this study. The dimensions for this storage rack are shown in this figure and the properties of Rack Type I given in Table 6-4 will be used for this study.

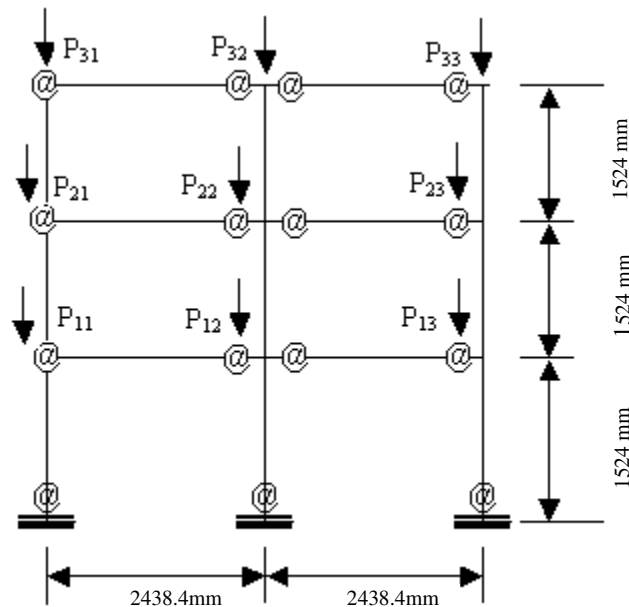


Figure 6-13: 2-bay by 3-storey storage rack example

For comparison, the results based on this study without the consideration of initial geometric imperfections are presented first. As discussed previously in section 6.3, once the beam-to-column

connection stiffness, R , values were obtained from the tests (Schuster, 2004), the corresponding end-fixity factor can be evaluated from Eq. (3.1). In this case, the end-fixity factor for the beam-to-column connection is 0.029 corresponding to the value of R of 3.537×10^7 N-mm/rad. Then following the steps given in Appendix A, the end-fixity factors for the lower and upper end of each individual column, $r_{l,ij}$ and $r_{u,ij}$ can be obtained for the purpose of evaluating the column lateral stiffness modification factors $\beta_{0,ij}$ and $\beta_{1,ij}$. The K factors values based on each storey can be determined from the 2nd - order approximation together with $r_{l,ij}$, $r_{u,ij}$, $\beta_{0,ij}$ and $\beta_{1,ij}$, and these results are presented in Tables 6-6. Also presented in this table are the results obtained from the alignment chart method.

Table 6-6: Comparison of K factors of two-bay by three-storey frame – Rack Type I

Storey	Col	Alignment chart	Current study ($\delta_0=0, \Delta_0=0$)				
		K factors	$r_{l,ij}$	$r_{u,ij}$	$\frac{12EI_{ij}}{L_{ij}^3} \beta_{0,ij}$ (kN/m)	$\beta_{1,ij}$ ($\times 10^{-2}$)	K factors
1	C ₁₁	2.080	1.000	0.122	102.146	9.787	1.692
	C ₁₂	1.919	1.000	0.198	116.917	9.671	1.692
	C ₁₃	2.080	1.000	0.122	102.146	9.787	1.692
2	C ₂₁	4.277	0.048	0.048	7.768	8.334	4.736
	C ₂₂	3.093	0.116	0.116	19.533	8.340	4.736
	C ₂₃	4.277	0.048	0.048	7.768	8.334	4.736
3	C ₃₁	3.565	0.122	0.159	23.965	8.345	2.954
	C ₃₂	2.623	0.198	0.274	42.417	8.372	2.954
	C ₃₃	3.565	0.122	0.159	23.965	8.345	2.954

From Table 6-6, compared to the proposed method, it is found that the alignment chart results are not in the conservative side for this frame. Also found in Table 6-6, the second storey is structurally unstable since its slenderness ratio KL/r is greater than 200. From the commentary of AISI, the slenderness ratio, KL/r , of all compression members preferably should not exceed 200 (AISI, 2004).

Presented in Table 6-7 are the results of the K factors accounting for the initial geometric imperfections for the pallet rack shown in Figure 6-13. The values for column lateral stiffness modification factors $\beta_{0,ij}$ and $\beta_{1,ij}$ associated with the initial geometric imperfections are also given in the table.

Table 6-7: *K* factors of two-bay by three-storey frame – Rack Type I

Storey	Col	Current study ($\delta_0=L/1000$, $\Delta_0=L/240$)		
		$\frac{12EI_{ij}}{L_{ij}^3}\beta_{0,ij}$ (kN/m)	$\beta_{1,ij}$ ($\times 10^{-2}$)	<i>K</i> factors
1	C ₁₁	95.352	10.380	1.806
	C ₁₂	108.165	10.250	1.806
	C ₁₃	95.352	10.380	1.806
2	C ₂₁	6.903	8.864	5.181
	C ₂₂	17.358	8.869	5.181
	C ₂₃	6.903	8.864	5.181
3	C ₃₁	21.108	8.876	3.247
	C ₃₂	37.303	8.909	3.247
	C ₃₃	21.108	8.876	3.247

From Tables 6-6 and 6-7, it is obvious that the column *K* factor values based on the initial geometric imperfections would increase while the column strength decreases. Similar to the case without consideration for the initial geometric imperfections, the slenderness ratio *KL/r* of second storey is greater than 200, consequently, the second storey becomes structurally unstable.

In the parametric studies, the following effects are demonstrated considering out-of-straightness, out-of-plumbness and these two effects combined on *K* factors in Tables 6-8 to 6-10.

Table 6-8: Effects of out-of-straightness - 2-bay by 3-storey

Column	<i>K</i> factors ($\Delta_0=0$)								
	$\delta_0=0$	$\delta_0=L/1000$	$\delta_0=L/800$	$\delta_0=L/600$	$\delta_0=L/500$	$\delta_0=L/400$	$\delta_0=L/300$	$\delta_0=L/240$	$\delta_0=L/200$
C ₁₁ = C ₁₂ = C ₁₃	1.692	1.740	1.753	1.774	1.792	1.819	1.867	1.919	1.974
C ₂₁ = C ₂₂ = C ₂₃	4.736	4.854	4.884	4.937	4.980	5.048	5.166	5.293	5.430
C ₃₁ = C ₃₂ = C ₃₃	2.954	3.027	3.047	3.079	3.107	3.149	3.223	3.302	3.388

Table 6-9: Effects of out-of-plumbness - 2-bay by 3-storey

Column	K factors ($\delta_0=0$)					
	$\Delta_0=0$	$\Delta_0=L/500$	$\Delta_0=L/400$	$\Delta_0=L/300$	$\Delta_0=L/240$	$\Delta_0=L/200$
$C_{11}=C_{12}=C_{13}$	1.692	1.723	1.730	1.743	1.756	1.769
$C_{21}=C_{22}=C_{23}$	4.736	4.883	4.920	4.983	5.047	5.112
$C_{31}=C_{32}=C_{33}$	2.954	3.052	3.077	3.119	3.162	3.206

Table 6-10: Effects of out-of-straightness and out-of-plumbness - 2-bay by 3-storey

Column	K factors					
	$\delta_0=0$	$\delta_0=L/1000$	$\delta_0=L/1000$	$\delta_0=L/800$	$\delta_0=L/600$	$\delta_0=L/400$
	$\Delta_0=0$	$\Delta_0=L/240$	$\Delta_0=L/500$	$\Delta_0=L/400$	$\Delta_0=L/300$	$\Delta_0=L/200$
$C_{11}=C_{12}=C_{13}$	1.692	1.806	1.772	1.793	1.829	1.904
$C_{21}=C_{22}=C_{23}$	4.736	5.181	5.008	5.081	5.207	5.479
$C_{31}=C_{32}=C_{33}$	2.954	3.247	3.131	3.178	3.261	3.440

Based on the results summarized in Tables 6-8 to 6-10, it is found that the K factors increase when the value of either one of the effects for initial imperfections increases. The combined effects of the initial geometric imperfections would have the most severe impact on the column K factors. For instance, the value of the K factor for the columns in storey 1 increased from 1.692 (perfect pallet rack) to 1.740 (out-of-straightness: $\delta_0 = L/1000$ alone) and from 1.692 (perfect pallet rack) to 1.756 (out-of-plumbness: $\Delta_0 = L/240$ alone). While the combined effects (out-of-straightness: $\delta_0 = L/1000$ and out-of-plumbness: $\Delta_0 = L/240$), the resulted K factor is increased to 1.806 from 1.692 (perfect pallet rack). It is also noted from Tables 6-8 and 6-9, the out-of-straightness has a greater influence than that of the out-of-plumbness, which is observed by comparing the K factors with respect to the imperfection values being $L/500$, $L/400$, $L/300$, $L/240$ and $L/200$.

6.5 Stability Analysis of Storage Racks Subjected to Variable Loading

6.5.1 Introduction

The elastic buckling load for storage racks subjected to variable loading using the approach discussed in Chapters 3 and 5 is presented in this section. As discussed previously, variable loading abandons the conventional assumption of proportional loading to instead of considering different load patterns that may cause a rack to buckle at different critical loading levels (Xu, 2002; Xu and Wang, 2007). The most critical or so-called lower bound of the buckling loads corresponding to the worst load patterns is the one that corresponds to the minimum magnitude of the total applied load for the rack. The minimum frame-buckling load together with its corresponding load pattern present a clear characterization of the buckling capacity of unbraced CFS racks subjected to variable loading. The proposed approach developed in Chapters 3 and 5 has realistically taken account for the volatility of magnitudes and patterns of loads applied to the storage racks as well as the initial geometric imperfections; therefore, it can be applied to the design of the storage racks.

6.5.2 Numerical Studies

Example of Geometric Perfect Storage Racks

The first numerical example carried out is the stability of a CFS rack subjected to variable loading without consideration for the effects of the initial geometric imperfections. As discussed previously in Chapter 3, following the procedures of decomposing a multi-storey unbraced frame into a series of single-storey frames presented in Appendix A, the lateral stability of the multi-storey unbraced frame subjected to variable loading can be formulated as a pair of problems seeking the maximum and minimum frame-buckling loads of the racks as described in Eqs. (3.13), (3.16) and (3.17).

The 3-bay by 3-storey CFS storage rack structure shown in Figure 6-20 studied by (Sarawit and Peköz, 2006) is investigated by using Rack Type I of column and beam sections together with their beam-to-column connection stiffness shown in Table 6-4. The beam-to-column connection stiffness obtained from the test is $R_1 = 313 \text{ k-in/rad}$ ($3.537 \times 10^7 \text{ N-mm/rad}$, Connection 1) (Schuster, 2004) in Rack Type I, the two different beam-to-column connection stiffness obtained of $R_2 = 10 \times R_1$ ($3.537 \times 10^8 \text{ N-mm/rad}$, Connection 2) and $R_3 = 50 \times R_1$ ($17.685 \times 10^8 \text{ N-mm/rad}$, Connection 3) are also considered in this study to demonstrate the influence of the semi-rigid connections to the variable

loading. Based on Eq. (3.1) in Chapter 3, the end-fixity factors associated with the foregoing three beam-to-column connection stiffness are evaluated and presented in Table 6-11. In this study, the column base connections are assumed to be rigid with a corresponding value of end-fixity factor of unity. Possible local buckling and distortional buckling of the members were not considered in this study. The effective length factor of the column associated with non-sway-buckling K_{braced} related to the rotational restraints of the column ends is used in the variable loading cases. K_{braced} is evaluated using Eq. (3.14).

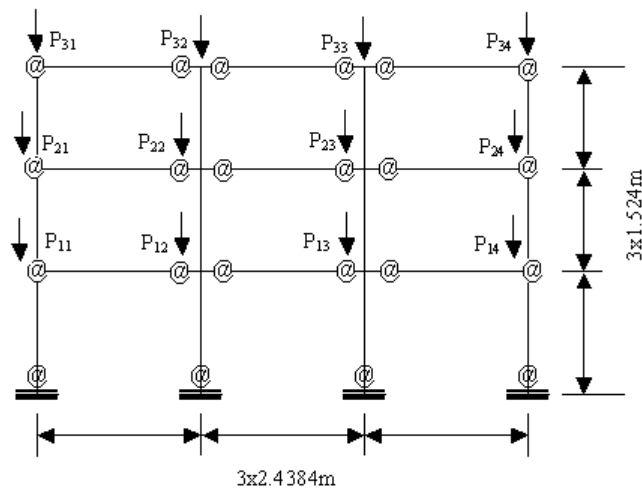


Figure 6-14: 3-bay by 3-storey storage rack example

Table 6-11: Three different end connections in study

Connection	Column base connection	Beam-to-column connection
1	$r = 1$	$r = 0.029$
2	$r = 1$	$r = 0.228$
3	$r = 1$	$r = 0.596$

Following the procedures described in Chapter 3, the frame-buckling loads with respect to the 3-bay by 3-storey storage rack being subjected to variable loading can be obtained from solving the

maximization and minimization problems stated in Eqs. (3.12), (3.15) and (3.16). For the foregoing three cases shown in Table 6-11, the maximum and minimum frame-buckling loads, together with their relative differences, are presented in Tables 6-12 to 6-14. For each case, the magnitudes of each variable load P_{ij} ($i=1, 2, 3; j = 1, 2, 3, 4$) associated with the maximum and minimum frame-buckling loads are presented so that the loading patterns corresponding to the critical buckling loads can be obtained. Also presented in the tables are influential column attributes, such as the end-fixity factors, the initial lateral stiffness $12EI_{ij}\beta_{0,ij}/L_{ij}^3$ ($i=1, 2, 3; j = 1, 2, 3, 4$) of the columns, the column effective length factor (K_{braced}) and the column buckling loads with respect to non-sway buckling. It can be observed from the tables that by increasing the column end-fixity factors would result in decreases of the column effective length factor, which consequently leads to increases of the magnitudes of column buckling loads in a non-sway mode. It is also observed that the column with the larger value of the end-fixity factor would yield to the larger value of $12EI_{ij}\beta_{0,ij}/L_{ij}^3$ that indicates the larger lateral stiffness against lateral instability.

Table 6-12: Results of the storage rack for Connection 1 ($r = 0.029$) –Figure 6-14

Col. <i>ij</i>	$r_{l,ij}$	$r_{u,ij}$	$\frac{12EI_{ij}}{L_{ij}^3} \beta_{0,ij}$ (kN/m)	$\beta_{1,ij}$	K_{braced}	$P_{u,ij}$ (kN)	Max. (kN)	Min. (kN)		
								$S_1 = 0$ $S_2 > 0$ $S_3 > 0$	$S_2 = 0$ $S_1 > 0$ $S_3 > 0$	$S_3 = 0$ $S_1 > 0$ $S_2 > 0$
11	1.000	0.123	102.343	0.098	0.681	861.400	-	401.010	-	
12	1.000	0.199	117.224	0.097	0.665	903.700	246.210	-	-	N/A
13	1.000	0.199	117.224	0.097	0.665	903.700	246.210	-	-	
14	1.000	0.123	102.343	0.098	0.681	861.400	-	84.460	-	
21	0.048	0.048	7.898	0.083	0.971	423.800	-	3.600	-	N/A
22	0.117	0.117	19.813	0.083	0.931	461.300	-	-	65.700	
23	0.117	0.117	19.813	0.083	0.931	461.300	-	-	1.700	
24	0.048	0.048	7.898	0.083	0.971	423.800	-	3.600	-	
31	0.123	0.160	24.203	0.084	0.917	475.400	-	3.600	-	N/A
32	0.199	0.276	42.810	0.084	0.863	536.900	-	-	15.300	
33	0.199	0.276	42.810	0.084	0.863	536.900	84.400	-	1.700	
34	0.123	0.160	24.203	0.084	0.917	475.400	-	73.660	-	
Critical frame buckling loads $\sum P_{ij} =$							578.820	569.930	84.400	N/A
$\sum S_i =$							$S_1=0.000$ $S_2=0.000$ $S_3=122.820$	$S_1=0.000$ $S_2=0.000$ $S_3=83.260$	$S_1=374.880$ $S_2=0.000$ $S_3=122.820$	N/A
Difference max. & min. loads							1.6%	585.5%	N/A	

Table 6-13: Results of the storage rack for Connection 2 ($r = 0.228$) – Figure 6-14

Col. <i>ij</i>	$r_{l,ij}$	$r_{u,ij}$	$\frac{12EI_{ij}}{L_{ij}^3} \beta_{0,ij}$ (kN/m)	$\beta_{1,ij}$	K_{braced}	$P_{u,ij}$ (kN)	Max. (kN)	Min. (kN)		
								$S_1 = 0$ $S_2 > 0$ $S_3 > 0$	$S_2 = 0$ $S_1 > 0$ $S_3 > 0$	$S_3 = 0$ $S_1 > 0$ $S_2 > 0$
11	1.000	0.476	176.561	0.097	0.665	902.100	-	371.860	-	
12	1.000	0.636	215.186	0.095	0.642	967.800	-	-	-	N/A
13	1.000	0.636	215.186	0.095	0.642	967.800	389.750	-	-	
14	1.000	0.476	176.561	0.097	0.665	902.100	-	0.700	-	
21	0.431	0.431	87.544	0.083	0.932	459.600	-	-	-	N/A
22	0.613	0.613	141.002	0.084	0.865	534.500	-	-	106.540	
23	0.613	0.613	141.002	0.084	0.865	534.500	0.050	-	26.720	
24	0.431	0.431	87.544	0.083	0.932	459.600	-	171.560	-	
31	0.476	0.625	120.396	0.084	0.865	534.500	-	171.550	-	N/A
32	0.636	0.769	171.926	0.084	0.793	634.900	-	-	26.720	
33	0.636	0.769	171.926	0.084	0.793	634.900	670.270	-	26.720	
34	0.476	0.625	120.396	0.084	0.865	534.500	-	171.560	-	
Critical frame buckling loads $\sum P_{ij} =$							1060.070	1058.780	670.320	N/A
$\sum S_i =$							$S_1=0.000$ $S_2=0.000$ $S_3=117.980$	$S_1=0.000$ $S_2=0.000$ $S_3=351.980$	$S_1=288.060$ $S_2=0.000$ $S_3=584.640$	N/A
Difference max. & min. loads							0.12%	58.1%		N/A

Table 6-14: Results of the storage rack for Connection 3 ($r = 0.596$) – Figure 6-14

Col. <i>ij</i>	$r_{l,ij}$	$r_{u,ij}$	$\frac{12EI_{ij}}{L_{ij}^3} \beta_{0,ij}$ (kN/m)	$\beta_{1,ij}$	K_{braced}	$P_{u,ij}$ (kN)	Max. (kN)	Min. (kN)		
								$S_1 = 0$ $S_2 > 0$ $S_3 > 0$	$S_2 = 0$ $S_1 > 0$ 0 $S_3 > 0$	$S_3 = 0$ $S_1 > 0$ $S_2 > 0$
11	1.000	0.739	242.135	0.096	0.654	934.800	-	-	-	N/A
12	1.000	0.848	272.585	0.095	0.627	1017.000	-	217.580	-	
13	1.000	0.848	272.585	0.095	0.627	1017.000	-	0.130	-	
14	1.000	0.739	242.135	0.096	0.654	934.800	195.320	-	-	
21	0.727	0.727	182.148	0.084	0.899	494.800	-	-	-	N/A
22	0.844	0.844	232.737	0.084	0.817	598.300	-	1.970	1058.760	
23	0.844	0.844	232.737	0.084	0.817	598.300	-	578.070	1.760	
24	0.727	0.727	182.148	0.084	0.899	494.800	395.290	-	-	
31	0.739	0.846	208.708	0.084	0.827	584.000	395.690	-	-	N/A
32	0.848	0.917	251.372	0.085	0.749	711.800	-	562.53	80.340	
33	0.848	0.917	251.372	0.085	0.749	711.800	-	-	1.760	
34	0.739	0.846	208.708	0.084	0.827	584.000	395.690	-	-	
Critical frame buckling loads $\sum P_{ij} =$							1382.800	1360.330	1142.620	N/A
$\sum S_i =$							$S_1=0.000$ $S_2=0.000$ $S_3=354.790$	$S_1=0.000$ $S_2=0.000$ $S_3=504.580$	$S_1=164.760$ $S_2=0.000$ $S_3=859.510$	N/A
Difference max. & min. loads							1.7%	21%		N/A

For Connection 1 the column base is rigidly connected and the beam-to-column connections are semi-rigidly connected with the end-fixity factor value of 0.029, which can be practically considered as a pinned connection. Consequently, the rack is flexible and it can be observed from Table 6-12 that the maximum frame-buckling loads is 576.82kN associated with both first and second stories becoming laterally unstable. The minimum frame-buckling loads associated with lateral instability of the first and second stories are 569.93 kN and 84.40 kN, respectively. Therefore, the relative difference between the maximum and minimum frame-buckling loads is 585.5%, which is rather significant and would cause some concern in the engineering practice. It is also observed from Table

6-12 that the load pattern corresponding to the maximum frame-buckling loads tends to place the loading only on the interior columns which are laterally stiffer than the exterior ones as characterized by the larger value of the column lateral stiffness $12EI_{ij}\beta_{0,ij}/L_{ij}^3$. Contrasting to the maximum loading, the load patterns associated with the minimum frame-buckling loadings are applied on the exterior columns when the first storey is laterally unstable and on the interior columns when the second storey is laterally unstable. With respect to the load patterns corresponding to the maximum and minimum frame-buckling loads obtained from the current study, verification results using MASTAN2 (McGuire et al., 2000) is given in Table 6-15. The results show that the applied load ratio of the elastic critical load is equal to one, which indicates the rack is within its critical load conditions.

Table 6-15: Results verification of rack shown in Figure 6-14 – Connection 1

Storey	Columns	Current study			
		Max. (kN)	Min. (kN)		
			$S_1 = 0$ $S_2 > 0$ $S_3 > 0$	$S_2 = 0$ $S_1 > 0$ $S_3 > 0$	$S_3 = 0$ $S_1 > 0$ $S_2 > 0$
1	11	-	401.010	-	N/A
	12	246.210	-	-	
	13	246.210	-	-	
	14	-	84.460	-	
2	21	-	3.600	-	N/A
	22	-	-	65.700	
	23	-	-	1.700	
	24	-	3.600	-	
3	31	-	3.600	-	N/A
	32	-	-	15.300	
	33	84.400	-	1.700	
	34	-	73.660	-	
MASTAN2 – Elastic critical load: applied load ratio		1.0030	1.0310	0.987	N/A

In Connection 2, the beam-to-column connections stiffness ($r = 0.228$) value is increased to ten times compared to Connection 1 ($r = 0.029$). The increase of the semi-rigid connection stiffness yields a stiffer frame, which is evidenced by increasing the columns lateral stiffness $12EI_{ij}\beta_{0,ij}/L_{ij}^3$ compared to that of Connection 1. Consequently, the maximum frame-buckling load of Connection 2 increases

to 1060.07 kN, and the corresponding minimum frame-buckling load decreases to 670.32 kN, which yields the relative difference between the maximum and minimum frame-buckling loads to be 58.1%, which is still very significant. The load patterns associated with the maximum and minimum frame-buckling loads are similar to that of Connection 1.

As the connection rigidity value of Connection 3 ($r=0.596$) is further increased to fifty times of Connection 1 ($r=0.029$), the storage rack becomes stiffer than Connection 2, and the magnitudes of the maximum and minimum frame-buckling loads are found to be increased to 1382.8 kN and 1142.62 kN, respectively. The relative difference between the maximum and minimum in Connection 3 is 21%. It is found that the load patterns associated with the maximum are applied for exterior columns, which are different compared to Connections 1 and 2. When either the first or second stories are laterally unstable, the load patterns associated with minimum frame-buckling loads are found to apply to the loading on the interior columns.

It is noted that for the three connections, the linear programming procedure could not find the maximum and minimum frame-buckling loads that only involves the lateral storey buckling of the third storey of the storage rack ($S_3=0$ and $S_1 > 0$, $S_2 > 0$), which indicates that for any given load pattern, the lateral storey instability will not occur in the third storey prior to such type of failure in the first and/or second storey. Therefore, the maximum and minimum frame-buckling loads with respect to the lateral instability of storey 3 are not considered in the following parametric study.

Example of Initial Geometric Imperfect Storage Racks

The second study is designed to investigate the effects of the initial geometric imperfections to the CFS storage racks stability subjected to variable loading. The numerical example of the 3-bay by 3-storey CFS rack (shown in Figure 6-14) with the end-fixity factor of Connection 2 (shown in Table 6-11) will be used and the effects of out-of-straightness (δ_0), out-of-plumbness (Δ_0) and combined the out-of-straightness (δ_0) and out-of-plumbness (Δ_0) are evaluated, respectively.

(1) Effect of out-of-Straightness (δ_0)

For stability of the 3-bay by 3-storey rack subjected to variable loading, the results of maximum and minimum frame-buckling loads influenced by out-of-straightness (δ_0) are presented in Tables 6-16 to

6-18. The relative difference between the maximum and minimum frame-buckling loads is given in Table 6-19.

Table 6-16: Effects of out-of-straightness (δ_0) to Maximum frame-buckling loads

Col. <i>ij</i>	Maximum frame-buckling loads (kN)						
	$\delta_0=0$	$\delta_0=L/100$ 0	$\delta_0=L/800$	$\delta_0=L/600$	$\delta_0=L/500$	$\delta_0= L/400$	$\delta_0= L/300$
11	-	-	-	-	-	-	-
12	-	183.360	184.080	0.900	172.310	166.670	157.070
13	389.750	183.350	177.160	350.920	172.110	166.670	158.210
14	-	-	-	-	-	-	-
21	-	-	-	-	-	-	-
22	-	-	3.870	72.600	588.110	504.040	2.180
23	0.050	2.170	6.350	180.810	5.300	27.820	184.480
24	-	-	-	-	-	-	-
31	-	-	-	-	-	-	-
32	-	406.390	102.380	180.810	5.300	27.820	186.660
33	670.270	228.550	516.210	180.810	5.300	27.820	186.660
34	-	-	-	-	-	-	-
ΣP_{ij}	1060.070	1003.820	990.060	966.840	948.420	920.850	875.250
ΣS_i	$S_1=0.000$ $S_2=0.000$ $S_3=117.980$	$S_1=0.000$ $S_2=0.000$ $S_3=112.700$	$S_1=0.000$ $S_2=0.000$ $S_3=116.820$	$S_1=0.000$ $S_2=0.000$ $S_3=284.680$	$S_1=0.000$ $S_2=0.000$ $S_3=521.230$	$S_1=0.000$ $S_2=0.000$ $S_3=475.600$	$S_1=0.000$ $S_2=0.000$ $S_3=228.600$

Table 6-17: Effects of out-of-straightness (δ_0) to minimum loading with lateral instability - storey 1: $S_1 = 0, S_2 > 0, S_3 > 0$

Col. <i>ij</i>	Minimum frame-buckling load (kN) ($S_1 = 0, S_2 > 0, S_3 > 0$)						
	$\delta_0=0$	$\delta_0=L/100$ 0	$\delta_0=L/800$	$\delta_0=L/600$	$\delta_0=L/500$	$\delta_0= L/400$	$\delta_0= L/300$
11	371.860	349.490	6.40	-	594.860	523.850	293.000
12	-	-	-	-	-	-	-
13	-	-	-	-	-	-	-
14	0.700	-	337.760	334.970	-	-	17.460
21	-	81.620	173.850	-	230.420	181.130	132.140
22	-	-	-	-	-	-	-
23	-	-	-	-	-	-	-
24	171.560	190.460	156.910	-	-	0.025	143.830
31	171.550	190.440	156.910	-	-	0.025	143.830
32	-	-	-	-	-	-	-
33	-	-	-	-	-	-	-
34	171.560	190.460	156.910	630.700	121.870	212.600	143.830
ΣP_{ij}	1058.780	1002.460	988.730	965.680	947.120	919.620	874.090
ΣS_i	$S_1=0.000$	$S_1=0.000$	$S_1=0.000$	$S_1=0.000$	$S_1=0.000$	$S_1=0.000$	$S_1=0.000$
	$S_2=0.000$	$S_2=0.000$	$S_2=0.000$	$S_2=0.000$	$S_2=0.000$	$S_2=0.000$	$S_2=0.000$
	$S_3=117.980$	$S_3=297.980$	$S_3=336.480$	$S_3=109.240$	$S_3=279.520$	$S_3=299.400$	$S_3=295.270$

Table 6-18: Effects of out-of-straightness (δ_0) to minimum loading with lateral instability - storey 2: $S_2 = 0, S_1 > 0, S_3 > 0$

Col. <i>ij</i>	Minimum frame-buckling loads (kN) ($S_2 = 0, S_1 > 0, S_3 > 0$)						
	$\delta_0=0$ Min.(kN)	$\delta_0=L/1000$ Min.(kN)	$\delta_0=L/800$ Min.(kN)	$\delta_0=L/600$ Min.(kN)	$\delta_0=L/500$ Min.(kN)	$\delta_0= L/400$ Min.(kN)	$\delta_0= L/300$ Min.(kN)
11	-	-	-	-	-	-	-
12	-	-	-	-	-	-	-
13	-	-	-	-	-	-	-
14	-	-	-	-	-	-	-
21	-	-	-	-	-	-	-
22	106.540	471.380	628.820	614.980	508.160	-	553.780
23	26.720	54.840	0.025	0.025	31.950	195.830	3.270
24	-	-	-	-	-	-	-
31	-	-	-	-	-	-	-
32	26.720	55.430	-	-	31.950	195.830	1.460
33	26.720	55.440	0.025	0.025	-	195.830	1.460
34	-	-	-	-	-	-	-
ΣP_{ij}	670.320	637.100	628.820	615.030	604.010	587.500	559.970
ΣS_i	$S_1=288.060$ $S_2=0.000$ $S_3=584.640$	$S_1=272.460$ $S_2=0.000$ $S_3=479.130$	$S_1=268.060$ $S_2=0.000$ $S_3=584.640$	$S_1=262.350$ $S_2=0.000$ $S_3=537.970$	$S_1=257.280$ $S_2=0.000$ $S_3=483.86$	$S_1=249.680$ $S_2=0.000$ $S_3=239.670$	$S_1=237.190$ $S_2=0.000$ $S_3=489.280$

Table 6-19: Difference between the maximum and minimum frame-buckling loads - out-of-straightness (δ_0)

out-of-straightness	Max. Frame buckling loads $\Sigma P_{ij} =$ (kN)	$S_1 = 0, S_2 > 0, S_3 > 0$		$S_2 = 0, S_1 > 0, S_3 > 0$	
		Min. Frame buckling loads $\Sigma P_{ij} =$ (kN)	Difference Max. & Min loads (kN)	Min. Frame buckling loads $\Sigma P_{ij} =$ (kN)	Difference Max. & Min loads (kN)
$\delta_0=0$	1060.070	1058.780	0.12%	670.320	58.1%
$\delta_0=L/1000$	1003.810	1002.460	0.13%	637.100	57.6%
$\delta_0=L/800$	990.060	988.730	0.13%	628.820	57.4%
$\delta_0=L/600$	966.840	965.680	0.12%	615.030	57.2%
$\delta_0=L/500$	948.420	947.120	0.14%	604.010	57.0%
$\delta_0=L/400$	920.850	919.620	0.13%	587.500	56.7%
$\delta_0=L/300$	875.250	874.090	0.13%	559.970	56.3%

In Tables 6-16 to 6-18, the results demonstrate that the maximum frame-buckling loads of the rack and minimum frame buckling loads corresponding to the lateral instability of stories 1 and 2, which are $S_1 = 0, S_2 > 0, S_3 > 0$ and $S_2 = 0, S_1 > 0, S_3 > 0$, respectively. Comparing the results to the geometric perfect rack, it is found that the maximum and minimum frame-buckling loads decrease as the values of out-of-straightness (δ_0) increase. In Table 6-17, for each value for out-of-straightness (δ_0), the load pattern corresponding to the maximum frame-buckling loads tends to place the loading only on the interior columns and the first and second stories are laterally unstable simultaneously. The results of Table 6-17 demonstrate for each value for out-of-straightness (δ_0) with respect to the lateral instability of storey 1, the load pattern corresponding to the minimum frame-buckling loads will tend to place the loading only on the exterior columns and second stories are laterally unstable simultaneously. While for the minimum frame-buckling loads with respect to the lateral instability of storey 2 shown in Table 6-18, it is observed that for each value of the out-of-straightness (δ_0), the

minimum frame-buckling loads decrease significantly and the corresponding load tends to place the loading only on the interior columns.

The results of the relative difference between the maximum and minimum frame-buckling loads with respect to lateral instability of stories 1 and 2 are presented in Table 6-19. For each value of out-of-straightness (δ_0), only 0.13% is noted for the relative difference between the maximum and minimum frame-buckling loads associated with the lateral instability of storey 1. A significant difference is found to be greater than 56% between the maximum and minimum frame-buckling loads with respect to lateral instability of storey 2.

(2)Effect of out-of-Plumbness (Δ_0)

The results of the maximum and minimum frame-buckling loads accounting for the effect of out-of-plumbness (Δ_0) are demonstrated in Tables 6-20 to 6-22. The relative difference between the maximum and minimum frame-buckling loads is presented in Table 6-23.

Table 6-20: Effects of out-of-plumbness (Δ_0) to maximum frame-buckling loads

Col. <i>ij</i>	Maximum frame-buckling loads (kN)					
	$\Delta_0=0$	$\Delta_0=L/500$	$\Delta_0=L/400$	$\Delta_0=L/300$	$\Delta_0=L/240$	$\Delta_0=L/200$
11	-	-	-	122.570	9.810	476.150
12	-	328.400	186.390	-	-	-
13	389.750	47.710	186.390	-	-	-
14	-	-	-	230.630	338.720	0.390
21	-	-	-	-	-	213.170
22	-	626.260	463.540	-	-	-
23	0.050	-	7.200	-	-	-
24	-	-	-	206.180	-	0.340
31	-	-	-	206.750	291.010	0.780
32	-	4.480	150.440	-	-	-
33	670.270	-	-	-	-	-
34	-	-	-	206.580	313.250	242.110
ΣP_{ij}	1060.070	1006.850	993.960	973.100	952.800	932.930
ΣS_i	$S_1=0.000$ $S_2=0.000$ $S_3=117.980$	$S_1=0.000$ $S_2=0.000$ $S_3=562.080$	$S_1=0.000$ $S_2=0.000$ $S_3=451.460$	$S_1=0.000$ $S_2=0.000$ $S_3=257.500$	$S_1=0.000$ $S_2=0.000$ $S_3=107.830$	$S_1=0.000$ $S_2=0.000$ $S_3=358.700$

Table 6-21: Effects of out-of-plumbness (Δ_0) to minimum loading with lateral instability - storey 1: $S_1 = 0, S_2 > 0, S_3 > 0$

Col. <i>ij</i>	Minimum frame buckling loads (kN) ($S_1 = 0, S_2 > 0, S_3 > 0$)					
	$\Delta_0=0$	$\Delta_0=L/500$ Min. (kN)	$\Delta_0=L/400$ Min. (kN)	$\Delta_0=L/300$ Min. (kN)	$\Delta_0=L/240$ Min. (kN)	$\Delta_0=L/200$ Min. (kN)
11	371.860	-	-	122.570	9.810	476.150
12	-	328.400	186.390	-	-	-
13	-	47.710	186.390	-	-	-
14	0.700	-	-	230.630	338.720	0.390
21	-	-	-	-	-	213.170
22	-	626.260	463.540	-	-	-
23	-	-	7.200	-	-	-
24	171.560	-	-	206.180	-	0.340
31	171.550	-	-	206.750	291.010	0.780
32	-	4.480	150.440	-	-	-
33	-	-	-	-	-	-
34	171.560	-	-	206.580	313.250	242.110
ΣP_{ij}	1058.780	1006.850	993.960	973.100	952.800	932.930
ΣS_i	$S_1=0.000$ $S_2=0.000$ $S_3=117.980$	$S_1=0.000$ $S_2=0.000$ $S_3=562.080$	$S_1=0.000$ $S_2=0.000$ $S_3=451.460$	$S_1=0.000$ $S_2=0.000$ $S_3=257.500$	$S_1=0.000$ $S_2=0.000$ $S_3=107.830$	$S_1=0.000$ $S_2=0.000$ $S_3=358.700$

Table 6-22: Effects of out-of-plumbness (Δ_0) to minimum loading with lateral instability - storey 2: $S_2 = 0, S_1 > 0, S_3 > 0$

Col. <i>ij</i>	Minimum frame buckling loads (kN) ($S_2 = 0, S_1 > 0, S_3 > 0$)					
	$\Delta_0=0$	$\Delta_0=L/500$	$\Delta_0=L/400$	$\Delta_0=L/300$	$\Delta_0=L/240$	$\Delta_0=L/200$
11	-	-	-	-	-	-
12	-	-	-	-	-	-
13	-	-	-	-	-	-
14	-	-	-	-	-	-
21	-	-	-	-	-	-
22	106.540	475.050	463.540	590.930	590.030	0.050
23	26.720	0.280	7.20	-	-	0.370
24	-	-	-	-	-	-
31	-	-	-	-	-	-
32	26.720	154.750	150.440	14.610	-	-
33	26.720	0.650	-	-	-	72.020
34	-	-	-	-	-	-
ΣP_{ij}	670.320	630.740	621.190	605.540	590.030	575.440
ΣS_i	$S_1=288.060$ $S_2=0.000$ $S_3=584.640$	$S_1=285.620$ $S_2=0.000$ $S_3=453.550$	$S_1=284.990$ $S_2=0.000$ $S_3=451.460$	$S_1=283.990$ $S_2=0.000$ $S_3=541.690$	$S_1=283.090$ $S_2=0.000$ $S_3=544.350$	$S_1=281.780$ $S_2=0.000$ $S_3=536.070$

Table 6-23: Difference between the maximum and minimum frame-buckling loads - out-of-plumbness (Δ_0)

out-of-plumbness	Max. Frame buckling loads $\Sigma P_{ij} =$ (kN)	$S_1 = 0, S_2 > 0, S_3 > 0$		$S_2 = 0, S_1 > 0, S_3 > 0$	
		Min. Frame buckling loads $\Sigma P_{ij} =$ (kN)	Difference Max. & Min loads (kN)	Min. Frame buckling loads $\Sigma P_{ij} =$ (kN)	Difference Max. & Min loads (kN)
$\Delta_0=0$	1060.070	1058.780	0.12%	670.320	58.1%
$\Delta_0=L/500$	1006.810	1006.810	0.0%	630.740	59.6%
$\Delta_0=L/400$	993.960	993.960	0.0%	621.190	60.0%
$\Delta_0=L/300$	973.100	973.100	0.0%	605.540	60.7%
$\Delta_0=L/240$	952.800	952.800	0.0%	590.030	61.5%
$\Delta_0=L/200$	932.930	932.930	0.0%	575.440	62.1%

From Tables 6-20 to 6-22, it is found that the magnitudes of the maximum and minimum frame-buckling loads are reduced with the presence of the initial out-of-plumbness. In Table 6-20, it is found when the rack is achieved to the maximum frame-buckling load, the first and second stories become laterally unstable simultaneously. It is also found from Tables 6-20 and 6-21, for each out-of-plumbness (Δ_0) value, there are no differences between the maximum and minimum frame-buckling loads including the load patterns with respect to the lateral instability of storey 1. It is also noted that the load patterns tend to place the loading only on the interior columns for out-of-plumbness with values of $\Delta_0=L/500$ and $\Delta_0=L/400$ and the load patterns tend to place the loading to the exterior columns for out-of-plumbness with values of $\Delta_0=L/300$, $\Delta_0=L/240$ and $\Delta_0=L/200$. In the case of the minimum frame-buckling loads with respect to the lateral instability of storey 2 shown in Table 6-22, it is seen that for each value of the out-of-plumbness (Δ_0), the minimum frame-buckling loads decrease significantly and the corresponding load tends to place the loading only on the interior columns.

The relative difference as noted is insignificant between the maximum and minimum frame-buckling loads with respect to the lateral instability of storey. The lateral instability with respect to the second storey, the relative difference between the maximum and minimum frame-buckling loads are found to be 59.6%, 60.0%, 60.7%, 61.5% and 62.1%, for each out-of-plumbness (Δ_0) of $\Delta_0=L/500$, $\Delta_0=L/400$, $\Delta_0=L/300$, $\Delta_0=L/240$ and $\Delta_0=L/200$, respectively.

(3) Combined Effects of out-of-Straightness (δ_0) and out-of-Plumbness (Δ_0)

The combined effects of out-of-straightness (δ_0) and out-of-plumbness (Δ_0) on the maximum and minimum frame-buckling loads together with their relative difference are discussed in this section. Comparing to only one of the effects for out-of-straightness or out-of-plumbness, the combined effects of out-of-straightness and out-of-plumbness have a greater impact on the maximum and minimum frame-buckling loads.

Table 6-24: Effects of both out-of-straightness (δ_0) and out-of-plumbness (Δ_0) to maximum frame-buckling loading

Col. <i>ij</i>	Maximum frame-buckling load (kN)					
	$\delta_0=0$ $\Delta_0=0$	$\delta_0=L/1000$ $\Delta_0=L/240$	$\delta_0=L/1000$ $\Delta_0=L/500$	$\delta_0=L/800$ $\Delta_0=L/400$	$\delta_0=L/600$ $\Delta_0=L/300$	$\delta_0=L/400$ $\Delta_0=L/200$
11	-	113.570	74.610	125.720	82.810	138.730
12	-	-	95.520	73.240	82.810	-
13	389.750	-	95.520	73.240	82.810	-
14	-	213.540	88.350	73.210	82.810	153.280
21	-	3.190	-	-	2.050	111.350
22	-	-	577.340	573.030	544.730	-
23	0.050	-	5.000	0.690	-	-
24	-	187.830	-	-	2.070	133.520
31	-	191.030	-	-	1.850	133.520
32	-	-	11.140	6.830	0.530	-
33	670.270	-	5.000	0.690	-	-
34	-	191.010	-	-	2.070	133.520
ΣP_{ij}	1060.070	900.160	952.480	926.630	884.530	803.920
ΣS_i	$S_1=0.000$ $S_2=0.000$ $S_3=117.980$	$S_1=0.000$ $S_2=0.000$ $S_3=239.990$	$S_1=0.000$ $S_2=0.000$ $S_3=525.670$	$S_1=0.000$ $S_2=0.000$ $S_3=520.020$	$S_1=0.000$ $S_2=0.000$ $S_3=502.570$	$S_1=0.000$ $S_2=0.000$ $S_3=270.370$

Table 6-25: Effects of both out-of-straightness (δ_0) and out-of-plumbness (Δ_0) to minimum loading with lateral instability - storey 1: $S_1 = 0, S_2 > 0, S_3 > 0$

Col. <i>ij</i>	Minimum frame-buckling loads (kN) ($S_1 = 0, S_2 > 0, S_3 > 0$)					
	$\delta_0=0$ $\Delta_0=0$	$\delta_0=L/100$ 0 $\Delta_0=L/240$	$\delta_0=L/100$ 0 $\Delta_0=L/500$	$\delta_0=L/800$ $\Delta_0=L/400$	$\delta_0=L/600$ $\Delta_0=L/300$	$\delta_0=L/400$ $\Delta_0=L/200$
11	371.860	113.570	74.610	125.720	82.810	138.730
12	-	-	95.520	73.240	82.810	-
13	-	-	95.520	73.240	82.810	-
14	0.700	213.540	88.350	73.210	82.810	153.280
21	-	3.190	-	-	2.050	111.350
22	-	-	577.340	573.030	544.730	-
23	-	-	5.000	0.690	-	-
24	171.560	187.830	-	-	2.070	133.520
31	171.550	191.030	-	-	1.850	133.520
32	-	-	11.140	6.830	0.530	-
33	-	-	5.000	0.690	-	-
34	171.560	191.010	-	-	2.070	133.520
ΣP_{ij}	1058.780	900.160	952.480	926.630	884.530	803.920
ΣS_i	$S_1=0.000$ $S_2=0.000$ $S_3=351.980$	$S_1=0.000$ $S_2=0.000$ $S_3=564.540$	$S_1=0.000$ $S_2=0.000$ $S_3=451.460$	$S_1=0.000$ $S_2=0.000$ $S_3=257.500$	$S_1=0.000$ $S_2=0.000$ $S_3=107.830$	$S_1=0.000$ $S_2=95.120$ $S_3=358.700$

Table 6-26: Effects of both out-of-straightness (δ_0) and out-of-plumbness (Δ_0) to minimum loading with lateral instability - storey 2: $S_2 = 0, S_1 > 0, S_3 > 0$

Col. <i>ij</i>	$S_2 = 0, S_1 > 0, S_3 > 0$					
	$\delta_0=0$ $\Delta_0=0$ Min. (kN)	$\delta_0=L/100$ 0 $\Delta_0=L/240$ Min. (kN)	$\delta_0=L/1000$ $\Delta_0=L/500$ Min. (kN)	$\delta_0=L/800$ $\Delta_0=L/400$ Min. (kN)	$\delta_0=L/600$ $\Delta_0=L/300$ Min. (kN)	$\delta_0=L/400$ $\Delta_0=L/200$ Min. (kN)
11	-	-	-	-	-	-
12	-	-	-	-	-	-
13	-	-	-	-	-	-
14	-	-	-	-	-	-
21	-	-	-	-	-	-
22	106.540	552.950	577.340	573.030	545.340	498.610
23	26.720	0.0270	5.000	0.680	-	0.0560
24	-	-	-	-	-	-
31	-	-	-	-	-	-
32	26.720	6.170	11.140	6.830	7.750	0.0560
33	26.720	0.0270	5.000	0.680	-	0.0570
34	-	-	-	-	-	-
ΣP_{ij}	670.320	559.170	598.490	581.220	553.090	498.780
ΣS_i	$S_1=288.060$ $S_2=0.000$ $S_3=584.640$	$S_1=267.510$ $S_2=0.000$ $S_3=511.750$	$S_1=270.270$ $S_2=0.000$ $S_3=525.670$	$S_1=266.800$ $S_2=0.000$ $S_3=520.020$	$S_1=258.370$ $S_2=0.000$ $S_3=500.050$	$S_1=243.570$ $S_2=0.000$ $S_3=466.230$

Table 6-27: Difference between the maximum and minimum frame-buckling loads – out-of-straightness (δ_0) and out-of-plumbness (Δ_0)

out-of-straightness and out-of-plumbness	Max. Frame buckling loads $\Sigma P_{ij} =$ (kN)	$S_1 = 0, S_2 > 0, S_3 > 0$		$S_2 = 0, S_1 > 0, S_3 > 0$	
		Min. Frame buckling loads $\Sigma P_{ij} =$ (kN)	Difference Max. & Min loads (kN)	Min. Frame buckling loads $\Sigma P_{ij} =$ (kN)	Difference Max. & Min loads (kN)
$\delta_0=0$ $\Delta_0=0$	1060.070	1058.780	0.12%	670.320	58.1%
$\delta_0=L/1000$ $\Delta_0=L/240$	900.160	900.160	0.0%	559.170	61.0%
$\delta_0=L/1000$ $\Delta_0=L/500$	952.480	952.480	0.0%	598.490	59.1%
$\delta_0=L/800$ $\Delta_0=L/400$	926.630	926.630	0.0%	581.220	59.4%
$\delta_0=L/600$ $\Delta_0=L/300$	884.530	884.530	0.0%	553.090	59.9%
$\delta_0=L/400$ $\Delta_0=L/200$	803.920	803.920	0.0%	498.780	61.2%

As presented in Tables 6-24 to 6-27, it is found that the results for the maximum and minimum frame-buckling loads decrease when the values of the out-of-straightness (δ_0) and out-of-plumbness (Δ_0) are both increased. From Table 6-24, it is noted when the rack is subjected to the maximum frame-buckling loads the first and second stories become laterally unstable simultaneously and the corresponding load patterns tend to place the loading on the both interior and exterior columns. Similar to the effect of out-of-plumbness (Δ_0), and the combined effects for out-of-straightness (δ_0) and out-of-plumbness (Δ_0), the maximum and minimum frame-buckling loads including the load values and patterns with respect to the lateral instability of storey 1 are identical. It is also noted that

the minimum frame buckling loads decrease significantly when the frame is associated with the lateral instability of storey 2 and the load pattern corresponding to this minimum frame-buckling loads tends to place the loading only on the interior columns. In Table 6-27, for each combined value of out-of-straightness (δ_0) and out-of-plumbness (Δ_0), the relative differences between the maximum and minimum frame-buckling loads is close to 60%, which is significant.

6.6 Conclusions

The section properties of perforated members together with their elastic buckling analyses using the computer program CU-TWP (Sarawit and Peköz, 2003) and CAN/CSA-S136-04 (CSA, 2004) were studied first in this chapter. The results indicate that the presence of perforations in the section will reduce the buckling strength. The beam-to-column connection test results provided by Schuster (2004) were used to obtain the end-fixity factors, then the proposed method discussed in Chapters 3 and 4 can be used to predict the stability for CFS storage rack structures. Similar to the studies presented in Chapters 3 and 4, the effective length factor in the design of CFS storage racks with and without the initial geometric imperfections was studied. In the case of geometric perfect frames, it is found that the value of K factors for storey 1 is close to 1.7, given as a default value in RIM specification (RMI, 2000). It is also found the K factors decrease as the values of beam-to-column connections increase. In the study of effective length factor accounting for initial geometric imperfections, it is observed that the K factors increase when the values of initial imperfections increase. The results also demonstrated the combined effects of out-of-straightness ($\delta_0=L/1000$) and out-of-plumbness ($\Delta_0=L/240$) have more impact on the K factors than the influence of out-of-straightness (δ_0) and out-of-plumbness (Δ_0) individually. In the study of CFS storage rack structures subjected to variable loading using the proposed method, the results demonstrated the similar trends discovered in Chapters 3 and 5. For instance, it is also demonstrated, in this study that the semi-rigid connections plays an important role in the frame stability and the relative difference between the extreme frame-buckling loads were decreased when increasing the beam-to-column connection stiffness. The presences of the initial geometric imperfections reduce the column lateral stiffness and consequently the maximum and minimum frame-buckling loads are all reduced.

Chapter VII

Conclusions and Future Research

Provided in this study is a contribution for the development in the methodology to carry out the storey-based stability analysis for the multi-storey unbraced frames. The proposed methodology includes the assessment of the integrity of the conventional steel structures and CFS storage racks subjected to variable loadings, a simplified equation to calculate the lateral stiffness modification factor β_{ij} , and a practical method to explicitly account for the initial geometric imperfections for the design of steel structures including storage racks.

7.1 Conclusions

7.1.1 Storey Stability of Multi-Storey Unbraced Frames Subjected to Variable Loading

The proposed method to determine the stability of unbraced frames subjected to variable loading for single storey unbraced frames proposed by Xu (2002) was extended to a multi-storey process. This extended method incorporates the development of a general stability equation for multi-storey unbraced frames subjected to variable loading. This can be characterized by the column lateral stiffness modification factor β_{ij} which provides a quantitative measurement of the stiffness interactions among the columns in a storey to resist lateral interactions among the columns in a storey to minimize lateral instability. The concept of storey-based buckling is used to formulate the problem of determining the critical frame-buckling loads to be a pair of constrained maximization and minimization problems subjected to elastic stability constraints. The variables and objective functions of the maximization and minimization problems are the applied column loads and the summation of applied column load variables. The stability constraints are imposed to ensure that lateral instability occurs in at least one storey of the frame. For each variable, an upper limit is imposed to ensure that the magnitude of the applied load will not exceed this limit defined as the buckling load associated with the non-sway buckling of the individual column. The following conclusions were formulated from this study:

- The maximum and minimum frame-buckling loads and their associated load patterns can be obtained by solving the maximization and minimization problems, with a linear programming method, respectively. The maximum and minimum frame-buckling loads represent the upper and lower bounds of the frame buckling loads of the structures, which characterize the stability capacity of the frame under extreme loading conditions.
- The minimization problem has to be solved for each storey and the maximization problem only needs to be solved once by using any one of the stories in the frame. The numerical examples showed that the maximum frame-buckling load always corresponds to the lateral instability of both the first and second storey frame simultaneously, which indicates that a further increase in any one of the applied loads is impossible as each storey has already reached the limit state of lateral instability.
- There might be several different load patterns associated with the minimum frame-buckling loads and the relative difference between the maximum and minimum frame-buckling loads are found to be substantial.
- The relative differences between the maximum and minimum frame-buckling loads are increased when decreasing the beam-to-column connection stiffness.
- In the case of variable loading, frame-buckling loads associated with proportional loading are always between the maximum and minimum loads subjected to variable loading. In contrast to current the frame stability analysis involving only proportional loads, the proposed approach permits individual applied loads on the frame to vary independently.
- The variable loading approach captures the load patterns that cause instability failure of frames at the minimum and maximum load levels. The approach clearly identifies the stability capacities of frames under the extreme load cases and such critical information is generally not available through the current proportional loading stability analysis.

7.1.2 Storey-Based Stability Analysis for Unbraced Frame with Initial Geometrical Imperfections

The stability of columns in multi-storey unbraced frames with initial geometric imperfections was investigated within the context of storey-based buckling using the end-fixity factor to characterize the beam-to-column rotational restraints. The investigated effects of the imperfections on the stability of column were contemplated in the evaluation of effective length factor via the lateral stiffness modification factor of column. Formulations and procedures of calculating the storey-based column effective length factor with explicitly accounting for the initial geometric imperfections were derived. From the derived formulations, and to obtain the critical load multiplier λ_{cr} together with the effective length factor K , a Taylor series expansion was employed to simplify the stability equation as a quadratic equation (2nd-order approximation), which can be further reduced to a linear equation (1st-order approximation). Numerical results were carried out to substantiate with the results from the storey-based buckling analysis. The following conclusions were obtained from the studies results as:

- An inequality expression $\lambda_{icr-2nd-order} < \lambda_{icr-1st-order}$ was obtained which indicated the effective length factors K was found to be on the conservative side based on the Taylor series expansion of 2nd-order approximation versus the 1st-order approximation.
- The results obtained from the investigation of the proposed method for the unbraced frames without considering the initial geometric imperfections show good agreements with the results presented in the literature.
- The numerical results from the 1st-order and 2nd-order approximations, and storey-based buckling analysis, the maximum differences of 1.3% and 0.68% are noted between the 1st and 2nd order approximations and the storey-based buckling analysis, respectively. The maximum difference of 0.61% is found between 1st- order and 2nd-order approximations.
- From the numerical examples using the 1st-order approximation, the results show the critical load multiplier can provide a satisfied estimation for column effective length factor K and it should be recommended for use in engineering practice.

- In comparing the results with and without initial geometric imperfection, it is clear that initial geometric imperfections have detrimental effects on both lateral stiffness and buckling strength of the columns.
- Parametric studies were carried out to investigate the individual and combined effects of the initial out-of-straightness and out-of-plumbness on the column effective length factor, where it was found that the increase of the effective length factor linearly increase either one of the initial geometrical imperfections.
- The study also discovers that the out-of-straightness has a greater detrimental impact than that of the out-of-plumbness. It was found that given the same value of initial geometric imperfection, the influence of the out-of-straightness on the column effective length factor is almost doubled as that of the out-of-plumbness. This finding is consistent with the current practice in which the tolerance for the out-of-straightness and the out-of-plumbness are $L/1000$ and $L/500$, respectively.
- The proposed method is able to help the design practitioner to investigate the impacts of the out-of-straightness and out-of-plumbness on column strength explicitly and independently for any given values. Therefore, the proposed method in this study is certainly in the interest of design engineers and should be recommended for engineering practice.

7.1.3 Multi-storey Unbraced Frames with Initial Geometric Imperfections Subjected to Variable Loading

Based on the maximization and minimization problems stated with Eqs. (3.13), (3.16) and (3.17) in Chapter 3, the lateral stiffness modification factors of $\beta_{0,ij}(r_{l,ij}, r_{u,ij})$ and $\beta_{1,ij}(r_{l,ij}, r_{u,ij})$ corresponding to these equations are replaced by $\beta_{0,ij}(r_{l,ij}, r_{u,ij}, \delta_0, \Delta_0)$ and $\beta_{1,ij}(r_{l,ij}, r_{u,ij}, \delta_0, \Delta_0)$ given in Eqs. (4.13) accounting for the initial geometric imperfections. Therefore, the problem of multi-storey unbraced frames subjected to variable loading with respect to initial geometric imperfections can be solved and a set of conclusions obtained as follows:

- The presence of the initial geometric imperfections increased the maximum difference between the maximum and minimum buckling loads to 21.2% for single-storey unbraced frame with either pinned or rigid column ends.
- In the case of multi-storey unbraced frames, the study found the column lateral stiffness decreased when increasing the value of the initial geometric imperfections. As a result of the decreasing lateral stiffness, the extreme frame-buckling loads were reduced.
- The numerical examples in the study further demonstrated the combined effects of member out-of-straightness and frame out-of-plumbness has a stronger impact than considering the effects of member out-of-straightness and frame out-of-plumbness individually.
- With respect to the same values of initial geometric imperfections, the extreme frame-buckling loads decreased when the beam-to-column and column base connections decreased.

7.1.4 Application of Storey-based Stability Analysis to CFS Storage Racks

The methodology discussed in Chapters 3 to 5 applies to the CFS storage racks in this study. The effective length factor K of CFS storage racks is evaluated with consideration of the test results for semi-rigid connections. The analytical and comprehensive investigation on instability failures of CFS storage racks subjected to variable loading was also studied. The following conclusions are made:

- Upon the test results for the semi-rigid connections, the K factors presented in the numerical example are close to the value of 1.7 defined as a default value in RIM Specification (RMI, 2000) for the first storey. And the numerical examples show that the K factors are greater than 4 for the second storey which indicated the second storey is in the most unstable condition.
- The effective length factor K decreased with the increased beam size and beam-to-column connections. It was also noted that when the column size increases, the K factors will increase.

- The effective length factor K increase when the value of either one of the effects for initial imperfections increases. The combined effects of the initial geometric imperfections have the most severe impact on the column K factors. With respect to the imperfection values being $L/500$, $L/400$, $L/300$, $L/240$ and $L/200$, the out-of-straightness has a greater influence than that of the out- of-plumbness.
- With respect to the variable loading for CFS storage racks, the maximum frame-buckling load also corresponds to the lateral instability of both the first and second storey simultaneously and the linear programming procedure did not find the maximum and minimum frame-buckling loads that only involves the lateral storey buckling of the third storey of the storage rack ($S_3=0$ and $S_1 > 0$, $S_2 > 0$).
- The relative difference between the maximum and minimum frame-buckling loads of 585.5% is noted when the beam-to-column connection stiffness is 313 k-in/rad (3.537×10^7 N-mm/rad) from the test. With the beam-to-column connection stiffness increased to 3130 k-in/rad (3.537×10^8 N- mm/rad), the relative difference between the maximum and minimum frame-buckling loads can be decreased to 58%.
- In the case of accounting for the initial geometric imperfections, with respect to beam-to-column connection stiffness of 3130 k-in/rad (3.537×10^8 N- mm/rad), the relative difference as noted is insignificant between the maximum and minimum frame-buckling loads corresponding to the lateral instability of storey 1.

7.2 Future Research

This proposed research develops a civil engineering methodology and a practical approach for the stability analysis of multi-storey unbraced frames including CFS storage racks, which is not currently available in the design/engineering practice. However, there are still a number of aspects from this study that could be extended to possibly increase the robustness of the proposed methodology investigated.

- The current study only applies to the column axial force with respect to the stability analysis in multi-storey unbraced frames. Future research could be conducted for more complex types of loadings, such as distributed loading on the beams.
- The proposed method in this study explicates the account for initial geometric imperfections of out-of-straightness and out-of-plumbness that is based on an elastic assumption. The inelastic behavior of multi-storey unbraced frames accounting for initial geometric imperfections can be considered in future research.
- It is noted that much of the research on frame stability including the current study are based on the two-dimensional (2D) flexural buckling analysis. The methodology developed in this study could be conducted on the real application of three-dimensional (3D) frame structures in future research.
- The linear programming method adopted for solving the optimization problems in the current research is based on the 1st-order approximation. Future research could be considered to include nonlinear programming with respect to a nonlinear constraint for such problems using the 2nd-order approximation.
- The experimental data used in the current study of CFS storage racks was obtained from the cantilever test which is commonly used to design beams and connections. The beam-to-column connection stiffness R obtained from the portal test for sidesway analysis could be conducted in future research to evaluate the frame stability.

Appendix A

Procedures and Example of Frame Decomposition

The procedure of decomposing a multi-storey unbraced frame to a series of single-storey frames can be described as following (Liu and Xu, 2005)

Step 1: Determination of the Rotational Stiffnesses of Beams

$R_{bu,ij}$ and $R_{bl,ij}$ represent the beam-to-column rotational-restraining stiffnesses at the upper and lower joints of column ij and can be expressed as

$$R_{bu,ij} = \sum_{k=1}^2 R_{bu,ijk} \quad (\text{A.1a})$$

$$R_{bl,ij} = \sum_{k=1}^2 R_{bl,ijk} \quad (\text{A.1b})$$

in which

$$R_{bu,ijk} = \frac{6r_{k,1}}{4 - r_{k,1}r_{k,2}} \frac{EI_{bu,ijk}}{L_{bu,ik}} (2 + r_{k,2}) \quad (\text{A.2a})$$

$$R_{bl,ijk} = \frac{6r_{k,1}}{4 - r_{k,1}r_{k,2}} \frac{EI_{bl,ijk}}{L_{bl,ik}} (2 + r_{k,2}) \quad (\text{A.2b})$$

and $r_{k,1}$ and $r_{k,2}$ are end-fixity factors associated with the near and far ends of beam k , and $R_{bu,ijk}$ and $R_{bl,ijk}$ are end rotational stiffnesses of the beams that are connected to the upper and lower ends of column ij , respectively.

Based on the principle that the distribution of beam-to-column restraining stiffness shall be proportional to the column end rotational stiffness at each joint, the end rotational-restrain stiffnesses of the upper and lower ends of column ij can be given as follows:

$$R_{u,ij} = \mu_{u,ij} R_{bu,ij} \quad (\text{A.3a})$$

$$R_{l,ij} = \mu_{l,ij} R_{bl,ij} \quad (\text{A.3b})$$

where $R_{u,ij}$ and $R_{l,ij}$ are the end restrain stiffnesses of the upper and lower ends of column ij ; $\mu_{u,ij}$ and $\mu_{l,ij}$ are the stiffness distribution factors and will be determined in the next step.

Step 2: Determination of the Stiffness Distribution Factors

In the study of Liu and Xu (2005), the distribution factors corresponding with the so-called frame-based stiffness distribution (FSD) approach for the upper end of column C_{ij} can be obtained from the following form

$$\mu_{u,ij} = \frac{\frac{EI_{c,ij}}{L_{c,ij}} \frac{3r_{l,ij}}{1+2r_{l,ij}}}{\frac{EI_{c,ij}}{L_{c,ij}} \frac{3r_{l,ij}}{1+2r_{l,ij}} + \frac{EI_{c,ij}}{L_{c,ij}} \frac{1}{1+EI_{c,ij}/R_{u,ij}L_{c,ij}}} \quad (\text{A.4a})$$

in which $R_{u,(i+1)j}=R_{bu,(i+1)j}$ is defined in Equation (A.1a) and $r_{l,ij}$ is defined in Equation (3.1a).

Also from the study of Liu and Xu (2005), the stiffness distribution factors for columns joined together satisfy the following equation:

$$\mu_{l,(i+1)j}=1-\mu_{u,ij} \quad (\text{A.4b})$$

Step 3: Determination of the End-Fixity Factors

Once we can obtain the distribution factors $\mu_{u,ij}$ and $\mu_{l,ij}$ from Step 2, then we can calculate the end-fixity factors defined in Eqs. (3.1) associated with the upper and lower column ij individually.

Equations (3.1) in Chapter 3 are presented again as follows:

$$r_{l,ij} = \frac{1}{1+3EI_{c,ij}/R_{l,ij}L_{c,ij}}; \quad r_{u,ij} = \frac{1}{1+3EI_{c,ij}/R_{u,ij}L_{c,ij}} \quad (\text{A.5a,b})$$

Step 4: Determination of the Column Lateral Stiffness Modification Coefficients

From Step 3, the end-fixity factors for each individual column can be obtained, therefore, the modification coefficients $\beta_{0,ij}(r_{l,ij}, r_{u,ij})$ and $\beta_{1,ij}(r_{l,ij}, r_{u,ij})$ corresponding to the columns can be calculated from Eqs. (3.10) in Chapter 3. Equations (3.10) in Chapter 3 are shown again:

$$\beta_{0,ij}(r_{l,ij}, r_{u,ij}) = \frac{r_{l,ij} + r_{u,ij} + r_{l,ij}r_{u,ij}}{4 - r_{l,ij}r_{u,ij}} \quad (\text{A.6a})$$

$$\beta_{1,ij}(r_{l,ij}, r_{u,ij}) = \frac{8(5 + r_{u,ij}^2) - (34 - r_{u,ij})r_{u,ij}r_{l,ij} + (8 + r_{u,ij} + 3r_{u,ij}^2)r_{l,ij}^2}{30(4 - r_{l,ij}r_{u,ij})^2} \quad (\text{A.6b})$$

The detailed hand calculation to demonstrate the procedure described above for Case 4 of Chapter 3 is given as follows:

In Case 4, the column bases are rigid connections. The beam-to-column connections of the exterior columns are rigid, and the interior columns are pinned connection. Due to the pinned condition between the interior beam-to-column connections, and the rigid condition of exterior beam-to-column connection, the $r_{k,1}$ and $r_{k,2}$, the end-fixity factors associated with the near and far ends of beam k can be determined for each beam. The detailed hand calculations are studied as follows:

1. Procedures to Calculate the End-Fixity Factors and Lateral Stiffness Modification Factors

(1) Calculate the Rotational Stiffnesses of Beams for the Frame

From Eqs. (A2) given in Appendix A, we can obtain the rotational stiffnesses associated with beams connected to the lower end of column ij . For instance, beam B_{11} is connected to columns C_{11} and C_{12} , and then the rotational stiffnesses of beam B_{11} can be calculated as follows:

$$R_{bu,112} = R_{bl,212} = 3 \frac{EI_{bu,112}}{L_{bu,112}} = \frac{3 \times 2 \times 10^5 \times 8.749 \times 10^8}{6016.8} = 8.725 \times 10^{10} \text{ N-mm/rad}$$

where the last subscript denotes whether the beam is in the left or right side of the column. For example, the last subscript 2 in $R_{bu,112}$ denotes that the beam is on the right side of column C_{11} as that shown in Figure 3-8.

Similarly, it can be found the following rotational stiffnesses associated with beams connected to the upper end of column ij :

$$R_{bu,121} = R_{bl,221} = 0 \text{ N-mm/rad}; \quad R_{bu,122} = R_{bl,222} = 0 \text{ N-mm/rad}; \quad R_{bu,131} = R_{bl,231} = 11.68 \times 10^{10} \text{ N-mm/rad};$$

$$R_{bu,212} = 6.981 \times 10^{10} \text{ N-mm/rad}; \quad R_{bu,221} = 0 \text{ N-mm/rad}; \quad R_{bu,221} = 0 \text{ N-mm/rad};$$

$$R_{bu,231} = 9.35 \times 10^{10} \text{ N-mm/rad};$$

(2) Evaluate the Beam-to-Column Restraining Stiffnesses

Once the rotational stiffness of beams obtained, the corresponding beam-to-column restraining stiffnesses based on Eqs. (A1) calculated as follows:

$$R_{bu,11} = R_{bu,112} = 8.725 \times 10^{10} \text{ N-mm/rad}; \quad R_{bu,12} = R_{bu,121} + R_{bu,122} = 0 \text{ N-mm/rad}$$

$$R_{bu,13} = R_{bu,131} = 11.68 \times 10^{10} \text{ N-mm/rad}; \quad R_{bu,21} = R_{bu,212} = 6.981 \times 10^{10} \text{ N-mm/rad}$$

$$R_{bu,22} = R_{bu,221} + R_{bu,222} = 0 \text{ N-mm/rad}; \quad R_{bu,23} = R_{bu,231} = 9.35 \times 10^{10} \text{ N-mm/rad}$$

$$R_{bl,21} = R_{bl,212} = 8.725 \times 10^{10} \text{ N-mm/rad}; \quad R_{bl,22} = R_{bl,221} + R_{bl,222} = 0 \text{ N-mm/rad}$$

$$R_{bl,23} = R_{bl,231} = 11.68 \times 10^{10} \text{ N-mm/rad}$$

(3) Determine the Stiffness Distribution Factors:

For rigid connection of column bases, the end-fixity factors are unity, thus $r_{l,11} = r_{l,12} = r_{l,13} = 1$. The beam-to-column restraining stiffness at the upper end of column C_{21} , $R_{u,21} = R_{bu,21} = 6.981 \times 10^{10}$ N-mm/rad, the distribution factor for the upper end of column C_{11} can be obtained from Equation (A4a), in which

$$\mu_{u,11} = \frac{\frac{EI_{c,11}}{L_{c,11}} \frac{3r_{l,11}}{1+2r_{l,11}}}{\frac{EI_{c,11}}{L_{c,11}} \frac{3r_{l,11}}{1+2r_{l,11}} + \frac{EI_{c,21}}{L_{c,21}} \frac{1}{1+EI_{c,21}/R_{u,21}L_{c,21}}} = 0.667$$

Therefore, the stiffness distribution factor for the lower end of column C_{21} is $\mu_{l,21} = 1 - \mu_{u,11} = 0.333$. Similarly, the distribution factors associated with the other columns can be obtained as follows:

$$\mu_{u,12} = 1, \mu_{l,22} = 0, \mu_{u,13} = 0.683, \mu_{l,23} = 0.317$$

(4) Compute the Corresponding End-Fixity Factors

The beam-to-column rotational-restraining stiffnesses contributed by beams B₁₁ and B₁₂ to columns C₁₁, C₁₂ and C₁₃, and beams B₂₁ and B₂₂ to columns C₂₁, C₂₂, C₂₃ are given as follows,

$$R_{u,11} = \mu_{u,11} R_{bu,11} = 4.712 \times 10^{10} \text{ N-mm/rad}$$

$$R_{u,12} = \mu_{u,12} R_{bu,12} = 0 \text{ N-mm/rad}$$

$$R_{u,13} = \mu_{u,13} R_{bu,13} = 7.983 \times 10^{10} \text{ N-mm/rad}$$

$$R_{l,21} = \mu_{l,21} R_{bu,21} = 2.326 \times 10^{10} \text{ N-mm/rad}$$

$$R_{l,22} = \mu_{l,22} R_{bu,22} = 0 \text{ N-mm/rad}$$

$$R_{l,23} = \mu_{l,23} R_{bu,23} = 2.961 \times 10^{10} \text{ N-mm/rad}$$

The corresponding end-fixity factors based on Equations (3.1) are given as:

$$r_{u,11} = \frac{1}{1 + 3EI_{c,11} / R_{u,11} L_{c,11}} = \frac{1}{1 + 3 \times 2 \times 10^5 \times 4.6 \times 8.3246 \times 10^7 / 3529.6} = 0.42$$

Using the same equation, we can obtain the following values for end-fixity factors:

$$r_{u,12} = 0, r_{u,13} = 0.705$$

$$r_{l,21} = 0.377, r_{l,22} = 0, r_{l,23} = 0.644$$

$$r_{u,21} = 0.644, r_{u,22} = 0, r_{u,23} = 0.851$$

(5) Evaluate the Column Lateral Stiffness Modification Coefficients

Since the modification coefficients $\beta_{0,1j}$ and $\beta_{1,1j}$ are the function of the end-fixity factors, they can be obtained from Eqs. (3.10).

$$\beta_{0,11}(r_{l,11}, r_{u,11}) = \frac{r_{l,11} + r_{u,11} + r_{l,11}r_{u,11}}{4 - r_{l,11}r_{u,11}} = \frac{1 + 0.42 + 1 \times 0.42}{4 - 1 \times 0.42} = 0.514$$

Similarly, we can get the values of other later stiffness modification factors:

$$\beta_{0,12} = 0.25, \beta_{0,13} = 0.731, \beta_{0,21} = 0.336, \beta_{0,22} = 0, \beta_{0,23} = 0.592$$

$$\beta_{1,11} = 0.094, \beta_{1,12} = 0.1, \beta_{1,13} = 0.094, \beta_{1,21} = 0.086, \beta_{1,22} = 0.083, \beta_{1,23} = 0.09$$

Appendix B

Formulation and Verification of the Minimization Problem of Equations (3.20) to (3.22) of Case 4 in Chapter 3

The process of evaluating and verifying the minimization problem of Eqs. (3.20) to (3.22) for Case 4 study in Chapter 3 is demonstrated as follows (Xu and Wang, 2007)

1. Evaluate the Upper Bound Load of Individual Column

The seeking of minimum frame-buckling needs a side constraint for each applied column load, which is to be less than an corresponding upper bound load $P_{u,ij}$. The upper bound load $P_{u,ij}$ is defined as:

$$P_{u,ij} = \frac{\pi^2 EI_{ij}}{K_{braced,ij}^2 L_{ij}^2}$$

in which $K_{braced,ij}$ is the non-sway-buckling effective length factor, and is defined in Eq. (3.15).

The upper bound load is imposed to ensure that the magnitude of the applied load will not exceed the buckling load associated with non- sway-buckling of the individual column.

Upon the end fixity fact factor obtained form previously calculation, it can be obtained the non-buckling effective length factor $K_{braced,ij}$ for each column. For column C_{11} , it has the following equation:

$$K_{braced,11}^2 = \frac{[\pi^2 + (6 - \pi^2)r_{u,11}] \times [\pi^2 + (6 - \pi^2)r_{l,11}]}{[\pi^2 + (12 - \pi^2)r_{u,11}] \times [\pi^2 + (12 - \pi^2)r_{l,11}]}$$

with $r_{l,11}=1$, $r_{u,11}=0.642$, we can get $K_{braced,11}=0.573$. Similarly, we can obtain the other non- sway-buckling effective length factor.

$$K_{braced,12} = 0.707, K_{braced,13} = 0.56, K_{braced,21} = 0.719, K_{braced,22} = 1, K_{braced,23} = 0.608$$

Therefore, the corresponding upper bound load $P_{u,11}$ can be calculated as follows:

$$P_{u,11} = \frac{\pi^2 EI_{11}}{K_{braced,11}^2 L_{11}^2} = \frac{\pi^2 \times 2 \times 10^5 \times 4.6 \times 8.3246 \times 10^7}{0.573^2 \times 3529.6^2} = 184600 \text{ kN}$$

Similarly, we can get the upper bound load for other columns:

$$P_{u,12} = 82570 \text{ kN}, P_{u,13} = 99130 \text{ kN}, P_{u,21} = 80370 \text{ kN}, P_{u,22} = 415700 \text{ kN}, P_{u,23} = 47880 \text{ kN}$$

2. Formulate and Verify the Minimization Problem

The minimization problem is stated in Eqs. (3.20) to (3.22) in Chapt 3, substituting the lateral stiffness modification factors of $\beta_{0,ij}$ and $\beta_{1,ij}$ from previous calculation to Eqs. (3.22a) and (3.22b), also substituting the upper bound load for each column obtained from above calculation, we will have the minimization problem expressed as follows:

$$\text{Minimum } Z = \min \{ Z_l = \sum_{i=1}^2 \sum_{j=1}^3 P_{ij} \mid l = 1, 2, 3 \} \quad (3.20)$$

$$\text{Minimize: } Z = P_{11} + P_{12} + P_{13} + P_{21} + P_{22} + P_{23} \quad (3.21)$$

Subject to:

$$\begin{aligned} S_1 &= \frac{12EI_{11}}{L_{11}^3} \beta_{0,11} - \frac{12}{L_{11}} \beta_{1,11} (P_{11} + P_{21}) + \frac{12EI_{12}}{L_{12}^3} \beta_{0,12} - \frac{12}{L_{12}} \beta_{1,12} (P_{12} + P_{22}) \\ &\quad + \frac{12EI_{13}}{L_{13}^3} \beta_{0,13} - \frac{12}{L_{13}} \beta_{1,13} (P_{13} + P_{23}) \\ &= 25610 - 0.319(P_{11} + P_{21}) - 0.34(P_{12} + P_{22}) - 0.32(P_{13} + P_{23}) = 0 \end{aligned} \quad (3.22a)$$

$$\begin{aligned} S_2 &= \frac{12EI_{21}}{L_{21}^3} \beta_{0,21} - \frac{12}{L_{21}} \beta_{1,21} P_{21} + \frac{12EI_{22}}{L_{22}^3} \beta_{0,22} - \frac{12}{L_{22}} \beta_{1,22} P_{22} \\ &\quad + \frac{12EI_{23}}{L_{23}^3} \beta_{0,23} - \frac{12}{L_{23}} \beta_{1,23} P_{23} \\ &= 9753 - 0.34P_{21} - 0.328P_{22} - 0.355P_{23} > 0 \end{aligned} \quad (3.22b)$$

$$0 \leq P_{11} + P_{21} \leq 184600 \text{ kN}; 0 \leq P_{12} + P_{22} \leq 82570 \text{ kN}; 0 \leq P_{13} + P_{23} \leq 99130 \text{ kN}$$

$$0 \leq P_{21} \leq 80370 \text{ kN}; 0 \leq P_{22} \leq 415700 \text{ kN}; 0 \leq P_{23} \leq 47880 \text{ kN} \quad (3.22c)$$

In the case of seeking the minimum buckling load, the minimization problem will be solved two times.

a. $S_1=0, S_2>0$

In this case, $S_1=0$ represents the first storey becomes lateral unstable and the second storey keep lateral stable. In this condition, we obtain the following values:

$Z_1=75323.53$ kN, the corresponding individual column loading are:

$P_{12}=45588.77$ kN, $P_{22}=29734.76$ kN, the other column loadings are all equal to zero.

It is found in this case that the second storey becomes lateral unstable simultaneously, which means S_2 reduces to zero ($S_2=0$) at the same time.

b. $S_2=0, S_1>0$

In this case, we assume the first storey is lateral stable while the second storey becomes lateral unstable. The following results can be obtained for this condition:

$Z_2=27473.24$ kN, the corresponding individual column loading are:

$P_{23}=27473.24$ kN, the other column loadings are all equal to zero.

The results found that in this case the first storey still is still in stable condition when second storey is lateral unstable. It is found $S_1=16818.56$ kN >0 .

Therefore, from Equation (3.20), the minimum buckling loads will be chose as follows:

Minimum $Z=\min\{Z_1, Z_2\}=27473.24$

Appendix C

Lateral Stiffness of an Axially Loaded Column with Initial Geometric Imperfections

In section 5 on page 9, an axially loaded column in an unbraced frame shown in Figure 3 is discussed with geometric imperfection. The details to evaluate the lateral stiffness S given in Eq.(3.2) are discussed in this appendix. Based on Eq. (4.4), the general solution of this equation is given as

$$y = c_1 \cos(\phi x / L) + c_2 \sin(\phi x / L) + (\Delta_1 + \Delta_0) + M_u / P + S(L - x) / P \quad (C.1)$$

where ϕ is the stiffness parameter defined in Eq. (3.3), and c_1 and c_2 are coefficients to be determined from the boundary conditions given in Eqs. (4.7) to (4.9). Substituting Eq. (4.5) and boundary conditions in Eqs. (16) to (18) into Eq. (C.1), the coefficients c_1 and c_2 are determined as

$$c_1 = \frac{\phi(\Delta_1 + \Delta_0 + C) - (C + \Delta_0 + \delta_0\pi) \sin \phi}{\phi(\cos \phi - 1) - C_l \sin \phi} \quad (C.2)$$

$$c_2 = \frac{(C + \Delta_0 + \delta_0\pi)(\cos \phi - 1) - C_l(\Delta_1 + \Delta_0 + C)}{\phi(\cos \phi - 1) - C_l \sin \phi} \quad (C.3)$$

and c_1 and c_2 satisfy the following equation

$$-(C_u + \phi \sin \phi)c_1 + \phi \cos \phi c_2 = (1 + C_u)C + C_u(\Delta_1 + \Delta_0) + \Delta_0 + \delta_0\pi \quad (C.4)$$

in which

$$C = \frac{SH}{P} = \frac{SL^3}{EI\phi^2} \quad (C.5)$$

$$C_l = \frac{1 - r_l}{3r_l} \phi^2 ; \quad C_u = \frac{1 - r_u}{3r_u} \phi^2 \quad (C.6a,b)$$

where r_l and r_u are the end-fixity factors for the upper and lower ends of the column defined in Eqs. (3.1). Therefore, the coefficient C can be obtained as

$$C = \frac{\delta_0 \pi \phi / 50 - ((1 + \Delta_0 / 100)(C_l + C_u) + \delta_0 \pi / 50) \phi \sin \phi + (\Delta_0 (C_u - C_l) / 100 + (1 + \Delta_0 / 100)(C_l C_u - \phi^2) + \delta_0 \pi / 100 (C_l + C_u)) \sin \phi}{-2\phi + (2 + C_l + C_u) \phi \cos \phi - (C_l + C_u + C_l C_u - \phi^2) \sin \phi} \quad (\text{C.7})$$

Based on Eq. (C.5), the lateral stiffness of the column can be expressed as

$$S = \frac{\phi^2 CEI}{L^3} = \beta \frac{12EI}{L^3} \quad (\text{C.8})$$

in which $\beta = \frac{C\phi^2}{12}$ is the lateral stiffness modification factor accounting for initial geometric imperfections. The equations of the modification factor β in terms of the end-fixity factors can be derived from Eqs. (C.5) to (C.8) as the following

$$\beta = \frac{\phi^3}{12} \frac{f_1 + (-f_1 + f_2 \phi^2) \cos \phi - (f_3 \phi^2 + f_4 + f_5 + f_6) \phi \sin \phi}{f_7 - (f_7 + f_8 \phi^2) \cos \phi + (f_9 \phi^2 + f_{10}) \phi \sin \phi} \quad (\text{C.9})$$

where

$$f_1 = -\frac{9}{50} \delta_0 \pi r_l r_u \quad (\text{C.10a})$$

$$f_2 = 3(1 + \frac{\Delta_0}{100})(r_l + r_u - 2r_l r_u) \quad (\text{C.10b})$$

$$f_3 = (1 + \frac{\Delta_0}{100})(1 - r_l - r_u + r_l r_u) \quad (\text{C.10c})$$

$$f_4 = \frac{3}{100} \Delta_0 (r_l - r_u - 3r_l r_u) \quad (\text{C.10d})$$

$$f_5 = \frac{3\Delta_0}{100} (r_l + r_u - 2r_l r_u) \quad (\text{C.10e})$$

$$f_6 = -9r_l r_u \quad (\text{C.10f})$$

$$f_7 = 18r_l r_u \quad (\text{C.10g})$$

$$f_8 = 3(r_l + r_u - 2r_l r_u) \quad (\text{C.10h})$$

$$f_9 = 1 - r_l - r_u + r_l r_u \quad (\text{C.10i})$$

$$f_{10} = 3(r_l + r_u - 5r_l r_u) \quad (\text{C.10j})$$

Appendix D

Values of Lateral Stiffness Coefficients β_0 , β_1 and β_2 Accounting for Initial Geometric Imperfections in Chapter 4

The coefficients of column lateral stiffness β_0 , β_1 and β_2 are calculated based on the Eqs. (4.13a), (4.13b) and (4.15) with respect to the variation of column end-fixity factors and the combined effects of out-of-straightness (δ_0) and out-of-plumbness (Δ_0).

**Table D-1: β_0 ($\times 10^{-1}$) values corresponding to the column end-fixity factors
($\delta_0=L/1000$ and $\Delta_0=L/500$)**

$r_j \backslash r_i$	0	0.1	0.2	0.3	0.4	0.5	0.6	0.7	0.8	0.9	1
0	0.000	0.179	0.359	0.538	0.717	0.896	1.076	1.255	1.434	1.613	1.793
0.05	0.109	0.299	0.489	0.680	0.871	1.062	1.254	1.477	1.640	1.833	2.027
0.1	0.219	0.419	0.620	0.823	1.026	1.230	1.435	1.642	1.849	2.058	2.267
0.15	0.328	0.540	0.752	0.967	1.183	1.400	1.619	1.840	2.063	2.288	2.514
0.2	0.438	0.660	0.885	1.112	1.341	1.572	1.806	2.043	2.282	2.523	2.767
0.25	0.547	0.781	1.018	1.258	1.501	1.747	1.996	2.249	2.505	2.764	3.027
0.3	0.657	0.902	1.152	1.405	1.662	1.924	2.189	2.459	2.732	3.011	3.293
0.35	0.766	1.024	1.286	1.554	1.826	2.103	2.439	2.672	2.965	3.263	3.568
0.4	0.876	1.146	1.422	1.703	1.991	2.284	2.584	2.890	3.203	3.522	3.849
0.45	0.985	1.268	1.558	1.845	2.157	2.468	2.786	3.112	3.446	3.788	4.139
0.5	1.094	1.391	1.694	2.006	2.326	2.654	2.991	3.338	3.694	4.060	4.663
0.55	1.204	1.513	1.832	2.159	2.496	2.843	3.200	3.569	3.948	4.340	4.743
0.6	1.313	1.637	1.970	2.313	2.668	3.034	3.413	3.804	4.208	4.626	5.059
0.65	1.423	1.760	2.109	2.469	2.842	3.228	3.628	4.043	4.473	4.920	5.384
0.7	1.532	1.884	2.248	2.626	3.018	3.425	3.848	4.288	4.745	5.222	5.719
0.75	1.642	2.008	2.388	2.784	3.195	3.624	4.071	4.537	5.024	5.532	6.064
0.8	1.751	2.132	2.529	2.943	3.375	3.826	4.298	4.791	5.308	5.851	6.420
0.85	1.860	2.257	2.671	3.104	3.557	4.031	4.529	5.051	5.600	6.178	6.787
0.9	1.970	2.382	2.813	3.266	3.740	4.239	4.763	5.316	5.899	6.515	7.167
0.95	2.079	2.507	2.957	3.429	3.926	4.450	5.002	5.587	6.205	6.861	7.558
1	2.189	2.633	3.100	3.593	4.113	4.663	5.246	5.863	6.519	7.218	7.963

**Table D-2: β_0 ($\times 10^{-1}$) values corresponding to the column end-fixity factors
($\delta_0=L/800$ and $\Delta_0=L/400$)**

$r_j \backslash r_i$	0	0.1	0.2	0.3	0.4	0.5	0.6	0.7	0.8	0.9	1
0	0.000	0.162	0.323	0.485	0.646	0.808	0.969	1.131	1.293	1.454	1.660
0.05	0.106	0.277	0.448	0.621	0.793	0.966	1.139	1.313	1.488	1.662	1.837
0.1	0.211	0.392	0.574	0.757	0.941	1.126	1.312	1.499	1.686	1.875	2.065
0.15	0.317	0.508	0.701	0.895	1.091	1.288	1.487	1.688	1.889	2.093	2.298
0.2	0.422	0.624	0.828	1.034	1.242	1.453	1.665	1.880	2.097	2.316	2.537
0.25	0.528	0.741	0.956	1.174	1.395	1.619	1.846	2.076	2.308	2.544	2.783
0.3	0.633	0.857	1.085	1.315	1.550	1.788	2.029	2.275	2.525	2.778	3.036
0.35	0.738	0.974	1.214	1.457	1.706	1.958	2.216	2.478	2.745	3.018	3.295
0.4	0.844	1.091	1.343	1.601	1.863	2.131	2.405	2.685	2.971	3.263	3.562
0.45	0.950	1.209	1.474	1.745	2.023	2.307	2.598	2.896	3.201	3.515	3.836
0.5	1.055	1.327	1.605	1.891	2.184	2.484	2.793	3.111	3.437	3.773	4.118
0.55	1.161	1.445	1.737	2.037	2.346	2.664	2.992	3.330	3.678	4.037	4.408
0.6	1.262	1.563	1.869	2.185	2.511	2.847	3.194	3.553	3.924	4.309	4.706
0.65	1.372	1.682	2.003	2.334	2.667	3.032	3.400	3.781	4.177	4.587	5.014
0.7	1.478	1.801	2.136	2.484	2.845	3.219	3.609	4.013	4.435	4.873	5.331
0.75	1.583	1.921	2.271	2.635	3.015	3.409	3.821	4.250	4.699	5.167	5.657
0.8	1.689	2.040	2.406	2.788	3.186	3.602	4.037	4.492	4.969	5.469	5.994
0.85	1.794	2.160	2.542	2.942	3.360	3.798	4.257	4.739	5.246	5.779	6.341
0.9	1.900	2.280	2.679	3.097	3.535	3.996	4.480	4.991	5.529	6.098	6.700
0.95	2.005	2.401	2.816	3.253	3.712	4.197	4.708	5.248	5.820	6.426	7.071
1	2.111	2.522	2.955	3.410	3.892	4.401	4.939	5.511	6.118	6.764	7.453

**Table D-3: β_0 ($\times 10^{-1}$) values corresponding to the column end-fixity factors
($\delta_0=L/600$ and $\Delta_0=L/300$)**

$r_i \backslash r_j$	0	0.1	0.2	0.3	0.4	0.5	0.6	0.7	0.8	0.9	1
0	0.000	0.132	0.264	0.396	0.528	0.661	0.793	0.925	1.057	1.189	1.321
0.05	0.099	0.240	0.381	0.522	0.664	0.806	0.948	1.091	1.234	1.378	1.522
0.1	0.198	0.348	0.498	0.649	0.801	0.953	1.106	1.260	1.415	1.571	1.727
0.15	0.297	0.456	0.616	0.777	0.939	1.102	1.267	1.433	1.600	1.769	1.938
0.2	0.396	0.564	0.734	0.905	1.078	1.253	1.430	1.608	1.789	1.971	2.155
0.25	0.495	0.673	0.853	1.035	1.219	1.406	1.595	1.787	1.981	2.178	2.378
0.3	0.594	0.782	0.972	1.165	1.362	1.561	1.764	1.969	2.178	2.390	2.606
0.35	0.694	0.891	1.092	1.297	1.506	1.718	1.934	2.155	2.379	2.608	2.841
0.4	0.793	1.001	1.213	1.430	1.651	1.877	2.108	2.344	2.584	2.831	3.082
0.45	0.892	1.110	1.334	1.564	1.798	2.038	2.284	2.536	2.794	3.059	3.330
0.5	0.991	1.221	1.456	1.698	1.947	2.201	2.463	2.732	3.009	3.293	3.585
0.55	1.090	1.331	1.579	1.834	2.097	2.367	2.645	2.932	3.228	3.533	3.848
0.6	1.189	1.442	1.702	1.971	2.248	2.535	2.830	3.136	3.452	3.779	4.118
0.65	1.288	1.553	1.826	2.109	2.402	2.705	3.019	3.344	3.682	4.032	4.396
0.7	1.387	1.664	1.951	2.248	2.557	2.877	3.210	3.556	3.917	4.292	4.683
0.75	1.486	1.775	2.076	2.388	2.713	3.052	3.405	3.773	4.157	4.559	4.979
0.8	1.585	1.887	2.201	2.529	2.872	3.229	3.602	3.993	4.403	4.833	5.284
0.85	1.684	1.999	2.328	2.672	3.032	3.408	3.804	4.219	4.655	5.114	5.598
0.9	1.783	2.111	2.455	2.815	3.193	3.591	4.008	4.449	4.913	5.404	5.923
0.95	1.882	2.224	2.583	2.960	3.357	3.775	4.217	4.684	5.178	5.701	6.258
1	1.981	2.337	2.711	3.106	3.522	3.963	4.429	4.923	5.449	6.008	6.604

**Table D-4: β_0 ($\times 10^{-1}$) values corresponding to the column end-fixity factors
($\delta_0=L/400$ and $\Delta_0=L/200$)**

$r_j \backslash r_i$	0	0.1	0.2	0.3	0.4	0.5	0.6	0.7	0.8	0.9	1
0	0.000	0.0731	0.146	0.219	0.293	0.366	0.439	0.512	0.585	0.658	0.731
0.05	0.086	0.166	0.245	0.325	0.405	0.486	0.566	0.647	0.728	0.809	0.890
0.1	0.172	0.258	0.345	0.432	0.519	0.607	0.695	0.784	0.873	0.963	1.053
0.15	0.258	0.351	0.445	0.539	0.634	0.730	0.826	0.923	1.021	1.120	1.219
0.2	0.344	0.444	0.545	0.647	0.750	0.854	0.959	1.065	1.173	1.281	1.391
0.25	0.431	0.538	0.646	0.756	0.867	0.980	1.094	1.210	1.327	1.446	1.556
0.3	0.517	0.631	0.748	0.866	0.986	1.108	1.232	1.357	1.485	1.615	1.747
0.35	0.603	0.725	0.850	0.977	1.106	1.237	1.371	1.508	1.647	1.788	1.933
0.4	0.689	0.819	0.952	1.088	1.227	1.368	1.513	1.660	1.811	1.966	2.123
0.45	0.775	0.914	1.055	1.200	1.349	1.501	1.657	1.816	1.980	2.147	2.319
0.5	0.861	1.008	1.159	1.341	1.473	1.636	1.803	1.975	2.152	2.334	2.521
0.55	0.947	1.103	1.263	1.428	1.597	1.772	1.952	2.137	2.328	2.525	2.728
0.6	1.033	1.198	1.368	1.543	1.724	1.910	2.103	2.302	2.508	2.721	2.942
0.65	1.119	1.293	1.473	1.659	1.851	2.050	2.257	2.470	2.692	2.923	3.162
0.7	1.205	1.389	1.579	1.776	1.980	2.192	2.413	2.642	2.881	3.129	3.388
0.75	1.291	1.484	1.685	1.893	2.110	2.336	2.572	2.817	3.074	3.342	3.622
0.8	1.378	1.580	1.792	2.012	2.242	2.482	2.733	2.996	3.271	3.560	3.863
0.85	1.464	1.677	1.899	2.132	2.357	2.630	2.898	3.178	3.473	3.784	4.111
0.9	1.550	1.773	2.007	2.252	2.510	2.780	3.065	3.364	3.681	4.015	4.368
0.95	1.636	1.870	2.116	2.374	2.646	2.932	3.235	3.555	3.893	4.252	4.633
1	1.722	1.967	2.225	2.497	2.784	3.087	3.408	3.749	4.111	4.496	4.907

**Table D-5: β_1 ($\times 10^{-2}$) values corresponding to the column end-fixity factors
($\delta_0=L/1000$ and $\Delta_0=L/500$)**

$r_j \backslash r_i$	0	0.1	0.2	0.3	0.4	0.5	0.6	0.7	0.8	0.9	1
0	8.994	9.015	9.097	9.186	9.336	9.528	9.764	10.040	10.360	10.730	11.130
0.05	8.998	9.002	9.050	9.140	9.275	9.453	9.676	9.944	10.260	10.620	11.020
0.1	9.012	8.999	9.029	9.104	9.223	9.387	9.597	9.854	10.160	10.510	10.910
0.15	9.036	9.006	9.019	9.077	9.180	9.330	9.527	9.772	10.070	10.410	10.810
0.2	9.069	9.022	9.019	9.060	9.147	9.282	9.465	9.699	9.985	10.330	10.720
0.25	9.111	9.048	9.028	9.053	9.124	9.244	9.414	9.636	9.912	10.240	10.630
0.3	9.162	9.084	9.048	9.056	9.112	9.216	9.372	9.581	9.847	10.170	10.560
0.35	9.223	9.129	9.077	9.070	9.110	9.199	9.341	9.538	9.793	10.110	10.490
0.4	9.294	9.185	9.118	9.095	9.119	9.193	9.321	9.505	9.749	10.060	10.430
0.45	9.373	9.251	9.169	9.131	9.140	9.199	9.312	9.483	9.717	10.020	10.390
0.5	9.462	9.327	9.231	9.178	9.172	9.217	9.316	9.474	9.697	9.988	10.350
0.55	9.561	9.413	9.303	9.237	9.217	9.247	9.332	9.478	9.690	9.973	10.330
0.6	9.668	9.509	9.387	9.307	9.273	9.290	9.362	9.496	9.697	9.972	10.330
0.65	9.786	9.616	9.483	9.390	9.343	9.347	9.406	9.528	9.719	9.986	10.340
0.7	9.120	9.733	9.589	9.485	9.426	9.418	9.465	9.575	9.757	10.020	10.370
0.75	10.050	9.861	9.707	9.593	9.523	9.503	9.539	9.639	9.812	10.070	10.410
0.8	10.190	9.999	9.838	9.714	9.634	9.604	9.63	9.721	9.885	10.130	10.480
0.85	10.350	10.150	9.980	9.848	9.760	9.720	9.737	9.820	9.979	10.220	10.570
0.9	10.510	10.310	10.130	9.996	9.900	9.853	9.863	9.939	10.090	10.340	10.690
0.95	10.690	10.480	10.300	10.160	10.060	10.000	10.010	10.080	10.230	10.470	10.830
1	10.870	10.60	10.480	10.330	10.230	10.170	10.170	10.240	10.390	10.640	11.000

**Table D-6: β_1 ($\times 10^{-2}$) values corresponding to the column end-fixity factors
($\delta_0=L/800$ and $\Delta_0=L/400$)**

$r_j \backslash r_i$	0	0.1	0.2	0.3	0.4	0.5	0.6	0.7	0.8	0.9	1
0	9.159	9.181	9.249	9.362	9.520	9.723	9.971	10.030	10.60	10.990	11.420
0.05	9.164	9.168	9.218	9.314	9.456	9.644	9.880	10.160	10.490	10.870	11.300
0.1	9.178	9.165	9.197	9.275	9.401	9.575	9.797	10.070	10.390	10.760	11.190
0.15	9.202	9.171	9.186	9.247	9.356	9.515	9.723	9.983	10.290	10.660	11.080
0.2	9.236	9.187	9.185	9.229	9.322	9.464	9.659	9.906	10.210	10.570	10.980
0.25	9.279	9.214	9.194	9.221	9.297	9.424	9.604	9.839	10.130	10.480	10.890
0.3	9.332	9.250	9.214	9.224	9.284	9.395	9.560	9.781	10.060	10.410	10.810
0.35	9.359	9.297	9.244	9.238	9.281	9.376	9.526	9.735	10.000	10.340	10.740
0.4	9.476	9.354	9.285	9.263	9.290	9.369	9.505	9.700	9.958	10.280	10.680
0.45	9.549	9.422	9.337	9.299	9.310	9.374	9.495	9.676	9.923	10.240	10.630
0.5	9.640	9.499	9.401	9.347	9.343	9.391	9.497	9.666	9.901	10.210	10.600
0.55	9.741	9.588	9.475	9.407	9.388	9.421	9.513	9.668	9.892	10.190	10.570
0.6	9.852	9.687	9.561	9.479	9.445	9.465	9.543	9.685	9.898	10.190	10.570
0.65	9.973	9.769	9.659	9.564	9.517	9.523	9.587	9.717	9.920	10.200	10.580
0.7	10.100	9.917	9.768	9.661	9.602	9.595	9.647	9.765	9.958	10.230	10.600
0.75	10.240	10.050	9.889	9.772	9.701	9.682	9.722	9.830	10.010	10.280	10.650
0.8	10.390	10.190	10.020	9.896	9.814	9.785	9.815	9.913	10.090	10.350	10.720
0.85	10.550	10.340	10.170	10.030	9.943	9.904	9.925	10.010	10.180	10.440	10.810
0.9	10.720	10.510	10.330	10.190	10.090	10.040	10.050	10.140	10.30	10.560	10.930
0.95	10.900	10.680	10.500	10.350	10.250	10.190	10.20	10.280	10.440	10.700	11.700
1	11.080	10.870	10.680	10.530	10.420	10.370	10.370	10.440	10.610	10.870	11.250

**Table D-7: β_1 ($\times 10^{-2}$) values corresponding to the column end-fixity factors
($\delta_0=L/600$ and $\Delta_0=L/300$)**

$r_j \backslash r_i$	0	0.1	0.2	0.3	0.4	0.5	0.6	0.7	0.8	0.9	1
0	9.434	9.459	9.532	9.655	9.826	10.050	10.320	10.640	11.000	11.420	11.890
0.05	9.439	9.444	9.499	9.603	9.758	9.963	10.220	10.530	10.890	11.30	11.760
0.1	9.454	9.440	9.476	9.562	9.699	9.888	10.130	10.430	10.770	11.180	11.640
0.15	9.479	9.447	9.463	9.531	9.651	9.823	10.050	10.330	10.670	11.070	11.530
0.2	9.514	9.463	9.462	9.511	9.613	9.769	9.980	10.250	10.580	10.970	11.420
0.25	9.560	9.491	9.471	9.502	9.586	9.725	9.921	10.180	10.490	10.880	11.320
0.3	9.615	9.528	9.491	9.504	9.570	9.692	9.873	10.110	10.420	10.790	11.240
0.35	9.681	9.577	9.522	9.517	9.566	9.671	9.836	10.060	10.360	10.720	11.160
0.4	9.756	9.636	9.564	9.542	9.574	9.662	9.811	10.020	10.310	10.660	11.090
0.45	9.842	9.707	9.618	9.579	9.594	9.665	9.799	9.998	10.270	10.610	11.040
0.5	9.937	9.788	9.684	9.629	9.627	9.682	9.800	9.984	10.240	10.580	11.000
0.55	10.040	9.880	9.761	9.690	9.673	9.712	9.815	9.985	10.230	10.560	10.970
0.6	10.160	9.983	9.850	9.765	9.732	9.757	9.844	10.000	10.230	10.550	10.960
0.65	10.280	10.100	9.952	9.853	9.806	9.816	9.889	10.030	10.260	10.560	10.970
0.7	10.420	10.220	10.070	9.955	9.894	9.890	9.950	10.080	10.290	10.590	11.000
0.75	10.570	10.360	10.190	10.070	9.997	9.980	10.030	10.150	10.350	10.640	11.040
0.8	10.720	10.510	10.330	10.200	10.110	10.090	10.120	10.230	10.430	10.720	11.110
0.85	10.890	10.670	10.480	10.340	10.250	10.210	10.240	10.340	10.520	10.810	11.210
0.9	11.060	10.840	10.650	10.500	10.400	10.350	10.370	10.460	10.650	10.930	11.330
0.95	11.250	11.020	10.830	10.670	10.570	10.510	10.530	10.610	10.790	11.070	11.480
1	11.450	11.220	11.020	10.860	10.750	10.690	10.700	10.790	10.960	11.250	11.670

**Table D-8: β_1 ($\times 10^{-2}$) values corresponding to the column end-fixity factors
($\delta_0=L/400$ and $\Delta_0=L/200$)**

$r_j \backslash r_i$	0	0.1	0.2	0.3	0.4	0.5	0.6	0.7	0.8	0.9	1
0	9.984	10.010	10.100	10.240	10.440	10.700	11.010	11.380	11.810	12.290	12.830
0.05	9.990	9.996	10.060	10.180	10.360	10.600	10.900	11.250	11.670	12.150	12.690
0.1	10.010	9.991	10.030	10.130	10.290	10.510	10.800	11.140	11.540	12.010	12.550
0.15	10.030	9.997	10.020	10.100	10.240	10.440	10.700	11.030	11.430	11.890	12.420
0.2	10.070	10.010	10.020	10.070	10.190	10.380	10.620	10.940	11.320	11.770	12.300
0.25	10.120	10.040	10.020	10.060	10.160	10.330	10.560	10.850	11.220	11.670	12.190
0.3	10.180	10.080	10.040	10.060	10.140	10.290	10.500	10.780	11.140	11.570	12.090
0.35	10.250	10.140	10.080	10.080	10.140	10.260	10.450	10.720	11.060	11.490	12.000
0.4	10.330	10.200	10.120	10.100	10.140	10.250	10.420	10.670	11.000	11.420	11.920
0.45	10.430	10.280	10.180	10.140	10.160	10.250	10.410	10.640	10.960	11.360	11.850
0.5	10.530	10.360	10.250	10.190	10.190	10.260	10.400	10.620	10.920	11.320	11.800
0.55	10.650	10.460	10.330	10.260	10.240	10.290	10.420	10.620	10.910	11.290	11.770
0.6	10.770	10.580	10.430	10.340	10.310	10.340	10.450	10.630	10.910	11.280	11.760
0.65	10.910	10.700	10.540	10.430	10.380	10.400	10.490	10.660	10.930	11.290	11.760
0.7	11.060	10.840	10.660	10.540	10.480	10.480	10.560	10.710	10.960	11.320	11.780
0.75	11.210	10.980	10.800	10.670	10.590	10.580	10.640	10.780	11.200	11.370	11.830
0.8	11.380	11.150	10.950	10.800	10.720	10.690	10.740	10.870	11.100	11.440	11.910
0.85	11.560	11.320	11.120	10.960	10.860	10.820	10.860	10.990	11.210	11.540	12.010
0.9	11.750	11.500	11.290	11.130	11.200	10.980	11.010	11.120	11.340	11.670	12.140
0.95	11.960	11.700	11.490	11.320	11.200	11.150	11.170	11.280	11.490	11.830	12.300
1	12.170	11.920	11.700	11.530	11.400	11.350	11.360	11.470	11.680	12.010	12.500

**Table D-9: β_2 ($\times 10^{-4}$) values corresponding to the column end-fixity factors
($\delta_0=L/1000$ and $\Delta_0=L/500$)**

$r_j \backslash r_i$	0	0.1	0.2	0.3	0.4	0.5	0.6	0.7	0.8	0.9	1
0	0.000	0.189	0.701	1.448	2.350	3.309	4.252	5.089	5.735	6.103	6.109
0.05	0.043	0.058	0.410	1.019	1.800	2.678	3.561	4.366	5.004	5.389	5.430
0.1	0.166	0.013	0.210	0.681	1.350	2.133	2.950	3.715	4.339	4.733	4.802
0.15	0.359	0.047	0.094	0.429	0.980	1.669	2.416	3.136	3.740	4.135	4.225
0.2	0.614	0.152	0.054	0.258	0.690	1.285	1.958	2.627	3.205	3.596	3.701
0.25	0.920	0.319	0.085	0.160	0.480	0.977	1.573	2.188	2.734	3.116	3.231
0.3	1.269	0.539	0.177	0.130	0.340	0.739	1.258	1.816	2.327	2.695	2.815
0.35	1.651	0.805	0.324	0.162	0.260	0.569	1.010	1.510	1.982	2.332	2.452
0.4	2.056	1.106	0.517	0.246	0.250	0.461	0.825	1.265	1.697	2.026	2.143
0.45	2.476	1.435	0.747	0.378	0.280	0.409	0.698	1.079	1.470	1.775	1.886
0.5	2.900	1.781	1.007	0.547	0.360	0.407	0.624	0.947	1.296	1.578	1.681
0.55	3.321	2.137	1.287	0.747	0.480	0.449	0.599	0.866	1.174	1.431	1.524
0.6	3.727	2.491	1.578	0.968	0.630	0.528	0.614	0.829	1.098	1.330	1.414
0.65	4.110	2.835	1.871	1.201	0.800	0.635	0.664	0.830	1.063	1.272	1.345
0.7	4.460	3.160	2.156	1.437	0.980	0.763	0.740	0.863	1.062	1.250	1.314
0.75	4.769	3.454	2.423	1.665	1.170	0.901	0.834	0.918	1.088	1.257	1.314
0.8	5.026	3.709	2.661	1.876	1.340	1.039	0.936	0.988	1.132	1.286	1.337
0.85	5.223	3.914	2.860	2.058	1.500	1.167	1.034	1.060	1.184	1.326	1.373
0.9	5.349	4.059	3.009	2.200	1.630	1.272	1.117	1.123	1.232	1.366	1.412
0.95	5.396	4.133	3.097	2.289	1.710	1.341	1.172	1.163	1.263	1.392	1.437
1	5.355	4.126	3.117	2.312	1.730	1.361	1.183	1.166	1.260	1.387	1.433

**Table D-10: β_2 ($\times 10^{-4}$) values corresponding to the column end-fixity factors
($\delta_0=L/800$ and $\Delta_0=L/400$)**

$r_j \backslash r_i$	0	0.1	0.2	0.3	0.4	0.5	0.6	0.7	0.8	0.9	1
0	0.000	0.200	0.739	1.528	2.475	3.492	4.487	5.370	6.051	6.440	6.446
0.05	0.044	0.061	0.435	1.079	1.907	2.831	3.763	4.612	5.286	5.691	5.734
0.1	0.171	0.013	0.224	0.724	1.431	2.259	3.122	3.929	4.588	5.003	5.075
0.15	0.369	0.046	0.101	0.459	1.043	1.773	2.562	3.322	3.959	4.376	4.470
0.2	0.631	0.152	0.057	0.277	0.740	1.368	2.080	2.788	3.397	3.809	3.919
0.25	0.946	0.322	0.085	0.171	0.515	1.042	1.674	2.325	2.902	3.304	3.425
0.3	1.304	0.547	0.177	0.136	0.363	0.791	1.341	1.933	2.473	2.861	2.986
0.35	1.696	0.819	0.325	0.164	0.280	0.608	1.078	1.608	2.108	2.477	2.603
0.4	2.113	1.128	0.520	0.247	0.257	0.490	0.880	1.348	1.806	2.153	2.276
0.45	2.544	1.465	0.756	0.379	0.289	0.431	0.742	1.149	1.564	1.887	2.004
0.5	2.981	1.820	1.021	0.550	0.368	0.424	0.661	1.007	1.378	1.676	1.785
0.55	3.412	2.185	1.307	0.753	0.486	0.463	0.629	0.917	1.246	1.518	1.617
0.6	3.830	2.549	1.606	0.978	0.636	0.540	0.640	0.873	1.161	1.409	1.497
0.65	4.224	2.903	1.906	1.217	0.809	0.647	0.688	0.870	1.120	1.343	1.422
0.7	4.584	3.236	2.198	1.458	0.994	0.776	0.763	0.900	1.115	1.316	1.385
0.75	4.901	3.539	2.472	1.692	1.182	0.916	0.856	0.953	1.138	1.320	1.381
0.8	5.165	3.801	2.717	1.909	1.362	1.056	0.959	1.002	1.180	1.346	1.402
0.85	5.367	4.012	2.922	2.096	1.523	1.187	1.058	1.094	1.231	1.385	1.436
0.9	5.497	4.161	3.076	2.241	1.652	1.294	1.142	1.157	1.279	1.424	1.474
0.95	5.546	4.238	3.166	2.333	1.736	1.365	1.198	1.198	1.309	1.449	1.499
1	5.503	4.231	3.181	2.358	1.762	1.385	1.209	1.200	1.306	1.443	1.494

**Table D-11: $\beta_2 (\times 10^{-4})$ values corresponding to the column end-fixity factors
($\delta_0=L/600$ and $\Delta_0=L/300$)**

$r_j \backslash r_i$	0	0.1	0.2	0.3	0.4	0.5	0.6	0.7	0.8	0.9	1
0	0.000	0.217	0.804	1.661	2.691	3.796	4.877	5.837	6.578	7.001	7.008
0.05	0.046	0.069	0.477	1.179	2.080	3.086	4.100	5.022	5.755	6.195	6.241
0.1	0.178	0.015	0.249	0.797	1.568	2.470	3.410	4.287	5.003	5.453	5.531
0.15	0.386	0.045	0.113	0.509	1.149	1.945	2.805	3.632	4.324	4.776	4.877
0.2	0.659	0.153	0.061	0.309	0.819	1.507	2.284	3.054	3.717	4.165	4.283
0.25	0.988	0.328	0.084	0.190	0.572	1.152	1.843	2.553	3.181	3.618	3.747
0.3	1.363	0.561	0.175	0.145	0.404	0.876	1.480	2.127	2.715	3.137	3.271
0.35	1.773	0.843	0.326	0.167	0.306	0.674	1.191	1.772	2.318	2.719	2.855
0.4	2.208	1.164	0.527	0.248	0.274	0.540	0.972	1.486	1.987	2.366	2.498
0.45	2.659	1.515	0.769	0.381	0.300	0.468	0.817	1.265	1.720	2.073	2.200
0.5	3.115	1.885	1.044	0.556	0.376	0.453	0.721	1.105	1.514	1.840	1.959
0.55	3.566	2.265	1.341	0.764	0.495	0.486	0.679	1.001	1.365	1.664	1.772
0.6	4.002	2.645	1.651	0.996	0.647	0.561	0.683	0.947	1.267	1.539	1.637
0.65	4.413	3.014	1.964	1.243	0.823	0.668	0.726	0.936	1.215	1.462	1.549
0.7	4.790	3.363	2.269	1.494	1.014	0.798	0.799	0.960	1.202	1.426	1.503
0.75	5.121	3.679	2.555	1.737	1.209	0.940	0.893	1.011	1.221	1.424	1.493
0.8	5.397	3.953	2.811	1.963	1.395	1.085	0.996	1.078	1.260	1.446	1.509
0.85	5.608	4.174	3.025	2.158	1.563	1.220	1.098	1.150	1.310	1.483	1.542
0.9	5.744	4.331	3.186	2.311	1.697	1.331	1.184	1.214	1.357	1.520	1.577
0.95	5.795	4.411	3.281	2.407	1.786	1.405	1.241	1.255	1.386	1.544	1.601
1	5.750	4.405	3.298	2.434	1.813	1.426	1.253	1.257	1.381	1.537	1.595

**Table D-12: β_2 ($\times 10^{-4}$) values corresponding to the column end-fixity factors
($\delta_0=L/400$ and $\Delta_0=L/200$)**

$r_j \backslash r_i$	0	0.1	0.2	0.3	0.4	0.5	0.6	0.7	0.8	0.9	1
0	0.000	0.252	0.932	1.927	3.122	4.404	5.659	6.773	7.632	8.123	8.131
0.05	0.050	0.082	0.561	1.379	2.428	3.596	4.773	5.843	6.692	7.203	7.255
0.1	0.194	0.016	0.299	0.942	1.842	2.893	3.984	5.003	5.833	6.354	6.441
0.15	0.386	0.043	0.137	0.609	1.360	2.290	3.291	4.252	5.055	5.578	5.693
0.2	0.716	0.154	0.068	0.373	0.977	1.785	2.692	3.588	4.357	4.875	5.009
0.25	1.073	0.339	0.083	0.227	0.687	1.372	2.182	3.009	3.739	4.245	4.392
0.3	1.480	0.588	0.172	0.164	0.484	1.047	1.758	2.514	3.200	3.688	3.842
0.35	1.925	0.890	0.328	0.174	0.360	0.804	1.418	2.100	2.737	3.204	3.359
0.4	2.398	1.236	0.539	0.251	0.309	0.639	1.155	1.726	2.349	2.790	2.943
0.45	2.887	1.614	0.796	0.385	0.323	0.543	0.966	1.498	2.033	2.446	2.593
0.5	3.382	2.015	1.090	0.566	0.393	0.510	0.843	1.303	1.786	2.169	2.306
0.55	3.872	2.426	1.409	0.785	0.512	0.533	0.780	1.170	1.603	1.955	2.082
0.6	4.346	2.838	1.743	1.032	0.668	0.602	0.770	1.095	1.478	1.800	1.916
0.65	4.792	3.238	2.080	1.296	0.853	0.708	0.804	1.068	1.406	1.700	1.804
0.7	5.201	3.616	2.410	1.565	1.055	0.841	0.873	1.082	1.378	1.646	1.740
0.75	5.561	3.960	2.720	1.828	1.262	0.990	0.966	1.127	1.386	1.631	1.716
0.8	5.861	4.259	2.998	2.071	1.462	1.143	1.072	1.192	1.420	1.646	1.724
0.85	6.090	4.499	3.231	2.283	1.642	1.286	1.178	1.264	1.466	1.678	1.752
0.9	6.238	4.670	3.407	2.449	1.778	1.405	1.268	1.329	1.512	1.713	1.785
0.95	6.292	4.759	3.512	2.555	1.884	1.484	1.328	1.370	1.540	1.735	1.807
1	6.244	4.753	3.532	2.587	1.915	1.507	1.340	1.370	1.533	1.724	1.797

Appendix E

Joint Spring Constant, $F (R)$ Results (Schuster, 2004)

Designation	d (in)	P _u (lb)	I _{c,y-net} (in ⁴)	L _c (in)	I _{xb} (in ⁴)	L _b (in)	δ _{0.85} (in)	P _{0.85} (lb)	F (k-in/rad)
BB1.5x2.0x16-1	2.04	246	2.58	30	0.395	24	2.15	209	58.3
BB1.5x2.0x16-2	2.04	250	2.58	30	0.395	24	2.03	212	62.9
BB1.5x2.0x16-3	2.04	244	2.58	30	0.395	24	1.93	208	64.9
BB1.5x2.0x14-1	2.04	258	2.58	30	0.474	24	2.41	219	54.1
BB1.5x2.0x14-2	2.04	247	2.58	30	0.474	24	2.08	210	60.2
BB1.5x2.0x14-3	2.04	250	2.58	30	0.474	24	2.25	212	56.1
ER1.5x2.0x14-1	2.04	206	1.13	30	0.474	24	0.84	175	130
ER1.5x2.0x14-2	2.04	222	1.13	30	0.474	24	0.90	189	131
ER1.5x2.0x14-3	2.04	215	1.13	30	0.474	24	1.11	183	101
Average									79.8
ER1.5x3.0x14-1	3.22	505	1.13	30	1.42	24	2.11	429	121
ER1.5x3.0x14-2	3.22	489	1.13	30	1.42	24	2.18	416	113
ER1.5x3.0x14-3	3.22	509	1.13	30	1.42	24	2.17	432	118
Average									117
BB1.5x4.0x14-1	4.01	601	2.58	30	2.40	24	1.62	511	186
BB1.5x4.0x14-2	4.01	602	2.58	30	2.40	24	1.61	511	188
BB1.5x4.0x14-3	4.01	572	2.58	30	2.40	24	1.57	486	183
ER1.5x4.0x14-1	4.01	670	1.13	30	2.40	24	1.78	570	190
ER1.5x4.0x14-2	4.01	650	1.13	30	2.40	24	1.87	553	175
ER1.5x4.0x14-3	4.01	630	1.13	30	2.40	24	1.78	536	179
BB2.0x4.0x14-1	4.01	578	2.58	30	2.94	24	1.50	491	193
BB2.0x4.0x14-2	4.01	600	2.58	30	2.94	24	1.28	510	236
BB2.0x4.0x14-3	4.01	584	2.58	30	2.94	24	1.44	497	203
ER2.0x4.0x14-1	4.01	602	1.13	30	2.93	24	1.85	511	163
ER2.0x4.0x14-2	4.01	617	1.13	30	2.93	24	1.79	525	173
ER2.0x4.0x14-3	4.01	606	1.13	30	2.93	24	1.84	515	165
ER2.0x4.0x14-4	4.01	611	1.13	30	2.93	24	1.77	520	174
Average									185
ER2.0x5.0x14-1	5.19	789	1.13	30	5.40	24	1.35	671	295
ER2.0x5.0x14-2	5.19	790	1.13	30	5.40	24	1.37	672	291
ER2.0x5.0x14-3	5.19	765	1.13	30	5.40	24	1.27	650	304
ER2.0x5.0x14-4	5.19	775	1.13	30	5.40	24	1.41	659	277
Average									292
BB2.0x7.0x14-1	7.16	892	2.58	30	11.7	24	1.28	759	347
BB2.0x7.0x14-2	7.16	861	2.58	30	11.7	24	1.5	732	285
BB2.0x7.0x14-3	7.16	856	2.58	30	11.7	24	1.55	728	274
ER2.0x7.0x14-1	7.16	949	1.13	30	11.7	24	1.23	807	390
ER2.0x7.0x14-2	7.16	879	1.13	30	11.7	24	1.37	747	322
ER2.0x7.0x14-3	7.16	896	1.13	30	11.7	24	1.72	762	260
ER2.0x7.0x14-4	7.16	858	1.13	30	11.7	24	1.39	730	310
Average									313

Note: The moment of inertia values I_{c,y-net} and I_{xb} were obtained from The Econo-Rack Group.

Bibliography

- AISC, Manual of Steel Construction: Allowable Stress Design, 9th Edition, American Institute of Steel Construction, Chicago, III, 1989.
- AISC, Code of Standard Practice for Steel Buildings and Bridges, American Institute of Steel Construction, Chicago, 1992.
- AISC, Manual of Steel Construction-load and Resistance Factor Design (LRFD), American Institute of Steel Construction, Chicago, III, 1994.
- AISC, Manual of Steel Construction: Load and Resistance Factor Design (LRFD), 3rd Edition, American Institute of Steel Construction, Chicago, III, 2001.
- AISC, Specification for Structural Steel Buildings, American Institute of Steel Construction, Chicago, 2005.
- AISI Specification for the Design of Cold-Formed Steel Structural Members, Washington (DC): American Iron and Steel Institute; 1996, 2004.
- AS/NZ 4600, Cold-Formed Steel Structure Code AS/NZ 4600: 1996. Sydney: Standards Australia/Standards New Zealand, 1996.
- Bhatt, P., Problems in Structural Analysis by Matrix Method, Longman Inc., New York, 1981.
- Bjorhovde, R., Effect of end restraint on column strength-practical applications, AISC, Engineering Journal, 1st Qtr., (1984) 1-13
- Bleich, F., Die knickfestigkeit elastischer stabverbindungen, Der Eisenbau, 10(1919) 27.
- Bridge, R.Q., and Fraster D.J., Improved G-factor method for evaluating effective lengths of column, Journal of Structure and Engineering, ASCE, 115(6), (1977) 1341-1356.
- BS5950, Structural use of steelwork in buildings, Part 5: Code of practice for the design of cold-formed sections, London: British Standards Institution, 1998.
- CSA, Limit States Design of Steel Structures, Canadian Standard Association/National Standard of Canada, 2000.
- CSA, North American Specification for the Design of CFS Structural Members, Canadian Standards Association, Mississauga, Ontario, Canada, 2004.
- CSA, User guide for steel storage racks/Standard for the design and construction of steel storage racks, Canadian Standards Association, Mississauga, Ontario, Canada, 2005.

- CEN, ENV 1993-1-3 Eurode 3, Design of Steel Structures, Part 1.1-General Rules and Rules for Buildings, European Committee for Standardization, Brussels, 1992.
- CEN, Design of steel structures: Part 1.3: General rules–Supplementary rules for cold-formed thin gauge members and sheeting, ENV 1993-1-3, Brussels, European Committee for Standardization, 1996.
- Chen, W.F. and Lui, E.M., Structural Stability-Theory and Implementation, ELSEVIER, 1987.
- Chen, W.F. and Lui, E.M., Stability Design of Steel Frames, Boca Raton, FL: CRC Press, 1991.
- Chen, W.F., Guo, Y. and Liew, J.Y.R., Stability Design of Semi-Rigid Frames, John Wiley & Son, Inc., 1996.
- Christopher, J.E. and Bjorhovde, R., Semi-rigid frame design methods for practicing engineering, AISC Engineering Journal, 36 (1), (1999), 12-28.
- Clarke, M.J., Bridge, R.Q., Hancock, G.J., and Trahair, N.S., Advanced analysis of steel building frames, Journal of Constructional Steel Research, 23, (1992), 1-19.
- Clarke, M.J. and Bridge, R.Q., The Notional Load Approach for the Design of Frames, The University of Sydney, School of Civil and Mining Engineering Research Report No. R718, 1995.
- Craig, B., Examining the range of end-fixity factors for semi-rigid connections subjected to ultimate and service load conditions, Research Report, Department of Civil Engineering, University of Waterloo, Canada, 2000.
- Davies, J.M., Recent research advances in cold-formed steel structures, Journal of Constructional Steel, Research 55, (2000), 267–288.
- Deierlein, G.G., An inelastic analysis and design system for steel frames partially restrained connections, Proc. Of Connections in Steel Structures II, edited by Bjorhovde, R., Colson, A., Haaijer, G. and Stark, J., American Institute of Steel Construction, (1992), 408-415.
- Duan, L. and Chen, W.F., Effective length factor for columns in braced frames, ASCE, Journal of Structural Engineering, 114(10), (1988) 2357-2370.
- Duan, L. and Chen, W.F., Effective length factor for columns in unbraced frames, ASCE, Journal of Structural Engineering, 115(1), (1989) 149-165.
- FEM 10.2.02, Design code for racking plus worked examples, Federation Europeene De La Manutention (FEM) Section X, 2001
- FEM 10.2.03, Specifiers code, Federation Europeene De La Manutention (FEM) Section X, Guidelines for the Safe Provision of Static Steel Racking and Shelving, Specifier's Guidelines, 2003.

- FEM 10.2.04, Specifiers code, Federation Europeene De La Manutention (FEM) Section X, Guidelines for the Safe Provision of Static Steel Racking and Shelving, User's Code, 2001.
- Freitas, A.M.S., Freitas, M.S.R. and Souza, F.T, Analysis of steel storage rack columns, Journal of Constructional Steel Research 61 (2005) 1135–1146.
- Galambos, T.V., Guide to Stability Design Criteria for Metal Structures, 4th ed. John Wiley and Sons, New York, 1988.
- Gerstle, K.H., Effect of connection on frames, Journal of Construction Steel Research, 10 (1988), 241-67.
- Hancock, G.J., Distortional buckling of steel storage rack columns, ASCE, Journal of Structural Engineering, 111(12) (1985), 2770–83.
- Hancock, G.J., Design of cold-formed steel structures, 3rd ed. Australian Institute of Steel Construction; 1998.
- Hancock, G.J., Cold-formed steel structures, Journal of Constructional Steel Research 59 (2003) 473-487.
- Julian, O.G. and Lawrence, L.S., Notes on J and L Nomographs for Determination of Effective Lengths, unpublished report, 1959.
- Kishi, N., Chen, W.F., and Goto, Y., Effective length factor of columns in semi-rigid unbraced frames, ASCE, Journal of Structural Engineering, 23(3), (1997), 313-320.
- Kwon, Y.B. and Hancock, G.J., Tests of cold-formed channels with local and distortional buckling, ASCE, Journal of Structural Engineering, 117(7) (1992), 1786–803.
- Lau, S.C.W. and Hancock, G.J., Distortional buckling formulas for channel columns. ASCE, Journal of Structural Engineering, 113(5), (1987), 1063–78.
- Lau, S.C.W. and Hancock, G.J., Inelastic buckling of channel columns in the distortional mode, Thin-Walled Structures, (1990) 59–84.
- LeMessurier, W.J., A practical method of second order analysis, part 2-rigid frame, AISC, Engineering Journal, 2nd Qtr., (1977) 49-67.
- Lewis, G.M., Stability of Rack Structures, Thin-Walled Structures, 12(2), (1991), 163-174.
- Liu, Y. and Xu, L., Storey-based stability analysis of multi-storey unbraced frames, (2005)
- Livesley, R.K., Matrix Methods, of Structural Analysis, 2nd Ed., Pergamon Press Led., Headingto Hill Hall, Oxford, 1975.
- Lui, E.M., A novel approach for K factor determination, AISC, Engineering Journal, 4th Qtr., (1992) 150-159.

- Majid, K.I., Non-Linear Structures, Butterworth & Co. Ltd., 1972.
- McGuire, W., Gallagher, R.H. and Ziemian, R.D., MANSTAN2, Matrix Structural Analysis, 2nd Edition, John Wiley & Sons, Inc., 2000.
- Monforton, G.R. and Wu, T.S., Matrix analysis of semi-rigid connected frames, ASCE, Journal of Structural Engineering, 89(ST6), (1963), 13-42.
- Muller-Berslau, H., Die Graphische Statik der Bau-Konstruktionen, Vol.II. 2, A. Kroner, Berlin, 1908.
- NEHRP, National Earthquake Hazards Reduction Program, Recommended Provisions for Seismic Regulations for New Buildings and other Structures, California, USA, 2003.
- Newmark, N.M., A simple approximate formula for effective fixity of columns, Journal of the Aeronautical Sciences, 16(1949), 116.
- Olsson, A.M.J., Sandberg, G.E. and Austrell, P.E., Load-carrying capacity of damaged steel columns with channel sections, Journal of Structural Engineering, 125(3), (1999), 338-343.
- Peköz, T., and Winter G., Cold-Formed Steel Rack Structures, Proceedings of the 2nd Specialty Conference of Cold-Formed Steel Structures, University of Missouri-Rolla, 1973.
- Peköz, T. and Rao, K., Design of industrial storage racks, Progress in structural engineering and materials, 3 (2001), 28-35.
- Prager, W., Elastic stability of plane frameworks, Journal of Aeronaut, Sci., Vol. 3, pp: 388, 1936.
- Rhodes, J. Design of Cold-Formed Steel Members, Elsevier Applied Science, London, 1991.
- RMI, Specification for the design testing and utilization of industrial steel storage rack, Rack Manufactures Institute, 1997, 2000.
- Roddis, W.M.K., Hamid, H.A., and Guo, C.Q., K factor for unbraced frames: alignment chart accuracy for practical frame variations, AISC, Engineering Journal, 3rd Qtr., (1998) 81-93.
- SA, AS4100-1990 Steel Structures, Standards Australia, Sydney, 1990
- Sarawit, A.T. and Peköz, T., Notional load method for industrial steel storage racks, Thin-Walled Structures 44 (2006) 1280-1286.
- Sarawit, A.T. and Peköz, T., CUTWP program, Cold-Formed Steel Structures Research Group, School of Civil and Environmental Engineering, Cornell University, USA, 2003.
- Schafer, B., Direct Strength Method (DSM) Design Guide, Design Guide CF06-1, American Iron and Steel Institute, 2006.
- Schmidt, J.A., Design of steel columns in unbraced frames using notional loads, Practice Periodical on Structural Design and Construction, 4 (1), 1999

- Schuster, R.M., CFS Design Manual, Solid Mechanics Division, University of Waterloo, Waterloo, Ontario, Canada, 1975.
- Schuster, R.M., CFS Design, CIVE 703 Course Notes, Department of Civil Engineering, University of Waterloo, Ontario, Canada, 2004.
- Schuster, R.M., Industrial pallet rack storage structure frame column-beam connection spring constant tests, Final Report, Canadian Cold Formed Steel Research Group, University of Waterloo, Canada, 2004.
- Shanmugan, N.E. and Chen, W.F., An assessment of K factor formulas, AISC, Engineering Journal, 1st Qtr., (1995), 3-11.
- Sivakumaran, K.S. and Abdel-Rahaman, N., A finite element analysis model for the behavior of cold-formed steel member, Thin-walled Structures 31, (1998), 305-324.
- SSRC, Structural Stability Research Council, 1996
- Trahair, N.S. and Bradford, M.A., The Behaviour and Design of Steel Structures, 2nd Edition, CHAPMAN AND HALL, 1988.
- Xu, L., Second-order analysis for semi-rigid steel frame design, Canadian Journal of Civil Engineering, 28 (2001) 59-76.
- Xu, L., Liu, Y. and Chen, J., Stability of unbraced frames under non-proportional loading, Structural Engineering and Mechanics - an International Journal 1(11), (2001), 1-16.
- Xu, L., and Liu, Y., Storey-based effective length factors for unbraced PR frames, AISC, Engineering Journal, 39(1), (2002) 13-29.
- Xu, L. The buckling loads of unbraced PR frames under non-proportional loading, Journal of Construction Steel Research 58 (2002) 443-465.
- Xu, L. A NLP approach for evaluating storey-buckling strengths of steel frames under variable loading, Struct Multidisc Optim 25, (2003), 141-150.
- Xu, L. and Wang, X.H., Stability of multi-storey unbraced steel frames subjected to variable loading, Journal of Constructional Steel Research, 63 (2007), 1506-1514.
- Xu, L. and Wang, X.H., Storey-based column effective length factors with accounting for initial geometric imperfections, Journal of Engineering Structures, (in pressed).
- Yu, W.W., Cold-formed steel design, 3rd Edition, John Wiley and Sons Inc, 2000.
- Yura, J.A., The effective length of columns in unbraced frames, AISC, Engineering Journal, 2nd Qtr., (1971), 37-42.

Zimmerman, H., Die Knickfestigkeit des Geraden Stabes mit Mehreren Feldern, Sitzungsberichte der preussischen Akademie der Wissenschaften, (1909), 180.